

# **DAMAGING NON- SYNONYMOUS SNPS IN ULK1 GENE AND SUSCEPTIBILITY TO HEPATITIS B INFECTION**

*Thesis submitted in fulfillment of the requirements  
for the degree of*

**DOCTOR OF PHILOSOPHY**

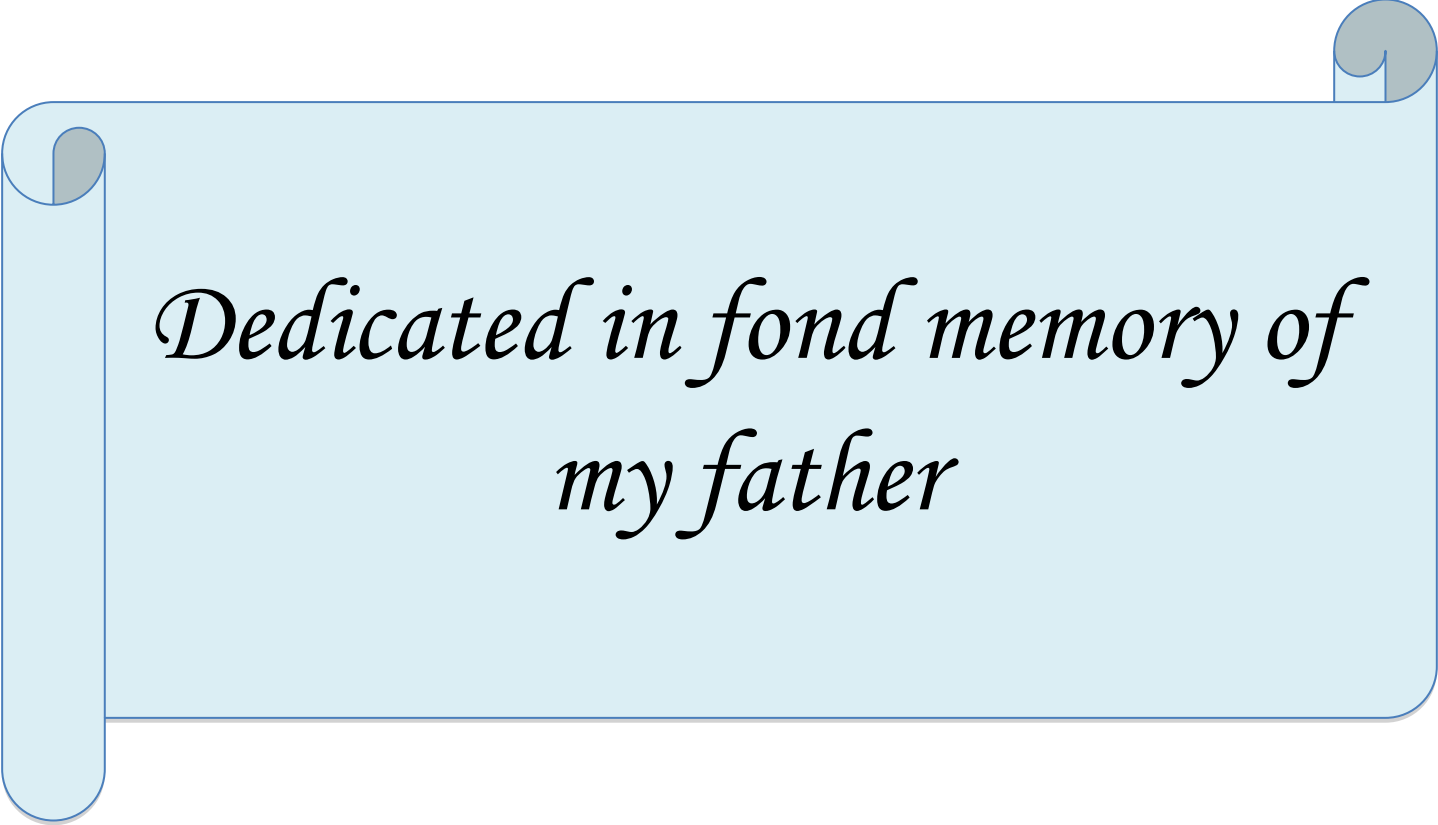
by  
**ROHIT RANDHAWA**



**Department of Biotechnology and Bioinformatics  
JAYPEE UNIVERSITY OF INFORMATION TECHNOLOGY  
WAKNAGHAT, DISTRICT SOLAN, H.P., INDIA**

**JANUARY, 2018**

Copyright  
@  
JAYPEE UNIVERSITY OF INFORMATION TECHNOLOGY,  
WAKNAGHAT  
January, 2018  
ALL RIGHTS RESERVED



*Dedicated in fond memory of  
my father*



# JAYPEE UNIVERSITY OF INFORMATION TECHNOLOGY

(Established by H.P. State Legislative Vide Act no. 14 of 2002)  
Waknaghat, P.O. Dumehar Bani, Kandaghat, Distt. Solan – 173215 (H.P.) INDIA

Website: [www.juit.ac.in](http://www.juit.ac.in)

Phone No. (91) 01792-257999(30 Lines).

Fax: (91) 01792 245362

## DECLARATION

I certify that:

- a. The work contained in this thesis is original and has been done by me under the guidance of my supervisor.
- b. The work has not been submitted to any other organisation for any degree or diploma.
- c. Wherever, I have used materials (data, analysis, figures or text), I have given due credit by citing them in the text of the thesis.

**Rohit Randhawa**

(Enrollment No. 126566)

Department of Biotechnology and Bioinformatics

Jaypee University of Information Technology, Waknaghat, India

Email: [rohitkangra001@yahoo.com](mailto:rohitkangra001@yahoo.com)

**Date:** 10-01-2018



## JAYPEE UNIVERSITY OF INFORMATION TECHNOLOGY

(Established by H.P. State Legislative Vide Act no. 14 of 2002)

Waknaghat, P.O. Dumehar Bani, Kandaghat, Distt. Solan – 173215 (H.P.) INDIA

Website: [www.juit.ac.in](http://www.juit.ac.in)

Phone No. (91) 01792-257999(30 Lines).

Fax: (91) 01792 245362

### CERTIFICATE

This is to certify that the thesis entitled, “**Damaging Non- Synonymous SNPs in ULK1 Gene and Susceptibility to Hepatitis B Infection**” which is being submitted by **Rohit Randhawa (Enrollment No. 126566)** in fulfillment for the award of degree of **Doctor of Philosophy in Biotechnology** at **Jaypee University of Information Technology, India** is the record of candidate’s own work carried out by him under my supervision. This work has not been submitted partially or wholly to any other University or Institute for the award of this or any other degree or diploma.

**Dr. Harish Changotra**

Associate Professor

Department of BT and BI

Jaypee University of Information Technology, India

**Email:** hchangotra@yahoo.com

**Date:** 10-01-2018

## ACKNOWLEDGEMENTS

***‘GOD provides inspiration to always keep going’***

*It is my earnest privilege to convey my gratitude to the following without whose guidance and support I would have never been able to complete my Ph. D. thesis.*

*I feel extremely fortunate to express my deep sense of respect for my distinguished mentor, **Dr. Harish Changotra**, for his pristine guidance, constructive criticism, constant encouragement and for providing requisite facilities to continue my research, which otherwise would have remained incomplete. His nurturing and gentle concern has been a stimulus, which I will always cherish. I also appreciate his untiring efforts during the entire tenure of my research work and patience during writing of this thesis. I have no words to express my gratitude for everything he has contributed in my Ph. D and without his blessings it was surely impossible for me to finish my work. I thank him from bottom of my heart.*

*I emphatically express my venerable thanks to **Prof. Dr. Vinod Kumar** (Vice Chancellor, JUIT), **Prof. Dr. Samir Dev Gupta** (Director, JUIT) and **Retd. Maj Gen Rakesh Bassi** (Registrar) for providing opportunity to pursue a Doctorate Degree, teaching assistantship and advanced lab infrastructure to accomplish this scientific venture of my life since ability is pint-sized without an opportunity.*

*I thankfully acknowledge the help rendered by **Dr. Sudhir Syal** (Acting HOD, Dept. of BT & BI) and **Prof. R. S. Chauhan** (Ex. Dean and HOD, Dept. of BT & BI) for his encouragement, timely help and cooperation throughout my research work. It gives me immense pleasure to express my gratitude to him for his ever smiling and positive disposition coming to my rescue in solving my problems and suggestions, which helped me in maintaining my confidence.*

*I also feel indebted to my former advisor, **Dr. Vikas Pahal** (Head Microbiology Dept, Dolphin PG College of Science and Agriculture) for his valuable advice and unconditional support throughout since my Masters days. I would like to convey my special sincere gratitude to **Dr. Uday Bhanu** (Assistant Professor (Senior Grade), Department of Pharmacy) for his valuable guidance and sustained support.*

*This document would be imperfect if I forget to mention the necessary ‘diet’ in the form of comments and suggestions received by **Dr. Tiratha Raj Singh, Dr. Ragini Raj Singh, and***

**Dr. Jata Shankar.** *I am short of words in expressing my thanks to them, for their innovative ideas that shaped this document. I wish to convey my sincere thanks to all the faculty members of Department of Biotechnology and Bioinformatics, for their help and guidance at the various stages of this study. I m also thankful to all the members of technical and non-technical staff of the department, especially **Mrs. Somlata Sharma, Mrs. Mamta, Mr. Baleshwar and Mr. Kamlesh** for their assistance and valuable contributions.*

*I am fortunate to have friends and family who always stood beside me in tough times. I extend my heartfelt thanks to my brother **Rajneesh** and friends, **Anil Kumar, Arun Sharma, Raman Thakur, Sanjay Singh, Vineet Mehta, Arun Prashar, Shivam Sharma, Varun Bhardwaj and Sampan Attri** who have been my brothers to me and always listened to my insane thoughts and ideas in spite of not understanding a bit of it. I am also grateful to my friends **Ambika Sharma, Avni Vij, Nutan Thakur, Poonam Katoch, Deepika, Tamanna, Kritika, Archit Sir, Nikhil Sir and Amit Sud** for they have played a very important role by being there so as to make me sail through all the twists and turns of this journey. It is my pleasure to express my gratitude to all research scholars of the Biotechnology & Bioinformatics Department for keeping me blessed with best wishes.*

*The purpose of this acknowledgement will be incomplete if I fail to appreciate the moral support and encouragement rendered by my wife **Mrs. Manika Sehgal Randhawa**, who has always been my inspiration and never let me felt abandoned. I am also pleased for the support rendered by my entire **family**. I express my love to my sweet nephew **Akshaj** whose innocence refreshed me during my difficult times.*

*The successful culmination of this thesis could not have been possible without the blessings of my mother (**Mrs. Inder Kaur**) and father (**Late K. C. Randhawa**) who always wish happiness and success for me. It is their blessings and love, which constantly motivated me and helped in the successful completion of my research work. Without their inspiration and assistance throughout I would have been greatly incapacitated.*

*At last, I would extend my sincere acknowledgment to all those who have directly or indirectly assisted me in my journey of the doctoral degree and I give heartfelt apologies if I have missed anyone.*

**Rohit Randhawa**

---



---

## TABLE OF CONTENTS

<b>CERTIFICATE</b>	<b>III</b>
<b>DECLARATION</b>	<b>IV</b>
<b>ACKNOWLEDGMENTS</b>	<b>V-VI</b>
<b>LIST OF TABLES</b>	<b>XIV-XVI</b>
<b>LIST OF FIGURES</b>	<b>XVII-XIX</b>
<b>ABSTRACT</b>	<b>XX</b>
<b>ABBREVIATIONS</b>	<b>XXI-XXIIIV</b>
<b>1. INTRODUCTION</b>	<b>1-7</b>
<b>2. REVIEW OF LITERATURE</b>	<b>8-40</b>
2.1 HEPATITIS B VIRUS.....	9
2.1.1 PRE-S/S ORF.....	9
2.1.2 SMALL SURFACE PROTEIN .....	11
2.1.3 MIDDLE SURFACE PROTEIN .....	11
2.1.4 LARGE SURFACE PROTEIN .....	11
2.1.5 PRE-C/C ORF.....	11
2.1.6 HEPATITIS B PRECORE PROTEIN.....	11
2.1.7 POLYMERASE ORF .....	12
2.1.8 HEPATITIS B X ORF.....	12
2.2 THE LIFE CYCLE OF HEPATITIS B VIRUS .....	13
2.3 DIFFERENT GENOTYPES OF HBV .....	14
2.3.1 SUB-GENOTYPES .....	16
2.4 EPIDEMIOLOGY .....	16
2.5 TRANSMISSION .....	18
2.6 CLINICAL STAGES OF HBV INFECTION .....	18



---

2.6.1 ACUTE HEPATITIS .....	19
2.6.2 CHRONIC HEPATITIS B (CHB).....	20
2.6.3 FULMINANT HEPATITIS.....	20
2.6.4 HEPATOCELLULAR CARCINOMA (HCC).....	20
2.7 BIOCHEMICAL MARKERS .....	21
2.8 SEROLOGICAL MARKERS FOR HBV .....	21
2.8.1 HEPATITIS B SURFACE ANTIGEN (HBSAG).....	21
2.8.2 ANTI-HBSAG .....	22
2.8.3 HEPATITIS B CORE ANTIGEN (HBCAG).....	22
2.8.4 ANTI-HBCAG.....	22
2.8.5 HEPATITIS B PRECORE ANTIGEN (HBEAG) .....	22
2.8.6 ANTI-HBEAG.....	22
2.8.7 HEPATITIS B X ANTIGEN (HBXAG) .....	23
2.8.8 HBV DNA .....	23
2.9 GENOME-WIDE ASSOCIATION STUDIES.....	23
2.10 CANDIDATE GENE APPROACH .....	25
2.11 CANDIDATE GENE APPROACH/GWAS AND INFECTIOUS DISEASES.....	26
2.11.1 MALARIA.....	26
2.11.2 HIV AND AIDS .....	26
2.11.3 MENINGOCOCCAL DISEASE.....	27
2.11.4 KAWASAKI DISEASE .....	27
2.11.5 GWAS AND HEPATITIS B VIRUS .....	28
2.12 AUTOPHAGY .....	28
2.12.1 CHAPERONE-MEDIATED AUTOPHAGY (CMA).....	29
2.12.2 MICROAUTOPHAGY.....	29
2.12.3 MACROAUTOPHAGY .....	29
2.13 AUTOPHAGY MACHINERY .....	30
2.13.1 INDUCTION .....	30
2.13.2 NUCLEATION.....	32
2.13.3 EXPANSION.....	32
2.13.4 MATURATION.....	33

<b>2.14 THE AUTOPHAGY-REGULATING KINASE ULK1 .....</b>	<b>33</b>
<b>2.14.1 ULK-FAMILY KINASES - ATG1-HOMOLOGS IN HIGHER ORGANISMS .....</b>	<b>33</b>
<b>2.14.2 CELLULAR FUNCTIONS OF ATG1/ULKS .....</b>	<b>34</b>
<b>2.14.3 REGULATION AND ROLE OF ATG1/ULK1 IN AUTOPHAGY .....</b>	<b>34</b>
<b>2.15 MECHANISM OF HBV-INDUCED AUTOPHAGY .....</b>	<b>36</b>
<b>2.16 EFFECT OF AUTOPHAGY ON HBV REPLICATION.....</b>	<b>38</b>
<b>2.17 HUMAN GENES INVOLVED IN HBV PATHOGENESIS AND SIGNIFICANCE OF THEIR POLYMORPHISMS.....</b>	<b>38</b>
<b>2.18 SNPs OF ULK1 IN DISEASES .....</b>	<b>40</b>
<b>2.18.1 ANKYLOSING SPONDYLITIS (AS).....</b>	<b>40</b>
<b>2.18.2 CROHN’S DISEASE.....</b>	<b>40</b>
<b>2.18.3 LATENT TUBERCULOSIS INFECTION .....</b>	<b>40</b>

### **3. MATERIALS AND METHODS 41-55**

<b>3.1 UNDERSTANDING ULK1: AN <i>IN SILICO</i> ANALYSIS .....</b>	<b>42</b>
<b>3.1.1 DATA RETRIEVAL .....</b>	<b>42</b>
<b>3.1.2 IDENTIFICATION OF SITE-SPECIFIC RESIDUES AND PHYLOGENETIC ANALYSIS FOR ULK1 .....</b>	<b>42</b>
<b>3.1.3 EVOLUTIONARY CONSERVED AND VARIABLE REGIONS.....</b>	<b>42</b>
<b>3.1.4 EVOLUTIONARY RELATIONSHIP ASSOCIATED WITH ULK1.....</b>	<b>42</b>
<b>3.1.5 IDENTIFICATION OF REGULATORY ELEMENTS AND OVER-REPRESENTED TFBS .....</b>	<b>43</b>
<b>3.1.6 IDENTIFICATION OF nsSNPs, THEIR PHENOTYPIC EFFECTS AND QUANTITATIVE STATISTICAL ANALYSES FOR GENETIC PARAMETERS .....</b>	<b>43</b>
<b>3.1.6.1 Mutation-based sequence stability analysis .....</b>	<b>44</b>
<b>3.1.6.2 Mutation-based structure stability analysis.....</b>	<b>44</b>
<b>3.1.6.3 Prediction of total energy for native and mutant structures .....</b>	<b>45</b>

<b>3.1.7</b> ELUCIDATION OF PUTATIVE PHOSPHORYLATION AND PALMITOYLATION SITES IN ULK1 .....	45
<b>3.1.8</b> PROTEIN–PROTEIN INTERACTION STUDIES FOR ULK1 .....	45
<b>3.2</b> GENOTYPING OF PREDICTED nsSNPS AND SELECTED SNPs OF ULK1 IN HBV INFECTED PATIENTS AND HEALTHY INDIVIDUALS .....	46
<b>3.2.1</b> STUDY SUBJECTS AND SAMPLE COLLECTION .....	46
<b>3.2.2</b> PROCESSING OF BLOOD SAMPLES .....	46
<b>3.3</b> LIVER FUNCTION TESTS.....	47
<b>3.3.1</b> <i>IN VITRO</i> DETERMINATION OF AST/GOT (ASPARTATE AMINOTRANSFERASE) IN HUMAN SERUM.....	47
<b>3.3.1.1</b> Principle .....	48
<b>3.3.1.2</b> Reagent composition.....	48
<b>3.3.1.3</b> Assay procedure.....	48
<b>3.3.1.4</b> Calculation .....	49
<b>3.3.2</b> <i>IN VITRO</i> DETERMINATION OF ALT/GPT (ALANINE AMINOTRANSFERASE) IN HUMAN SERUM.....	49
<b>3.3.2.1</b> Principle .....	49
<b>3.3.2.2</b> Reagent composition.....	50
<b>3.3.2.3</b> Assay procedure.....	50
<b>3.3.2.4</b> Calculation .....	50
<b>3.4</b> ISOLATION OF HBV DNA .....	51
<b>3.4.1</b> PROCEDURE.....	51
<b>3.5</b> GENOTYPE ANALYSIS OF SNPs IN ULK1 GENE .....	52
<b>3.5.1</b> PCR- RESTRICTION FRAGMENT LENGTH POLYMORPHISM (PCR-RFLP): DETECTION PROCEDURE TO IDENTIFY THE ALLELE-SPECIFIC PRODUCT .....	53
<b>3.5.2</b> TETRA PRIMER ARMS-PCR BASED ASSAY FOR GENOTYPING rs12303764.....	54
<b>3.6</b> HAPLOTYPE ANALYSIS .....	55
<b>3.7</b> STATISTICAL ANALYSIS .....	55

<b>4. RESULTS</b>	<b>56-104</b>
<b>4.1 <i>IN SILICO</i> ANALYSIS OF ULK1</b> .....	57
<b>4.1.1 THE CONSERVATIONAL AND PHYLOGENETIC EVALUATION</b> .....	57
<b>4.1.2 THE TRANSCRIPTION FACTOR BINDING SITES IN ULK1 GENE</b> .....	58
<b>4.1.3 POST-TRANSLATIONAL MODIFICATION SITES WITH THEIR</b> <b>ANNOTATIONS ON ULK1 PROTEIN DOMAIN STRUCTURE</b> .....	63
<b>4.1.4 LINKAGE DISEQUILIBRIUM ANALYSIS REVEALS SIGNIFICANT</b> <b>GENETIC VARIANTS AND HAPLOTYPES</b> .....	66
<b>4.1.5 PREDICTION OF NSSNPS THAT HAVE DAMAGING/DELETERIOUS</b> <b>EFFECT</b> .....	67
<b>4.2 <i>IN SILICO</i> MUTATIONAL ANALYSIS ON ULK1 SEQUENCE AND</b> <b>STRUCTURE</b> .....	68
<b>4.2.1 CHANGE IN THE PROTEIN STABILITY UPON MUTATIONS AT</b> <b>SEQUENCE LEVEL</b> .....	68
<b>4.2.2 CHANGE IN PROTEIN STABILITY UPON MUTATIONS AT</b> <b>STRUCTURE LEVEL</b> .....	70
<b>4.2.3 TOTAL ENERGY OF THE PROTEIN UPON MUTATIONS</b> .....	71
<b>4.3 VALIDATION OF <i>IN SILICO</i> ANALYSIS</b> .....	72
<b>4.3.1 STUDY SUBJECTS</b> .....	72
<b>4.3.2 LIVER FUNCTION TESTS (LFT)</b> .....	72
<b>4.3.3 QUANTIFICATION AND GROUPING OF HBV INFECTED PATIENTS</b> 74	
<b>4.3.4 GENETIC CORRELATION OF NSSNP IN HEPATITIS B PATIENTS</b> <b>AND HEALTHY CONTROLS</b> .....	74
<b>4.3.4.1 Genotyping nsSNP rs79965940 A/C (N148T)</b> .....	74
<b>4.3.4.1.1 PCR-RFLP</b> .....	74
<b>4.3.4.1.2 Genetic correlation of nsSNP rs79965940 in hepatitis B</b> <b>patients</b> .....	76
<b>4.3.4.1.3 Genetic correlation of nsSNP rs79965940 in hepatitis B</b> <b>patients with different clinical groups</b> .....	77
<b>4.3.4.2 Genotyping nsSNP rs55824543 C/T (T503M)</b> .....	79

<b>4.3.4.2.1</b> PCR-RFLP .....	79
<b>4.3.4.2.2</b> Genetic correlation of nsSNP rs55824543 (C/T) in hepatitis B patients.....	81
<b>4.3.4.2.3</b> Genetic correlation of nsSNP rs55824543 (C/T) in different HBV clinical groups.....	81
<b>4.3.4.3</b> Genotyping of nsSNP rs56364352 C/T (S298L) .....	84
<b>4.3.4.3.1</b> PCR-RFLP .....	84
<b>4.3.4.3.2</b> Role of nsSNP rs56364352 C/T in HBV susceptibility...	86
<b>4.3.4.3.3</b> Genetic correlation of nsSNP rs56364352 C/T in different clinical groups of HBV infection.....	86
<b>4.3.4.4</b> Genotyping nsSNP rs61942435 C/T (A991V) .....	89
<b>4.3.4.4.1</b> PCR-RFLP .....	89
<b>4.3.4.4.2</b> Genetic correlation of nsSNP rs61942435 C/T in hepatitis B patients and healthy controls.....	91
<b>4.3.4.4.3</b> Genetic correlation of nsSNP rs61942435 (C/T) in hepatitis B patients with different clinical groups .....	91
<b>4.3.4.5</b> Genotyping of SNP rs12303764 (G/T).....	94
<b>4.3.4.5.1</b> T-ARMS PCR.....	94
<b>4.3.4.5.2</b> Role of rs12303764 in genetic susceptibility of HBV infection in north Indian population .....	96
<b>4.3.4.5.3</b> Genetic correlation of rs12303764 in HBV infected patients at different stages of infection .....	96
<b>4.3.4.6</b> Genotyping SNP rs3923716 (G/T) .....	99
<b>4.3.4.6.1</b> PCR-RFLP .....	99
<b>4.3.4.6.2</b> Role of rs3923716 G/T in genetic susceptibility of HBV infection .....	101
<b>4.3.4.6.3</b> Genetic correlation of rs3923716 G/T in hepatitis B patients with different clinical groups.....	101
<b>4.3.5</b> HAPLOTYPE ANALYSIS OF nsSNPs OF ULK1 .....	104

<b>5. DISCUSSION</b>	<b>105-112</b>
5.1 <i>IN SILICO</i> ANALYSIS .....	108
5.1.1 PHYLOGENETIC ANALYSIS REVEALS ULK1 AS EVOLUTIONARY CONSERVED GENE.....	108
5.1.2 IMPERATIVE REGULATORY ELEMENTS AND TRANSCRIPTION FACTOR BINDING SITES DISTRIBUTED THROUGHOUT THE ULK1 GENE.....	108
5.1.3 PUTATIVE FUNCTIONAL SITES PRESENT IN ULK1 .....	108
5.1.4 PREDICTION OF nsSNPS DESTABILIZE ULK1 PROTEIN .....	109
5.2 GENOTYPING OF PREDICTED nsSNPS AND NONCODING SNPs.....	110
5.2.1 nsSNPS rs79965940 A/C (N148T), rs56364352 C/T (S298L) AND NONCODING SNP rs3923716 G/T INCREASE RISK TO HBV INFECTION, WHILE rs12303764 (G/T) SHOW PROTECTIVE ROLE AGAINST HBV INFECTION .....	110
5.2.2 NO SIGNIFICANT ASSOCIATION WAS OBSERVED FOR nsSNP rs61942435 C/T (A991V) AND rs55824543 (C/T) (T503M).....	112
 <b>6. CONCLUSION</b>	 <b>113-116</b>
 <b>REFERNCES</b>	 <b>117-149</b>
 <b>APPENDIX</b>	 <b>150-157</b>
 <b>LIST OF PUBLICATIONS</b>	 <b>158-160</b>

## LIST OF TABLES

Tables	Title	Page No.
Table 2.1	HBV genotypes along with their distribution pattern	15
Table 2.2	Gene polymorphisms associated with susceptibility to chronic hepatitis B	39
Table 3.1	Information of ULK1 polymorphisms, their genotype analysis platform and primer sequences used	52
Table 3.2	Thermocycling conditions used for genotyping polymorphisms of ULK1 gene	53
Table 3.3	The reaction conditions used in RFLP analysis for the nsSNPs of ULK1 gene	53
Table 4.1	Regulatory elements, their types and transcription factors which are related to UTR and intron regions of ULK1 gene	60
Table 4.2	Top ten transcription factors with their occurrence and importance rates	60
Table 4.3	oPOSSUM showing over-represented transcription factor binding sites, their Z score and Fisher score. Here Transcription Factors selected have Z score > 1	62
Table 4.4	The class-wise classification of the transcription factors detected in ULK1 gene	63
Table 4.5	Experimentally verified phosphorylation sites in ULK1	64
Table 4.6	The putative palmitoylation sites in ULK1. Four novel putative palmitoylation sites were identified applying CSS-PALM	66
Table 4.7	The significant SNPs in <i>ULK1</i> gene with their allelic information	67
Table 4.8	The non-synonymous single nucleotide polymorphisms in the coding region of ULK1 with putative damaging effects	69
Table 4.9	Prediction of protein stability change upon mutations in terms of Gibbs free energy from protein sequence by using iPTREE-STAB and i-MUTANT2.0	70
Table 4.10	Prediction of protein stability change upon mutations in terms of Gibbs free energy from protein structure by using DUET and ERIS	71
Table 4.11	Computation of total energy (CHARMm energy) of the native and mutant structures for mutations N148T and A991V in structures 4WNO and ULK1A predicted by CHARMm force field	71
Table 4.12	Base-line biochemical and demographic characteristics of patients	73
Table 4.13	The primer sequences and expected banding pattern for nsSNP rs79965940 A/C	75

<b>Table 4.14</b>	The standardized PCR parameters for nsSNP rs79965940 A/C (N148T)	75
<b>Table 4.15</b>	The optimized PCR conditions for genotyping rs79965940 nsSNP	75
<b>Table 4.16</b>	Genotypic and allelic frequencies of ULK1 polymorphism rs79965940 in HBV cases and healthy control samples (N= total number of samples)	76
<b>Table 4.17</b>	The allelic frequencies of ULK1 polymorphism rs79965940 in HBV subgroup and healthy control samples (N = Total number of samples)	77
<b>Table 4.18</b>	Analysis of the virological and biochemical parameters of HBV infected patients with rs79965940 (A/C) genotype	78
<b>Table 4.19</b>	The primer sequences and expected banding pattern for nsSNP rs55824543 (C/T)	79
<b>Table 4.20</b>	The optimized components for PCR amplification for genotyping of rs55824543 (C/T)	79
<b>Table 4.21</b>	The optimized PCR conditions for genotyping nsSNP rs55824543 (C/T)	80
<b>Table 4.22</b>	Genotypic and allelic frequencies of ULK1 polymorphism rs55824543 (C/T) in HBV cases and healthy control samples (N = total number of samples)	81
<b>Table 4.23</b>	The allelic frequencies and odds ratio of ULK1 polymorphism rs55824543 (C/T) in HBV subgroup and healthy control samples (N = total number of samples)	82
<b>Table 4.24</b>	Analysis of the virological and biochemical parameters of HBV infected patients with rs55824543 (C/T) genotype	83
<b>Table 4.25</b>	The primer sequences and expected banding pattern for nsSNP rs56364352 C/T	84
<b>Table 4.26</b>	The optimized conditions for genotyping of rs56364352 C/T	84
<b>Table 4.27</b>	The optimized PCR conditions for genotyping nsSNP rs56364352 C/T	85
<b>Table 4.28</b>	Genotypic and allelic frequencies of ULK1 polymorphism rs56364352 C/T in HBV cases and healthy control samples (N = total number of samples)	86
<b>Table 4.29</b>	The allelic frequencies and odds ratio of ULK1 polymorphism rs56364352 C/T in HBV subgroup and healthy control samples (N = total number of samples)	87
<b>Table 4.30</b>	Analysis of the virological and biochemical parameters of HBV infected patients with rs56364352 C/T genotype	88



<b>Table 4.31</b>	The primer sequences and expected banding pattern for nsSNP rs61942435 C/T	89
<b>Table 4.32</b>	The standardized conditions for genotyping of rs61942435 C/T	89
<b>Table 4.33</b>	The optimized PCR conditions for genotyping nsSNP rs61942435 C/T	90
<b>Table 4.34</b>	Genotypic and allelic frequencies of ULK1 polymorphism rs61942435 C/T in HBV cases and healthy control samples (N = total number of samples)	91
<b>Table 4.35</b>	The allelic frequencies and odds ratio of ULK1 polymorphism rs61942435 in HBV subgroup and healthy control samples (N = total number of samples)	92
<b>Table 4.36</b>	Analysis of the virological and biochemical parameters of HBV infected patients with rs61942435 (C/T) genotype	93
<b>Table 4.37</b>	The primer sequences and expected banding pattern for nsSNP rs12303764 (G/T)	94
<b>Table 4.38</b>	The standardized conditions for genotyping of rs12303764 (G/T)	95
<b>Table 4.39</b>	The optimized PCR conditions for genotyping rs12303764 (G/T)	95
<b>Table 4.40</b>	The genotypic and allelic frequencies of ULK1 polymorphism rs12303764 in HBV cases and healthy control samples (N = total number of samples)	96
<b>Table 4.41</b>	The allelic frequencies and odds ratio of <i>ULK1</i> polymorphism rs12303764 in HBV subgroup and healthy control samples (N = total number of samples)	97
<b>Table 4.42</b>	Analysis of the virological and biochemical parameters of HBV infected patients with rs12303764 (G/T) genotype	98
<b>Table 4.43</b>	Depiction of the primer sequences, amplified product size, restriction enzyme and expected fragment sizes of rs3923716 G/T after the RFLP analysis	99
<b>Table 4.44</b>	Optimized condition for genotyping rs3923716 G/T	99
<b>Table 4.45</b>	The optimized PCR conditions for genotyping SNP rs3923716 G/T	100
<b>Table 4.46</b>	Genotypic and allelic frequencies of ULK1 polymorphism rs3923716 G/T in HBV cases and healthy control samples (N = total number of samples)	101
<b>Table 4.47</b>	The allelic frequencies and odds ratio of ULK1 polymorphism rs3923716 G/T in HBV subgroup and healthy control samples (N = total number of samples)	102
<b>Table 4.48</b>	Analysis of the virological and biochemical parameters of HBV infected patients with rs3923716 G/T genotype	103

## LIST OF FIGURES

Figures	Title	Page No.
<b>Figure 1.1</b>	The pathway involved in autophagy	6
<b>Figure 2.1</b>	Schematic representation of hepatitis B virus. The nucleocapsid encloses the DNA and the viral polymerase, which is further bordered by the lipid-containing envelope and viral surface proteins	10
<b>Figure 2.2</b>	The genomic organization of hepatitis B virus	10
<b>Figure 2.3</b>	The life cycle of hepatitis B virus	13
<b>Figure 2.4</b>	The worldwide geographical prevalence of HBV infection as per World Health Organization (W.H.O.)	16
<b>Figure 2.5</b>	The geographic incidence of HBV across India; representing the number of reported outbreaks (N=291) in the country	17
<b>Figure 2.6</b>	The progression and complications in patients with hepatitis B infection	19
<b>Figure 2.7</b>	Overview of the genome-wide association studies	25
<b>Figure 2.8</b>	Schematic representation of autophagy	30
<b>Figure 2.9</b>	Regulation of autophagy via signaling pathways, hormones, growth factors and stress conditions. Here, purple and yellow lines depict events that positively and negatively regulate autophagy. The green lines portray pathways that are mTOR-independent. (IKK $\beta$ , inhibitor of nuclear factor $\kappa$ B kinase $\beta$ ; PI3K, phosphatidylinositol-3 kinase; PTEN, phosphatase and tensin homolog; MAPK, mitogen-activated protein kinase; TSC1/2, tuberousclerosis complexes 1 and 2; and EF, elongation factor)	31
<b>Figure 2.10</b>	Autophagy is induced by HBV expression and enhances HBV replication	37
<b>Figure 3.1</b>	Strategy used for designing TARMS-PCR primers for rs12303764	54
<b>Figure 4.1</b>	<b>A)</b> The multiple sequence alignment of ULK1 gene in eight species highlighting conserved regions. <b>B)</b> Mutations or variations in residues among the regions found in the ULK1 gene of eight species	57
<b>Figure 4.2</b>	Evolutionary relationship among the eight species included in the study. The phylogenetic tree was reconstructed using MEGA5 software by MP method, a character-based method	58

	for deducing phylogenetic trees by minimizing the total number of evolutionary steps	
<b>Figure 4.3</b>	The transcription factor binding sites in ULK1 gene. (A) Distant regulatory elements of co-regulated genes (DiRE) showed that 75% of the total transcription factors were present in UTR and remaining 25% in the intron region	59
<b>Figure 4.4</b>	The sequence logos of transcription factors identified in ULK1	61
<b>Figure 4.5</b>	The ULK1 domain structure with newly identified phosphorylation sites. NetPhos algorithm was used for prediction of phosphorylation sites at S, T and Y residues. A total of 58 new phosphorylation sites were identified out of which 25 are in kinase domain, 29 are in Ser/Thr rich domain and only 4 are in the CT domain	65
<b>Figure 4.6</b>	The linkage disequilibrium plot for ULK1	66
<b>Figure 4.7</b>	The CATT haplotype was prominently found with frequency of 0.774 in the studied population	67
<b>Figure 4.8</b>	The comparison of protein stability change upon mutations between iPTREE-STAB and i-MUTANT2.0 in terms of $\Delta\Delta G$	68
<b>Figure 4.9</b>	The comparison of protein stability change upon mutations between DUET and ERIS in terms of $\Delta\Delta G$	70
<b>Figure 4.10</b>	<b>A)</b> Structural representation of nsSNP rs79965940 (N148T) on the PDB structure of ULK1 (4WNO). (A) Native structure 4WNO with amino acid Asparagine at position 148. (B) Mutant structure N148T 4WNO with amino acid substitution as Threonine at position 148. (C) Superimposed native (4WNO) and mutant structures (N148T 4WNO). <b>B)</b> Structural representation of nsSNP rs61942435 (A991V) on the modeled structure of ULK1 (ULK1A). (A) Native structure ULK1A with amino acid Alanine at position 991 (B) Mutant structure A991V ULK1 with amino acid substitution as Valine at position 991. (C) Superimposed native (ULK1A) and mutant structures (A991V ULK1A)	72
<b>Figure 4.11</b>	Category-wise liver function test levels in hepatitis B infected patients	73
<b>Figure 4.12</b>	The HBV DNA levels in Hepatitis B infected patients	74
<b>Figure 4.13</b>	The representative agarose gel image for genotyping nsSNP rs79965940 in HBV infected as well as in healthy control	76

	samples (UD- undigested; CC-822bp; AA-625bp, 197bp; AC- 822bp, 625bp and 197bp)	
<b>Figure 4.14</b>	The representative agarose gel picture for genotyping nsSNP rs55824543 (C/T) in HBV infected as well as healthy control samples (UD- undigested; CC- 703bp; TT- 365bp and 338bp; CT- 703bp, 365bp and 338bp)	80
<b>Figure 4.15</b>	The representative agarose gel picture for genotyping nsSNP rs56364352 C/T in HBV infected as well as healthy control samples (UD- undigested; CC-866bp; TT- 458bp and 408bp; CT- 866bp,458bp and 408bp)	85
<b>Figure 4.16</b>	The representative agarose gel picture for genotyping nsSNP rs61942435 C/T in HBV infected as well as healthy control samples (UD- undigested; CC-322bp; TT- 223bp and 99bp; CT- 322bp, 223bp and 99bp)	90
<b>Figure 4.17</b>	Control genotypes obtained by sequencing amplified DNA fragments	95
<b>Figure 4.18</b>	. The representative agarose gel picture showing all genotypes of rs12303764	95
<b>Figure 4.19</b>	The representative agarose gel picture for genotyping rs3923716 G/T in HBV samples	100
<b>Figure 4.20</b>	The haplotype analysis of four nsSNPs of ULK1	104
<b>Figure 5.1</b>	Representation of overall conclusion of the study	116

---

---

## Abstract

Hepatitis B infection is simply an inflammation of the liver tissue which is intensifying at an alarming pace and demands emergent attention. According to W.H.O. 2017 report, approximately 257 million people are chronically infected with hepatitis B around the world and an estimate of 8.8 million people die every year due to complications caused by hepatitis B virus (HBV) infection. India constitutes 17.6% (1324 million) of the world's population (7600 million) and accounts for 10–15% of the worldwide HBV burden. Importantly, it has been shown that hepatitis B virus uses autophagy machinery for its own survival and proliferation *via* its X and S protein. In mammals, ULK1 is the principal gene of autophagy pathway, which gets activated first and further initiates autophagy downstream genes. Till date, the genetic variations in ULK1 have been studied with a handful of diseases which includes *Mycobacterium tuberculosis* infection, Behçet's disease (BD) and Vogt-Koyanagi-Harada (VKH) syndrome, congenital heart malformation, and Crohn's disease. Despite of strong association studies of autophagy with Hepatitis B infection available in literature, there are no genetic association studies reported between ULK1 and Hepatitis B. Owing to these facts, the current study investigated whether nsSNPs rs61942435, rs79965940, rs55824543 and rs56364352 and non-coding SNPs rs12303764 and rs3923716 in ULK1 gene might be linked with the susceptibility to HBV infection or its progression to various stages of HBV infection. On comprehensive analysis and assessment, it was found that rs79965940, rs56364352 and rs3923716 are associated with higher risk of HBV infection developing from initial asymptomatic infection to more severe chronic infection. In conclusion, we anticipate that these analyzed SNPs can be used as genetic biomarkers and can act as a bridge between the research gap on autophagy and HBV relation.

---

**ABBREVIATIONS**

AASLD	American Association for the Study of Liver Diseases
ALT	Alanine Aminotransferase
AST	Aspartate Aminotransferase
ATP	Adenosine 5'-triphosphate
cccDNA	Covalently closed circular DNA
CD	Crohn's Disease
CFH	Complement Factor H
CHB	Chronic Hepatitis B
CMA	Chaperone-Mediated Autophagy
COPI	COat Protein complex I
CTLs	Cytotoxic T-Lymphocytes
dbSNP	Single Nucleotide Polymorphism Database
DNA	Deoxyribonucleic acid
dNTP	2'-deoxynucleotide 5'-triphosphate
dsDNA	double strand DNA
EASL	European Association for the Study of the Liver
EDTA	Ethylene Diamine Tetraacetic Acid
EF	Elongation Factor
EHMT2	Euchromatic Histone-lysine-MethylTransferase 2
ELISA	Enzyme-Linked Immune-Sorbent Assay
EM	Electron Microscopy
ER	Endoplasmic Reticulum
ESCRT	Endosomal Sorting Complex Required for Transport
EtBr	Ethidium bromide
GWAS	Genome-Wide Association Studies
HAV	Hepatitis A Virus
HBcAg	Hepatitis B core antigen
HBeAg	Hepatitis B early antigen

HBsAg	Hepatitis B surface antigen
HBV	Hepatitis B Virus
HBx	HBV X protein
HCC	Hepatocellular Carcinoma
HLA	Human Leukocyte Antigen
H-W	Hardy-Weinberg
IKK $\beta$	Inhibitor of nuclear factor $\kappa$ B Kinase $\beta$
IM	Isolation Membrane
Kb	Kilobase
KD	Kawasaki disease
KEGG	Kyoto Encyclopedia of Genes and Genomes
KIR	Killer Immunoglobulin-like Receptor
LAMP2A	Lysosome-Associated Membrane Protein type-2A
LC	Liver Cirrhosis
LD	Linkage Disequilibrium
LFT	Liver Function Test
LHBs	Large hepatitis Surface antigen
M	Molarity
MAF	Minor Allele Frequency
MAPK	Mitogen-Activated Protein Kinase
MD	Meningococcal Disease
mg	Milligram
MHBs	Medium Hepatitis Surface antigen
min	Minutes
ml	Milliliter
mM	Millimolar
MP	Maximum Parsimony
mRNA	messenger RNA
MSA	Multiple Sequence Alignment

---



---

mTOR	Mammalian Target Of Rapamycin
MVBs	Multivesicular Bodies
N	Normality
NASH	Non-Alcoholic SteatoHepatitis
NCBI	National Center for Biotechnology Information
ng	Nanograms
nm	Nanometer
nsSNPs	Non-Synonymous Single Nucleotide Polymorphisms
NTCP	Sodium-Taurocholate Cotransporting polypeptide
OR	Odds ratio
ORF	Open Reading Frame
PCD	programmed cell death
PCR	Polymerase Chain Reaction
PDB	Protein Data Bank
PE	PhosphatidylEthanolamine
PI3K	Phosphatidylinositol-3 Kinase
pgRNA	Pregenomic RNA
PHALISA	Phage-Linked Immune-Sorbent assay
PI3P	Phosphatidylinositol-3-Phosphate
PolyPhen	Polymorphism Phenotyping
PPIs	Protein-Protein Interactions
PTEN	Phosphatase and Tensin homolog
RMSD	Root Mean Square Deviation
RNase	Ribonuclease
S	Serine
SIFT	Sorting Intolerant From Tolerant
SGOT	Serum Glutamic Oxaloacetic Transaminase
SGPT	Serum Glutamic Pyruvic Transaminase
SHBs	Small Hepatitis Surface antigen
SNP	Single Nucleotide Polymorphism



T	Threonine
TARMS	Tetra-primer Amplification Refractory Mutation System
Taq	<i>Thermus aquaticus</i>
TCF19	Transcription Factor 19
TE	Tris-EDTA
TFs	Transcription Factors
TGN	Trans-Golgi Network
TNF- $\alpha$	Tumour necrosis factor-alpha
TSC1/2	Tuberousclerosis Complexes 1 and 2
UC	Ulcerative colitis
ULKs	Unc-51 Like Kinases
ULK1	Unc-51 Like Autophagy Activating Kinase 1
Unc-51	Uncoordinated-51
UPR	Unfolded Protein Response
UTR	Untranslated regions
WHO	World Health Organization
$\alpha$	Alpha
$\beta$	Beta
$\gamma$	Gamma
%	Percentage
$\mu\text{g}$	Microgram
$\mu\text{l}$	Microlitre
$\mu\text{M}$	Micromolar

# INTRODUCTION

## **1. Introduction**

Human genetic studies have a central goal to categorize genetic risk factors for frequent and multifaceted diseases such as schizophrenia and type II diabetes, and for rare Mendelian diseases such as cystic fibrosis and sickle cell anemia [1]. The genome-wide association studies (GWAS) measures and examines the DNA sequence variations across the human genome to spot genetic risk factors for diseases that are common in the population [2]. The ultimate goal of GWAS is to use genetic risk factors to make predictions about who is at risk and to spot out the biological factors of disease susceptibility for building up new prevention and treatment strategies [2]. Understanding the biological basis of genetic effects will lead to a significant role in building new pharmacologic therapies. One of the most flourishing appliances of GWAS has been in the area of pharmacogenetics, which gives rise to a new field called personalized medicine that aims to modify healthcare to individual patients based on their genetic background and other biological features [3]. GWAS studies, for better or for worse, have guided in this exciting era of personalized medicine and personal genetic testing [4].

Various GWAS of infectious diseases has identified a variety of genetic markers that show sturdy confirmation of association [5]. These studies have also established some previously reported links from candidate-gene and linkage studies, as well as identifying strong associations between common infectious disease phenotypes and novel genes and pathways involved [5]. Several Single-Nucleotide Polymorphisms (SNPs) have been revealed via GWAS studies and are deposited in the public databases (e.g. the National Center for Biotechnology Information [<http://www.ncbi.nlm.nih.gov>], Ensembl [<http://asia.ensembl.org/index.html>], and the MEXT Integrated Database Project [<http://dbcls.rois.ac.jp>]) through international SNP discovery projects such as the Human Genome Project, the International HapMap project, and the 1000 Genomes project [6]. With the development of more advanced technologies for analyzing large-scale SNP genotyping, GWAS data using thousands of SNPs permit the discovery of candidate genetic loci for multifactorial diseases [7-9]. The disease-associated SNPs have also been deposited in public databases, such as the database of Genotypes and Phenotypes ([www.ncbi.nlm.nih.gov/gap](http://www.ncbi.nlm.nih.gov/gap)) [10]. Moreover, a number of SNPs associated with complex genetic traits have been very well accounted, such as body mass index [11], height [12] and hair thickness [13]. In a GWAS, associations of certain variants with a particular trait are detected by

comparing the two groups of participants to detect the examining differences in allele and/or genotype frequencies of all SNPs, which exist across the entire genome [14-16]. By using an autonomous set of participants with a superior number of samples, GWAS facilitates the efficient detection of associated variations which are in strong linkage disequilibrium (LD) [17]. However, it would be tricky to spot the association of SNPs in a SNP-based GWAS with low minor allele frequency (below 1–5%; known as rare variants) because of inadequate statistical power due to the low sample number [18]. Till date, GWAS have been reported for various infectious diseases including HIV [19], malaria [20], tuberculosis [21], leprosy [22], meningococcal meningitis [23], kawasaki's disease [24] and viral hepatitis B and C [25-28].

Worldwide, hepatitis infection is intensifying at an alarming pace and demands emergent attention [29]. Hepatitis is simply an inflammation of the liver tissue [30]. Some people show no warning sign of the infection whereas others show poor appetite, tiredness, vomiting, yellow discoloration of the skin and whites of the eye, abdominal pain, and diarrhea [31]. Hepatitis may be short-term (acute) or long-term (chronic) depending on the duration of the infection, whether it lasts for less than or more than six months [32]. Acute hepatitis can sometimes cure on its own and if not, further progress to more severe chronic hepatitis, or on the odd occasions result in acute liver failure [33]. The most common cause of hepatitis infection worldwide is viruses of *Hepadnaviridae* family (humans, apes, and birds serve as natural hosts) [34]. Other causes include profound alcohol use, certain drugs, toxins, other infections, autoimmune diseases, and non-alcoholic steatohepatitis (NASH) [35].

According to W.H.O. 2017 report, approximately 257 million people are chronically infected with hepatitis B around the world [36] and an estimate of 8.8 million people die every year due to complications caused by hepatitis B virus (HBV) infection (WHO fact sheet, 2017 ) [37]. With the highest prevalence in sub-Saharan Africa and East Asia, around 5–10% of the adult population is chronically infected. An assessment states that 2–7% of the general population is chronically infected in the Middle East and the Indian subcontinent [38]. Till date, India constitutes 17.6% (1324 million) of the world's population (7600 million) and accounts for 10–15% of the worldwide HBV burden [39].

Human HBV is the member of the *Hepadnaviridae* family whose natural hosts are humans, apes, and birds. Currently, this virus family is divided into 2 genera: *Avihepadna* virus (infect birds) and *Orthohepadna* virus (infect mammals). The human HBV genome is a 3.2 kb circular and partially double-stranded DNA (dsDNA) that includes four overlapping open reading frames (ORFs) encoding the surface; (preS1, preS2, and S), core (C and pre-core), polymerase (P), and X proteins [40]. Hepatitis B surface antigen (HBsAg), a foremost indicator of HBV prevalence is commonly used for evaluating HBV endemicity around the world. The mode of transmission of this virus from a person is usually through blood or body fluids. Despite effective vaccinations, HBV infections are still very common globally as the virus replicates by reverse transcription using a viral polymerase lacking proof-reading ability which results in the emergence of mutant viruses that remain undetected by host immunity or viral therapeutic agents. Other mutations result in a change within the HBV surface antigen, resulting in a loss of detection by some diagnostic assays [41]. The virus is organized into four overlapping ORFs (C, P, S, and X) that encode 7 viral proteins [42]. A single core protein, three envelope glycoproteins, and the viral DNA polymerase are incorporated into mature virus particles. A sixth protein, the so-called HBV X protein, is a trans-activator of viral replication that is not incorporated into the virion. The protein, known as the HBe antigen, contains the full amino acid sequence of the core protein, and is not incorporated into the virus particle, but is secreted in a soluble form by an infected hepatocyte [43]. Four HBV serotypes have been identified based on peptide differences in the hepatitis B surface antigen (HBsAg). The common determinant a and two pairs of mutually exclusive determinants, d/y and w/r, enable the distinction of four major subtypes: adr, adw, ayr, and ayw [44]. Additional sub-determinants of w (w1-w4) have allowed the definition of six more serotypes. Currently, the introduction of molecular typing techniques has made this classification obsolete.

HBV strains are classified into ten main genomic groups that have distinct geographical distributions [45-48]. Genotype A is widespread around the world but is most prevalent in Northern Europe, North America, and South Africa. Genotypes B and C are the most common in Asia and the Pacific. The genotype D has the broadest distribution around the world, with the highest prevalence in the Mediterranean area, the Middle East, and India. The genotype E is

mainly found in (West) Africa. The genotype F and H are most frequent in South and Central America. The exact epidemiology of genotype G has yet to be determined [49].

From decades, extensive evidence suggests an important role of hepatitis B virus X protein, a small soluble cytoplasmic protein in the host cells, which modulates gene expression or intracellular signal pathway through interaction with either transcriptional machinery or signaling components involved in cell proliferation, apoptosis, and DNA repair [50, 51]. Importantly, it has been shown that hepatitis B virus uses autophagy machinery for its own survival and proliferation *via* its X and S protein [52-54]. The clinical presentation of the disease in patients with chronic hepatitis B infection depends on several host and viral factors. Out of these, autophagy machinery is one of the chief factors contributing to the progression and replication of HBV [55]. Autophagy, an evolutionary conserved and regulated catabolic process is primarily involved in the degradation of cellular components through lysosomal machinery. This process is indispensable in many cellular events including differentiation, survival, development, and homeostasis [56]. The autophagy process involves the sequestration of bulk cytoplasm within a cytosolic double-membrane vesicle termed the autophagosome, which eventually fuses with the lysosome (or the vacuole in yeast) as portrayed in Figure 1.1 [57]. Fusion results in the discharge of the internal vesicle, now termed an autophagic body, into the lysosome lumen [58]. Within the lysosome, the engulfed material is degraded and the products are recycled [59]. Autophagy has been reported in a number of human diseases and conditions, including cancer, neurodegenerative disorders, certain myopathies, aging, infectious diseases and defense against pathogens [60].

From a total of 33 autophagy-related genes (ATG) identified till date [61], ATG1/ULK1 (uncoordinated 51-like kinase 1) complex plays a central role in autophagy. It works by integrating signals from the upstream mechanistic target of rapamycin (mTOR) and 5' AMP-activated protein kinase (AMPK) and transduces them to the downstream autophagy pathway. While autophagy occurs at the basal levels under standard conditions, it is often activated in response to cellular stresses such as endoplasmic reticulum (ER) stress, nutrient starvation, hypoxia, and pathogen infection. Upon these stress conditions, the cell utilizes autophagy either

to redistribute its resources to tide over the period of stress or to degrade injurious components (such as, damaged mitochondria or invading pathogens) via lysosomal degradation [62].

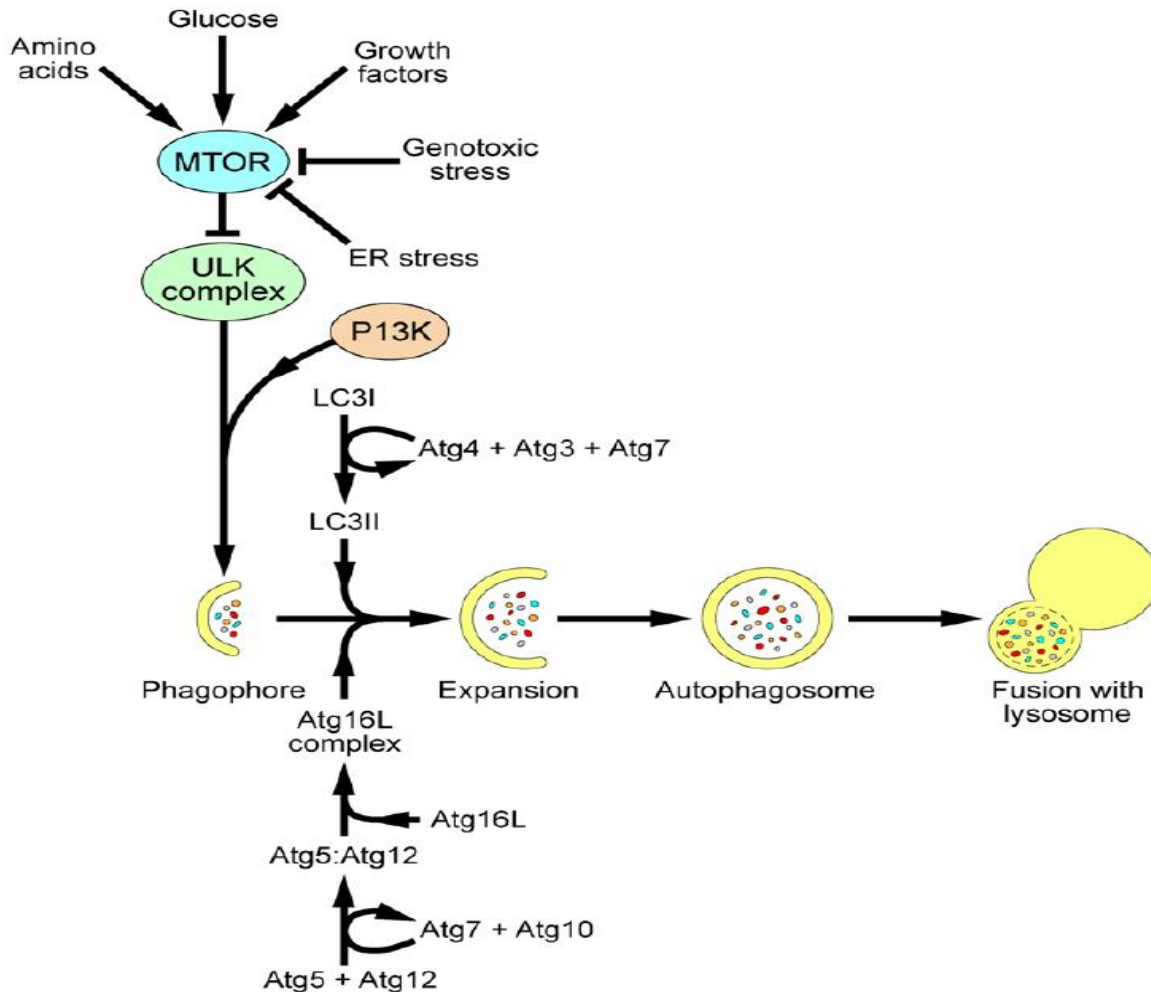


**Figure 1.1** The pathway involved in autophagy (Maier HJ *et al.* 2012)

Recently, Sir *et al.* revealed the enhancement of HBV DNA replication by autophagy [63], they further confirmed the role of autophagy in the production of HBV virions *in vivo* using HBV transgenic mice. They also reported that the formation of autophagosome is essential for HBV DNA synthesis in the cytoplasm [64]. In particular, ULK1, an ortholog of yeast autophagy-related gene (ATG1), is a critical mammalian kinase regulator of autophagy [65, 66]; as evident from studies depicting the correlation between autophagy induction and HBV expression [67, 68]. In mammals, ULK1 is the principal gene of autophagy pathway, which gets activated first and further initiates autophagy downstream genes. Till date, the genetic variations in ULK1 have been studied with a handful of diseases which includes *Mycobacterium tuberculosis* infection,

Behçet's disease (BD) and Vogt-Koyanagi-Harada (VKH) syndrome, congenital heart malformation, and Crohn's disease [69-73]. Despite of strong association studies of autophagy with Hepatitis B infection available in literature [74], there are no genetic association studies reported between ULK1 and Hepatitis B. Therefore, assuming the hypothesis that ULK1 controls the induction of autophagy by forming complex with ATG13, FIP200, and ATG10 and variations in ULK1 gene can alter its interaction with its partners and could be associated with Hepatitis B infection. In this study, we analyzed the four predicted damaging non-synonymous SNPs (nsSNPs) by *in-silico* analysis and two earlier reported SNPs i.e. rs3923716 (G/T) and rs12303764 (G/T) in ULK1 known to be associated with Crohn's Disease [73, 75] in a New Zealand Population for their association with Hepatitis B infection susceptibility. Keeping in view the research gap, our study mainly focuses on the association of polymorphisms in ULK1 gene and their susceptibility to HBV infection in North Indian Population.

### **Objectives of the study**

*Objective 1.* To predict the damaging nsSNPs in ULK1 gene through *in-silico* analysis

*Objective 2.* To analyze the effect of damaging nsSNPs on ULK1 stability

*Objective 3.* To optimize T-ARMS-PCR and PCR-RFLP assays for earlier reported SNPs and predicted nsSNPs

*Objective 4.* Genotyping of SNPs and their association with HBV infection risk



# REVIEW OF LITERATURE

## 2. Review of Literature

### 2.1 Hepatitis B Virus

The Hepatitis B Virus (HBV) is an envelope, hepatotropic and non-cytopathic virus [76]. Despite safe vaccines available for HBV, it still remains a severe civic health problem particularly in Asia, Africa, South America and may possibly results in death [77]. HBV infection can give rise to a variety of clinical symptoms , ranging from asymptomatic carrier state to acute hepatitis, chronic hepatitis, liver cirrhosis (LC) and hepatocellular carcinoma (HCC). Development of chronic hepatitis B (CHB) to severe liver disorder, like LC and HCC, is determined by viral factors, genetic characteristics of the host and environmental factors [78]. The HBV or Dane particle is an enveloped partially double-stranded circular DNA virus with a diameter of 42nm (Figure 2.1). The envelope is made up of phospholipids and hepatitis B surface antigen (HBsAg) and is 7 nm thick. It contains a 27 $\mu$ m inner nucleocapsid core of viral DNA and a tightly bound 19 kilo Dalton hepatitis B core antigen (HBcAg). The viral core also contains DNA polymerase and protein kinase activity [79]. The genome of HBV is partially double-stranded relaxed circular (RC) DNA molecule with a single stranded region of variable length [80]. The antisense strand is the longer strand designated as L (-) and the sense strand is the shorter strand designated as S (+). The S (+) strand varies from 50 to 70 % of the L (-) strand, which consists of 3200 bases. The positions of the 5'-end of both the strands are fixed whereas the position of the 3'-end of the plus strand (short strand) is not fixed. A 224 base pair 5'-cohesive terminus maintains the circularization of the genome [81]. The minus strand contains four open reading frames (ORFs) and carries all the protein coding capacity of the virus [82]. Critically, these cover in a frameshifted way with each other so the short strand is perused one and a half time. The longest ORF encodes the viral polymerase (pol). The ORF for the envelope gene is completely located within the Polymerase ORF and the ORF for the core (*Pre-C/C*) and X gene partially overlap with Pol ORF. The HBV encodes more than one protein from one ORF by using multiple internal AUG codons within an ORF, creating additional start sites for protein biosynthesis [80].

#### 2.1.1 Pre-S/S ORF

The gene for the HBV surface antigen consists of a single ORF divided into three coding regions, preS1, preS2 and S, each starting with an in-frame ATG codon as illustrated in Figure 2.2 [83]. By translation initiation at the first AUG, the large hepatitis surface antigen (LHBs)

encompassing PreS1, PreS2 and S is synthesized; by initiation at the second AUG the middle surface protein (MHBs, encompassing PreS2+ S) and is synthesized by initiation at the third, the small surface protein (SHBs) is synthesized. The HBsAg contains small (SHBs), medium (MHBs), and large (LHBs) proteins, all of which are glycosylated, type II transmembrane proteins that can form multimers stabilized by disulfide bridges formed by cysteine residues present in the S domain [84]. All these proteins exist in two forms differing in the extent of glycosylation. [85].

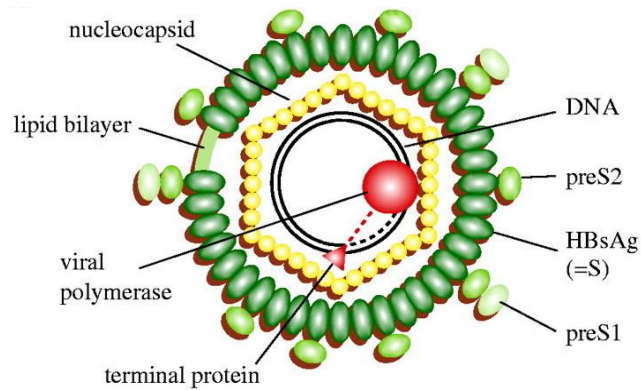


**Figure 2.1** Schematic representation of hepatitis B virus. The nucleocapsid encloses the DNA and the viral polymerase, which is further bordered by the lipid-containing envelope and viral surface proteins [86]

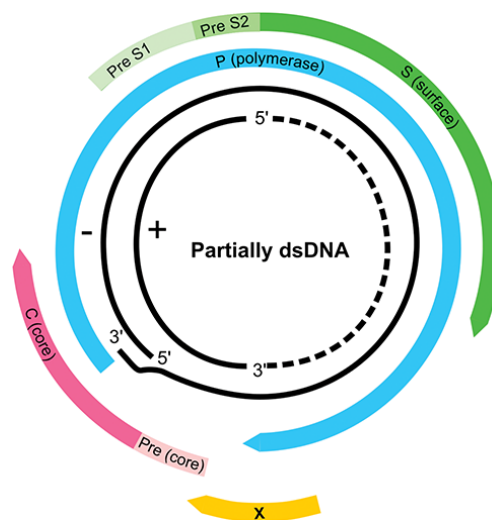


**Figure 2.2** The genomic organization of hepatitis B virus.

### **2.1.2 Small Surface protein**

The SHBs domain is 226 amino acids long and is the most abundant protein of all three HBV - associated particles. The SHBs is found in a glycosylated and a non-glycosylated form [87].

### **2.1.3 Middle Surface protein**

The MHBs Pre-S2 domain is a minor component of the virion or HBs particle and consists of the S and a 55-amino-acid N-terminal extension. It is either single or double glycosylated [88].

### **2.1.4 Large surface protein**

The LHBs contains a further N-terminal extension to the M protein of 108 or 119 amino acids (depending on the subtype/genotype) and is more prevalent than MHBs in virions and filaments but less prevalent in HBs spheres. The LHBs contains three domains, PreSI, Pre-S2, and S, and is glycosylated [89].

### **2.1.5 Pre-C/C ORF**

The Pre-CtC ORF encodes the core protein P21, which is the major polypeptide of the nucleocapsid and expresses the HBcAg [90]. The HBc protein is either 183, 185, or 195 amino acids long, depending on the genotype of the virus [91]. The ORF C is preceded upstream by a short, in-phase ORF called the Pre-core region from which the soluble hepatitis B early antigen (HBeAg) is made. The core protein expressed this way assembles itself into core particles that display core antigenicity [79].

### **2.1.6 Hepatitis B precore protein**

The core protein ORF is preceded by an in-frame initiation codon positioned 29 codons upstream. The sequence encompassing these 29 codons has been termed the 'precore' sequence and the protein translated from the upstream initiation codon has been termed as the 'precore' protein [80]. Although the precore protein contains the entire sequence of the core protein and the amino terminal extension of 29 amino acids, it is not a precursor of the core protein [92]. HBeAg is a soluble secretory protein and is regarded as an accessory protein of the virus. The first 19 amino acids of the precore protein form a secretion signal that allows the translocation of the precore protein into the lumen of the endoplasmic reticulum (ER). These 19 amino acids are

cleaved off by a host cell signal peptidase, leaving the precore protein derivative P22. The P22 is then secreted through the ER and Golgi apparatus and further modified by C-terminal cleavage of upto 34 amino acids, resulting in the secretion of a heterogeneous population of proteins of 15 to 18 kDa, serologically defined as HBeAg [93].

### **2.1.7 Polymerase ORF**

The Pol gene is the longest ORF, spanning almost 80% of the genome and overlapping the other three ORFs. The Pol protein is translated from pregenomic RNA [80]. The 834 to 845 codons found in the Pol ORF have sequence homology to reverse transcriptases and most parts of the ORF are essential for viral replication. The 90-kDa product of the Pol ORF is a multifunctional protein that has at least four domains [94]. The N-terminal domain encodes the terminal protein that is covalently linked to the S end of the minus strand of virion DNA. This part of Pol ORF is necessary for priming of minus-strand synthesis [95]. An intervening domain with no specific recognized function is referred to as the spacer or tether region. The third domain encodes the RNA and DNA-dependent DNA polymerase, i.e. the reverse transcriptase. The C-terminal domain encodes ribonuclease (RNase) H that cleaves the RNA in the RNA-DNA hybrids during reverse transcription [96]. The terminal protein's role in protein priming of reverse transcription includes the provision of the substrate tyrosine at amino acid 63 of the HBV Pol for the formation of the covalent bond between the enzyme and the first nucleotide (G) of the minus-strand DNA [97].

### **2.1.8 Hepatitis B X ORF**

The X ORF encodes a 154 amino acids long polypeptide in length (HBx) with a molecular weight of 17 kDa [98]. This is the second accessory protein of HBV and is conserved in a similar form across all the mammalian hepadna viruses. The expression of full-length HBx protein is dispensable for virus production *in vitro* but is a critical component of the infectivity process *in vivo* [99]. HBx behaves as a transcriptional trans-activator of a number of viral and cellular gene promoters through direct interaction with transcription factors [100].

## 2.2 The life cycle of hepatitis B virus

The HBV virion binds to a receptor on the surface of the hepatocyte [101]. A number of candidate receptors have been identified, including the transferrin receptor, the asialoglycoprotein receptor molecule, and human liver endonexin. The mechanism of HBsAg binding to a specific receptor to enter cells has not been established yet. Figure 2.3 shows how the viral nucleocapsids enter the cell and reach the nucleus, where the viral genome is delivered [102]. In the nucleus, second-strand DNA synthesis is completed and the gaps in both strands are repaired to yield a supercoiled covalently closed circular DNA (cccDNA) molecule. In the lipid membrane of the ER, the envelope proteins get inserted and become an integral membrane protein [103]. Pregenomic RNA (pgRNA) is packaged along with HBV polymerase and a protein kinase into core particles where it assists as an outline for reverse transcription of negative-strand DNA [80]. The RNA to DNA conversion takes place inside the core particles. The new, mature, viral nucleocapsids further follow two different intracellular pathways, one of which leads to the formation and secretion of new virions, whereas the other leads to amplification of the viral genome inside the cell nucleus [104].

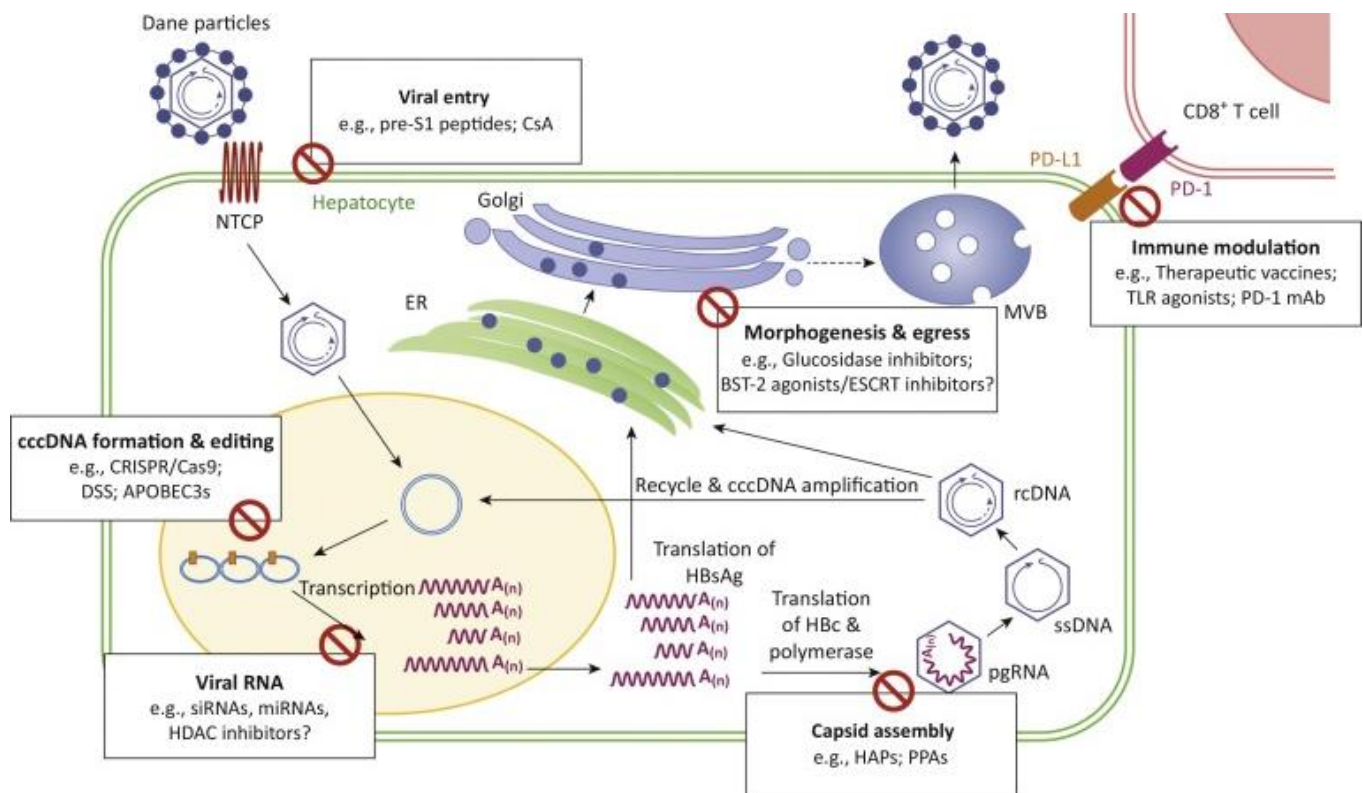


**Figure 2.3** The life cycle of hepatitis B virus [105]

In the virion assembly pathway, the nucleocapsids reach the ER, where they associate with the envelope proteins and bud into the lumen of the ER, from which they are secreted *via* the Golgi apparatus out of the cell. In the genome amplification pathway, the nucleocapsids deliver their genome to amplify the intranuclear pool of cccDNA [104]. The precore polypeptide is transported into the ER lumen, where its amino- and carboxy-termini are trimmed and the resultant protein is secreted as precore antigen (HBeAg). The X protein contributes to the efficiency of HBV replication by interacting with different transcription factors and is capable of stimulating both cell proliferation and cell death. The HBV polymerase is a multifunctional enzyme [106]. The products of the P gene are involved in multiple functions of the viral life cycle, including a priming activity to initiate minus-strand DNA synthesis, a polymerase activity, which synthesizes DNA by using either RNA or DNA templates, a nuclease activity which degrades the RNA strand of RNA-DNA hybrids, and the packaging of the RNA pregenome into nucleocapsids [95].

### **2.3 Different genotypes of HBV**

At least ten HBV genotypes (A–J) and several subtypes have been identified for the HBV genome so far (summarized in **Table 2.1**). Genotype A is mostly prevalent in sub-northern Europe, Saharan Africa, Western Africa and India. Genotypes B and C are frequent in Asia. Genotype C is largely present in East and Southeast Asia. Genotype D is widespread in Africa, the Mediterranean region, Europe, and India. Genotype E is limited to West Africa. Genotype F is found in Central and South America. Genotype G has been found in Germany, France, and the United States. Genotype H is found in Central America [107]. Modes of transmission are correlated with the geographic distribution of HBV genotype throughout the world. For example, highly endemic areas have widespread genotypes B and C where vertical transmission is the main mode of infection, whereas areas where horizontal transmission is the main mode of infection, the remaining genotypes were found [108].

In a study conducted in Japan, patients with genotype A have higher persistence of HBV infection as compared to genotype B and genotype C [109]. Delayed HBeAg seroconversion and longer HBV replication period were observed in HBV genotype C [110]. As compared to

genotype B patients, genotype C patients are more prone to advanced fibrosis, cirrhosis, and even HCC [111]. Higher rates of unprompted HBsAg seroclearance was observed in patients with genotype A and B as compared to patients with genotype C and D [112]. Patients infected with genotype C have higher HBV viral load as compared genotype B patients [113]. Several studies have also shown age as the major risk factor for HCC development, younger mean age is associated with higher HCC development in genotype C patients than in genotype B patients [114, 115]. Similar results were observed with genotype D when compared to genotype A in various studies.

**Table 2.1** HBV genotypes along with their distribution pattern

Genotype	Serotype	Geographical Distribution	Genome (bp)	HBV proteins (aa)		
				PreS1	Pol	Core
<b>A</b> (A1-A6)	adw2	Africa, Europe, USA, Australia	3221	119	845	185
<b>B</b> (B1-B9)	adw2, ayw1	South East Asia, China, Japan	3215	119	843	183
<b>C</b> (C1-C16)	adw2,ayr,adrq-,adrq+	South East Asia, China, Korea, Japan, Polynesia, Australia	3215	119	843	183
<b>D</b> (D1-D7)	ayw2,3 and 4	Mediterranean area, Middle East, East Europe, India	3282	108	832	183
<b>E</b> (ND)	adw4	West and Central Africa	3212	118	842	183
<b>F</b> (F1-F4)	adw4q-	Southe America, Central America, Alsaka, Polynesia	3215	119	843	183
<b>G</b> (ND)	adw2	Europe, North America (Coinfection with Genotype A)	3248	118	842	195
<b>H</b> (ND)	adw4	Central America, Mexico, South United States	3215	119	843	183
<b>I</b> (ND)	adw	Vietnam, Laos, India	3215	119	843	183
<b>J</b> (ND)		Japan	3182	108	832	183

ND- No sub-genotypes identified so far



### 2.3.1 Sub-genotypes

Sub-genotypes are described as a divergence of  $>4\%$  (but less than  $7.5\%$ ) in the nucleotide sequence within the complete genome [116]. In HBV, genotypes from A-D and F upto 40 sub-genotypes have been reported [117]. The difference of  $< 4\%$  between sub-genotypes is indicated to be as clades. According to Pourkarim *et. al.* (2014), misclassification of HBV genotypes can be dodged by applying phylogenetic analysis over a full-length genome sequence rather than partial sequence [116].

### 2.4 Epidemiology

According to World Health Organization (WHO), the global epidemiology of HBV is best reviewed among the six regions: Western Pacific, Europe, Eastern Mediterranean, Africa, South-East Asia and the Americas. Every geographical area can then be designated by its endemicity, which is defined as the prevalence of HBsAg in the overall population of that specific geographical area [118]. In addition, the Western Pacific region (defined by the World Health Organization as 37 countries including China, Japan, South Korea, Philippines, and Vietnam) reports for nearly 60% of all HBV infections globally [119]. Prior to implementation of the vaccination program, the Asian-Pacific region was divided into three categories in terms of HBsAg prevalence [120]. Figure 2.4 portrays the high-prevalence ( $>8\%$ ) regions including China, Hong Kong, Taiwan, Korea, Mongolia, Philippines, Thailand, and Vietnam. The intermediate-prevalence ( $2-8\%$ ) regions included central Asia, the Indian subcontinent, Indonesia, Malaysia, and Singapore. Low-prevalence ( $<2\%$ ) regions included Australia and New Zealand, although prevalence has increased in recent years due to immigrants from high-prevalence countries [121].

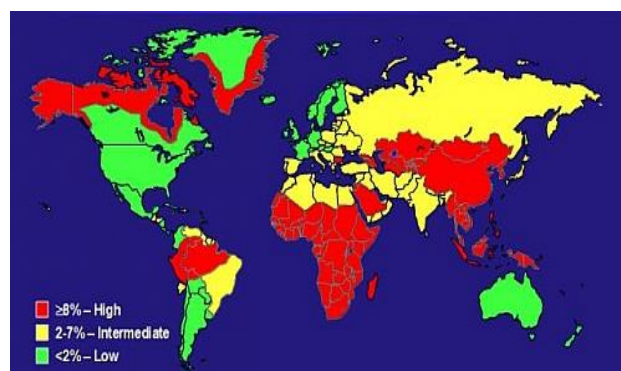


**Figure 2.4** The worldwide geographical prevalence of HBV infection as per World Health Organization (W.H.O).

In India, a study conducted on approximately 8575 pregnant women in 1987 had shown a 3.7% incidence of HBV infection [122], another study of 20,104 pregnant women conducted in 2011 revealed a prevalence of around 1.1%. The precise reasons for the decreased incidence of HBV infection could be the introduction of the HBV vaccination [123]. However, similar to other countries the prevalence of hepatitis B is variable all over India with a gradient of commonly growing prevalence from north to south (**Figure 2.5**). The lowermost prevalence is 2.3% in a larger cohort of 20,000 blood donors in northern India [124] while it was maximum reported as 5.7% in a community-centered study in nearly 2000 people from southern India [125].

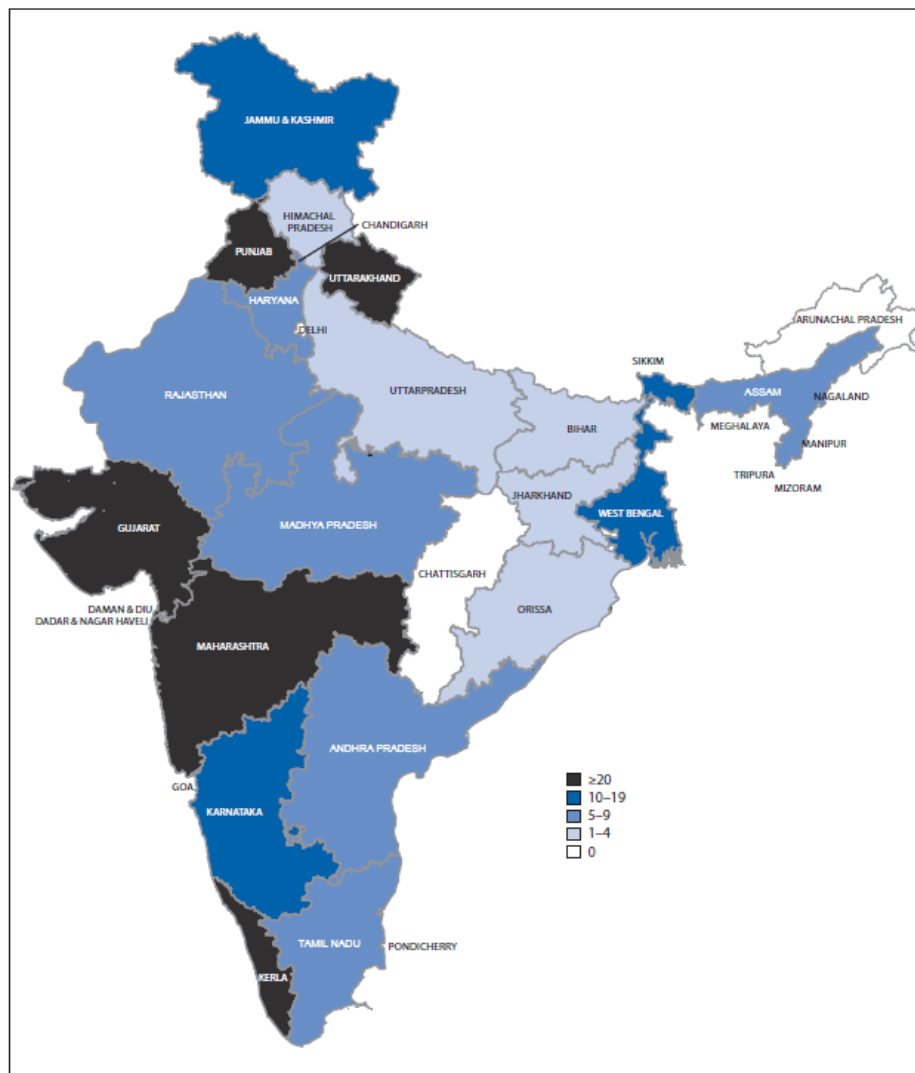


**Figure 2.5** The geographic incidence of HBV across India; representing the number of reported outbreaks (N=291) in the country [126].

## **2.5 Transmission**

Currently, there are four recognized modes of transmission, which include i) prenatal- from mother to child at birth, ii) horizontal- by contact with an infected person, or exposure to blood or other infected fluids, iii) sexual contact, and iv) intra-familial- frequent or household contact with the infected person. There is a considerable variation between areas, countries and continents and the age at which most transmission takes place. The presence of the virus has been detected in a variety of body fluids such as saliva, nasopharyngeal, semen and menstrual blood [127] and the virus has not been detected in feces, probably due to viral inactivation by enzymes within the intestinal mucosa or bacterial flora [128]. One of the most effective routes, which allow the virus to enter an unexposed individual, is through the percutaneous introduction (i.e. needle-stick injuries, etc.) [129]. However, the sexual transmission could range between a mere 1-3% for a single unprotected sexual encounter or increase to 15%-30% due to a regular infected partner [130]. Homosexual men are reported to be at 10-20 times greater risk than the general population [131]. The hepatitis B virus is stable on environmental surfaces for at least a week and an indirect inoculation could occur via inanimate objects or by contact with mucous membranes or bruised skin [132]. The infectious HBV can be present in blood without detectable HBsAg, and the failure to detect the antigen does not exclude the presence of the infectious virus [133].

## **2.6 Clinical stages of HBV infection**

The course of hepatitis B could be extremely variable with different clinical manifestations depending on the patient's age at infection, the immune status and the stage at which the disease is recognized [134]. During the incubation phase of the disease (6 to 24 weeks), the patients feel unwell with possible nausea, vomiting, diarrhea, anorexia, and headaches. Patients then become jaundiced, although low-grade fever and loss of appetite may improve. Sometimes neither jaundice nor obvious symptoms are observed in HBV infection [135]. The asymptomatic cases are generally identified by detecting biochemical or virus-specific serologic alterations in their blood. It is quite likely that they become silent carriers of the virus and constitute a reservoir for further transmission to others [135]. Most adult patients recover completely from their HBV infection, but others (about 5 to 10%) do not clear the virus and progress to become asymptomatic carriers or develop chronic hepatitis, possibly resulting in cirrhosis and/or liver

cancer. Rarely, some patients develop fulminant hepatitis and die [136]. In general, the occurrence of clinical disease rises with age [137]. A small number of long-established chronic carriers apparently terminate their active infection and become HBsAg-negative (about 2% per year) [138]. The four major clinical types of hepatitis are discussed further wherein Figure 2.6 evidently reveals the transformation among different clinical stages.

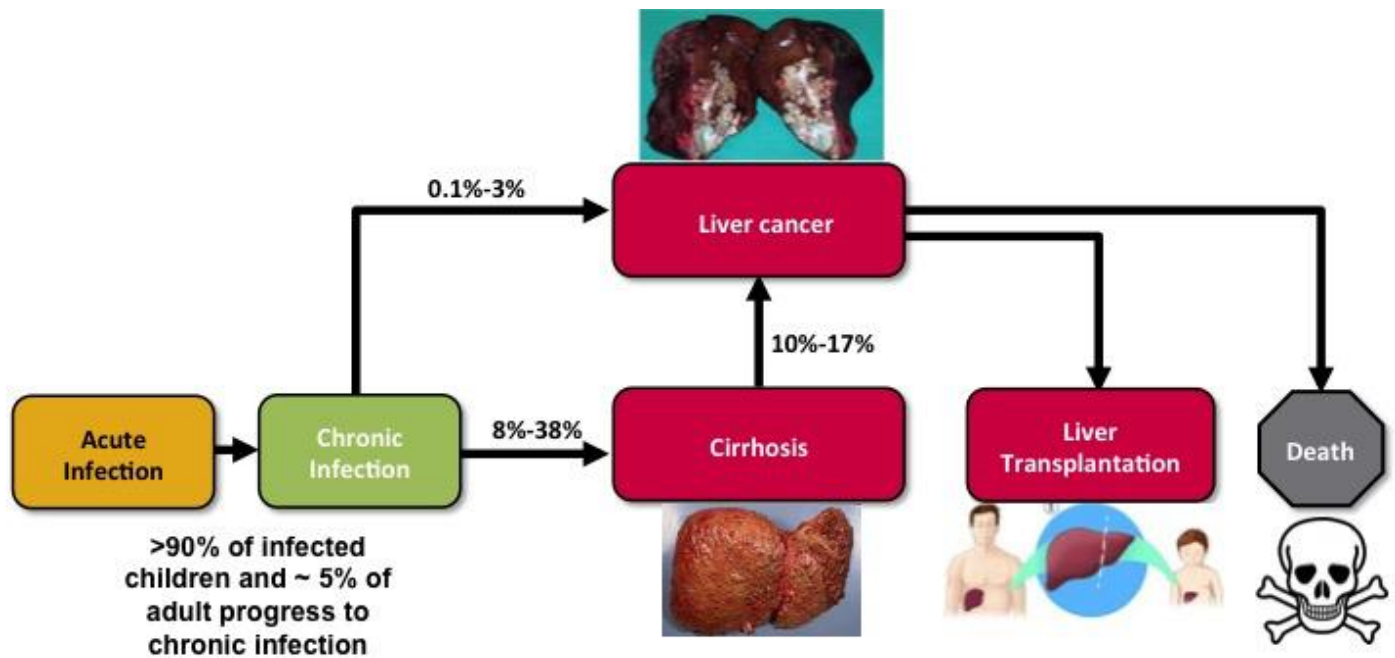


**Figure 2.6** The progression and complications in patients with hepatitis B infection.

### 2.6.1 Acute Hepatitis

The clinical course of HBV runs similar to that of Hepatitis A Virus (HAV) but tends to be more severe, at times associated with the serum-sickness-like syndrome [139]. The mildest attacks are asymptomatic and are detectable only by an increase in serum transaminase levels. Alternatively, the patient may be anicteric with gastrointestinal and influenza-like symptoms. These patients are likely to remain undiagnosed unless a clear history of exposure is available. The severity of infection varies from the symptomatic and icteric (from which recovery is typical) to fulminant and fatal viral hepatitis. Icteric attacks in adults are marked by a prodromal period (typically 3-4 days extending up to 2-3 weeks) during which a patient feels sick, suffering from digestive symptoms such as anorexia and nausea and may, in the later stages, have mild pyrexia. Other common symptoms are rigors, mild pyrexia, loss of desire to drink alcohol or smoke, malaise,

and occasionally severe headaches. The prodromal period is followed by the darkening of urine and lightening of feces, followed by the development of jaundice [140].

### **2.6.2 Chronic hepatitis B (CHB)**

Although most adult patients recover completely from an acute episode of hepatitis B, in a significant proportion of 5 to 10%, the virus persists in the body and become chronic carriers. This figure is much higher in children: 70 to 90% of infants infected in their first few years of life become chronic carriers of HBV [141]. Surprisingly, some of the patients infected persistently might have no clinical or biochemical evidence of liver disease. Chronic hepatitis B is a prolonged (>6 months) infection with persistent serum levels of HBsAg and IgG anti-HBcAg and the absence of an anti-HBsAg antibody response. HBV DNA and HBeAg are often detectable at high concentrations but may disappear if viral replication ceases or if mutations occur; preventing the synthesis of the viral pre-core protein precursor of HBeAg. The associated inflammatory liver disease is variable in severity. It is always much milder than in acute hepatitis B, but can last for decades and proceed to cirrhosis, and is associated with a 100-fold increase in the risk of developing a hepatocellular carcinoma [142].

### **2.6.3 Fulminant Hepatitis**

This is a rare form of the disease, which usually overwhelms the patient within 10 days. This form develops so quickly that the jaundice is inconspicuous and the disease may be confused with acute psychosis or meningoencephalitis. The foreboding signs could be repeated vomiting, fetor hepaticas, confusion, and drowsiness. The 'flapping' tremor may only be transient, but rigidity is usual. The serum bilirubin and transaminases are poor prognostic indicators as transaminase levels may actually decrease as the patient's clinical condition worsens [143]. Prothrombin is the best indicator of prognosis. The frequency of the fulminant course varies depending upon the type of viral hepatitis and prevalence of hepatitis B carriage [144].

### **2.6.4 Hepatocellular Carcinoma (HCC)**

Hepatocellular carcinoma (HCC) is the third leading cause of cancer-related deaths and sixth most common cancer worldwide [145]. There is an alarming increase in the incidence and mortality of rates for HCC, particularly in eastern/south-eastern Asia and in Africa [146]. HCC

prognosis is strongly correlated with the diagnostic delay. To date, no ideal screening modality has been developed for HCC.

## **2.7 Biochemical markers**

Laboratory evaluation of hepatitis B usually consists of liver enzyme tests, including levels of alanine aminotransferase (ALT) and/or aspartate aminotransferase (AST), alkaline phosphatase (ALP), and gamma-glutamyl transpeptidase (GGT), as well as liver function tests (LFTs) that include total and direct serum bilirubin, albumin, and measurement of the international normalized ratio (INR) [147]. Hematologic and coagulation studies also include a platelet count and a complete blood count (CBC). Ammonia levels may be obtained, but the results often create diagnostic confusion in clinicians [148]. Serum transaminases, considered to be sensitive and specific markers of liver disease can be affected by stage of the HBV infection. That's why there are limitations of its use as an independent diagnostic marker. Increased levels of serum transaminase in association with the levels of HBV DNA are evocative of CHB infection. The prediction of the severity of HBV infection to fibrosis at the end has been correlated with the combinations of the serum markers present [149, 150].

## **2.8 Serological markers for HBV**

The HBV infection can be easily diagnosed by a variety of serological markers. During the infection, these markers vary depending on whether the infection is acute or chronic and these are identified as follows:

### **2.8.1 Hepatitis B surface antigen (HBsAg)**

HBsAg can be detected in the serum several weeks before the onset of symptoms, which can last for months after onset. HBsAg is present in serum during the acute infections and persists in chronic infections. In fact, in some chronic cases, HBsAg is spontaneously removed after long persistence. The presence of HBsAg indicates that the person is possibly infectious [151]. It is useful for the diagnosis of HBV infection and screening of blood. Recently, an MI3 phage, PHH2, was isolated which had the ability to bind HBsAg. The HBsAg binding phage was used in an assay referred to as "PHALISA", an abbreviation for Phage-Linked Immune-Sorbent assay.

This assay was at least 20-100 times more sensitive in the detection of HBV antigen than conventional enzyme-linked immune-sorbent assay (ELISA) [152].

### **2.8.2 Anti-HBsAg**

This is the specific antibody to hepatitis B surface antigen. Its appearance in 1 to 4 months after the onset of symptoms indicates clinical recovery and subsequent immunity to HBV. Anti-HBs can neutralize HBV and provide protection against HBV infection. The anti-HBs replaces HBsAg as the acute HBV infection is resolving. Anti-HBs generally persists for a lifetime in over 80% of patients and indicates immunity [153, 154].

### **2.8.3 Hepatitis B core antigen (HBcAg)**

Hepatitis B core antigen is derived from the protein envelope that encloses the viral DNA, and it is not detectable in the bloodstream. An immune response is induced when HBcAg peptides are expressed on the surface of hepatocytes, which is crucial for killing infected cells [155]. The HBcAg is an accurate index of active viral replication [156].

### **2.8.4 Anti-HBcAg**

It is the first antibody to appear on HBV infection and is the specific antibody of core antigen. The antibodies related to HBcAg belong to IgM and IgG class. The presence of IgM identifies an early acute infection [157]. During the acute infection, IgM anti-HBc is present in high titer and it usually disappears within 6 months [158]. An absence of HBsAg and anti-HBs suggests a recent infection. IgG with no IgM type antibodies may be present in chronic as well as the resolved type of hepatitis and generally remains detectable for a lifetime.

### **2.8.5 Hepatitis B precore antigen (HBeAg)**

HBeAg appearing during weeks 3 to 6 indicates an acute active disease related with higher viral replication. Progression to chronic infection is indicated by the presence of this virological marker beyond 10 weeks. The constant presence of anti-HBe specifies chronic liver disease [141].

### **2.8.6 Anti-HBeAg**

This is the specific antibody to HBeAg. For the resolution of infection at acute stage, seroconversion from e antigen to anti-e antibody acts as a prognostic marker [159]. In the absence of HBsAg, anti-HBs and core HBV mutants, if anti HBeAg is present along with anti-HBc in the blood then it is said to be less contagiousness and convalescence recovery. Anti-HBe appears after anti-HBc and its presence correlates to a decreased infectivity [160].

### **2.8.7 Hepatitis B x antigen (HBxAg)**

Hepatitis B x antigen is detected in HBeAg positive blood in patients with both acute and chronic hepatitis [161]. HBxAg is reportedly involved in transcriptional regulation [135]. It has also been well reported that autophagy is induced by HBV through the HBx protein [162]. The enzymatic activity of PI3KC3 was also increased, which mediates PI3P formation further enhancing autophagosome formation [63].

### **2.8.8 HBV DNA**

The HBV DNA is detectable by hybridization assays or Polymerase chain reaction (PCR) one week after initial infection. The tests are generally performed for monitoring the antiviral treatment or to detect mutants that escape detection by current methods [163].

These serological markers are vital in determining the characterizing stage of HBV infection whereas the genome level understanding is also vital in inferring suitable therapeutic interventions. The genome-wide association studies (GWAS) or whole genome association studies (WGA) has gained immense attention in recent past as it stipulates the channel for determining the genetic variants and its association with diseases.

## **2.9 Genome-Wide Association Studies**

Many phenotypes are quantitative in nature, and multifaceted in etiology, with several environmental and genetic reasons [164]. In recent days, linkage disequilibrium (LD) based GWAS is utilized in humans to map modern complex diseases [165]. The GWAS is an investigational design used to identify associations between the genetic variants and traits in desired populations [166]. The key goal is to better understand the biology of disease, beneath



the hypothesis that a better understanding will lead to prevention or better treatment. The trail from GWAS to biology is not so straightforward because an association between a genetic variant and a trait is not directly informative [167]. GWAS have also been productively put into practice for better defining the relative role of genes and the environment in disease risk, supporting in risk prediction (allowing preventative and personalized medicine), and exploring natural selection and population differences.

A number of steps are critical for an effective GWAS as depicted in Figure 2.7, which comprises of a well distinct cohort of cases, suitably matched controls, quality control evaluation of samples and genotyping data. Data analysis should be corrected for multiple hypotheses testing with a  $p$ -value mandatory for statistical significance of associations usually set at less than  $5 \times 10^{-8}$ . Since the  $p$ -value cut-off is merely 'statistical', a number of optional analytical approaches have been developed including pathway-based approaches and network analyses whereby the biological role of genes is assessed alongside its statistical association [168].

Regardless of the analytical approach, all GWAS results necessitate replication and should be validated additionally by the measurement of proteins, gene expression or function [169]. The replication studies should have adequate sample sizes to detect the effect. Confidence in the result is increased if the effect is observed from the same SNP or another SNP in high LD with the candidate SNP and is in the same direction [166].

Now a days, linkage disequilibrium based GWAS is in trend for mapping modern complex trait in humans [170]. GWAS involves correlating allele frequencies with trait variation in a population-based sample studies [171]. One of the major advantages of the GWAS approach is that it is unbiased with respect to genomic structure and previous knowledge of the trait etiology, in contrast to candidate gene studies, where knowledge of the trait is used to identify candidate loci contributing to the trait of interest. Therefore, the results obtained from GWAS holds the promise to disclose the role of causal genes which are not previously suspected in disease etiology [172].

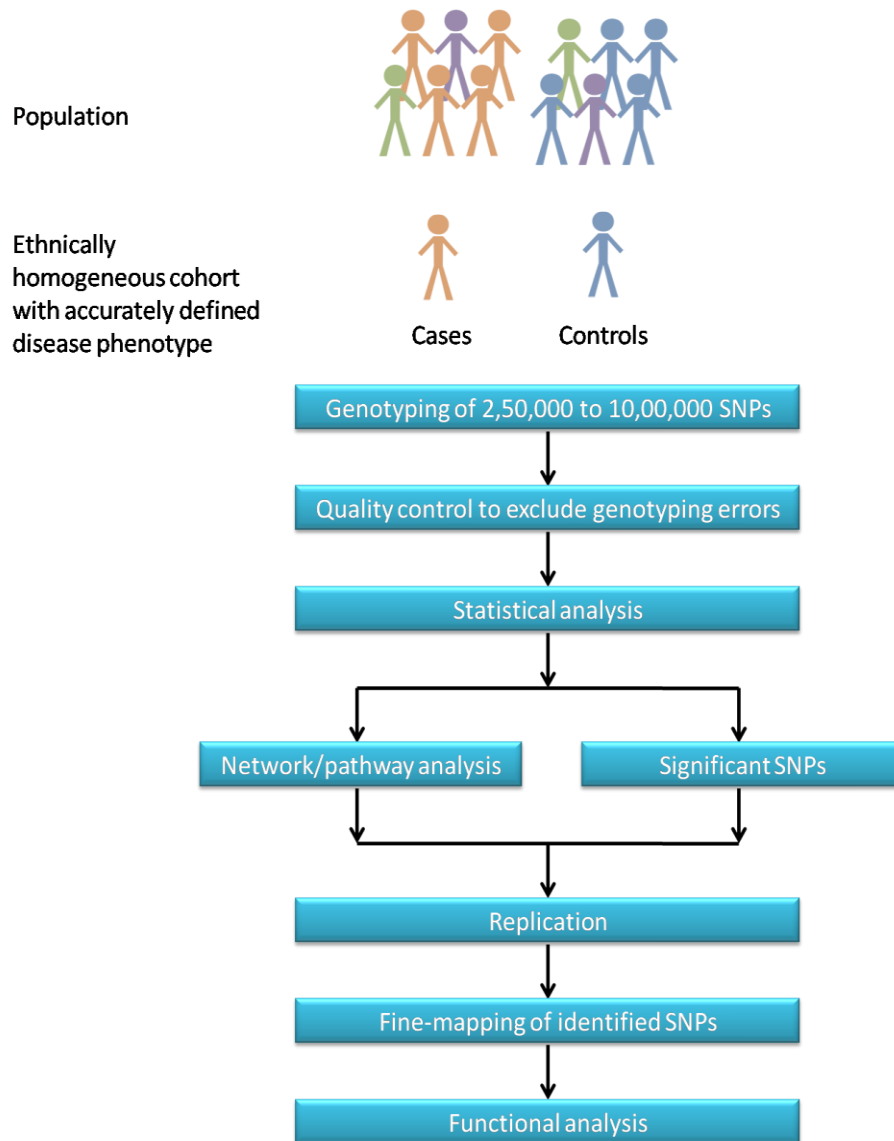


**Figure 2.7** Overview of the genome-wide association studies.

### 2.10 Candidate gene approach

Candidate gene studies have been at the first place of genetic association studies i.e. to point out the risk variants associated with a particular disease. The advantage of candidate gene approach over GWAS is that it is relatively cheap, quick to perform and are focused on the selection of genes that have been in some way related to the disease previously and thus come with prior knowledge about gene function. This approach initiates with the selection of putative candidate gene according to its relevance in the disease being investigated [173]. This is pursued by considering and selecting polymorphisms which are having a functional consequence, either by

affecting gene regulation or its protein product [174]. The underlying principle of these studies is that the SNPs under examination detain information about the causal genetic variability of the gene under consideration, though the SNPs may not serve as the true disease-causing variants. Ultimately, the gene variant is confirmed for disease association by scrutinizing its occurrence in random test subjects (cases) having the disease and the selected healthy control subjects which do not have the disease; and is then assessed for its association with disease prognosis and diagnosis and its future potential as a biomarker. This makes the knowledge derived from candidate gene approach precious and clinically pertinent as a prospective disease diagnostic tool and for personalised medicine initiatives in future treatments of genetic disorders [175].

## **2.11 Candidate gene approach/GWAS and infectious diseases**

Candidate gene approach/GWAS have been used to characterize the genetic architecture of susceptibility to common infections and of response to vaccination. The largest body of data in this area comes from candidate gene studies for infection with bacterial, viral, fungal, and parasitic pathogens.

### **2.11.1 Malaria**

Malaria is transmitted by female Anopheles mosquitoes, which carry parasites of Plasmodium spp. (*P. falciparum*, *P. vivax*, *P. ovale*, *P. malariae*, and *P. knowlesi*) [176]. The initial GWAS in the case of malaria has been studied in association with hemoglobin subunit beta (HBB) gene [20]. Later, GWAS proceeded with more genes associated with more severe malaria and was replicated in ATPase Plasma Membrane Ca<sup>2+</sup> Transporting 4 (*ATP2B4*), *16q22*, *ABO* and CD40 Ligand (*CD40LG*) [177-179]. A recent study of severe malaria with 5291 controls and 5130 cases have identified a novel highly significant SNP (rs184895969) flanked by FRAS1 Related Extracellular Matrix 3 (*FREM3*) and genes encoding receptors which code *P. falciparum* (*GYP A*, *GYP B*, *GYP E*). A haplotype at this locus showed protection against severe disease (OR = 0.67, 95% CI, 0.60–0.76, p-  $9.5 \times 10^{-11}$ ) [180].

### **2.11.2 HIV and AIDS**

Susceptibility to HIV-1 infection and the disease progression are the different phenotypes, which have been examined via host genetic studies using both candidate-gene and genome-wide

strategies [181, 182]. Both candidate-gene and genome-wide strategies have inspected a range of diverse phenotypes, including susceptibility to the HIV-1 acquisition, viral load following infection, and disease progression. Various robust associations between HIV-1 phenotypes and polymorphisms have been identified with various genes like the chemokine receptor 5–chemokine receptor 2 (*CCR5–CCR2*) locus [183, 184], the human leukocyte antigen (*HLA*) class I region [185, 186] and killer immunoglobulin-like receptor (*KIR*) loci [187]. The first reported GWAS of this infectious disease in European ancestry identified *HLA* SNPs (rs2395029 and rs9264942) that were extremely associated with the viral load during the asymptomatic period of HIV-1 infection [19].

### **2.11.3 Meningococcal disease**

In 2010, the first GWAS for meningococcal disease (MD) was reported where 475 disease cases from the UK and 4703 controls were included which identified 79 SNPs with significance [23]. The results were replicated first in 553 Western European cases and 839 matched controls, where two highly significant SNPs in complement factor H (*CFH*) were identified in a combined analysis, further this study was replicated in a second cohort from Spain of 415 cases and 537 controls. Individuals carrying the minor allele were protected against the disease with a relative risk of ~0.6 as compared to the individuals carrying wild-type allele. An additional study identified three SNPs, which have genome-wide significance in a mutual analysis in the neighboring gene *CFHR3*. All SNPs decline disease susceptibility for carriers of the minor allele.

### **2.11.4 Kawasaki disease**

Several GWAS have been performed on Kawasaki disease (KD), a systemic vasculitis of unknown etiology. The first GWAS study on KD was completed in Dutch Caucasian population using a case-control design [24]. The study was replicated further with 2173 cases and 9383 controls using a case-control and family-based plan. The confirmed results included a functional SNP in *FCGR2A*, an SNP near *MIA* and *RAB4B*, and an SNP in *ITPKC* gene. The SNP in *FCGR2A* association was replicated in a Japanese cohort of 428 cases and 3379 controls, jointly with two replication studies including 754 cases and 947 controls [188]. The genes recognized in these GWAS clearly contribute to disease occurrence and propose that KD is activated by

environmental factors or infectious agents in children whose immune system is genetically determined to react in a different way when matched up to unaffected children.

### **2.11.5 GWAS and Hepatitis B Virus**

Various GWAS have been reported in association with HBV infection, its progression, and recovery. A GWAS recognized sturdy associations among variants in HLA-DPA1 and HLA-DPB1 in the HLA class II region and protection against chronic HBV infection in an Asian population [25]. This study was replicated and further studies have confirmed the findings and suggest that these variants are associated with the HBV clearance [189-191]. These variants possibly will also influence HLA mRNA expression levels, and lower expression of HLA-DPA1 and HLA-DPB1 has seen to be related to an increased risk of chronic HBV [192]. Another GWAS of HLA-DPA1 and HLA-DPB1 genes followed by a replication analysis using samples from HBV carriers and spontaneously HBV-resolved individuals as well as healthy controls in Japanese and Korean population has demonstrated that these genes were considerably associated with defensive effects against CHB [193]. Apart from vast studies from Asia, few studies have also been reported that looked at an association between HLA-DP variants and constant HBV infection in non-Asian countries [194-196]. A Korean group found two novel variants in the euchromatic histone-lysine-methyltransferase 2 (EHMT2) gene and transcription factor 19 (TCF19) that were associated with susceptibility to chronic HBV infection [197]. Recently, sodium-taurocholate cotransporting polypeptide (NTCP), which is encoded by SLC10A1, has been shown to be a well-built cellular receptor for HBV and hepatitis D virus [198]. Further *in-vitro* investigation of SLC10A1 variant (rs2296651) resulted in loss of HBV-receptor function [199]. Recently, ULK1 (autophagy initiating gene) has been intensively studied and found to be associated with HBV infection, which promotes autophagy in hepatocytes *via* the activation of ULK1 [200]. Autophagy promotion is suggested to help the HBV replication and the inhibition of hepatocyte autophagy might be a new target for HBV infection [55, 64].

### **2.12 Autophagy**

Autophagy (*auto-phagin* from Greek meaning ‘Self-Eating’) is a cellular catabolic degradation pathway which gets activated in response to starvation or stress in which cellular proteins, organelles, and cytoplasm are engulfed, degraded and recycled to maintain cellular metabolism.

There are three major types of autophagy in eukaryotes: chaperone-mediated autophagy (CMA), microautophagy and macroautophagy [201].

### **2.12.1 Chaperone-mediated autophagy (CMA)**

It is known to be associated with higher eukaryotes. It involves a direct translocation of cytosolic proteins across the lysosomal membrane [202]. Proteins containing a pentapeptide motif (KFERQ or similar sequences) are recognized by Hsc70, which facilitates protein unfolding and delivery of the protein to the CMA receptor lysosome-associated membrane protein type-2A (LAMP2A), a lysosomal membrane protein [203]. CMA is dynamic in cells under basal circumstances but it is excellently triggered in retort to stressors like oxidative stress, hypoxia, DNA damage and prolonged starvation [204]. The CMA activity is coordinated with other autophagic pathways and even with the ubiquitin/proteasome system. Thus, cells retort to obstruction of CMA both *in vitro* and *in vivo* by enhancing macroautophagy and the ubiquitin/proteasome system [205].

### **2.12.2 Microautophagy**

It is characterized mainly in yeast and is the process by which cytoplasmic material become sequestered through a direct invagination of the vacuole membrane [206]. It is generally thought that microautophagy accounts for the basal rate of intracellular protein degradation in normal non-stimulated conditions, though later discoveries in yeast showed that this pathway can also be induced by various conditions [207]. Microautophagy has the capacity to sequester large structures such as entire organelles through both selective and non-selective mechanisms [208]. Moreover, certain cargo, e.g. mitochondria can be degraded both by micro- and macroautophagy, but how this selectivity is regulated is not known [57]. Very recently, a microautophagy-like process was characterized in eukaryotic cells, involving delivery of cytosolic materials to the intraluminal vesicles of late endosome/multivesicular bodies (MVBs) in an ESCRT (Endosomal sorting complex required for transport)-dependent manner [209].

### **2.12.3 Macroautophagy**

Hereafter referred to simply as autophagy, is the best characterized form of autophagy. It was first identified and characterized in mammalian cells by electron microscopy (EM) studies [210].

This process (**Figure 2.8**) involves nucleation of a membrane, named the phagophore or isolation membrane (IM), which expands to form a double-membrane vesicle called the autophagosome. The autophagosome either fuses directly with the lysosome or with endocytic vesicles, generating an amphisome that eventually fuses with the lysosomal compartment resulting in the formation of an autolysosome where the sequestered material becomes degraded by lysosomal hydrolases [211].

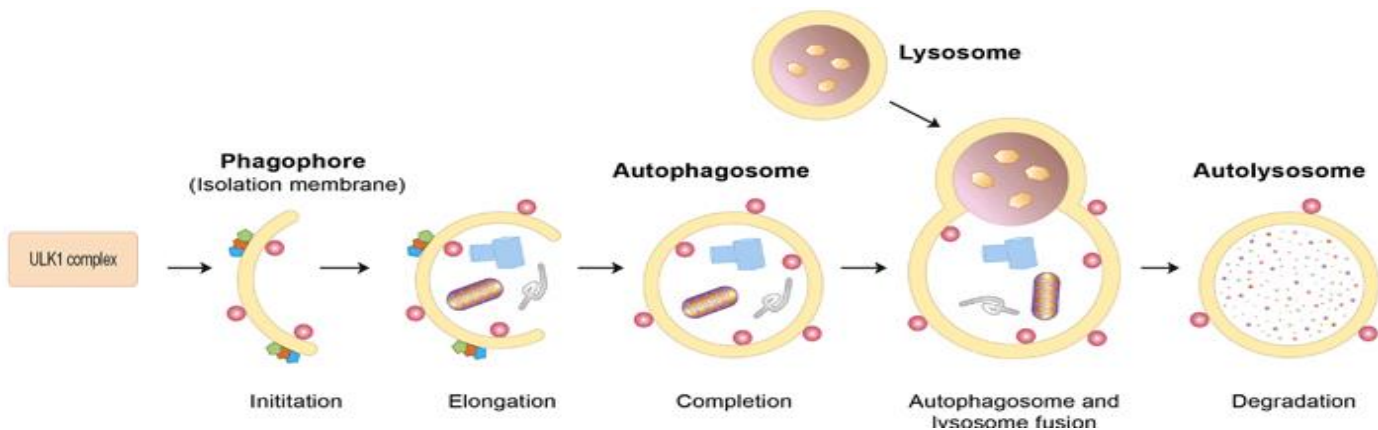


**Figure 2.8** Schematic representation of autophagy.

### 2.13 Autophagy Machinery

The discovery of Atg genes initiated an exciting era in research and has provided a growing understanding of the complex process of autophagy and its role in various physiological and pathological conditions, including starvation responses, anti-aging, immunity, differentiation, lipid metabolism, development and protection from cell death [212]. Furthermore, autophagy is associated with various diseases, including cancer, neuro-degeneration (clearance of intracellular aggregate-prone proteins) and infectious diseases (removal of pathogens) [213]. However, there is still much to be learnt about the mechanism underlying autophagy, a process that can be broken down into several steps; (A) induction, (B) nucleation, (C) expansion and (D) maturation. Our current understanding of each step will be described in below.

#### 2.13.1 Induction

Autophagy can be induced by several conditions, including nutrient limitation (starvation), energy depletion and lack of growth factors (insulin/IGF) [214]. It can also be stimulated by numerous cellular stressors such as heat and oxidative stress. It is still uncertain that how many

major signaling pathways controlling autophagy directly affect autophagy, while it is clear that the mammalian target of rapamycin (*mTOR*) plays a key role in integrating several signals as demonstrated in **Figure 2.9** [215]. Inhibition of *mTOR* leads to activation of autophagy likely through the release of *mTOR*-mediated inhibitory phosphorylation of Atg1 orthologues (*ULK-1/2*) in mammalian cells [216]. The class I PI3K inhibits autophagy through activation of *mTOR*, whereas the activity of class III PI3K/*Vps34* is required for induction of autophagy. Identification of the inhibitory action of 3-methyladenine (3-MA), provided the first evidence for a regulatory effect of protein kinases and phosphatases in autophagy and it was later found that 3-MA is a PI3K inhibitor [217].

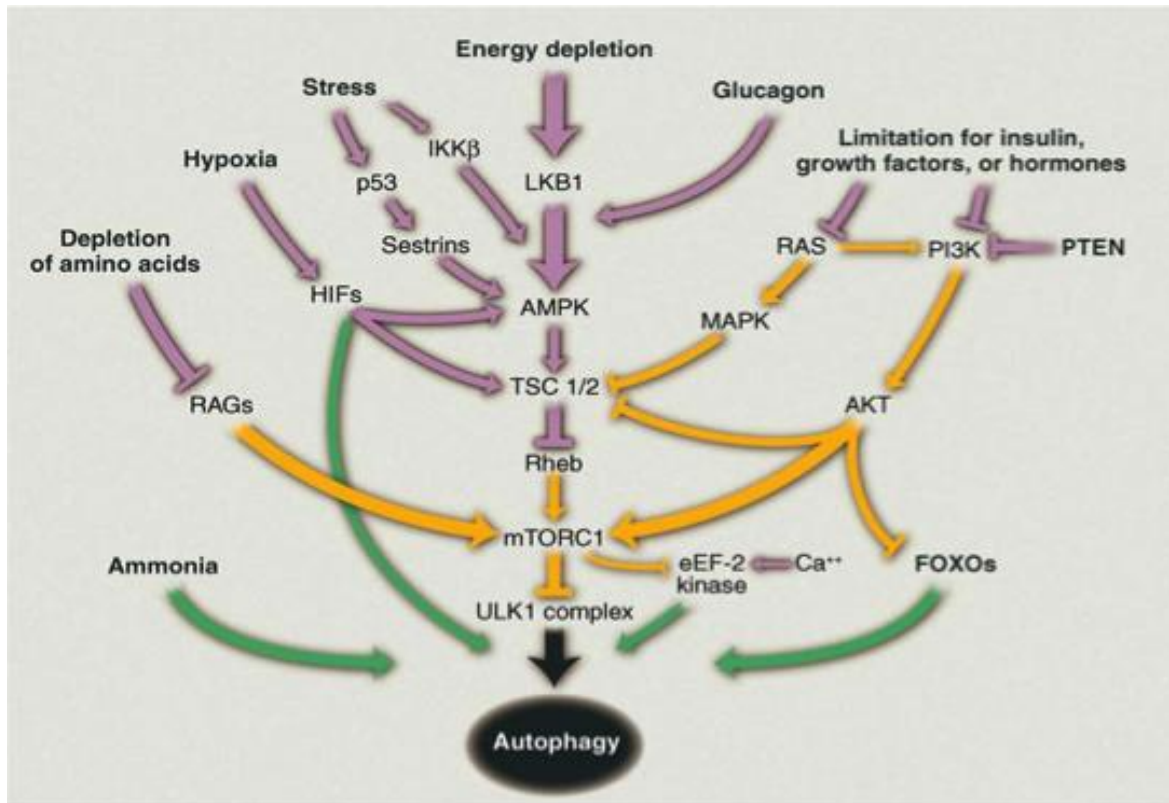


**Figure 2.9** Regulation of autophagy via signaling pathways, hormones, growth factors and stress conditions. Here, purple and yellow lines depict events that positively and negatively regulate autophagy. The green lines portray pathways that are *mTOR*-independent. (IKK $\beta$ , an inhibitor of nuclear factor  $\kappa$ B kinase  $\beta$ ; PI3K, phosphatidylinositol-3 kinase; PTEN, phosphatase and tensin homolog; MAPK, mitogen-activated protein kinase; TSC1/2, tuberousclerosis complexes 1 and 2; and EF, elongation factor) [218].



### **2.13.2 Nucleation**

Ever since the discovery of autophagy, the exact source of the autophagosomal membranes has been under deep discussion [219]. In mammalian cells, autophagy is initiated by the formation and elongation of the phagophore/isolation membrane (IM) [220]. In yeast, the IM arises from the pre-autophagosomal structure (PAS), whereas the IM in mammalian cells has been recommended to arise in different areas of the cytoplasm [221]. In yeast, Atg9 is transported to the PAS from a compartment to the mitochondria and as Atg9 is required for PAS formation, it is likely that it mediates transport of the lipids required to create this structure [222]. The sorting mechanism for the shuttling of Atg9 from mitochondria to the PAS is unknown but seems to require actin. mAtg9, however, cycles from the trans-Golgi network (TGN) to a peripheral Rab7-positive endosomal pool and is present on autophagosomes after starvation, in a Unc-51-like kinase (ULK1) -dependent manner [223]. The yeast ULK1 homologue, Atg1, is also responsible for the recruitment of other Atg proteins to the PAS. The role of Atg1/ULKs in autophagy induction has not yet been properly characterized, however, the activity of ULK kinase increases during starvation, and kinase-dead mutants of ULK exert a dominant negative effect on autophagosome formation [65].

### **2.13.3 Expansion**

The process of membrane elongation and completion to form the autophagosome requires two ubiquitin-like proteins Atg12 and Atg8 and their conjugation systems [224]. The Atg12-Atg5 conjugate associates with a small coiled-coil membrane-bound protein, Atg16L (an ortholog of yeast Atg16), to form an Atg12-Atg5-Atg16L complex [225]. Atg16L directs the Atg12-Atg5 complex to the IM, and this complex has been proposed to work in an E3-like mode for the conjugation of LC3 [226]. The Atg12-Atg5-Atg16L complex also determines the sites of LC3 lipidation. Before conjugation to PE, the carboxy-terminal residue of LC3 is cleaved off by the cysteine protease Atg4, exposing a critical Glycine residue at the C terminus which becomes covalently conjugated to PE [227]. Soluble LC3 is called LC3-I whereas the membrane bound, autophagosome associated form is referred to as LC3-II. LC3 can mediate membrane tethering and may contribute to autophagosome membrane expansion. LC3 might also assist the final fusion to close the autophagosome, a poorly understood step [228].

### 2.13.4 Maturation

After the final closure of the autophagosome, it matures by fusion with endocytic compartments, creating amphisomes, and prior to fusion with lysosomes, creating the autolysosome in which the cargo is degraded [229]. Several factors have been reported to be important for the convergence of autophagic and endocytic vesicles, such as coat protein complex I (COPI) and ESCRT. COPI is found at early endosomes which function as a sorting station for the endocytic cargo, whereas ESCRTs are required for the formation of MVBs and sorting of endocytic cargo targeted for lysosomal degradation into MVBs [230]. Recently, the endosomal PI3P 5-kinase has been shown to be involved in maturation, indicating that also endocytic membrane lipids are important for proper autophagosome maturation [231]. In mammalian cells, the fusion of autophagosomes with lysosomes is facilitated by microtubules and seems to require dynein, structures which are not required for fusion of yeast autophagosomes with the vacuole [232]. Interestingly, the Rab7, PI3P, and LC3 binding protein FYCO1 were found to promote microtubule plus end directed transport of autophagosomes, thereby connecting transport of autophagosomes to the fusion with lysosomes [233].

## 2.14 The autophagy-regulating kinase ULK1

### 2.14.1 ULK-family kinases - Atg1-homologs in higher organisms

Atg1 is a serine/threonine kinase initially recognized in genetic screens for autophagy genes in *S. cerevisiae* [234]. The orthologs related to this gene have been found in all higher eukaryotes; based on the Atg1-relative in *C. elegans*, Unc-51, they are referred to as Unc-51 like kinases (ULKs) [235]. In mammalian cells, two clear Atg1-orthologs are present, the kinases ULK1 and ULK2. Both genes are ubiquitously expressed, although their relative abundance differs among various tissues [236]. Like Atg1, ULK1/2 are composed of three modular regions, an N-terminal kinase domain, followed by a serine/ proline rich spacer region, and a C-terminal region [65]. The alignment of Atg1 and its mammalian and *Drosophila* orthologs shows a high degree of homology for the kinase domain with some conservation at the C-terminus. The ULK1 and ULK2 share 55% overall identity on the protein level and 78% identity in their kinase domains, including residues in the conserved T-loop activation domain [65]. ULK1/2 forms a unique family in the human genome, together with three more distantly related kinases, ULK3 and ULK4 [237]. Sequence conservation between these three kinases and ULK1/2 is limited to the

kinase domain and excludes the regulatory spacer and C terminal regions, which are important for ULK1/2-function, suggesting that the cellular role of ULK3/4 differs from that of ULK1/2 [238].

### **2.14.2 Cellular functions of Atg1/ULKs**

Atg1 was first described in yeast as a critical regulator of autophagy induction, whereas its *C. elegans* ortholog, Unc-51 (uncoordinated-51) was originally identified as an axonal guidance mutant [239] only later, it was also shown to be required for dauer-formation, a specialized autophagy-related developmental stage entered in response to an unfavorable environment [240]. Both, the role in autophagy and that in neuronal processes are conserved up to mammals, and ULK1, as well as ULK2, have been shown to function in either context, although ULK1 has been studied to a greater extent [241]. ULK1 and ULK2 are required for fiber formation in cerebellar granular neurons and regulate filopodia extension and axon-branching of sensory neurons by non-clathrin-coated endocytosis [242]. A role in autophagy has been clearly determined for ULK1, yet, in the case of ULK2, contradictory findings were reported [65].

### **2.14.3 Regulation and role of Atg1/ULK1 in autophagy**

With regard to their function during autophagy, yeast Atg1 and mammalian ULK1, together with their complex partners (m) Atg13 and Atg17/FIP200 display common features but also major differences [243]. First, both the proteins are the most upstream component of the autophagy machinery and to receive inputs from multiple regulatory signaling pathways, i.e. the (m)TOR and the PKA-pathway, atleast in yeast [244]. In either case, the signal transferred to Atg1/ULK1 is inhibitory. When mTOR or PKA are suppressed, Atg1/ULK1 is depressed and further initiates autophagy. Yet, the mechanism of autophagy induction by Atg1/ULK1 is not well understood. To date, only two substrates have been described for ULK1, besides from its associated proteins mAtg13 and FIP200 namely the focal adhesion protein Paxillin and the class III PI3-kinase complex subunit Ambra 1 [245]. However, the mechanism by which Paxillin regulates autophagy remains to be elucidated, and Ambra 1 is not conserved in yeast, suggesting that Atg1/ULK1 phosphorylates additional Atg-proteins [245]. It should be noted that the requirement for Atg1/ULK1 for autophagy induction seems to be general and independent to the inducing stimulus. Second, Atg1 and ULK1 regulate the trafficking of (m)Atg9 to the peripheral

compartments [246]. Yet, the precise mechanism for this has not been elucidated until now. Third, full activation of Atg1 and ULK1 requires their binding partners (m)Atg13 and Atg17/FIP200, further increasing kinase activities (although only moderately in mammalian cells) upon starvation. Furthermore, (m)Atg13 enhances the interaction of Atg1/ULK1 with Atg17/FIP200 [247].

On the other hand, regulatory and functional differences between Atg1 and ULK1 have been reported, indicating that certain findings in one organism are not readily transferable to others. First, in yeast, hyperphosphorylation of Atg13 by TOR under nutrient-rich conditions prevents its binding to Atg1, which occurs only with the nutrient deprivation and dephosphorylation of Atg13 [248]. A direct interaction between TOR and the Atg1-complex has not been demonstrated. Mammalian ULK1 however, is constitutively associated with mAtg13, Atg101, and FIP200 [249]. Under the nutrient rich conditions, mTORC1, via raptor, also binds to ULK1 and directly phosphorylates not only to mAtg13 but also to ULK1 itself. Upon starvation, mTORC1 dissociates from the ULK1-mAtg13-Atg101-FIP200-complex and ULK1 phosphorylates mAtg13 and FIP200 [250]. Second, the kinase activity of yeast Atg1, although increased with starvation, which is not required for initial recruitment of other Atg-proteins, including Atg8, to the PAS but only for subsequent membrane extension and dissociation of these Atg-proteins from the PAS [251]. This suggests that Atg1 itself acts as a scaffold. One exception is Atg2, which localizes to the PAS, in an Atg1-kinase-activity-dependent manner [252]. In contrast, ULK1-kinase activity is also required for the localization of Atg8-homolog LC3 to the isolation membranes [253]. Third, in yeast, the interaction of Atg1 and Atg17 seems to be completely dependent on Atg13, whereas ULK1 also directly binds to FIP200, although this association is enhanced by mAtg13 [254]. Furthermore, studies in yeast also demonstrated additional regulatory influences on the Atg1-complex that have not yet been examined in mammalian cells. In particular, Atg1 and Atg13 can be phosphorylated by PKA, which prevents the localization of these proteins to PAS [255]. Moreover, Atg1 has been shown to phosphorylate its own activation loop upon exposure to pro-autophagic stimuli, and this event requires Atg13 and Atg17, which is essential for initiation of autophagy [256].

### 2.15 Mechanism of HBV-induced autophagy

The HBV has exhibited to induce autophagy *in vitro*, in the liver of transgenic mice that carry the entire HBV genome, during natural infection [63, 67]. However, different mechanisms regarding how HBV induces autophagy have been proposed [257]. It has been reported that the HBV X protein (HBx), a regulatory protein, could activate the Beclin-1 promoter to induce the expression of Beclin-1, which can further activate the PI3KC3 complex [162]. This induction of Beclin-1 by HBx enhanced autophagy when cells were nutrient starved (**Figure 2.10**) [68]. In a separate study, Sir *et al.* did not observe the induction of Beclin-1 by HBV or the HBx protein. However, they found that HBx, whether by itself or when it was expressed from the HBV DNA genome, could bind to and activate PI3KC3 [63]. This activation of PI3KC3 led to the production of a high level of phosphatidylinositol-3-phosphate (PtdIns(3)P) in cells and an increased amount of autophagic vacuoles including autophagosomes and autolysosomes [258]. Interestingly, this increase of autophagic vacuoles by HBx did not lead to an increase of the autophagic protein degradation rate, suggesting that the increased amount of autophagic vacuoles induced by HBx did not sequester more cellular proteins or organelles for degradation [259]. The induction of autophagic vacuoles was not only observed in cells that expressed HBx but also in the cells productively replicating HBV and in the liver of transgenic mice that carried the complete HBV genome [260]. However, it was not observed in mice carrying the HBV genomic mutant that was not capable of expressing HBx [261].

The accumulation of unfolded or misfolded proteins in the ER can lead to ER stress, which can activate IRE1, PERK, and ATF6; resulting in the activation of a cascade of downstream signaling events collectively called the unfolded protein response (UPR) [262]. HBV is known to use this pathway to induce autophagy without promoting the autophagic protein degradation. It was found that this induction of ER stress and UPR was mediated by SHBs, and the effect of SHBs on autophagy was abolished if the expression of any of the three sensors of the ER stress (i.e., IRE1, PERK and ATR6) was suppressed with siRNAs [263]. The HBV genomic mutant incapable of expressing SHBs is unable to trigger UPR and induce autophagy. Although the activation of UPR can persuade autophagy and hepatitis C virus has been shown to induce autophagy *via* this mechanism; the finding that HBV could use SHBs to induce ER stress and autophagy were rather surprising [264]. This is because of the fact that

previous studies on HBV indicated that HBx, LHBs and the LHBs mutant with a deletion in the pre-S2 region could induce the ER stress. In contrast, SHBs was not known to induce ER stress and, instead, a reduction of its expression could actually cause the accumulation of LHBs in the ER lumen, resulting in the induction of ER stress and hepatocellular injury [265]. Besides the product of HBV gene, various HBV genotypes may also impact the ability of HBV to induce autophagy. It was found that HBV genotype C virus was more potent than genotype B virus in the induction of autophagy [266]. The HBV genotype C is also associated with a more severe liver disease outcome than genotype B [267]. It is unclear whether the increased virulence of genotype C HBV is related to its increased ability to induce autophagy.

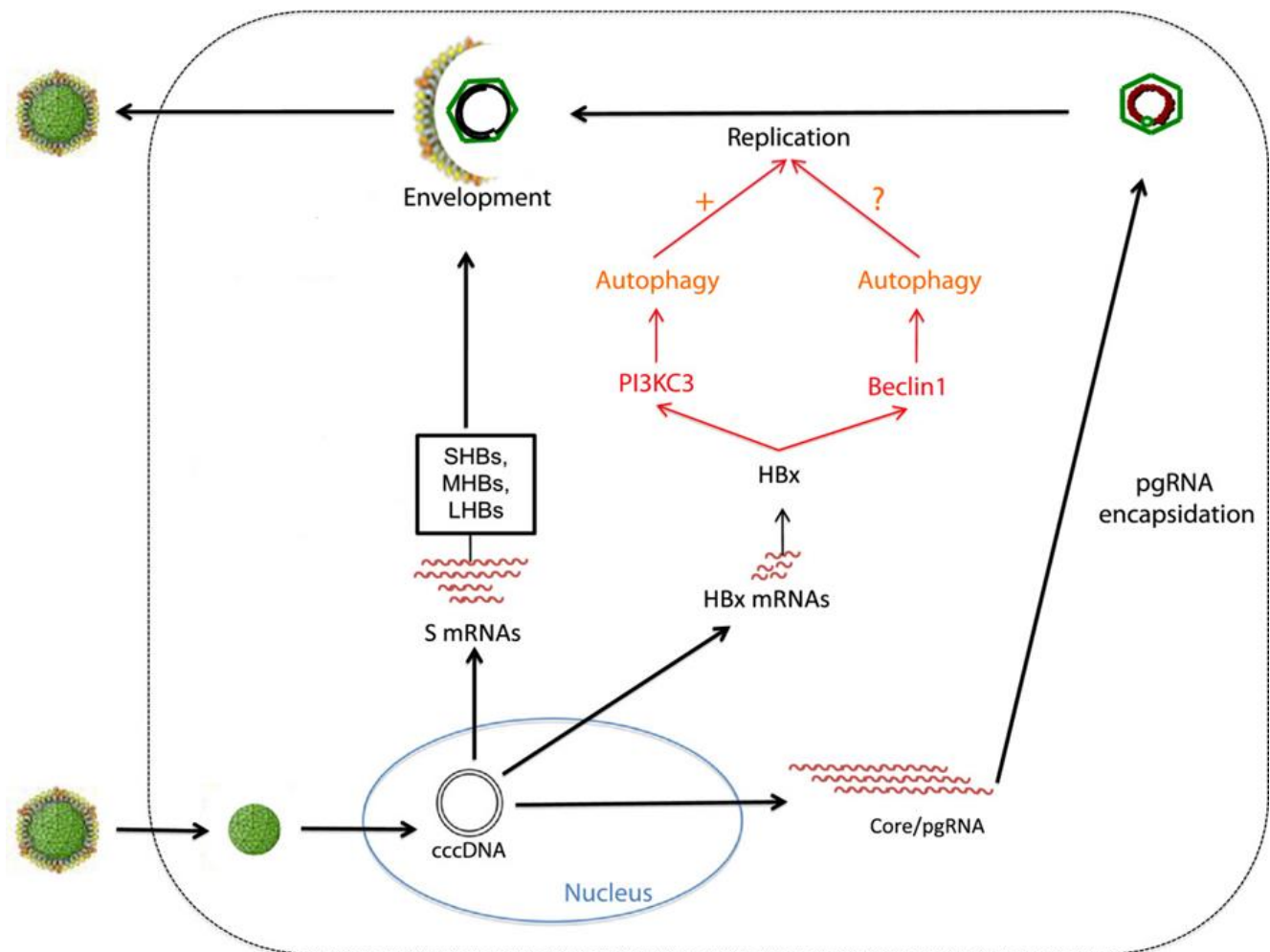


**Figure 2.10** Autophagy is induced by HBV expression and enhances HBV replication [259]

### 2.16 Effect of Autophagy on HBV replication

In addition, autophagy also plays a constructive role in the replication of HBV, as the inhibition of autophagy led to the reduction of HBV replication in cells (**Figure 2.10**) [64]. The suppression of PI3KC3 and Atg7 with the siRNA leads to the inhibition of HBV DNA replication with only a small effect on HBV RNA transcription, protein synthesis or the packaging of the pgRNA into the core particle [268]. Similar results were found where the activity of PI3KC3 was repressed using its inhibitor 3-methyladenine [63]. This finding was supported by the studies conducted using HBV transgenic mice, which carried the entire HBV genome and actively replicated HBV in the liver [269]. How autophagy is involved in HBV DNA replication is unclear. However, it does have a profound effect on the subcellular localization of the HBV core protein, as the HBV core protein was localized primarily to the nuclei of the hepatocytes in wild-type mice but it was diffusely localized to the cytoplasm in the hepatocytes of mice with liver-specific knockout of Atg5 [64]. Curiously, in the studies conducted by Li *et al.*, it was shown that the inhibition of autophagy with 3-methyladenine or with siRNA knockdown of either Beclin-1 or Atg5, had little effect on the HBV RNA and DNA syntheses, but it inhibited the release of enveloped viral particles. Based on the observation that SHBs co-localized with the autophagosomes and co-immuno precipitated with LC3, they suggested that HBV might use autophagosomes as the scaffold for viral envelopment [270]. The possibility that HBV may use autophagosomes for viral envelopment certainly requires further investigation, as the report by Sir *et al.* indicated the co-localization of both HBV core/precure protein and surface proteins with autophagic vacuoles [63].

### 2.17 Human genes involved in HBV pathogenesis and significance of their polymorphisms

Different viral, environmental and genetic components are considered to play a major role in HBV infection. The individual's genome and ethnic differences show differential severity, infection, and the outcome of HBV infection [271]. The liver as we know is a rich source of innate and adaptive immune cells, cytokines, and chemokines. An over abundance of candidate gene studies has shown that polymorphisms in certain immunity and inflammation-related genes are significantly associated with HCC risk [272]. Various genes whose polymorphisms play important role in response to HBV infection are listed as under in **Table 2.2**.

**Table 2.2** Gene polymorphisms associated with susceptibility to chronic hepatitis B

Gene/Loci	Population	Sample size	p-value	Reference
HLA B 44-Cw 1601	Caucasian	563	0.02	[273]
HLA B 44-Cw 0501	Caucasian	563	0.006	[273]
HLA-DRB1 0301	Chinese	190	0.0074	[274]
HLA-DR6	Korean	1272	< 0.001	[275]
HLA-DQA1 0501	Chinese	190	0.0157	[274]
HLA-DQA1 0501	African American	91	0.05	[276]
HLA -DQB1 0301	African American	91	0.01	[276]
HLA-DQB1 0301	Chinese	190	0.0075	[274]
HLA B 08	Caucasian	563	0.03	[273]
TNF-alpha-863	Korean	1400	-	[277]
TNF-alpha-238	Chinese	355	0.02	[278]
TNF-alpha-238	Chinese	455	0.02	[279]
NKG2D	Han Chinese	500	0.04	[280]
Interleukin-16- TT	Iran	744	0.02	[281]
Interleukin-16- GG	Iran	744	< 0.001	[281]
PRKAA1- 424	Han Chinese	276	0.03	[282]
RKAA1-707	Han Chinese	276	0.03	[282]
PRKAA1-822	Han Chinese	276	0.02	[282]
TNF-alpha-308	Iran	240	<0.001	[283]
TNF-alpha-857	Iran	240	0.008	[283]
TNF-alpha-863	Iran	240	0.008	[283]



## 2.18 SNPs of ULK1 in diseases

### 2.18.1 Ankylosing spondylitis (AS)

It is a form of arthritis that mainly affects the spine, and also other joints of the body. It causes inflammation of the vertebrae which can lead to severe, chronic pain and discomfort. In more severe cases this inflammation can lead to ankylosis in which a new bone formation occurs in the spine due to which sections of the spine get fused in a fixed, immobile position. AS has been acknowledged as a polygenic inheritable disease. A large number of genes, implicated in IBD and/or CD, have already been associated with AS and they share a common pathway [284]. Since autophagy plays a significant role in several immune-related diseases which have substantial overlaps in genetic association, a recent case-control study has explored the role of the ULK1 autophagy gene in the development of AS [285]. The findings of the study suggest that the rs9652059 variation (C→T) could increase AS susceptibility and the three haplotypes rs9652059<sup>C</sup>-rs4964879<sup>G</sup>, rs9652059<sup>C</sup>-rs11616018<sup>T</sup> and rs9652059<sup>T</sup>-rs11616018<sup>T</sup> may be associated with AS susceptibility.

### 2.18.2 Crohn's disease

Crohn's disease (CD) is considered to be caused by the interactions among many genes that regulate the immune response against environmental factors such as intestinal bacteria [286]. Association of ULK1 gene with CD has been studied in the New Zealand population [75]. The results suggest a novel association between one haplotype tagging SNP (rs12303764) in the ULK1 gene and CD. The findings from another study also provide some evidence to suggest that genetic variation in ULK1 may play a role in interindividual differences in CD susceptibility and clinical outcome [73].

### 2.18.3 Latent Mycobacterium tuberculosis infection (LTBI)

Latent tuberculosis infection (LTBI) is characterised by the presence of immune responses to previously acquired *Mycobacterium tuberculosis* infection lacking clinical evidence of active tuberculosis (TB). In 2016, first candidate gene association study of autophagy-related genes and LTBI was reported. The results found were satisfactory showing *ULK1* polymorphisms were associated with LTBI in Asian individuals, with a reduction of >80% in the LTBI risk for each copy of the minor allele [287].

# MATERIALS AND METHODS

### 3. Materials and Methods

#### 3.1 Understanding *ULK1*: An *In silico* analysis

##### 3.1.1 Data Retrieval

In this *in-silico* analysis, an extensive examination of the *ULK1* gene was carried out both at nucleotide and protein levels. The analyses initiated with the retrieval of human protein/gene sequence of *ULK1* (GenBank Accession Number: AAC32326) from the National Center for Biotechnology Information (NCBI).

##### 3.1.2 Identification of site-specific residues and phylogenetic analysis for *ULK1*

Apart from the human protein sequence of *ULK1* (GenBank Accession Number: AAC32326), corresponding protein sequences for other seven species of families Hominidae (*Pan troglodytes*; GenBank Accession Number: JAA43195), Bovidae (*Bos taurus*; GenBank Accession Number: NP\_001192856), Cricetidae (*Cricetulus griseus*; GenBank Accession Number: EGW02429), Pteropodidae (*Pteropus alecto*; GenBank Accession Number: ELK14239), Muridae (*Rattus norvegicus*; GenBank accession Number: NP\_001101811, *Mus musculus*; GenBank Accession Number: NP\_033495), Pipidae (*Xenopus (Silurana) tropicalis*; GenBank Accession Number: NP\_001106388) were also retrieved and further deliberated for their evolutionary conservation.

##### 3.1.3 Evolutionary conserved and variable regions

The genetic variations leading to different phenotypes were analyzed by observing the variable regions in the multiple sequence alignment (MSA) generated for the *ULK1* gene. The latter was carried out using multiple sequence comparison by log-expectation (MUSCLE) [288] and multiple alignment using fast Fourier transform (MAFFT) [289]. These programs use log-expectation scores and fast fourier transform methods respectively for providing better average accuracy and speed compared to other MSA algorithms. These programs were used with their default parameters.

##### 3.1.4 Evolutionary relationship associated with *ULK1*

Highly conserved regions play an imperative role in phylogenetic tree construction. Therefore, the evolutionary relationship among eight species was elucidated on the basis of sequence similarities by applying molecular evolutionary genetics analysis 5 (MEGA5) which helps to

estimate the rates of molecular evolution and deduce ancestral affiliations [290]. The phylogenetic reconstruction was achieved by means of maximum parsimony (MP), a character-based method for deducing phylogenetic trees by minimizing the total number of evolutionary steps required for explanation of a given set of data. The bootstrap analysis was also performed for the verification of inferred tree by taking 1000 bootstrap replicates to generate the statistically significant phylogenetic tree.

### **3.1.5 Identification of regulatory elements and over-represented TFBS**

Identification of regulatory elements like enhancers, silencers, and repressors involved in controlling the expression of ULK1 provides useful insights into how the gene is regulated and expressed under the influence of these factors. Distant regulatory elements of co-regulated genes (DiRE) [291] and oPOSSUM 3 [292] were used for detection of the regulatory elements in ULK1 and over-represented transcription binding sites, respectively. Additionally, JASPAR database [293] was also explored for similar kind of datasets to identify various classes, families and sequence logos for transcription factors (TFs) and their binding sites.

### **3.1.6 Identification of nsSNPs, their phenotypic effects and quantitative statistical analyses for genetic parameters**

The nsSNPs are the nucleotide changes that result in the altered amino acid in the protein sequence. This altered amino acid may or may not affect the function of the protein. The affected protein function in case of modifying nsSNPs is due to change in its (1) structure, (2) stability and (3) by influencing functional binding sites. We have used Sorting Intolerant From Tolerant (SIFT) and Polymorphism Phenotyping (PolyPhen) tools to identify nsSNPs which are popular standard tools to predict intolerant or damaging variants. These are based on sequence homology, conservation, structure and SWISS-PROT annotations. For identification of known SNPs, we computationally analyzed *ULK1* gene initially as experimental methods are complicated, expensive and time consuming. The nsSNPs were further analyzed for their phenotypic effect in coding sequences. SIFT algorithm was used for identification of genetic variations, leading to diverse phenotypes in ULK1 [294]. The prediction is based on the generated SIFT score and focuses on the phenomenon of protein conservation which states that protein evolution has a strong correlation with protein function. PolyPhen was also used for

validating these phenotypic consequences which predicts on the basis of sequence, structural, evolutionary annotations, and substitutions in the proteins [295]. The profile scores for the two amino acid positions (native and mutant) were calculated and assessed for evaluating their phenotypic effects. On the basis of the scores, PolyPhen categorizes the substitutions into three classes i.e. ‘benign’, ‘possibly damaging’ and ‘probably damaging’. The genotype data from CEU (CEPH—Utah Residents with Northern and Western European Ancestry) population for the ULK1 gene was retrieved from The International Hap Map project [296] and was analyzed for various quantitative genetic parameters: linkage disequilibrium (LD), haplotype and SNPs. These parameters represent the combination of alleles on neighboring loci on the chromosome being transmitted together and involvement of alleles in a non-random mode of inheritance in the population. This analysis was performed using Haploview [297] and the parameters analyzed for genetic association were  $D'$  and  $r^2$ . The  $D'$  value provides the measure of LD between the two blocks and its value closer to zero shows a higher amount of historical recombination between the two blocks and  $r^2$  gives the correlation coefficient between the two loci under study.

### **3.1.6.1 Mutation-based sequence stability analysis**

IPTREE-STAB and i-Mutant2.0 tools were used to predict the change in protein stability on encountering mutations. The iPTREE-STAB is a sequence-based web server that predicts stability change upon single amino acid substitution [298]. Whereas, i-Mutant2.0 tool is a support vector machine (SVM)-based tool for the prediction of change in protein stability in terms of  $\Delta\Delta G$  values [299].

### **3.1.6.2 Mutation-based structure stability analysis**

One nsSNP i.e. rs79965940 (N148T) out of the four nsSNPs was mapped on the partial available protein structure of ULK1 (PDB ID: 4WNO). As there was no PDB structure available for the complete sequence of ULK1, we used Robetta (Rosetta Comparative Modeling and *Ab Initio* Modeling) web-based server (<http://robetta.bakerlab.org>) for the prediction of full-chain protein structure by comparative modelling [300]. The second nsSNP i.e. rs61942435 (A991V), was mapped onto the structure (ULK1 modelled structure A-ULK1A) obtained from Robetta. Further, DUET and Eris tools were used for predicting the protein stability change incurred upon mutations [301, 302].

### **3.1.6.3 Prediction of total energy for native and mutant structures**

Mutant structures for the mutations N148T in 4WNO and A991V in ULK1A were generated using PyMOL (Molecular Graphics System, Version 1.8 Schrödinger, LLC). These mutant structures (N148T in 4WNO and A991V in ULK1A), as well as their native structures (4WNO and ULK1A), were submitted for carrying out energy minimizations and total energy computation using CHARMM force field (Discovery Studio 4.1).

### **3.1.7 Elucidation of putative phosphorylation and palmitoylation sites in ULK1**

Most of the processes occurring in a cell are controlled by signaling cascade dependent on phosphorylation/dephosphorylation. ULK1 is a kinase which itself is controlled by phosphorylation events and phosphorylates its substrates for modulating their activity [303, 304]. Hence, detection of phosphorylation sites in ULK1 may unravel important functional aspects regarding its involvement in various disorders [305-307]. The NetPhos algorithm was used for the prediction of phosphorylation sites at serine (S), threonine (T) and tyrosine (Y) residues in the ULK1 amino acid sequence [308]. This algorithm utilizes an artificial neural network (ANN) based method which is trained from PhosphoBase a database of experimentally validated phosphorylated proteins [309]. Detection of palmitoylation sites is also an important component of this study. The palmitoylation sites were obtained from CSS-PALM, a tool based on the clustering and scoring strategy (CSS) algorithm for the prediction of palmitoylation sites [310].

### **3.1.8 Protein–Protein Interaction studies for ULK1**

The complex interaction networks involving ULK1 protein which is often implicated in different or same pathways have been constructed by Search Tool for Retrieval of Interacting Genes and proteins (STRING) version 9.05 [311]. The tool predicts the interactions between various proteins based on a confidence score and validates the connections using databases, text mining and gene fusion support. The interaction studies were performed in various modes and by changing parameters to obtain a robust network model for ULK1 and its associated interacting partners. The different modes include confidence view, evidence view, action mode and the interactive view to infer the most appropriate interactions among nodes in the network.

### **3.2 Genotyping of predicted nsSNPs and selected SNPs of ULK1 in HBV infected patients and healthy individuals**

#### **3.2.1 Study subjects and sample collection**

The studied population represents 700 subjects of North Indian region. The median age was 35 ±14 years for HBV infected patients, and 37±13 years for control subjects. Out of these total participants, 500 were HBV infected patients, which were enrolled in the study for the period of 3 years from 2013 to 2016, and 200 healthy controls. HBV Infected blood samples were collected from Department of Hepatology, Post Graduate Institute of Medical Education and Research (PGIMER), Chandigarh. Diagnosis of hepatitis B was based on the presence of Hepatitis B surface antigen (HBsAg), anti-HBs, anti-HBC total, HBeAg, anti HBe, aspartate aminotransferase (AST), Alanine aminotransferase (ALT) and HBV DNA levels. The basic demographic data for all the patients were recorded. Patients or their legal representatives gave their consent for the study. The chronic HBV infection was diagnosed by detection of HBsAg over a period of 6 months. The blood samples from patients and healthy controls were collected in sterile, vacutainers (Red cap for *serum* and Purple cap for *DNA* isolation) and transferred to the laboratory under proper cold chain conditions for further processing.

#### **Inclusion and Exclusion criteria:**

The inclusion criteria were all patients who were serum HBsAg positive for at least six months with elevated ALT levels (>1.5 times the upper limit of normal; 65 U/L). All of the patients were diagnosed after they had been previously followed for at least 12 months. The exclusion criteria were patients with acute HAV, HBV, HCV, or HDV, patients with evidence for hepatocellular carcinoma (HCC), or concomitant of HCV, HDV, HIV infection, metastatic or autoimmune liver disease and drug induced acute hepatitis.

#### **3.2.2 Processing of blood samples**

Two ml venous blood was collected from the patients and healthy subjects in Na<sub>2</sub>EDTA coated tubes. The blood sample was then stored at -20°C until further use.

**Isolation of genomic DNA from a whole blood sample (Miller et.al., 1988; with minor modifications):**

- A 400µl blood sample was pipetted in a 2ml eppendorf. To this, RBC lysis buffer was added (three times the volume of blood sample) and was kept for incubation on a rocker at room temperature until RBCs completely lysed.
- The solution was centrifuged at 5000 rpm for 2 min to obtain a creamish white WBC pellet.
- The supernatant was discarded and the WBC pellet was thoroughly suspended in 300 µl TE buffer (pH 8.0) using a vortexing machine.
- 22µl of 10% SDS solution was added to the suspended pellet solution and the mixture was incubated at 56°C for 30 min in a dry bath.
- Subsequently, 160 µl of 7.5 M ammonium acetate was added to the solution and was mixed vigorously for about 1 min per sample on a vortexer. The mixture was centrifuged at 13,000 rpm at RT for 15 mins, thereby resulting in separation of the precipitated proteins as a pellet.
- The clear supernatant was transferred to a fresh sterile micro-centrifuge. To this chilled absolute ethyl alcohol was added (twice the volume of clear supernatant). The tube was gently rocked a couple of times to allow the precipitation of genomic DNA.
- The genomic DNA precipitate was centrifuged at 13,000 rpm for 10 min to pellet at the bottom of the tube. The latter were subsequently washed in 150 µl of 70% ethanol and air-dried at RT for about 10-15 mins.
- The dried pellet was dissolved in 60 µl TE buffer (pH 7.3) by incubating at 65°C for 10 mins. The dissolved DNA was finally stored at 20°C until further use.
- The DNA quantification was done using Nano Drop plus Spectrophotometer (GE Healthcare, US). The concentration of DNA was read by measuring the absorbance of a sample at A° 260 on a spectrophotometer.



### 3.3 Liver function tests

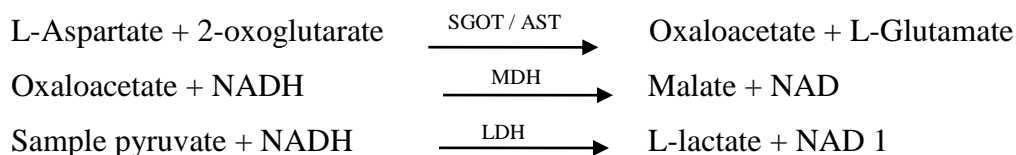
The biochemical estimations (Serum glutamic oxaloacetic transaminase and serum glutamate pyruvate transaminase) in serum were carried out using Erba diagnostic kits (ERBA diagnostics, Germany).

#### 3.3.1 In vitro determination of AST/GOT (Aspartate Aminotransferase) in human serum

SGOT /ASAT is widely distributed with high concentrations in the heart, liver, skeletal muscle, kidney and erythrocytes. Damage or disease to any of these tissues such as myocardial infarction, viral hepatitis, liver necrosis, cirrhosis and muscular dystrophy may result in raised levels of SGOT / ASAT.

##### 3.3.1.1 Principle

This reagent is based on IFCC recommendations, without pyridoxal phosphate. The series of reactions involved in the assay system is as follows: LDH



- SGOT / ASAT present in the sample catalyzes the transfer of the amino group from L-aspartate to 2-oxoglutarate forming oxaloacetate and L-glutamate.
- Oxaloacetate in the presence of NADH and Malate dehydrogenase (MDH) is reduced to L-malate. In this reaction, NADH is oxidized to NAD. The reaction is monitored by measuring the rate of decrease in absorbance at 340 nm due to the oxidation of NADH to NAD.
- Addition of Lactate dehydrogenase (LDH) to the reagent is necessary to achieve rapid and complete reduction of endogenous pyruvate so that it does not interfere with the assay.

### 3.3.1.2 Reagent composition

#### R1

Tris Buffer (pH 7.8)	110 mmol/l
L-Aspartate	340 mmol/l
LDH	≥ 4000 U/l
MDH	≥ 750 U/l

#### R2

CAPSO	20 mmol/l
2-Oxoglutarate	85 mmol/l
NADH	1.05 mmol/l

### 3.3.1.3 Assay procedure

Wavelength	340 nm, Hg 334 nm, Hg 365 nm
Cuvette	1 cm
Working solution	1.000 ml
Sample	0.100 ml

- Mix, incubate 1 min at 37°C and then measure the initial absorbance of calibrator and sample against reagent blank.
- Measure the absorbance change exactly after 1, 2 and 3 min.
- Calculate 1 minute absorbance change ( $\Delta A/\text{min}$ ).

### 3.3.1.4 Calculation

$$\bullet \quad |AST/GOT(U/l) = \Delta A_{sam}/min \div \Delta A_{cal}/min * C_{cal}$$

$C_{cal}$  = calibrator concentration

- Using factor:  $AST/GOT = f \times \Delta A/\text{min}$   
f = factor

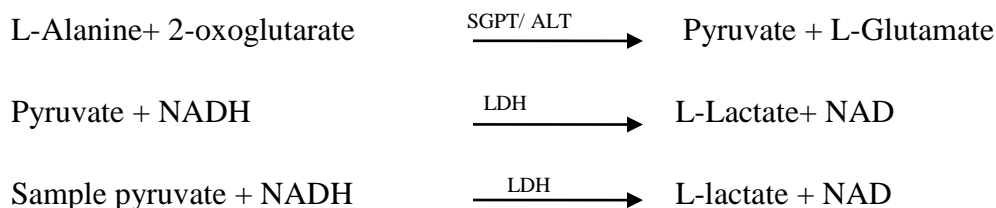
### 3.3.2 *In vitro* determination of ALT/GPT (Alanine Aminotransferase) in human serum

The ALT/GPT is present in high concentration in liver and to a lesser extent in kidney, heart, skeletal muscle, pancreas, spleen and lung. However, increased levels of ALT/GPT are generally

a result of liver disease associated with some degree of hepatic necrosis such as cirrhosis, viral or toxic hepatitis and obstructive jaundice. Characteristically, ALT/GPT is generally higher than AST/GPT in acute viral or toxic hepatitis, whereas, for most patients with the chronic hepatic disease, ALT/GPT levels are generally lower than AST/GPT levels. Elevated ALT/GPT levels have also been found in extensive trauma and muscle disease, circulatory failure with shock, hypoxia, myocardial infarction and haemolytic disease.

### **3.3.2.1 Principle**

This ALT/GPT reagent is based on the recommendations of the IFCC without pyridoxal phosphate. The series of reactions involved in the assay system is as follows:



- The amino group is enzymatically transferred by SGPT / ALAT present in the sample from alanine to the carbon atom of 2-oxoglutarate yielding pyruvate and L-glutamate.
- Pyruvate is reduced to lactate by LDH present in the reagent with the simultaneous oxidation of NADH to NAD. The reaction is monitored by measuring the rate of decrease in absorbance at 340 nm due to the oxidation of NADH.
- Endogenous sample pyruvate is rapidly and completely reduced by LDH during initial incubation period to avoid interference during the assay.

### **3.3.2.2 Reagent composition**

#### **R1**

Tris Buffer (pH 7.5)	137.5 mmol/l
L-Alanine	709 mmol/l
LDH (microbial)	≥ 2000U/l

#### **R2**

CAPSO	20 mmol/l
2-oxoglutarate	85 mmol/l
NADH	1.05 mmol/l

### 3.3.2.3 Assay procedure

Wavelength	340 nm, Hg 334 nm, Hg 365 nm
Cuvette	1 cm
Working solution	1.000 ml
Sample	0.100 ml

- Mix, incubate 1 min. at 37°C and then measure the initial absorbance of calibrator and sample against reagent blank.
- Measure the absorbance change exactly after 1, 2 and 3 min.
- Calculate 1 minute absorbance change ( $\Delta A/\text{min}$ ).

### 3.3.2.4 Calculation

- $$|ALT/GPT(U/l) = \Delta A_{sam}/min \div \Delta A_{cal}/min * C_{cal}$$
  
 $C_{cal}$  = calibrator concentration
- Using factor:  $ALT/GPT (U/l) = \Delta A/\text{min} \times f$   
 $f$  = factor

## 3.4 Isolation of HBV DNA

HBV DNA was isolated from a total of 500 HBV infected samples using QIAamp DNA Blood Mini Kit (QIAGEN Inc, Valencia, CA).

### 3.4.1 Procedure

1. Pipet 20  $\mu\text{l}$  QIAGEN Protease (or proteinase K) into the bottom of a 1.5 ml microcentrifuge tube.
2. Add 200  $\mu\text{l}$  serum sample to the microcentrifuge tube.
3. Add 200  $\mu\text{l}$  Buffer AL to the sample. Mix by pulse-vortexing for 15 s
4. Incubate at 56°C for 10 minutes.
5. Briefly centrifuge the 1.5 ml microcentrifuge tube to remove drops from the inside of the lid.
6. Add 200  $\mu\text{l}$  ethanol (96–100%) to the sample and mix again by pulse-vortexing for 15 s. After mixing, briefly centrifuge the 1.5 ml microcentrifuge tube to remove drops from the inside of the lid.

7. Carefully apply the mixture from step 6 to the QIAamp Mini spin column without wetting the rim. Close the cap, and centrifuge at 6000 x g (8000 rpm) for 1 min. Place the QIAamp Mini spin column in a clean 2 ml collection tube (provided), and discard the tube containing the filtrate.
8. Carefully open the QIAamp Mini spin column and add 500 µl Buffer AW1 without wetting the rim. Close the cap and centrifuge at 6000 x g (8000 rpm) for 1 min. Place the QIAamp Mini spin column in a clean 2 ml collection tube (provided), and discard the collection tube containing the filtrate.
9. Carefully open the QIAamp Mini spin column and add 500 µl Buffer AW2 without wetting the rim. Close the cap and centrifuge at full speed (20,000 x g; 14,000 rpm) for 3 min.
10. Place the QIAamp Mini spin column in a new 2 ml collection tube (not provided) and discard the old collection tube with the filtrate. Centrifuge at full speed for 1 min. Place the QIAamp Mini spin column in a clean 1.5 ml microcentrifuge tube (not provided), and discard the collection tube containing the filtrate. Carefully open the QIAamp Mini spin column and add 200 µl Buffer AE or distilled water. Incubate at room temperature (15–25°C) for 1 min, and then centrifuge at 6000 x g (8000 rpm) for 1 min.

### 3.5 Genotype analysis of SNPs in *ULK1* gene

For amplification of the fragment of DNA containing polymorphisms in *ULK1* gene, the isolated DNA was subjected to PCR for the total six selected polymorphisms, rs79965940, rs61942435, rs55824543, rs56364352, rs3923716 and rs12303764 using genespecific primers mentioned below in **Table 3.1**.

**Table 3.1** Information of *ULK1* polymorphisms, their genotype analysis platform, and primer sequences used

Gene of Interest	Polymorphism	Genotype analysis	Primer Name	Primer Sequence (5' to 3')
ULK1	rs79965940	PCR-RFLP	Fwd	TGGTAGATGGACAGGACCCG
			Rev	ATGGTGTGTTTACCTTGGCC
ULK1	rs61942435	PCR-RFLP	Fwd	GGTCATCTGGTTCCAGGCAGT

			Rev	AAGCTGTGCATTGAGCGGA
ULK1	rs55824543	PCR-RFLP	Fwd	AAAGCTAAGGGGCCAACTCC
			Rev	GTGGAACAGAAGCCAACTGC
ULK1	rs56364352	PCR-RFLP	Fwd	CCCCTCGGTCAGGAAATGTG
			Rev	AGCATGAGTAGGGTTGCAGG
ULK1	rs3923716	PCR-RFLP	Fwd	CTGCGAGTGGCTTGTGAGTCCG
			Rev	TAGGGTGGCCGAGGCAGGAA
ULK1	rs12303764	TARMS-PCR	Outer Fwd	GGTGAATGAGGAAACCAACCAGGGAC G
			Outer Rev	CCAAGTGGCTACAGTGCTGACAGATG
			Inner Fwd	CAGGCGTGGCTGGGGCATG
			Inner Rev	GGAAGGGCTCCTGCCACCCA

The PCR in a total volume of 25 µl was carried out with various components and was performed using The Veriti Thermal Cycler (Applied Biosystems, Foster, USA) following the cycling conditions mentioned in **Table 3.2**.

**Table 3.2** Thermocycling conditions used for genotyping polymorphisms of ULK1 gene

PCR Condition	Cycles	rs79965940	rs61942435	rs55824543	rs56364352	rs3923716	rs12303764
		Initial Denaturation - 95°C/ 5 mins					
<b>Denaturation</b>	35	95°C/30s	95°C/30s	95°C/30s	95°C/30s	95°C/30s	95°C/30s
<b>Annealing</b>		57°C/45s	58°C/45s	60°C/40s	60°C/45s	58°C/40s	58°C/45s
<b>Extension</b>		72°C/60s	72°C/60s	72°C/60s	72°C/60s	72°C/60s	72°C/60s
		Final Extension- 72°C/ 5 mins					

### 3.5.1 PCR- Restriction Fragment Length Polymorphism (PCR-RFLP): Detection Procedure to identify the allele-specific product

Further, the amplified products were digested with the restriction enzyme in order to detect the genotype present in a particular individual at a particular position. For the restriction digestion

analysis of rs79965940, rs61942435, rs55824543, rs56364352 and rs3923716, 10µl aliquots of the PCR products were digested overnight with 1 unit of MmeI, HindIII, NspI, BbvI and BseRI (New England Biolabs, UK Ltd.) restriction enzymes, respectively. The reaction conditions in RFLP for the nsSNPs are mentioned in **Table 3.3**.

**Table 3.3** The reaction conditions used in RFLP analysis for the nsSNPs of *ULK1* gene

Reaction components	rs79965940	rs61942435	rs55824543	rs56364352	rs3923716
	MmeI	HindIII	NspI	BbvI	BseRI
Enzyme	0.1	0.1	0.1	0.1	0.1
Buffer	1.5	1.5	1.5	1.5	1.5
Water	3.4	3.4	3.4	3.4	3.4
PCR product	10	10	10	10	10
Total	15	15	15	15	15

### 3.5.2 Tetra primer ARMS-PCR based assay for genotyping rs12303764

The *ULK1* polymorphism rs12303764 was amplified using primers designed manually and their specificity was checked by NCBI-BLAST tool.

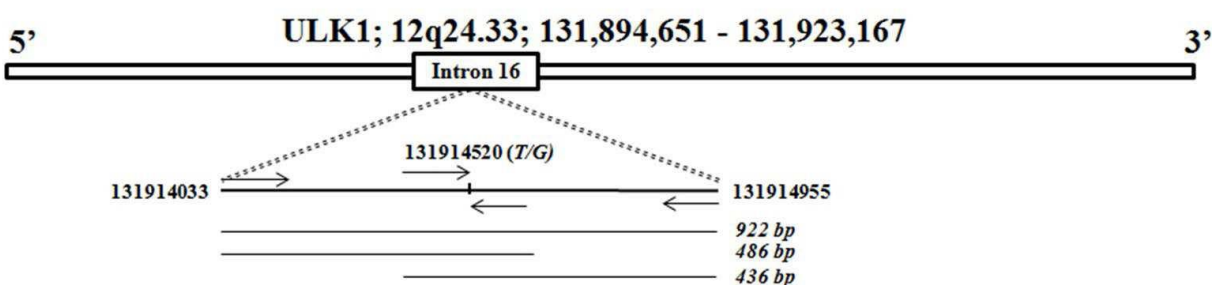


Figure 3.1 Strategy used for designing TARMS-PCR primers for rs12303764

As mentioned above in figure 3.1, the primers were designed in a way that the two allele-specific amplicons would have different lengths and could easily be separated by standard agarose gel electrophoresis. Since the control amplicon is always amplified irrespective of other amplicons corresponding to one of the alleles it provides an internal control for amplification failure. For the standardization of amplification conditions, gradients of annealing temperature (range 48–

65°C), Taq DNA polymerase (0.5U–5.0 U; Promega, Madison, US) and primers (5–15 pmol) were run. PCR was performed in 25 µl containing 20 ng of genomic DNA, 0.2 mM of each dNTP, 5mM MgCl<sub>2</sub>, 50mM NaCl, 50mM Tris–HCl (pH 9.0), 10 µg activated calf thymus DNA; 0.1 mg/ml BSA. The PCR cycling conditions were 5 min of initial denaturation at 95°C, 35 cycles of 95°C for 30 s, annealing at (48–65°C) for 40 s, 72°C for 2 min and a final extension at 72°C for 5 min. At high annealing temperature, low primers, and Taq concentration, the number of specific bands was either less or absent, while at the low annealing temperature, higher primers and Taq concentrations, there was an amplification of a number of non-specific bands. Optimal amplification of specific bands was observed at 58°C of annealing temperature, 2.5U of Taq DNA polymerase and 10 pmol of each of the four primers. Amplified PCR products were separated on 3% agarose gel and visualized by ethidium bromide.

### **3.6 Haplotype analysis**

The haplotype analysis was conducted to examine the genetic association of the predicted nsSNPs of ULK1 with hepatitis B infection. Haplotypes were analysed using SNPSTATS software (<http://bioinfo.iconlogica.net>) [312].

### **3.7 Statistical analysis**

The genotypes and alleles frequencies were estimated by direct counting. The genotype frequencies were assessed for Hardy–Weinberg equilibrium with  $X^2$  test. Quantitative variables were compared using independent Student t- Test. The results were expressed as odds ratio (OR), 95% confidence intervals (95% CI) and p-values. All the statistical analyses were performed using SPSS v.17.0 for Windows. A *p*-value of <0.05 was considered to be statistically significant in the study. Power of the study for each SNP was estimated using OSSE - an Online Sample Size Estimator and power calculator.



# RESULTS

## 4. Results

### 4.1 *In silico* analysis of ULK1

#### 4.1.1 The conservational and phylogenetic evaluation

The conserved regions in protein sequences generally signify the integrity and stability of genome, which further affect the basic cellular processes [313]. The conserved positions are considered to be involved in important functions, active sites of enzymes and binding sites of the protein receptors [314]. The multiple sequence alignment (MSA) generated from MUSCLE and MAFFT tools for the ULK1 protein was found to be quite similar and various important conserved patterns were identified as shown in Figure 4.1 (A and B). These patterns may have an important association with diseased states and evolutionary relationship among *Pan troglodytes*, *Xenopus (Silurana) tropicalis*, *Mus musculus*, *Rattus norvegicus*, *Pteropus alecto*, *Cricetulus griseus*, and *Bos taurus*. The Figure 4.1A illustrates MSA for the eight sequences where highly conserved regions are highlighted inside the red blocks whereas Figure 4.1B clearly demonstrates the mutations or variations in residues among the regions found in the ULK1 gene of eight species. The maximum conserved blocks were present in the kinase domain followed by S/T rich region and C-terminal domain (CTD). The dots represent conservation with respect to human ULK1 sequence, while variable characters are shown as amino acids. As discussed, these sequence similarities (conserved regions) reflect the evolutionary relationship among the species.

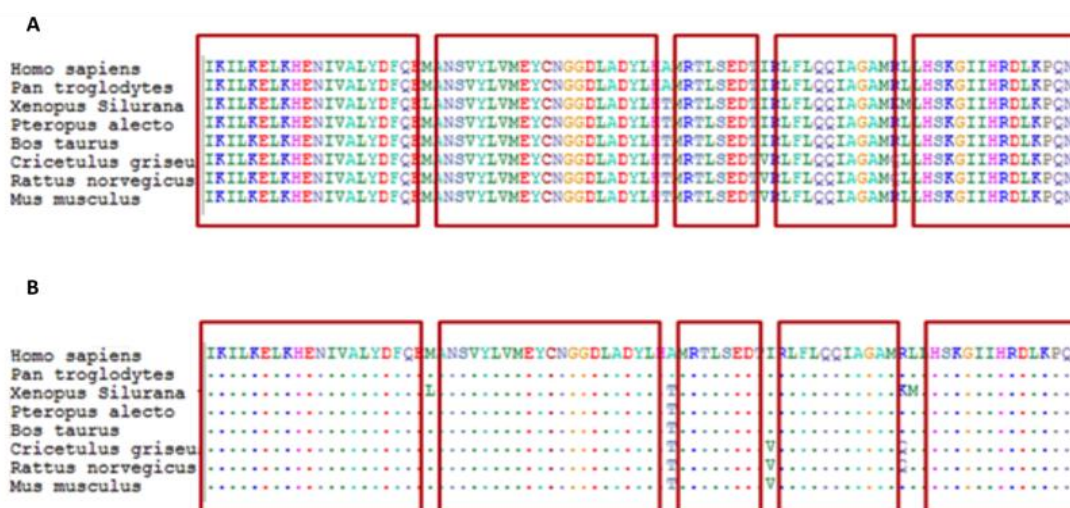


**Figure 4.1** A) The multiple sequence alignment of *ULK1* in eight species highlighting conserved regions. B) Mutations or variations in residues among the regions found in the *ULK1* of eight species.

For the phylogenetic analysis, the ULK1 protein sequence of the eight different species was selected based on the availability of completely validated protein sequence data. MEGA5 was used with 1000 bootstrap replicates using maximum parsimony (MP) method and an evolutionary tree was reconstructed as shown in Figure 4.2. The generated phylogenetic tree supports a clear understanding of the evolutionary relationship between the different species.

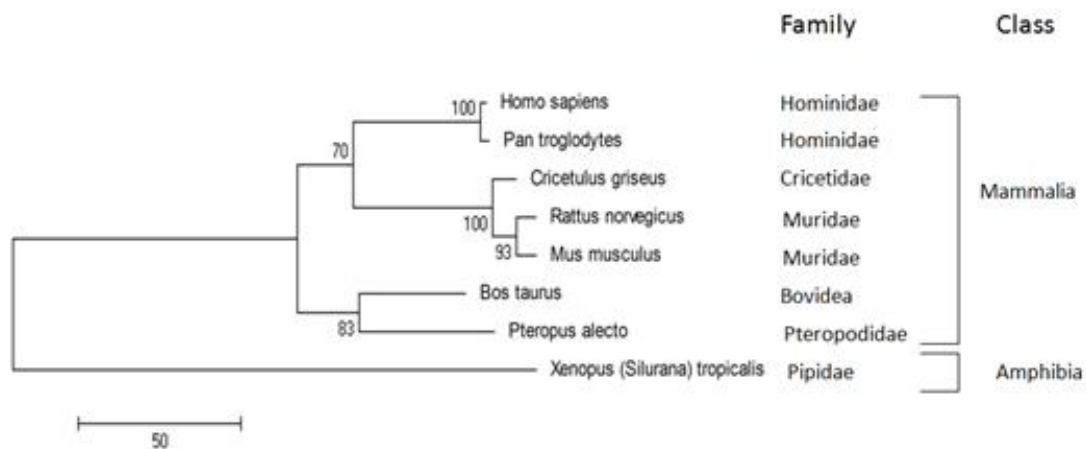


**Figure 4.2** Evolutionary relationship among the eight species included in the study. The phylogenetic tree was reconstructed using MEGA5 software by MP method, a character-based method for deducing phylogenetic trees by minimizing the total number of evolutionary steps.

Here, as shown by the bootstrap values, *H. sapiens* and *P. troglodytes* have 100% evolutionary relationship depicting that the *ULK1* gene present in these species is quite identical and could have originated from the same ancestor. Similarly, *R. norvegicus* and *M. musculus* have 93% similarity and could have the same ancestral origin as *C. griseus*, showing the bootstrap value of 100. The *X. (Silurana) tropicalis*, a species of amphibian family shows a vast difference in its origin and evolution from others when studied on the basis of the protein sequence of *ULK1*. From this data, we could conclude that these sequences tend to be related closely to a family compared to others.

#### 4.1.2 The transcription factor binding sites in ULK1 gene

The regulatory elements in *ULK1* gene were analyzed using DiRE software with the default value for a random set of genes as 5000. This *in silico* approach demonstrated a total of four potential regulatory elements in *ULK1* gene; out of which, three are un-translated regions (UTR)

that correspond to 75% of the total regulatory region in *ULK1* and one intron representing 25% of the total regulatory region as shown in Figure 4.3A. Among the three UTR regions, two are 3' UTRs and one is 5' UTR. The presence of regulatory elements at 5' and 3' indicates that *ULK1* is a complex gene and it could be regulated from both the ends [315].

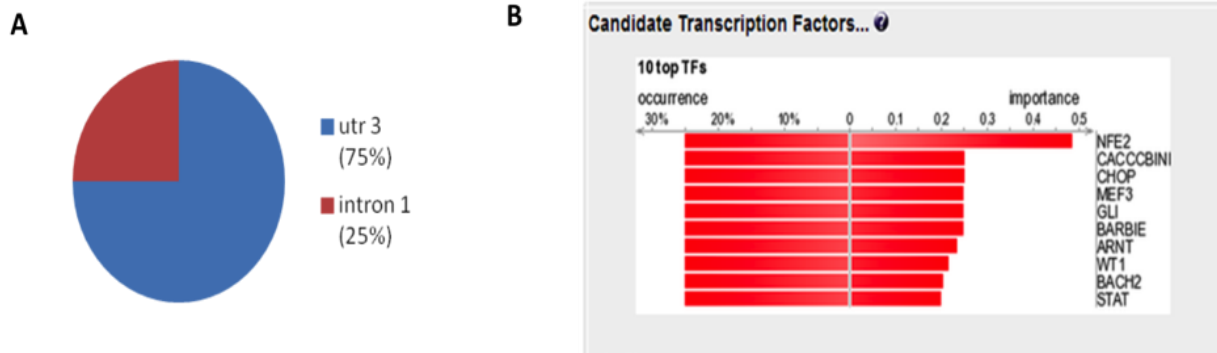


**Figure 4.3** The transcription factor binding sites in *ULK1* gene. (A) Distant regulatory elements of co-regulated genes (DiRE) showed that 75% of the total transcription factors were present in UTR and remaining 25% in the intron region.

Additionally, it is proposed that the neighbouring generic locations might play a critical role in *ULK1* regulation and ultimately in autophagy [315]. A total of 23 TFs in UTR and intron regions were identified using DiRE and are displayed along with their locus, positions, and score in **Table 4.1**. These TFs either bind directly or in the form of complex to the transcriptional regulatory region of *ULK1*, which could further control its expression. Among these detected transcription factors, CHOP, E2F1, NFE2, and STAT have already been studied for their role in a *ULK1* expression where CHOP and E2F1 enhance the autophagy process whereas NFE2 and STAT suppress the process of autophagy [316, 317]. All these TFs have an equal occurrence rate of 25% (**Table 4.2**). Based on the high importance rate (0.48555), nuclear factor (erythroid-derived) 2 (NFE2) is of utmost significance when compared to the rest of the TFs (importance rate of <0.24984) found in the analysis (**Table 4.2**). The distribution of TFBS all over the *ULK1* gene suggests multiple points of their action and this information could further be utilized to understand its regulation [318].

**Table 4.1** Regulatory elements, their types and transcription factors which are related to UTR and intron regions of ULK1 gene

#	REGULATORY ELEMENT	TYPE	SCORE	LOCUS	GENE	CANDIDATE TFBS (RELATIVE POSITIONS)
1	chr12:130946862-130947195	Intron	2.544	chr12:130905754-130979065	ULK1	CACCCBINDINGFACTOR(120)
						NFE2(129)
						BACH2(130)
						GLI(207)
						WT1(214)
						RFX1(307)
						PR(324)
GRE(324)						
2	chr12:130945120-130945301	UTR5	1.221	chr12:130905754-130979065	ULK1	PAX5(4)
						NRF1(6)
						HIC1(9)
						MTF1(37)
						ZBRK1(45)
3	chr12:130972084-130972437	UTR3	2.027	chr12:130905754-130979065	ULK1	SMAD4(32)
						MYOGNF1(122)
						STAT(169)
						HSF1(205)
						BARBIE(233)
4	chr12:130973189-130973466	UTR3	2.784	chr12:130905754-130979065	ULK1	ARNT(65)
						CHOP(82)
						ERR1(151)
						MEF3(217)
						PPARG(258)

**Table 4.2** Top ten transcription factors with their occurrence and importance rates

#	TRANSCRIPTION FACTOR	OCCURRENCE	IMPORTANCE
1	NFE2	25%	0.48555
2	CACCCBINDINGFACTOR	25%	0.24984
3	CHOP	25%	0.24961
4	MEF3	25%	0.24805
5	GLI	25%	0.24727
6	BARBIE	25%	0.24727
7	ARNT	25%	0.23340
8	WT1	25%	0.21587
9	BACH2	25%	0.20391
10	STAT	25%	0.19805

These multiple hotspots could be utilized to control the regulation of ULK1 in an efficient way. Furthermore, to substantiate these results, we used oPOSSUM tool to find the over-represented TFBS in the promoter region of ULK1. The identified TFs are exhibited in the form of sequence logos in Figure 4.4 and represented in detail in **Tables 4.3**. The recognition of TFBS depends on features that consider the search parameters of JASPAR >8 bits and >75% as the threshold of position specific scoring matrices.

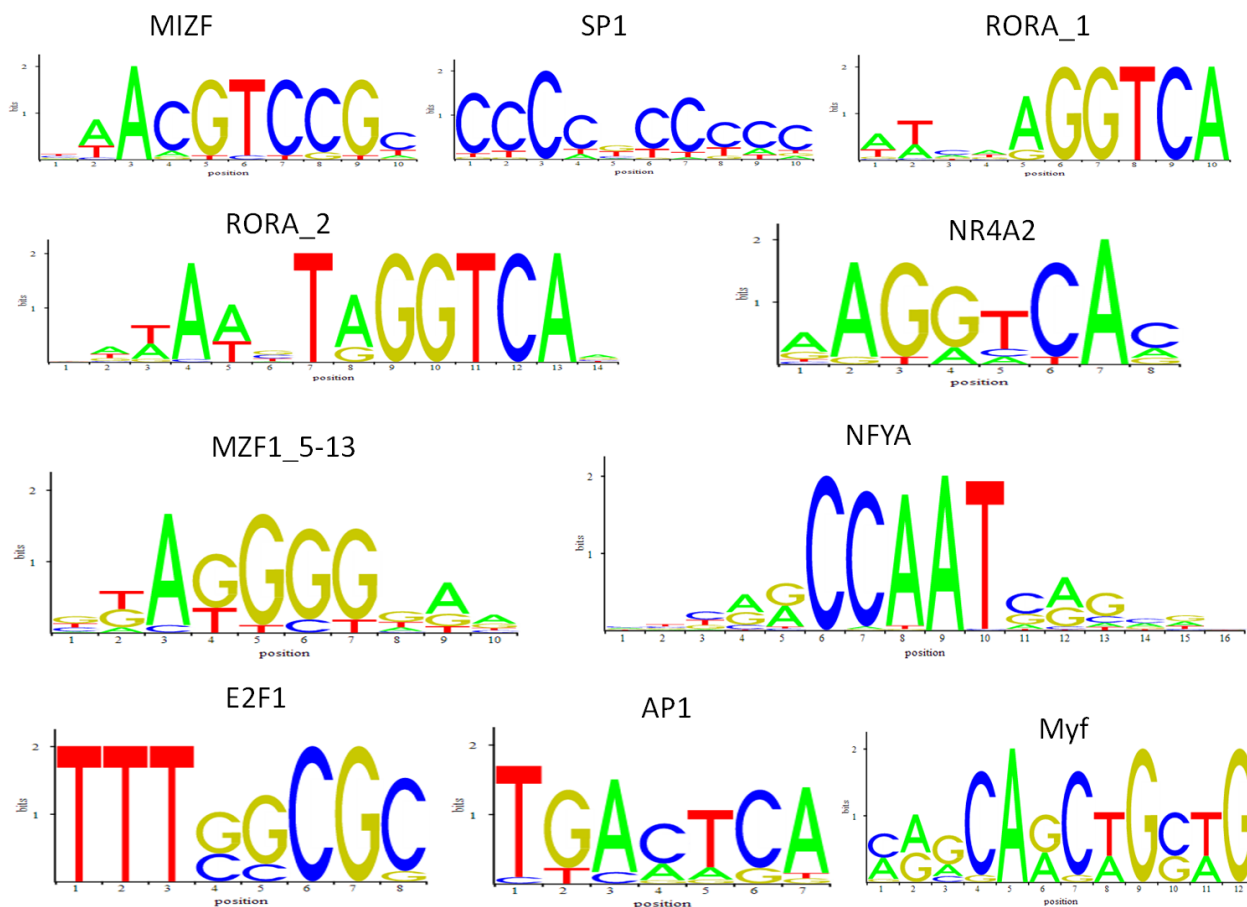


**Figure 4.4** The sequence logos of transcription factors identified in ULK1.

On further grouping based on their class, we observed that major over-represented TFBS (43/58) in ULK1 were of zinc-coordinating class (**Table 4.4**), followed by winged helix–turn–helix, zipper type, alpha helix and Ig-fold. Zinc coordinating class of TFs contains zinc fingers (ZnFs), a widespread protein domain, and the spacing of these zinc-coordinating residues gives rise to diverse classes of ZnFs.

**Table 4.3** oPOSSUM showing over-represented transcription factor binding sites, their Z score and Fisher score. Here Transcription Factors selected have Z score > 1

TF	JASPAR ID	CLASS	FAMILY	TARGET GENE HITS	TARGET TFBS HITS	Z-SCORE	FISHER SCORE
Zfx	MA0146.1	Zinc-coordinating	BetaBetaAlpha-zinc finger	1	5	16.721	0.919
Tcfcp2l1	MA0145.1	Other	CP2	1	4	12.964	0.849
Klf4	MA0039.2	Zinc-coordinating	BetaBetaAlpha-zinc finger	1	8	11.997	0.596
MIZF	MA0131.1	Zinc-coordinating	BetaBetaAlpha-zinc finger	1	1	11.047	2.476
Egr1	MA0162.1	Zinc-coordinating	BetaBetaAlpha-zinc finger	1	2	9.729	1.358
SP1	MA0079.2	Zinc-coordinating	BetaBetaAlpha-zinc finger	1	6	8.687	0.692
RORA_2	MA0072.1	Zinc-coordinating	Hormone-nuclear Receptor	1	1	8.63	1.936
NR4A2	MA0160.1	Zinc-coordinating	Hormone-nuclear Receptor	1	5	7.765	0.577
RORA_1	MA0071.1	Zinc-coordinating	Hormone-nuclear Receptor	1	2	6.65	1.054
NFYA	MA0060.1	Other Alpha-Helix	NFY CCAAT-binding	1	1	5.88	1.44
Zfp423	MA0116.1	Zinc-coordinating	BetaBetaAlpha-zinc finger	1	1	5.353	1.47
ZEB1	MA0103.1	Zinc-coordinating	BetaBetaAlpha-zinc finger	1	8	4.153	0.349
Foxa2	MA0047.2	Winged Helix-Turn-Helix	Forkhead	1	2	2.758	0.753
MZF1_5-13	MA0057.1	Zinc-coordinating	BetaBetaAlpha-zinc finger	1	3	2.147	0.612
E2F1	MA0024.1	Winged Helix-Turn-Helix	E2F	1	1	2.033	1.115
GABPA	MA0062.2	Winged Helix-Turn-Helix	Ets	1	1	1.883	0.973
AP1	MA0099.2	Zipper-Type	Leucine Zipper	1	4	1.584	0.412
Stat3	MA0144.1	Ig-fold	Stat	1	1	1.386	0.918
Esrrb	MA0141.1	Zinc-coordinating	Hormone-nuclear Receptor	1	1	1.181	0.89
Myf	MA0055.1	Zipper-Type	Helix-Loop-Helix	1	1	1.031	0.891

**Table 4.4** The class-wise classification of the transcription factors detected in ULK1 gene

CLASS NAME	TFS	TOTAL GENE HITS	TFBS HITS
Zinc-coordinating	Zfx, Klf4, MIZF, Egr1, SP1, RORA_1, RORA_2, NR4A2, Zfp423, ZEB1, MZF1_5-13, Esrrb	12	43
Other	Tcfcp2l1	1	4
Other Alpha-Helix	NFYA	1	1
Winged Helix-Turn-Helix	Foxa2, E2F1, GABPA	3	4
Zipper-Type	AP1, Myf	2	5
Ig-fold	Stat3	1	1

The interactions of these classes of TFs with the ULK1 gene could be utilized to modulate its expression, which in turn could alter autophagy pathway. The latter recently has been shown to involve in various 324 diseases and its manipulation could be utilized for therapeutic interventions [319-321].

#### 4.1.3 Post-translational modification sites with their annotations on ULK1 protein domain structure

Phosphorylation and palmitoylation sites play a crucial role in protein–protein interactions, hence in the functions of a protein [322, 323]. As mentioned earlier, ULK1 activity is controlled by phosphorylation events and in addition, it also phosphorylates its substrates for modulating their activity [304, 306]. Most of the processes occurring in a cell are controlled by signaling cascade dependent on phosphorylation/de-phosphorylation. Hence, detection of the phosphorylation sites in ULK1 could be helpful to understand its various functional aspects as well as its involvement in various diseases like bone cancer, cervical adenocarcinoma, gastric cancer and lung cancer [305]. For prediction of phosphorylation sites at serine (S), threonine (T), and tyrosine (Y) amino acids in ULK1, the NetPhos algorithm was used; representing the prediction score  $\geq 0.5$  as phosphorylated. The ordered information retrieved from NetPhos includes protein ID, phosphorylated AA in the sequence, a stretch of 9 AAs with the phosphorylated residue at the center and the score. A complete list of all the phosphorylation sites identified in ULK1 is shown in **Appendix B.Table 1**. Some of the predicted phosphorylation sites have already been verified experimentally and the corresponding PubMed IDs are represented in **Table 4.5**.



**Table 4.5** Experimentally verified phosphorylation sites in ULK1

NAME	POSITION	CONTEXT SEQUENCE	SCORE	PREDICTION	PREDICTED KINASE	PUBMED IDS
ULK1_HUMAN	225	FQASSPQDL	0.993	*S*	-	19807128
ULK1_HUMAN	317	ASPPSLGEM	0.732	*S*	PKC $\alpha$	22932492
ULK1_HUMAN	403	GRTSPSPSP	0.924	*S*	GSK3 $\beta$	22932492
ULK1_HUMAN	405	TPSPSPPCS	0.987	*S*	GSK3 $\beta$	21383122
ULK1_HUMAN	411	PCSSSPSPS	0.895	*S*	GSK3 $\beta$ , ERK1	22932492
ULK1_HUMAN	460	TPRSSAIRR	0.962	*S*	-	22932492
ULK1_HUMAN	465	AIRRSGSTS	0.984	*S*	-	16964243
ULK1_HUMAN	467	RRSGSTSPL	0.986	*S*	AMPK, PKC $\delta$	19807128
ULK1_HUMAN	469	SGSTSPLGF	0.975	*S*	ERK1	21383122
ULK1_HUMAN	477	FARASPSPP	0.989	*S*	ERK1	18691976
ULK1_HUMAN	479	RASPSPPAH	0.891	*S*	CDC2, CDK5	21383122
						18691976
						19807128
ULK1_HUMAN	495	ARKMSLGG G	0.969	*S*	AMPK AKT PKA PKC $\delta$ PKC $\mu$	22932492
ULK1_HUMAN	533	RGGRSPRPG	0.994	*S*	CDK5	21383122
ULK1_HUMAN	544	APEHSPRTS	0.986	*S*	CDC2 CDK5	22932492
ULK1_HUMAN	556	CRLHSAPNL	0.807	*S*	AMPK	21383122
						21205641
						18669648
						18846507
ULK1_HUMAN	694	GRSFSTSRLL	0.987	*S*	AKT	22932492
ULK1_HUMAN	716	PDPGSTESL	0.894	*S*	CK1	22932492
ULK1_HUMAN	719	GSTESLQEK	0.574	*S*	CK1	22932492
ULK1_HUMAN	747	AGGTSSPSP	0.551	*S*	-	16964243
ULK1_HUMAN	761	GSPPSGSTP	0.575	*S*	-	16964243
ULK1_HUMAN	775	TRMFSAGPT	0.983	*S*	-	21383122
ULK1_HUMAN	866	ALKGSASEA	0.886	*S*	-	19807128
ULK1_HUMAN	1042	ERRLSALLT	0.99	*S*	AMPK PKA	19807128
ULK1_HUMAN	456	TQFQTPRSS	0.971	*T*	-	18669648
ULK1_HUMAN	636	DFPKTPSSQ	0.671	*T*	CDK5	22932492
ULK1_HUMAN	695	RSFSTSRLLT	0.975	*T*	-	22932492

Among these phosphorylation sites, the newly identified phosphorylation sites are portrayed in **Figure 4.5** with their position in the domains of the ULK1 protein. We found a new phosphorylation site in ULK1 at amino acid position 295 of Y residue in the kinase domain with the significant score (0.809), which has not been verified experimentally and could further be studied to unravel its impact on the protein function. This tyrosine phosphorylation site is present in the kinase domain of the gene and thus may regulate the phosphotransferase activity of the protein.

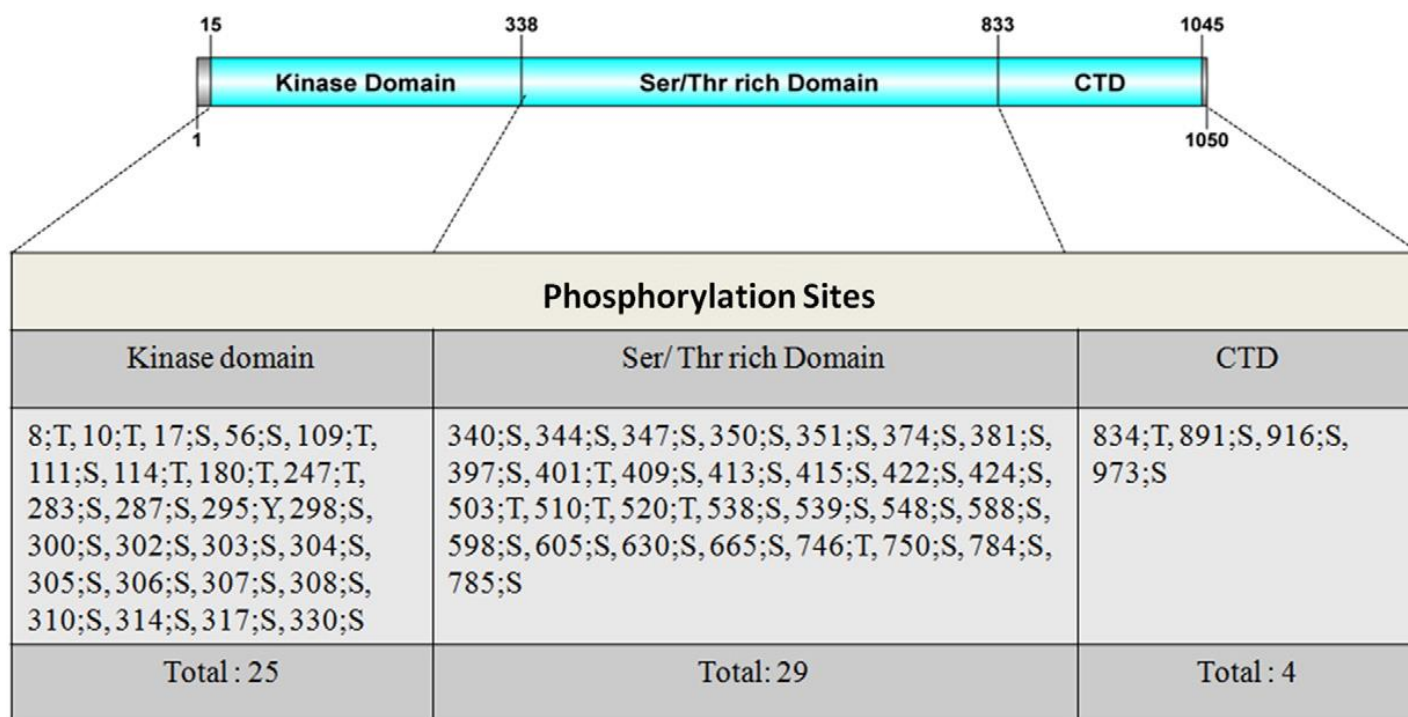


**Figure 4.5** The ULK1 domain structure with newly identified phosphorylation sites. The NetPhos algorithm was used for prediction of phosphorylation sites at S, T and Y residues. A total of 58 new phosphorylation sites were identified out of which 25 are in the kinase domain, 29 are in Ser/Thr rich domain and only 4 are in the CT domain.

In ULK1, we found 4 palmitoylation sites at positions 426, 927, 1003 and 1049 (**Table 4.6**) which could further be investigated for their role in trafficking and protein–protein interactions. These are the putative positions where the palmitic acid may attach to the protein at cysteine residues for its attachment to the membrane.

**Table 4.6** The putative palmitoylation sites in ULK1. Four novel putative palmitoylation sites were identified applying CSS-PALM

Protein	Position	Peptide
ULK1	426	GPFSSSRCGASVPIP
ULK1	927	QIRAGKLCLSSTVKQ
ULK1	1003	MFQHREGCVPRYHKA
ULK1	1049	SALLTGICA

#### 4.1.4 Linkage disequilibrium analysis reveals significant genetic variants and haplotypes

In order to analyze various genetic parameters (including linkage disequilibrium (LD), haplotypes and SNPs) for *ULK1* gene, the genotype data of CEU (CEPH—Utah Residents with Northern and Western European Ancestry) was obtained from The International HapMap Project. The evaluation yields the information about the predisposition to various diseases due to these genetic variants upon extensive statistical analysis. These parameters act as vital biomarkers for the functional association with a variety of diseases. In this study, the LD analysis revealed an important block in the *ULK1* gene with five important SNPs having non-random associations as represented in **Figure 4.6**. The five critical SNPs out of seven SNPs identified were rs9652059, rs1134574, rs7953348, rs11615995 and rs11616018 with minor allele frequencies (MAF) of 0.2, 0.085, 0.198, 0.228 341 and 0.207 respectively (**Table 4.7**).

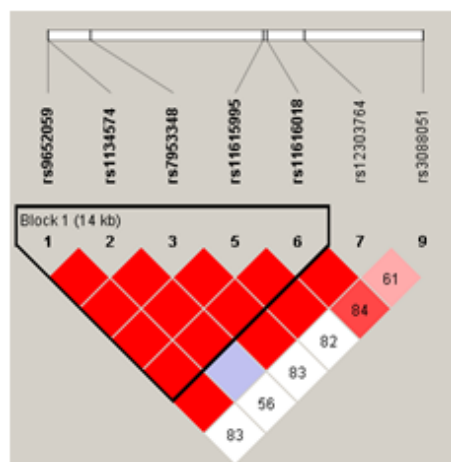


**Figure 4.6** The linkage disequilibrium plot for ULK1

**Table 4.7** The significant SNPs in *ULK1* gene with their allelic information

S.No	Name	ObsHET	PredHET	HWpval	%Genotype	MAF	Alleles
1	rs9652059	0.267	0.32	0.331	100	0.2	C:T
2	rs1134574	0.169	0.155	1	98.9	0.085	A:G
3	rs7953348	0.259	0.318	0.2774	96.7	0.198	T:C
4	rs11615995	0.316	0.352	0.6146	94.4	0.228	T:C
5	rs11616018	0.276	0.328	0.3664	96.7	0.207	T:C
6	rs12303764	0.552	0.471	0.3335	96.7	0.379	T:G
7	rs3088051	0.424	0.387	0.7676	97.8	0.263	A:G

These SNPs also had  $r^2 \geq 0.8$ , which further validated the higher correlation between the loci. Furthermore, we identified one haplotype block in the *ULK1* gene where 5 SNPs and 4 haplotypes were recognized with different population frequencies (**Figure 4.7**). The CATTT haplotype was prominently found with frequency 0.774 in the studied population.

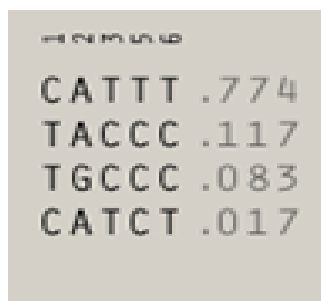


**Figure 4.7** The CATTT haplotype was prominently found with a frequency of 0.774 in the studied population.

#### 4.1.5 Prediction of nsSNPs that have damaging/deleterious effect

Numerous *in silico* tools like Sorting Intolerant From Tolerant (SIFT), Polymorphism Phenotype (PolyPhen2), PredictSNP (CADD, DANN, FATHMM, FunSeq2, and GWAVA) have been used to predict the nsSNPs and their effects on the ULK1 protein function. The coding nsSNPs may have a significant impact on the function of a protein and such SNPs could be damaging or

deleterious [324]. The predicted impact of the change in amino acid may be tolerated or damaging/deleterious based on the tolerance index and probability scores. Out of 13 nsSNPs present in ULK1, we identified 4 nsSNPs i.e. rs79965940, rs61942435, rs55824543 and rs56364352 which could have harmful functional effects on the ULK1 protein (**Table 4.8**).

## 4.2 *In silico* mutational analysis on ULK1 sequence and structure

### 4.2.1 Change in the protein stability upon mutations at sequence level

Protein stability change was predicted by iPTREE-STAB and I-MUTANT2.0 in terms of Gibbs free energy change ( $\Delta\Delta G$ ) values as shown in **Table 4.9**. The  $\Delta\Delta G$  value less than '0' signifies a decrease in protein stability while  $\Delta\Delta G$  value more than 0 signifies an increase in protein stability (**Figure 4.8**).

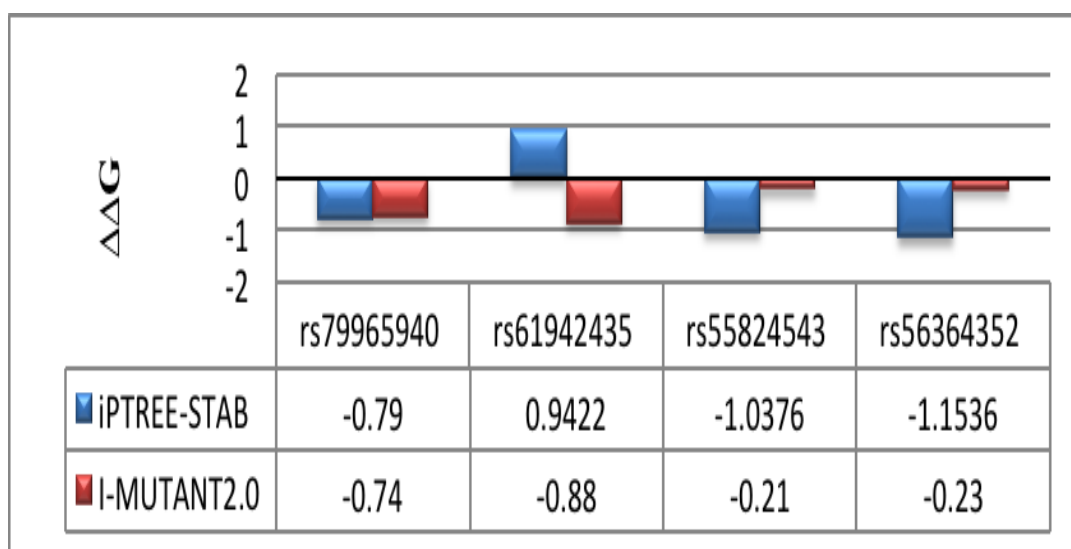


**Figure 4.8** The comparison of protein stability change upon mutations between iPTREE-STAB and i-MUTANT2.0 in terms of  $\Delta\Delta G$ .

**Table 4.8** The non-synonymous single nucleotide polymorphisms in the coding region of ULK1 with putative damaging effects

SNP	Amino	SIFT	PolyPhen-2	PredictSNP <sup>2</sup>				
	acid change			CADD	DANN	FATHMM	FunSeq2	GWAVA
rs11546871	P714L	TOLERATED	TOLERATED	TOLERATED	TOLERATED	TOLERATED	TOLERATED	TOLERATED
rs11609348	A816T	TOLERATED	TOLERATED	TOLERATED	TOLERATED	TOLERATED	TOLERATED	TOLERATED
rs12827141	P478L	TOLERATED	TOLERATED	TOLERATED	TOLERATED	TOLERATED	TOLERATED	TOLERATED
rs34936984	G745V	TOLERATED	TOLERATED	TOLERATED	TOLERATED	TOLERATED	TOLERATED	TOLERATED
rs55815560	S665L	TOLERATED	TOLERATED	TOLERATED	TOLERATED	TOLERATED	TOLERATED	TOLERATED
<b>rs55824543</b>	T503M	<b>DAMAGING</b>	TOLERATED	TOLERATED	<b>DAMAGING</b>	<b>DAMAGING</b>	<b>DAMAGING</b>	TOLERATED
<b>rs56364352</b>	S298L	TOLERATED	<b>DAMAGING</b>	TOLERATED	<b>DAMAGING</b>	<b>DAMAGING</b>	<b>DAMAGING</b>	<b>DAMAGING</b>
rs61731335	D343N	TOLERATED	TOLERATED	TOLERATED	TOLERATED	TOLERATED	TOLERATED	TOLERATED
rs61731338	A362V	TOLERATED	TOLERATED	TOLERATED	TOLERATED	TOLERATED	TOLERATED	TOLERATED
<b>rs61942435</b>	A991V	<b>DAMAGING</b>	TOLERATED	<b>DAMAGING</b>	<b>DAMAGING</b>	<b>DAMAGING</b>	<b>DAMAGING</b>	<b>DAMAGING</b>
rs74749868	T452S	TOLERATED	TOLERATED	TOLERATED	TOLERATED	TOLERATED	TOLERATED	TOLERATED
<b>rs79965940</b>	N148T	<b>DAMAGING</b>	TOLERATED	TOLERATED	TOLERATED	TOLERATED	<b>DAMAGING</b>	<b>DAMAGING</b>
rs112712246	L962M	TOLERATED	TOLERATED	TOLERATED	TOLERATED	TOLERATED	TOLERATED	TOLERATED

**Table 4.9** Prediction of protein stability change upon mutations in terms of Gibbs free energy from protein sequence by using iPTREE-STAB and i-MUTANT2.0

ULK1 nsSNP	Amino acid substitution	iPTREE-STAB $\Delta\Delta G$ Value (kcal/mol)	Stability prediction	IMUTANT2.0 $\Delta\Delta G$ Value (kcal/mol)	Stability prediction
rs79965940	N148T	-0.79	Decrease	-0.74	Decrease
rs61942435	A991V	0.9422	Increase	-0.88	Decrease
rs55824543	T503M	-1.0376	Decrease	-0.21	Decrease
rs56364352	S298L	-1.1536	Decrease	-0.23	Decrease
$\Delta\Delta G < 0$ : Decrease Stability; $\Delta\Delta G > 0$ : Increase Stability					

#### 4.2.2 Change in protein stability upon mutations at structure level

The protein stability change at structure level was predicted for rs79965940 and rs61942435 (as full protein structure of ULK1 is still not identified) by DUET and ERIS tools in terms of Gibbs free energy change ( $\Delta\Delta G$ ) values as shown in **Table 4.10**. The  $\Delta\Delta G$  value less than 0 signifies a decrease in protein stability while  $\Delta\Delta G$  value more than 0 denotes an increase in protein stability for DUET and for ERIS tool,  $\Delta\Delta G$  value less than 0 signifies an increase in protein stability while  $\Delta\Delta G$  value more than 0 signifies a decrease in protein stability. The results by DUET indicate that both mutations (N148T and A991V) decrease the protein stability; while the results from ERIS suggest that the mutation N148T decreases the protein stability and the mutation A991V increases the protein stability (**Figure 4.9**).

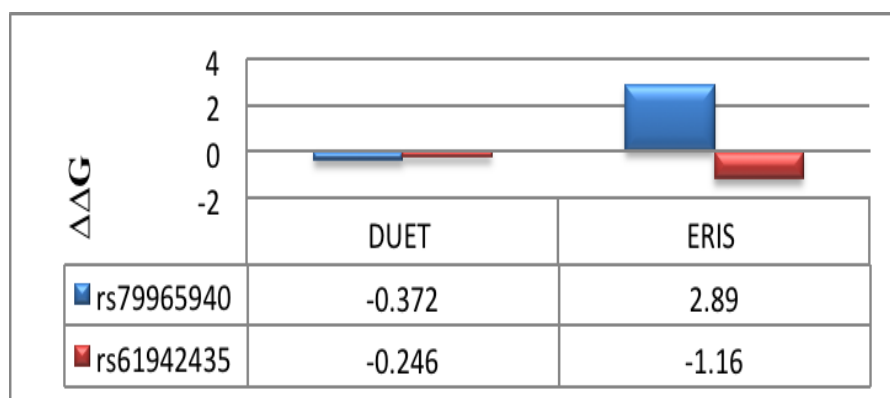


**Figure 4.9** The comparison of protein stability change upon mutations between DUET and ERIS in terms of  $\Delta\Delta G$ .

**Table 4.10** Prediction of protein stability change upon mutations in terms of Gibbs free energy from protein structure by using DUET and ERIS

ULK1 nsSNP	ULK1 structure	Amino acid substitution	DUET $\Delta\Delta G$ Value (kcal/mol)	Stability prediction	ERIS $\Delta\Delta G$ Value (kcal/mol)	Stability prediction
rs79965940	4WNO	N148T	-0.372	Decrease	2.89	Decrease
rs61942435	ULK1A <sup>1</sup>	A991V	-0.246	Decrease	-1.16	Increase

#### 4.2.3 Total energy of the protein upon mutations

Mutant structures for the mutations N148T in 4WNO and A991V in ULK1A were generated using PyMOL (Molecular Graphics System, Version 1.8 Schrödinger, LLC) and are represented in **Figure 4.10A** and **Figure 4.10B**. The energy minimization was carried out and total energy was computed using CHARMM force field (Discovery Studio 4.1) and the results are illustrated in **Table 4.11**. The total energy of native and mutant structures was compared and from the results, it was observed that the mutation N148T increased the total energy of the structure and hence could be considered as a destabilizing mutation. Whereas, the mutation A991V was found to decrease the total energy of the structure and therefore it could increase the stability of the protein.

**Table 4.11** Computation of total energy (CHARMm energy) of the native and mutant structures for mutations N148T and A991V in structures 4WNO and ULK1A predicted by CHARMM force field

S. No.	Structure	Force field	Potential energy/CHARMm energy (Kcal/mol)	Vander Waals energy (Kcal/mole)	Electrostatic energy (Kcal/mole)	Final RMS gradient (Kcal/mole X Å <sup>0</sup> )
Native	4WNO	CHARMm	-23179.83	-2145.89	-23558.82	157.4
N148T	4WNO	CHARMm	-23112.05	-2097.40	-23652.33	112.9
Native	ULK1A*	CHARMm	-4259.87	-452.66	-4320.24	24.1

<sup>1</sup>Full chain structure of ULK1 predicted and modeled by Robetta wherein  $\Delta\Delta G < 0$ : Decrease Stability;  $\Delta\Delta G > 0$ : Increase Stability (For DUET) and  $\Delta\Delta G < 0$ : Increase Stability;  $\Delta\Delta G > 0$ : Decrease Stability (For ERIS)



A991V	ULK1A*	CHARMm	-4268.66	-449.41	-4346.36	24
-------	--------	--------	----------	---------	----------	----

\* Full chain structure of ULK1 predicted and modeled by Robetta.

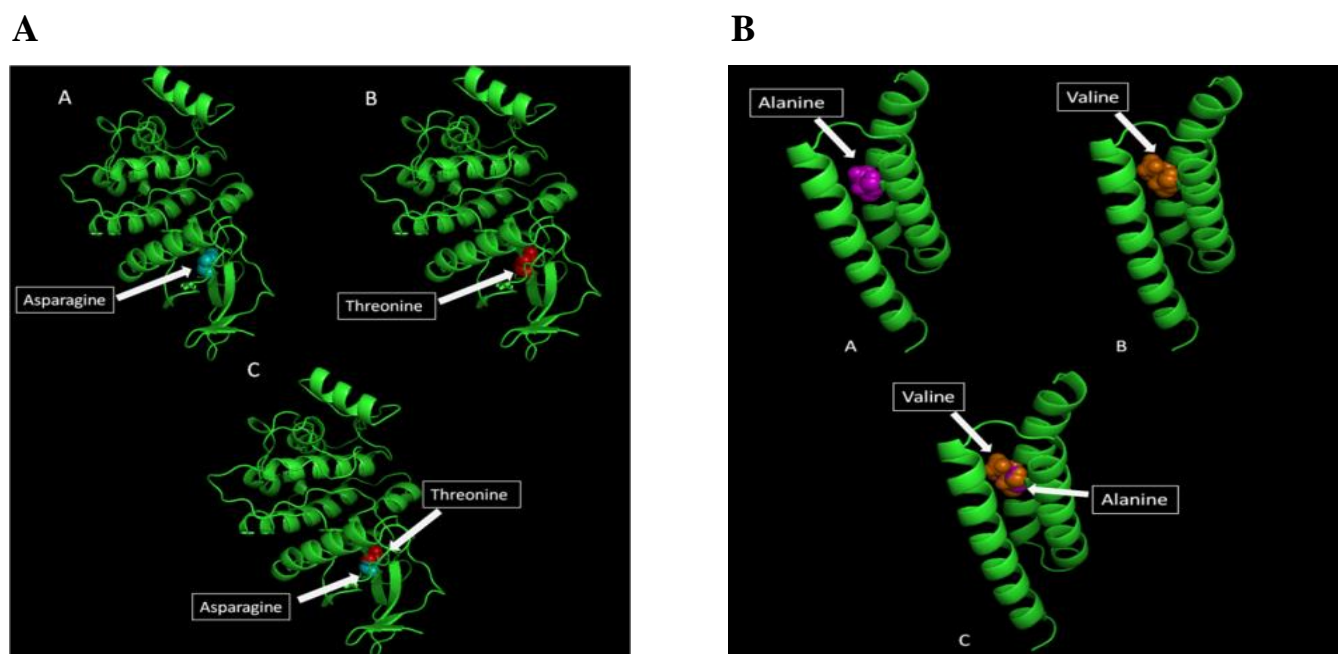


**Figure 4.10** **A**) Structural representation of nsSNP rs79965940 (N148T) on the PDB structure of ULK1 (4WNO). (A) Native structure 4WNO with amino acid Asparagine at position 148. (B) Mutant structure N148T 4WNO with amino acid substitution as Threonine at position 148. (C) Superimposed native (4WNO) and mutant structures (N148T 4WNO). **B**) Structural representation of nsSNP rs61942435 (A991V) on the modeled structure of ULK1 (ULK1A). (A) Native structure ULK1A with amino acid Alanine at position 991 (B) Mutant structure A991V ULK1 with amino acid substitution as Valine at position 991. (C) Superimposed native (ULK1A) and mutant structures (A991V ULK1A).

### 4.3 Validation of *in silico* analysis

#### 4.3.1 Study subjects

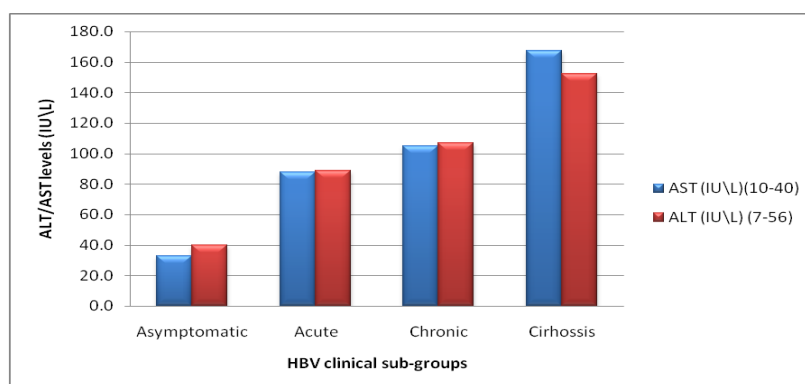
The detail of the base-line biochemical and demographic characteristics of the patients investigated in this study are described in **Table 4.12**.

#### 4.3.2 Liver function tests (LFT)

Collected serum of 500 patients was used for the analysis of LFT for enzyme Aspartate Aminotransferase (AST), also known as Serum Glutamic Oxaloacetic Transaminase (SGOT) and Alanine Aminotransferase (ALT), also known as Serum Glutamic Pyruvic Transaminase (SGPT) (**Figure 4.11**). These biochemical values were further used for differentiating patients into various clinical groups.

**Table 4.12** Base-line biochemical and demographic characteristics of patients

Characteristics	Patients Characteristics	Control subjects
<b>Gender (male/female)</b>	314/186	110/90
<b>Age [Mean ± SD]</b>	35±14	37±13
<i>History of alcohol consumption</i>		
<b>Yes (%)</b>	296 (59.2%)	20 (10%)
<b>No (%)</b>	204 (40.8%)	180 (90%)
<b>HBsAg</b>	+ve	-ve
<b>HCV</b>	-ve	-ve
<b>HIV</b>	-ve	-ve
<b>ALT (Mean ± SD)</b>	89.10±86.35	33.4±13.4
<b>AST (Mean ± SD)</b>	87.95±72.88	25.6±8.8
<i>Clinical diagnosis</i>		
<b>Asymptomatic carrier</b>	142 (28.4%)	-ve
<b>Acute Hepatitis</b>	114 (22.8%)	-ve
<b>Chronic Hepatitis</b>	207 (41.4%)	-ve
<b>Liver cirrhosis</b>	37 (7.4%)	-ve

**Figure 4.11** Category-wise liver function test levels in hepatitis B infected patients.

### 4.3.3 Quantification and grouping of HBV infected patients

The HBV DNA from 500 patients was isolated and subjected to quantification of viral load by quantitative RT-PCR. As shown in **Figure 4.12**, there was a significant increase in HBV DNA levels with respect to the severity of HBV infection among the patients.

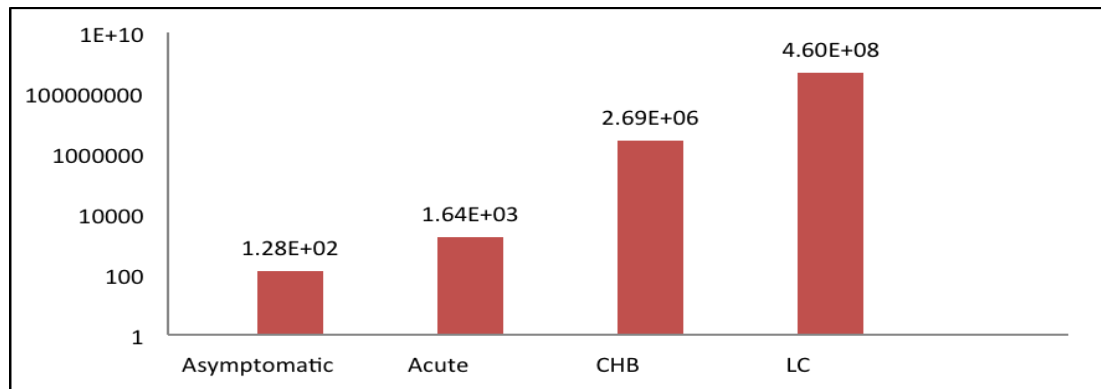


**Figure 4.12** The HBV DNA levels in Hepatitis B infected patients.

### 4.3.4 Genetic correlation of nsSNP in Hepatitis B patients and healthy controls

#### 4.3.4.1 Genotyping nsSNP rs79965940 A/C (N148T)

The dbSNP database was used to retrieve the information of nsSNP rs79965940 A/C and to design the specific primers for amplification of the polymorphic site. The amplified product were then digested with the enzyme *MmeI* at the specific position of the SNP. The primers pair was checked for their specificity using the primer-BLAST tool which was further checked for their specificity using the BLAST tool and IDT Oligo Analyzer tool (<https://eu.idtdna.com/calc/analyzer>) [325, 326]. **Table 4.13** shows the primer sequences, amplified product size and the expected fragment sizes after RFLP analysis.

##### 4.3.4.1.1 PCR-RFLP

PCR was carried using the specific primers for genotyping the nsSNP rs79965940. For best PCR results, major parameters of the PCR cycle (annealing temperature, Taq DNA polymerase concentration, and primer concentration) were optimized as mentioned in the **Table 4.14**. The amplified PCR products were analyzed on 1.5% agarose gel with ethidium bromide.

**Table 4.13** The primer sequences and expected banding pattern for nsSNP rs79965940 A/C

ULK1 SNP	Primer sequences 5'– 3'	Amplified product size (bp)	Restriction enzyme	Banding pattern (bp)
rs79965940 (A/C)	F:TGGTAGATGGACAGGACCCG R:ATGGTGTGTTTACCTTGCC	822 bp	<i>MmeI</i>	CC-822 bp; AA-625 bp, 197 bp;AC- 822 bp,625 bp and 197 bp

**Table 4.14** The standardized PCR parameters for nsSNP rs79965940 A/C (N148T)

ULK1 Polymorphism	PCR components	Gradient range	Optimal condition
rs79965940 (A/C)	Annealing temperature	48–65 °C	58 °C
	Taq DNA polymerase	0.5 U–5.0 U	2.5U
	Primers	0.05 - 0.4 µmol	0.2µmol

The optimized PCR amplification conditions were used to amplify DNA segments from 500 HBV infected samples and 200 healthy control samples in order to genotype the nsSNP rs79965940. The optimized PCR amplification conditions are shown in **Table 4.15**. Amplified PCR products were digested with *MmeI* with reaction conditions as shown in **Table 3.3** in section material and methods and we observed the homozygous wild type genotype AA (625bp, 197bp), heterozygous genotype AC (822bp, 625bp, and 197bp bands) and homozygous mutant genotype CC (822 bp) in different HBV infected individuals as well as in healthy control samples. The representative agarose gel picture is shown in **Figure 4.13**.

**Table 4.15** The optimized PCR conditions for genotyping rs79965940 nsSNP

PCR Step	Temperature	Duration
Initial Denaturation	95°C	2 minutes
Denaturation	95°C	45seconds
Annealing	<b>58°C</b>	1 minute
Extension	72°C	45 seconds
Final extension	72°C	5 minutes

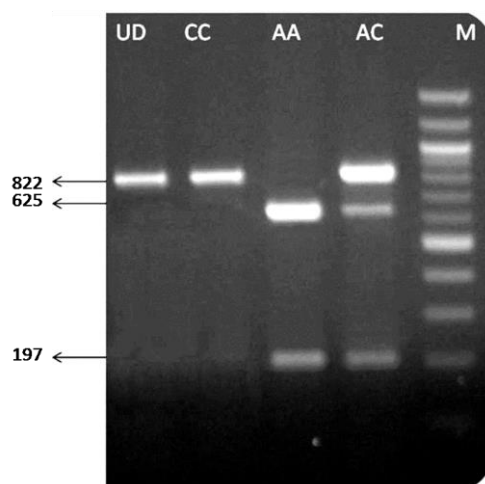


**Figure 4.13** The representative agarose gel image for genotyping nsSNP rs79965940 in HBV infected as well as in healthy control samples (UD- undigested; CC-822bp; AA-625bp, 197bp; AC- 822bp, 625bp and 197bp).

#### 4.3.4.1.2 Genetic correlation of nsSNP rs79965940 in hepatitis B patients

The genotyping data were compiled and compared for calculating the allelic and genotyping frequencies in HBV infected and healthy control samples. The nsSNP rs79965940 was found to be associated with HBV infection susceptibility (OR- 1.4; 95% CI-1.08 to 1.81; p-0.01) in allelic model and homozygous model (OR- 1.85; 95% CI-1.11 to 3.10; p-0.01) (**Table 4.16**).

**Table 4.16** Genotypic and allelic frequencies of ULK1 polymorphism rs79965940 in HBV cases and healthy control samples (N = total number of samples)

ULK1 nsSNP rs79965940 (A/C)	HBV (N=500 )	Control (N =200)	Odds ratio [95% CI]	p-value
AA	260 (52 %)	118 (59 %)	Ref.	
AC	150 (30 %)	60 (30 %)	1.13 (0.78-1.64)	0.50
CC	90 (18 %)	22 (11 %)	<b>1.85 (1.11-3.10)</b>	<b>0.01</b>
AC+CC	240 (48 %)	82 (41 %)	1.32 (0.95-1.85)	0.09
AC+AA	410 (52 %)	178 (89 %)	1.04 (0.79-1.38)	0.75
A	670 (67 %)	296 (74 %)	Ref.	
C	330 (33 %)	104 (26 %)	<b>1.40 (1.08-1.81)</b>	<b>0.01</b>

#### 4.3.4.1.3 Genetic correlation of nsSNP rs79965940 in hepatitis B patients with different clinical groups

The study patients were broadly stratified into four clinical categories (according to Asian Pacific Association for the Study of the Liver (APASL) guidelines) based on the severity of HBV infection, which includes asymptomatic, acute, chronic and liver cirrhosis [327]. When these clinical groups were compared to healthy individuals, regression analysis for ULK1 nsSNP rs79965940 provided a supportive and remarkable outcome which supports our above mentioned results. As shown in **Table 4.17**, nsSNP rs79965940 also showed a significant association with two clinical categories, i.e. acute patients group (OR 1.5; 95% CI-1.08 to 2.18; p-0.01) and chronic hepatitis B (CHB) patients group (OR- 1.4; 95% CI-1.03 to 1.90; p-0.02), but no such association was seen with asymptomatic patients group and liver cirrhosis patients group.

**Table 4.17** The allelic frequencies and odds ratio for ULK1 polymorphism rs79965940 in HBV subgroup and healthy control samples (N = Total number of samples)

ULK1 nsSNP	Clinical Subgroup (N)	Allele frequency			OR (95% CI)	p-value
			HBV	Controls		
rs79965940 (A/C)	Asymptomatic (142)	A	194 (68%)	296 (74%)	1.3 (0.94-1.84)	0.1
		C	90 (32%)	104 (26%)		
	Acute Hepatitis (114)	A	148 (65%)	296 (74%)	<b>1.5 (1.08-2.18)</b>	<b>0.01</b>
		C	80 (35%)	104 (26%)		
	Chronic Hepatitis (207)	A	277 (67%)	296 (74%)	<b>1.4 (1.03-1.90)</b>	<b>0.02</b>
		C	137 (33%)	104 (26%)		
	Liver cirrhosis (37)	A	51 (69%)	296 (74%)	1.2 (0.74-2.20)	0.36
		C	23 (31%)	104 (26%)		

A 'p-value' <0.05 was considered significant. The significant values are shown in bold.

**Table 4.18** Analysis of the virological and biochemical parameters of HBV infected patients with rs79965940 (A/C) genotype

HBV infection category (N= no. of samples)	Genotypes (n= no. of samples)	Viral load (IU/ml) [Mean±SD]	p value	AST (U/L) [Mean±SD]	p value	ALT (U/L) [Mean±SD]	p value	Bilirubin (mg/dL) [Mean±SD]	p value
Asymptomatic (N=142)	AA (n=77)	129.6±108.4	0.09*	49.2±38.5	0.10*	88.5±81.5	0.90*	0.87±0.46	0.81*
	AC (n=40)	96.2±84.4	0.11**	62.1±44.1	<b>0.0004**</b>	86.5±84.5	0.94**	0.85±0.40	0.62**
	CC (n=25)	172.6±140.5	0.69#	84±48.4	0.61#	87.2±68.9	0.41#	0.82±0.36	0.45#
	AC+AA(n=117)	118.21±101.6	0.56###	54±41	<b>0.0016###</b>	88.5±81.2	0.94###	0.77±0.56	0.66###
	AC+CC (n=65)	125.2±114.6	0.97†	70.5±47	0.90†	88.6±81.4	0.82†	0.80±0.50	0.95†
Acute (N=114)	AA (n=58)	1141.4±1312	<b>0.04*</b>	56.0±35	0.08*	89±86.6	0.87*	0.87±0.46	0.09*
	AC (n=32)	1808.5±1788.3	<b>0.01**</b>	76±73.1	0.64**	86.3±60.5	0.97**	0.87±0.44	0.64**
	CC (n=24)	1948.8±1427.2	<b>0.004#</b>	83.4±35	0.48#	86.8±63.7	0.48#	0.87±0.46	0.10#
	AC+AA(n=90)	1552.5±1501	0.24###	63.4±52.3	0.07###	89±86.4	0.11###	0.87±0.46	0.53###
	AC+CC (n=56)	1868.6±1631	0.08†	79.70±59.4	0.77†	86.7±63.5	0.29†	0.87±0.46	0.41†
Chronic (N=207)	AA (n=105)	2115240±3521145	0.43*	87.6±73	0.12*	88.6±86.5	0.24*	0.9±0.5	0.21*
	AC (n=67)	2848452± 8561436	<b>0.02**</b>	87.4±71.3	0.24**	87.9±81.0	0.53**	0.9±0.5	0.80**
	CC (n=35)	4102654.2 ±6338537.5	0.44#	87±71.3	0.35#	88±81.1	0.21#	0.88±0.46	0.32#
	AC+AA(n=172)	2400851± 5996641.3	0.13###	87.9±73	0.31###	89.2±86.5	0.76###	0.88±0.46	0.72###
	AC+CC (n=102)	3278816± 7860079.2	0.75†	87.2±71.2	0.25†	87.8±81	0.65†	0.88±0.46	0.77†
Cirrhosis (N=37)	AA (n=20)	66475177.4±19098763	<b>0.05*</b>	87.6±71.6	0.24*	88.3±81.3	0.11*	0.87±0.46	0.81*
	AC (n=11)	1108100518±2313018546	<b>0.05**</b>	88.9±49.9	0.15**	89.8±56.7	0.37**	0.89±0.45	0.87**
	CC (n=6)	10727784828±25097159870	0.21#	86±73.8	0.22#	85.8±88.1	0.13#	0.86±0.46	0.93#
	AC+AA(n=31)	436084169±1428371570	<b>0.02###</b>	87.4±71.3	0.57###	88±81.1	0.25###	0.87±0.46	0.69###
	AC+CC (n=17)	4503283215±14920841461	0.75†	87.8±71.7	0.51†	88.5±81.5	0.06†	0.87±0.46	0.99†

\* Student's t test (AA vs. AC), \*\* (CC vs. AA), # (AC vs. CC), ### (AC+AA vs. CC), † one-way ANOVA - (b/w all pairs), p value <0.05 was considered significant, ALT: Alanine aminotransferase; AST: Aspartate aminotransferase.

#### 4.3.4.2 Genotyping nsSNP rs55824543 C/T (T503M)

The dbSNP database was used to retrieve the information of the nsSNP rs55824543 (C/T) and to design the specific primers for amplification of the DNA fragment that contain polymorphic site. The amplified product was then digested with the enzyme *NspI* at a specific position of the SNP. The primer pairs were checked for their specificity using the primer-BLAST tool and were further checked for their specificity using the BLAST tool and IDT Oligo Analyzer tool [325, 326]. The **Table 4.19** shows the primer sequences, amplified product size, restriction enzyme and the expected fragment sizes after RFLP analysis of nsSNP rs55824543 (C/T).

**Table 4.19** The primer sequences and expected banding pattern for nsSNP rs55824543 (C/T)

ULK1 SNP	Primer sequences 5'– 3'	Amplified product size (bp)	Restriction enzyme	Banding pattern (bp)
rs55824543 (C/T)	F:AAAGCTAAGGGGCCAACTCC R:GTGGAACAGAAGCCAACTGC	703 bp	<i>NspI</i>	CC-703 bp; TT- 365 bp and 338 bp; CT- 703 bp,365 bp and 338 bp

##### 4.3.4.2.1 PCR-RFLP

The PCR was carried using the specific primers for genotyping the nsSNP rs55824543 (C/T). For best PCR results, the cycling parameters of the PCR amplification (annealing temperature, Taq DNA polymerase concentration, and primer concentration) were optimized as mentioned in the **Table 4.20**. The amplified PCR products were analyzed on 1.5% agarose gel with ethidium bromide.

**Table 4.20** The optimized components for PCR amplification for genotyping of rs55824543 (C/T)

ULK1 Polymorphism	PCR components	Gradient range tried	Optimal condition
rs55824543 (C/T)	Annealing temperature	48–65 °C	60 °C
	Taq DNA polymerase	0.5 U–5.0 U	2.5U
	Primers	0.05 - 0.4 µmol	0.2µmol



The optimized PCR conditions were used to amplify the DNA segments from 500 HBV infected samples and 200 healthy control samples in order to genotype the nsSNP rs55824543 (C/T). The optimized PCR amplification parameters are presented in **Table 4.21**. Amplified PCR product was digested with *NspI* and all the genotypes were observed i.e. homozygous wild type genotype CC (703bp), heterozygous genotype CT (703bp, 365bp, and 338bp) and homozygous mutant genotype TT (365bp and 338bp) in different HBV infected as well as in control samples. The representative agarose gel image is shown in **Figure 4.14**.

**Table 4.21** The optimized PCR conditions for genotyping nsSNP rs55824543 (C/T)

PCR Step	Temperature	Duration
Initial Denaturation	95°C	2 minutes
Denaturation	95°C	45seconds
Annealing	60°C	40seconds
Extension	72°C	45 seconds
Final extension	72°C	5 minutes

} 35 cycles

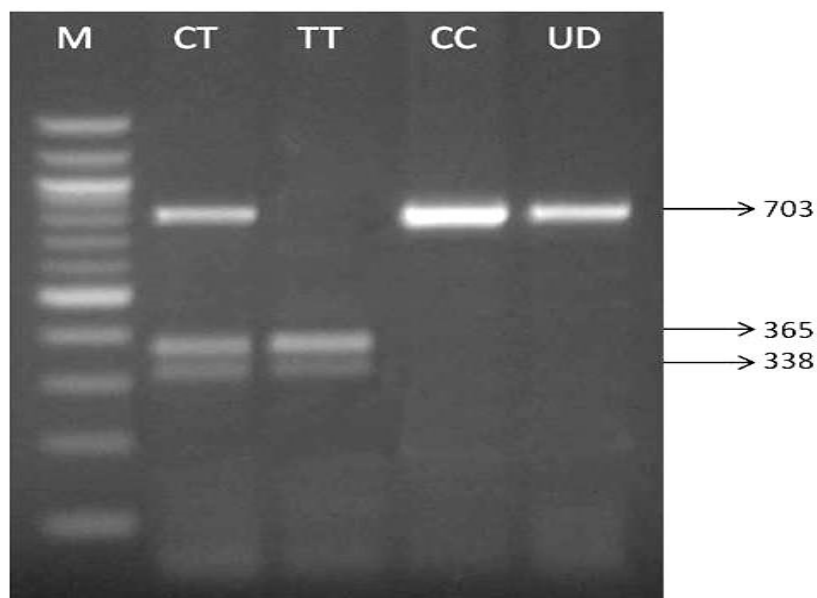


**Figure 4.14** The representative agarose gel picture for genotyping nsSNP rs55824543 (C/T) in HBV infected as well as healthy control samples (UD- undigested; CC- 703bp; TT- 365bp and 338bp; CT- 703bp, 365bp and 338bp).

#### 4.3.4.2.2 Genetic correlation of nsSNP rs55824543 (C/T) in hepatitis B patients

The genotyping data were compiled and compared for calculating the allelic and genotyping frequencies in 500 HBV infected and 200 healthy control samples. The nsSNP rs55824543 (C/T) was not found to be associated with HBV susceptibility in the allelic model (OR- 0.83; 95% CI- 0.63 to 1.10; p-0.20), as well as in any other genetic model analyzed as illustrated in **Table 4.22**.

**Table 4.22** Genotypic and allelic frequencies of ULK1 polymorphism rs55824543 (C/T) in HBV cases and healthy control samples (N = total number of samples)

ULK1 nsSNP rs55824543 (C/T)	HBV (N=500 )	Control (N =200)	Odds ratio [95% CI]	p-value
CC	350 (70%)	130 (65%)	Ref.	
CT	96 (19.2%)	46 (23%)	0.77 (0.51-1.16)	0.21
TT	54 (10.8%)	24 (12%)	0.83 (0.49-1.40)	0.49
CT+TT	150 (30%)	70 (35%)	0.79 (0.56-1.12)	0.19
CT+CC	446 (89.2%)	176 (88%)	0.94 (0.72-1.22)	0.65
C allele	796 (79.6%)	306 (76.5%)	Ref.	
T allele	204 (20.4%)	94 (23.5%)	0.83(0.63-1.10)	0.20

#### 4.3.4.2.3 Genetic correlation of nsSNP rs55824543 (C/T) in different HBV infection clinical groups

Based on the severity of HBV infection, the patients population under study was broadly stratified into four clinical categories, which includes asymptomatic, acute, chronic and liver cirrhosis categories. When these clinical groups were compared to healthy individuals, regression analysis for ULK1 nsSNPs rs55824543 (C/T) did not show any significant association with any of the clinical categories of HBV infection as depicted in **Table 4.23**.

**Table 4.23** The allelic frequencies and odds ratio of ULK1 polymorphism rs55824543 (C/T) in HBV subgroup and healthy control samples (N = total number of samples)

ULK1 SNP	Clinical Group	Allele frequency			OR (95% CI)	<i>p</i> -value
			HBV	Controls		
rs55824543 (C/T)	Asymptomatic (142)	C	229 (80%)	306 (76.5%)	0.78 (0.53- 1.13)	0.19
		T	55 (20%)	94 (23.5%)		
	Acute Hepatitis (114)	C	172 (75%)	306 (76.5%)	1.05 (0.72- 1.54)	0.76
		T	56 (25%)	94 (23.5%)		
	Chronic Hepatitis (207)	C	333 (80%)	306 (76.5%)	0.79 (0.56- 1.10)	0.17
		T	81 (20%)	94 (23.5%)		
	Liver cirrhosis (37)	C	62 (84%)	306 (76.5%)	0.63 (0.32- 1.21)	0.07
		T	12 (16%)	94 (23.5%)		

A '*p*-value' <0.05 was considered significant. Significant values are shown in bold.

**Table 4.24** Analysis of the virological and biochemical parameters of HBV infected patients with rs55824543 (C/T) genotype

HBV infection category (N= no. of samples)	Genotypes (n= no. of samples)	Viral load (IU/ml) [Mean±SD]	p value	AST (U/L) [Mean±SD]	p value	ALT (U/L) [Mean±SD]	p value	Bilirubin (mg/dL) [Mean±SD]	P value
Asymptomatic (N=142)	CC (n=100)	127.2±113.4	0.39*	61.4±50.0	0.44*	49.3±57.7	0.58*	0.57±0.24	0.69*
	CT (n=29)	107.6±86.1	0.15**	54.1±20.1	0.48**	58.1±118.4	0.32**	0.55±0.25	0.58**
	TT(n=13)	176.3±131.5	<b>0.05</b> #	51.6±24.2	0.72#	33.5±16.9	0.46#	0.53±0.28	0.64#
	CC+CT(n=129)	122.3±107.5	0.09###	59.1±45.3	0.55###	51.6±74.0	0.38###	0.60±0.24	0.32###
	CT+TT (n=42)	129.6±105.2	0.27†	53.7±21.4	0.13†	51.0±98.5	0.56†	0.60±0.30	0.56†
Acute (N=114)	CC (n=73)	1864.7±1608.7	<b>0.007</b> *	50.6±29.7	<b>0.004</b> *	84.8±44.5	0.56*	0.92±0.43	0.21*
	CT (n=26)	950.6±979.4	0.73**	83.2±81.1	0.01**	92.7±88.7	0.52**	0.80±0.40	0.67**
	TT (n=15)	1711.2±1309.9	0.04#	74.8±54.9	0.72#	76.8±41.6	260.51#	0.87±0.40	0.59#
	CC+CT(n=99)	1624.1±1519.1	0.83###	66.4±49.1	0.54###	86.2±58.4	<0.55###	0.90±0.41	0.79###
	CT+TT (n=41)	1228.0±1156.9	0.15†	79.8±72.3	0.29†	86.0±74.9	0.19†	0.83±0.40	0.59†
Chronic (N=207)	CC (n=148)	2759109.8±6360608.6	<b>0.03</b> *	98.0±57.5	<b>0.04</b> *	99.3±56.1	0.12*	1.1±0.51	1.00*
	CT (n=37)	224144.3±6301945.6	0.69**	131.6±159.7	0.68**	128.8±199.5	0.14**	1.1±0.56	0.15**
	TT (n=22)	2210874.0±3211929.3	0.17#	103.0±21.8	0.41#	117.2±39.5	0.79#	0.94±0.36	0.23#
	CC+CT(n=185)	197513.2±6331894.5	0.14###	104.9±88.7	0.95###	105.2±102.3	<0.57###	1.09±0.54	0.20###
	CT+TT (n=59)	2511715.6±5332955.6	0.85†	120.8±127.1	0.35†	124.8±158.3	0.78†	1.02±0.40	0.97†
Cirrhosis (N=37)	CC (n=29)	2653568178±11499277882	0.67*	170±82.2	0.96*	158±92.6	0.54*	0.95±0.30	0.19*
	CT (n=4)	158143393.3±162019591.0	0.66**	168.3±42.0	0.53**	129.0±47.1	0.55**	0.74±0.25	0.20**
	TT (n=4)	74816866±696008690.5	0.82#	144.3±21.8	0.34#	129.3±31.9	1.00#	0.81±0.50	0.81#
	CC+CT(n=33)	2351092447.1±10788453143.8	0.67###	170.7±78.2	0.51###	155.2±88.8	0.56###	0.92±0.30	0.52###
	CT+TT (n=15)	116480130.0±123735763.5	0.75†	156.0±33.2	0.42†	129.5±37.4	0.86†	0.77±0.38	0.15†

\*Student's t test (CC vs. CT), \*\* (CC vs. TT), # (CT vs. TT), ### (CT+CC vs. TT), † one-way ANOVA - (b/w all pairs), p value <0.05 was considered significant, ALT: Alanine aminotransferase; AST: Aspartate aminotransferase.

#### 4.3.4.3 Genotyping of nsSNP rs56364352 C/T (S298L)

The dbSNP database was used to retrieve the information of the nsSNP rs56364352 C/T and to design the specific primers for amplification of DNA fragment that contains the polymorphic site. The amplified product was then digested with the enzyme *BbvI* at a specific position of the SNP. The primer pair was checked for their specificity using the primer-BLAST tool and was further checked for their specificity using the BLAST tool and IDT Oligo Analyzer tool [325, 326]. The **Table 4.25** shows the primer sequences, amplified product size, restriction enzyme and expected fragment sizes after RFLP analysis.

**Table 4.25** The primer sequences and expected banding pattern for nsSNP rs56364352 C/T

ULK1 nsSNP	Primer sequences 5'– 3'	Amplified product size (bp)	Restriction enzyme	Banding pattern (bp)
rs56364352 (C/T)	F:CCCCTCGGTCAGGAAATGTG R:AGCATGAGTAGGGTTGCAGG	866 bp	<i>BbvI</i>	CC-866 bp; TT- 458 bp and 408 bp; CT- 866 bp,458 bp and 408 bp

##### 4.3.4.3.1 PCR-RFLP

PCR was carried using the specific primers for genotyping the nsSNP rs56364352 C/T. For best PCR results, the three major parameters of the PCR cycle (annealing temperature, Taq DNA polymerase concentration, and primer concentration) were optimized as mentioned in the **Table 4.26**. Amplified PCR products were analyzed on 1.5% agarose gel stained with ethidium bromide.

**Table 4.26** The optimized conditions for genotyping of rs56364352 C/T

ULK1 Polymorphisms	PCR components	Gradient range tried	Optimal conditions
rs56364352 (C/T)	Annealing temperature	48–65 °C	60 °C
	Taq DNA polymerase	0.5 U–5.0 U	2.5U
	Primers	0.05 - 0.4 µmol	0.2µmol

The DNA segments were amplified using optimized PCR conditions in 500 HBV infected samples and 200 healthy control samples in order to genotype the nsSNP rs56364352 C/T. The optimized PCR conditions are shown in **Table 4.27**. The amplified PCR products were further incubated overnight and digested with *BbvI* for its genotyping analysis. We observed the homozygous wild type genotype CC (866bp), heterozygous genotype CT (866bp, 458bp, and 408bp bands) and homozygous mutant genotype TT (458bp and 408bp) in different HBV as well as in control samples. The representative agarose gel picture is shown in **Figure 4.15**.

**Table 4.27** The optimized PCR conditions for genotyping nsSNP rs56364352 C/T

PCR Stage	Temperature	Duration
Initial Denaturation	95°C	2 minutes
Denaturation	95°C	45seconds
Annealing	60°C	45 minute
Extension	72°C	45 seconds
Final extension	72°C	5 minutes

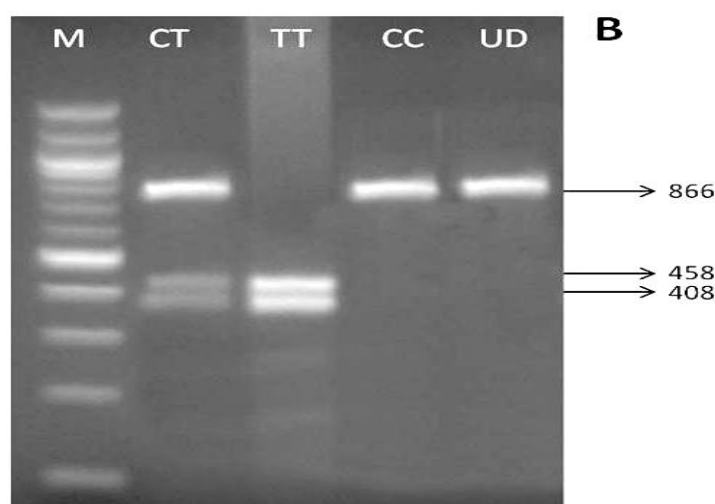


**Figure 4.15** The representative agarose gel picture for genotyping nsSNP rs56364352 C/T in HBV infected as well as healthy control samples (UD- undigested; CC-866bp; TT- 458bp and 408bp; CT- 866bp,458bp and 408bp).

#### 4.3.4.3.2 Role of nsSNP rs56364352 C/T in HBV susceptibility

Genotyping data was compiled and compared for calculating the allelic and genotyping frequencies in 500 HBV and 200 control samples. The nsSNP rs56364352 C/T was found to be associated with HBV susceptibility in allelic model (OR- 1.68; 95% CI-1.30 to 2.16;  $p < 0.01$ ). This nsSNP was also found to be associated in heterozygous model (OR- 1.72; 95% CI-1.10 to 2.47;  $p < 0.01$ ), homozygous model (OR- 2.36; 95% CI-1.40 to 3.97;  $p < 0.01$ ) and in dominant model (OR- 1.87; 95% CI-1.34 to 2.61;  $p < 0.01$ ) (**Table 4.28**).

**Table 4.28** Genotypic and allelic frequencies of *ULK1* polymorphism rs56364352 C/T in HBV cases and healthy control samples (N = total number of samples)

ULK1 nsSNP rs56364352 (C/T)	HBV (N=500)	Control (N =200)	Odds ratio [95% CI]	p-value
CC	197 (39.4%)	110 (55%)	Ref.	
CT	210 (42%)	68 (34%)	<b>1.72 (1.10-2.47)</b>	<b>&lt;0.01</b>
TT	93 (18.6%)	22 (11%)	<b>2.36 (1.40-3.97)</b>	<b>&lt;0.01</b>
CT+TT	303 (60.6%)	90 (45%)	<b>1.87 (1.34-2.61)</b>	<b>&lt;0.01</b>
CT+CC	407 (81.4%)	178 (89%)	1.27 (0.95-1.71)	0.10
C allele	604 (60.4%)	288 (72%)	Ref.	
T allele	396 (39.6%)	112 (28%)	<b>1.68 (1.30-2.16)</b>	<b>&lt;0.01</b>

#### 4.3.4.3.3 Genetic correlation of nsSNP rs56364352 C/T in different clinical groups of HBV infection

When the different clinical groups were compared to healthy individuals, regression analysis for *ULK1* nsSNP rs56364352 C/T provided outcome supports our above results mentioned in **Table 4.28**. As shown in **Table 4.29**, nsSNP rs56364352 C/T also showed a significant association with two clinical categories, i.e. acute patients group (OR 1.5; 95% CI-1.08 to 2.18;  $p < 0.01$ ) and chronic hepatitis B patients group (OR- 1.4; 95% CI-1.03 to 1.90;  $p < 0.02$ ), but no such association was seen with asymptomatic patients group and liver cirrhosis patients group.

**Table 4.29** The allelic frequencies and odds ratio of ULK1 polymorphism rs56364352 C/T in HBV subgroup and healthy control samples (N = total number of samples)

ULK1 SNP	Clinical Group	Allele frequency			OR (95% CI)	p-value
			HBV	Controls		
rs56364352 (C/T)	Asymptomatic (142)	C	170 (60%)	288 (72%)	<b>1.72 (1.20-2.30)</b>	<b>&lt;0.01</b>
		T	114 (40%)	112 (28%)		
	Acute Hepatitis (114)	C	129 (57%)	288 (72%)	<b>1.97 (1.40-2.77)</b>	<b>&lt;0.01</b>
		T	99 (43%)	112 (28%)		
	Chronic Hepatitis (207)	C	249 (60%)	288 (72%)	<b>1.70 (1.27-2.28)</b>	<b>&lt;0.01</b>
		T	165 (40%)	112 (28%)		
	Liver cirrhosis (37)	C	56 (76%)	288 (72%)	0.82 (0.46-1.46)	0.51
		T	18(24%)	112 (28%)		

A 'p-value' <0.05 was considered significant. Significant values are shown in bold.



**Table 4.30** Analysis of the virological and biochemical parameters of HBV infected patients with rs56364352 C/T genotype

HBV infection category (N=no of samples)	Genotypes (n=no of samples)	Viral load (IU/ml) [Mean±SD]	P value	AST (U/L) [Mean±SD]	P value	ALT (U/L) [Mean±SD]	P value	Bilirubin (mg/dL) [Mean±SD]	P value
Asymptomatic (N=142)	CC (n=53)	123.5±98.3	0.79*	61.8±56.1	0.06*	43.6±51.1	0.33*	0.49±0.24	0.08*
	CT (n=64)	118.5±105.5	0.18**	57.9±37.1	0.62**	57.5±93.1	1.00**	0.57±0.25	<0.001**
	TT(n=25)	160.4±143.7	0.13#	55.9±27.4	0.80#	43.6±38.5	0.47#	0.69±0.20	0.03#
	CC+CT(n=117)	120.8±101.9	0.10##	59.6±46.4	0.70##	51.2±77	0.63##	0.53±0.25	0.003##
	CT+TT (n=89)	130.3±118.2	0.91†	57.3±34.5	0.89†	53.6±81.5	0.82†	0.60±0.24	0.75†
Acute (N=114)	CC (n=39)	1532.5±1487	0.78*	60.9±38.8	0.61*	75.8±36	0.36*	0.87±0.46	0.98*
	CT (n=51)	1450.8±1375.4	0.10**	64.8±33.4	0.12**	83.4±50.2	0.08**	0.87±0.37	0.59**
	TT (n=24)	2197.5±1641.4	0.04#	84.5±82.6	0.14#	103.3±88.3	0.21#	0.93±0.37	0.51#
	CC+CT(n=90)	1486.2±1417.2	0.03##	63.1±35.7	0.06##	80.1±44.5	0.07##	0.87±0.41	0.51##
	CT+TT (n=75)	1689.8±1496.2	0.42†	71.1±54.4	0.61†	89.8±64.9	0.39†	0.89±0.37	0.11†
Chronic (N=207)	CC (n=83)	1292038±2232985	0.31*	92.5±30.4	0.06*	95.3±47.3	0.22*	1.0±0.43	1.00*
	CT (n=83)	1864473±4658982	<0.001**	118.4±124.8	0.14**	115.3±142.1	0.05**	1.0±0.5	0.03**
	TT (n=41)	7184121±10444774	<0.001#	102.4±44.1	0.42#	113.1±47.1	0.92#	1.2±0.57	0.04#
	CC+CT(n=166)	1578255±3653450	0.51##	105.4±91.2	0.83##	105.3±106	0.64##	1.0±0.47	0.20##
	CT+TT (n=124)	3623389±750812	0.75†	113.1±105.1	0.53†	114.6±119.1	0.55†	1.1±0.53	0.74†
Cirrhosis (N=37)	CC (n=22)	3031909247±13163170714	0.09*	171.6±54.2	0.52*	146.7±82.5	0.31*	0.87±0.32	0.11*
	CT (n=12)	916739007±2255720770	0.61**	166.1±110.4	0.47**	166±99.2	0.53**	0.96±0.38	0.97**
	TT (n=3)	60815561±9376719	0.71#	140.6±3.7	0.28#	139.66±10.4	0.33#	1.0±0.30	0.21#
	CC+CT(n=34)	2285378574±10630659255	0.65##	169.7±77.1	0.87##	153.5±87.8	0.75##	0.90±0.34	0.89##
	CT+TT (n=15)	745554318±2030648486	0.15†	161.06±98.5	0.74†	160.73±88.7	0.96†	0.98±0.35	0.77†

\* Student's t test (CC vs. CT), \*\* (CC vs. TT), # (CT vs. TT), ## (CT+CC vs. TT), † one-way ANOVA - (b/w all pairs), p value <0.05 was considered significant, ALT: Alanine aminotransferase; AST: Aspartate aminotransferase.

#### 4.3.4.4 Genotyping nsSNP rs61942435 C/T (A991V)

The dbSNP was used to retrieve the information of the nsSNP rs61942435 C/T and to design specific primers for amplification of the DNA strand that contain the polymorphic site. The desired amplified product was then incubated and digested by the restriction enzyme *HindIII* at a specific position of the SNP for genotyping analysis. The primers pair was checked for their specificity using the primer-BLAST tool and was further checked for their specificity using the BLAST tool and IDT Oligo Analyzer tool [325, 326]. The **Table 4.31** displays the primer sequences, amplified product size and expected fragment sizes after RFLP analysis.

**Table 4.31** The primer sequences and expected banding pattern for nsSNP rs61942435 C/T

ULK1 nsSNP	Primer sequences 5'– 3'	Amplified product size (bp)	Restriction enzyme	Banding pattern (bp)
rs61942435 (C/T)	F:GGTCATCTGGTTCCAGGCAGT R:AAGCTGTGCATTGAGCGGA	322 bp	<i>HindIII</i>	CC-322 bp; TT- 223 bp and 99 bp; CT- 322 bp, 223 bp and 99 bp

##### 4.3.4.4.1 PCR-RFLP

PCR was carried using the primers mentioned in **Table 4.31** for genotyping the nsSNP rs61942435 C/T. For best PCR results, the three major parameters of the PCR cycle (annealing temperature, Taq DNA polymerase concentration, and primer concentration) were optimized to amplify the product, as mentioned in the **Table 4.32**. Amplified PCR products were analyzed on 2.5% agarose gel with ethidium bromide.

**Table 4.32** The standardized conditions for genotyping of rs61942435 C/T

ULK1 Polymorphisms	PCR components	Gradient range used	Optimal condition
rs61942435 (C/T)	Annealing temperature	48–65 °C	58 °C
	Taq DNA polymerase	0.5 U–5.0 U	2.5U
	Primers	0.05 - 0.4 µmol	0.2µmol

The optimized PCR conditions were used to amplify the DNA segments from 500 HBV infected samples and 200 healthy control samples in order to genotype the nsSNP rs61942435 C/T. The optimized PCR amplification parameters are presented in **Table 4.33**. Amplified PCR product was digested with *HindIII* and all the genotypes were observed ie. the homozygous wild type genotype CC (322bp), heterozygous genotype CT (322bp, 223bp, and 99bp bands) and homozygous mutant genotype TT (223bp and 99bp) in different HBV as well as in control samples. The representative agarose gel picture is shown in **Figure 4.16**.

**Table 4.33** The optimized PCR conditions for genotyping nsSNP rs61942435 C/T

PCR Steps	Temperature	Duration
Initial Denaturation	95°C	2 minutes
Denaturation	95°C	45seconds
Annealing	<b>58°C</b>	45seconds
Extension	72°C	45 seconds
		} 35 cycles
Final extension	72°C	5 minutes

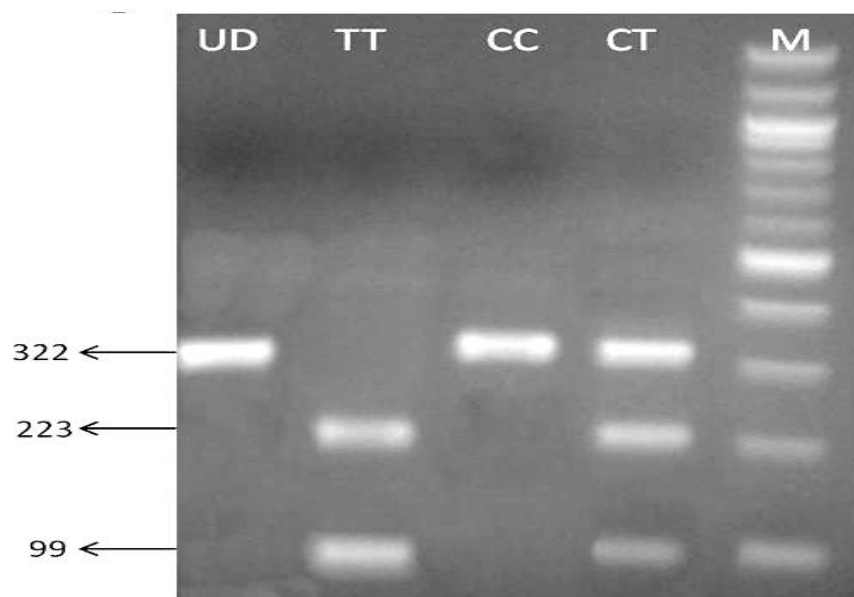


**Figure 4.16** The representative agarose gel picture for genotyping nsSNP rs61942435 C/T in HBV infected as well as healthy control samples (UD- undigested; CC-322bp; TT- 223bp and 99bp; CT- 322bp, 223bp and 99bp).

#### 4.3.4.4.2 Genetic correlation of nsSNP rs61942435 C/T in hepatitis B patients and healthy controls

The genotyping data thus generated was collected and evaluated for calculating the allelic and genotypes frequencies in 500 HBV infected and 200 healthy control samples. The nsSNP rs61942435 C/T was not found to be associated with HBV susceptibility in allelic model or in any of the other genetic models tested (**Table 4.34**).

**Table 4.34** Genotypic and allelic frequencies of ULK1 polymorphism rs61942435 C/T in HBV cases and healthy control samples (N = total number of samples)

ULK1 nsSNP rs61942435 (C/T)	HBV (N=500)	Control (N =200)	Odds ratio [95% CI]	p-value
CC	350 (70%)	130 (65%)	Ref.	-
CT	96 (19.2%)	46 (23%)	0.77 (0.51-1.16)	0.21
TT	54 (10.8%)	24 (12%)	0.83 (0.49-1.40)	0.49
CT+TT	150 (30%)	70 (35%)	0.79 (0.56-1.12)	0.19
CT+CC	446 (89.2%)	176 (88%)	0.94 (0.72-1.22)	0.65
C allele	796 (79.6%)	306 (76.5%)	Ref.	-
T allele	204 (20.4%)	94 (23.5%)	0.83 (0.63-1.10)	0.20

#### 4.3.4.4.3 Genetic correlation of nsSNP rs61942435 (C/T) in hepatitis B patients with different clinical groups

When the stratified clinical groups were compared to healthy individuals, regression analysis for *ULK1* nsSNP rs61942435 did not show any significant association with clinical groups (**Table 4.35**).

**Table 4.35** Allelic frequencies of ULK1 polymorphism rs61942435 in HBV subgroup and healthy control samples (N = total number of samples)

ULK1 SNP	Clinical Group	Allele frequency		OR (95% CI)	p-value	
		HBV	Controls			
<b>rs61942435 (C/T)</b>	Asymptomatic (142)	C	218(77%)	306(76.5%)	0.93 (0.65-1.33)	0.70
		T	66(23%)	94(23.5%)		
	Acute Hepatitis (114)	C	174(76%)	306(76.5%)	0.95 (0.65-1.39)	0.81
		T	54 (24%)	94(23.5%)		
	Chronic Hepatitis (207)	C	317(77%)	306(76.5%)	0.94 (0.68-1.30)	0.72
		T	97(23%)	94(23.5%)		
	Liver cirrhosis (37)	C	66(89%)	306(76.5%)	0.37 (0.17-0.80)	0.01
		T	8(11%)	94(23.5%)		

A 'p-value' <0.05 was considered significant. The significant values are shown in bold.

**Table 4.36** Analysis of the virological and biochemical parameters of HBV infected patients with rs61942435 (C/T) genotype

HBV infection category (N= no. of samples)	Genotypes (n= no. of samples)	Viral load (IU/ml) [Mean±SD]	p value	AST (U/L) [Mean±SD]	p value	ALT (U/L) [Mean±SD]	p value	Bilirubin (mg/dL) [Mean±SD]	p value
Asymptomatic (N=142)	CC (n=89)	128.6±112.5	0.38*	59 ±42	0.87*	47 ±55	0.59*	0.57±0.25	0.37*
	CT (n=40)	147.5±117.5	<b>0.03**</b>	60.3±50.5	<b>0.72**</b>	54.5±103	0.60**	0.53±0.21	0.68**
	TT(n=13)	61±33	<b>0.01#</b>	54.4±33.4	400.69#	55.5±57.4	0.97#	0.60±0.23	0.31#
	CC+CT(n=129)	134.5±113.7	<b>0.02##</b>	59.4±44.6	0.69##	49.2±73.4	0.76##	0.55±0.25	0.49##
	CT+TT (n=53)	126.3±109.2	0.81†	58.3±46.5	0.61†	54.7±93.5	0.78†	0.54±0.24	0.55†
Acute (N=114)	CC (n=65)	1625.5±1413	0.62*	64.4±29.8	0.26*	86.2±44	0.97*	0.88±0.43	0.80*
	CT (n=44)	1768.8±1644.4	0.11**	75.4±70.4	0.10**	86.6±73.7	0.13**	0.90±0.40	0.54**
	TT (n=5)	605.6±138.4	0.12#	42.2±13.6	0.30#	56.3±21.3	0.36#	1.0±0.35	0.59#
	CC+CT(n=109)	1683.2±1505.2	0.11##	68.8±50.4	0.23##	86.1±57.5	0.24##	0.88±0.41	<0.001#
	CT+TT (n=49)	1649.8±1597.2	0.69†	71.9±67.4	0.78†	83.8±70.9	0.51†	0.88±0.36	0.41†
Chronic (N=207)	CC (n=117)	2121414.7±3879090.9	0.11*	101.3±87.4	0.92*	101.3±97.3	0.45*	1.0±0.43	1.00*
	CT (n=83)	3495844±8329055	<b>&lt;0.001**</b>	102.4±54.8	<b>0.02**</b>	111.3±88.1	<b>0.35**</b>	1.0±0.5	0.30**
	TT (n=7)	259697.2±3499520.8	0.31#	186.4±201.1	<b>0.004#</b>	141.1±173.1	0.43#	1.2±1.2	0.37#
	CC+CT(n=200)	2691802.8±6149647.5	0.30##	101.4±75.2	<b>0.007##</b>	105.3±94	0.33##	1.0±0.46	0.29##
	CT+TT (n=90)	425931.7±8049911.2	0.15†	109.1±78.1	0.36†	114.2±96.1	0.15†	1.1±0.6	0.84†
Cirrhosis (N=37)	CC (n=29)	2624720867±11504142617	0.56*	173.6±79.2	0.31*	163.7±88.5	0.22*	0.91±0.4	<0.001*
	CT (n=8)	221051633±397692951.1	-	143.1±50.4	-	122.1±55.2	-	0.90±0.30	-
	TT (n=0)	-	-	-	-	-	-	-	-
	CC+CT(n=37)	2105008600±0196680722	-	167.4±74.2	-	152.4±84.2	-	0.90±0.33	-

\* Student's t test (CC vs. CT), \*\* (CC vs. TT), # (CT vs. TT), ## (CT+CC vs. TT), † one-way ANOVA - (b/w all pairs), p value <0.05 was considered significant, ALT: Alanine aminotransferase; AST: Aspartate aminotransferase.

#### 4.3.4.5 Genotyping of SNP rs12303764 (G/T)

The polymorphic information of nsSNP rs12303764 (G/T) was retrieved from dbSNP. Since, no restriction enzyme was available for rs12303764 (G/T), specific T-ARMS primers were designed in a way that the two allele-specific amplicons would have different lengths and easily be separated by standard agarose gel electrophoresis. The control amplicon is always amplified irrespective of other amplicons corresponding to one of the alleles; it provides an internal control for amplification failure. The primer pairs were checked for their specificity using the primer-BLAST tool [325]. The **Table 4.37** shows the primer sequences, amplified product size and the expected fragment sizes after T-ARMS PCR analysis.

**Table 4.37** The primer sequences and expected banding pattern for nsSNP rs12303764 (G/T)

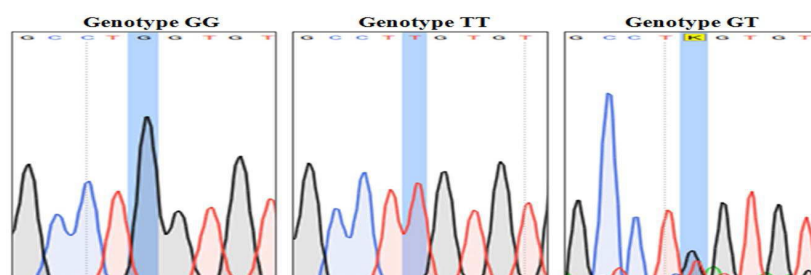
ULK1 SNP	Primer sequences 5'– 3'	Banding pattern (bp)
rs12303764 (G/T)	Outer Forward: GGTGAATGAGGAAACCAACCAGGGACG	TT: 922, 486 bp
	Outer Reverse: CCAAGTGGCTACAGTGCTGACAGATG	GG: 922,436 bp
	Inner Forward (G): CAGGCGTGGCTGGGGCATG	GT: 922, 486
	Inner Reverse (T): GGAAGGGCTCCTGCCACCCA	and 436 bp

##### 4.3.4.5.1 T-ARMS PCR

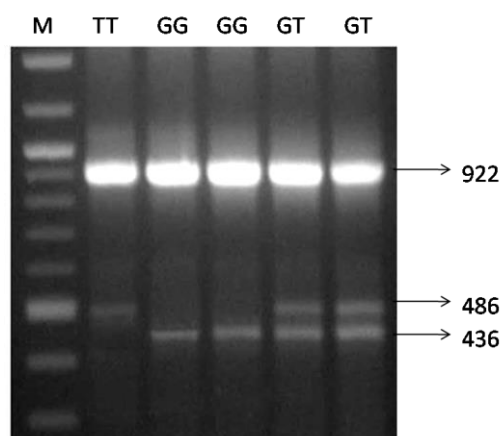
For genotyping rs12303764 (G/T) T-ARMS PCR was carried using the specific primers. Annealing temperature, Taq DNA polymerase concentration, and primer concentration were adjusted to retrieve ideal results as mentioned in the **Table 4.38**. Control samples for this analysis were obtained by sequencing of the amplified DNA fragments corresponding to the desired genotypes, as mentioned in **Figure 4.17** and these were used to optimize PCR reaction and amplification conditions. The amplified PCR products were analyzed on 3% agarose gel stained with ethidium bromide. The optimized T-ARMS PCR conditions were used to amplify DNA fragments in 500 HBV infected samples and 200 healthy control samples as indicated in **Table 4.39**. All the three genotypes were observed in HBV infected and healthy control samples. The representative agarose gel picture is shown in **Figure 4.18**.

**Table 4.38** The standardized conditions for genotyping of rs12303764 (G/T)

ULK1 Polymorphisms	PCR components	Gradient range	Optimal condition
rs12303764 (G/T)	Annealing temperature	48–65 °C	58 °C
	Taq DNA polymerase	0.5 U–5.0 U	2.5U
	Primers	0.05 - 0.4 μmol	0.2μmol

**Figure 4.17** Control genotypes obtained by sequencing amplified DNA fragments**Table 4.39** The optimized PCR conditions for genotyping rs12303764 (G/T)

PCR Steps	Temperature	Duration
<b>Initial Denaturation</b>	95°C	2 minutes
<b>Denaturation</b>	95°C	45seconds
<b>Annealing</b>	<b>58°C</b>	1 minute
<b>Extension</b>	72°C	45 seconds
<b>Final extension</b>	72°C	5 minutes

**Figure 4.18.** The representative agarose gel picture showing all genotypes of rs12303764.



#### 4.3.4.5.2 Role of rs12303764 in genetic susceptibility of HBV infection in north Indian population

The **Table 4.40** shows genotyping data we obtained after analysing all the collected samples including 500 HBV infected and 200 healthy control samples. GG, GT and TT genotypes were present in 207, 229 and 64 HBV patients while in case of normal healthy controls the proportion of the genotypes obtained were 120, 55 and 25. The nsSNP rs12303764 was found to be associated with HBV protection in allelic model (OR 0.64; 95% CI-0.49 to 0.82;  $p < 0.05$ ), (**Table 4.40**). Whereas, it was found to be associated with HBV infection susceptibility in heterozygous (OR 2.41; 95% CI-1.66 to 3.49;  $p < 0.01$ ), dominant (OR 2.12; 95% CI-1.52 to 2.96;  $p < 0.01$ ) and recessive (OR 1.44; 95% CI- 1.08 to 1.92;  $p < 0.01$ ) models.

**Table 4.40** The genotypic and allelic frequencies of ULK1 polymorphism rs12303764 in HBV cases and healthy control samples (N = total number of samples)

ULK1 rs12303764 (G/T)	HBV (N=500)	Control (N =200)	Odds ratio [95% CI]	p-value
TT	207 (41.2%)	120 (60%)	Ref.	
GT	229 (45.8%)	55 (27.5%)	<b>2.41(1.66-3.49)</b>	<b>&lt;0.01</b>
GG	64 (12.8%)	25 (12.5%)	1.48 (0.88-2.48)	0.13
GT+GG	293 (58.6%)	80 (40%)	<b>2.12 (1.52-2.96)</b>	<b>&lt;0.01</b>
GT+TT	436 (87%)	175 (87.5%)	<b>1.44 (1.08-1.92)</b>	<b>0.01</b>
T	643 (64.3%)	295 (73.7%)	Ref.	
G	357 (35.7%)	105 (26.3%)	0.64 (0.49–0.82)	0.04

#### 4.3.4.5.3 Genetic correlation of rs12303764 in HBV infected patients at different stages of infection

When the stratified clinical groups of HBV infected patients were compared to healthy individuals, regression analysis for *ULK1* SNP rs12303764 did not show any significant association with HBV infection as described in **Table 4.41**. On analysing data of different clinical groups, significant protective association of the SNP was observed in acute (OR 0.51;

95% CI- 0.36 to 0.72; p-0.0002) and chronic (OR- 0.59; 95% CI- 0.44 to 0.79; p-0.0006) hepatitis B patient groups, whereas no association was seen in asymptomatic and liver cirrhosis group.

**Table 4.41** The allelic frequencies and odds ratio of *ULK1* polymorphism rs12303764 in HBV subgroup and healthy control samples (N = total number of samples)

ULK1 SNP	Clinical Group	Allele frequency		OR (95% CI)	<i>p</i> -value	
		HBV	Control			
<b>rs12303764</b> (G/T)	Asymptomatic (142)	G	91(32%)	105(73.7%)	0.79 (0.56-0.10)	0.17
		T	193(68%)	295(26.3%)		
	Acute Hepatitis (114)	G	88(39%)	105(73.7%)	0.51 (0.36-0.72)	0.0002
		T	140(61%)	295(26.3%)		
	Chronic Hepatitis (207)	G	159(38%)	105(73.7%)	0.59 (0.44-0.79)	0.0006
		T	255(62%)	295(26.3%)		
	Liver cirrhosis (37)	G	19(26%)	105(73.7%)	0.98 (0.54-1.78)	0.9579
		T	55(74%)	295(26.3%)		

A '*p*-value' <0.05 was considered significant. The significant values are shown in bold.

**Table 4.42** Analysis of the virological and biochemical parameters of HBV infected patients with rs12303764 (G/T) genotype

HBV infection category (N= no. of samples)	Genotypes (n= no. of samples)	Viral load (IU/ml) [Mean±SD]	p value	AST (U/L) [Mean±SD]	p value	ALT (U/L) [Mean±SD]	p value	Bilirubin (mg/dL) [Mean±SD]	p value
Asymptomatic (N=142)	GG (n=15)	95.1±96.0	0.82*	60.9±24.0	0.93*	57.3±40.7	0.45*	0.70±0.20	0.03*
	GT(n=61)	101.6±94.5	<b>0.05**</b>	59.9±48.1	0.77**	45.1±60.4	0.83**	0.55±0.25	0.01**
	TT(n=66)	159.3±120.5	<b>0.003#</b>	57.6±43.2	0.77#	52.5±83.9	0.58#	0.53±0.24	0.64#
	GG+GT(n=76)	100.3±94.5	<b>0.001##</b>	60.1±44.3	0.74##	47.6±57.0	0.68##	0.58±0.24	0.21##
	GT+TT (n=127)	131.6±112.2	0.17†	58.7±45.4	0.22†	49.0±74.56	0.77†	0.54±0.24	0.65†
Acute (N=114)	GG (n=15)	1252.7±1440.7	<b>0.44*</b>	59.6±26.7	0.69*	71.8±28.5	0.52*	0.87±0.47	0.80*
	GT (n=58)	1566.6±1411.4	0.19**	63.2±37.1	0.34**	78.7±40.7	0.18**	0.90±0.40	0.81**
	TT (n=41)	1874.2±1603.9	0.29#	76.8±67.9	0.20#	99.0±78.6	0.09#	0.86±0.38	0.61#
	GG+GT(n=73)	1502.1±1413.1	0.20##	62.4±35.1	0.12##	77.2±38.4	<b>&lt;0.0001##</b>	0.90±0.42	0.62##
	GT+TT (n=99)	1694.0±1493.9	0.45†	68.8±52.3	0.77†	87.0±59.9	0.69†	0.88±0.39	0.33†
Chronic (N=207)	GG (n=33)	918785.8±1622859.6	<b>0.02*</b>	105.0±78.5	0.77*	96.3±125.1	0.48*	1.06±0.40	0.70*
	GT (n=93)	3135252.3±5632472.0	0.13**	111.6±111.7	0.45**	113.8±117.5	0.66**	1.1±0.56	0.91**
	TT (n=81)	2896802.0±7475771.9	0.81#	97.0±35.8	0.26#	103.2±45.5	0.47#	1.05±0.46	0.52#
	GG+GT(n=126)	2554749.2±4998090.5	0.69##	109.9±103.7	0.31##	109.2±119.3	<b>&lt;0.0001##</b>	1.09±0.52	0.57##
	GT+TT (n=174)	3024249.6±6536739.6	0.45†	104.8±85.1	0.33†	108.8±91.3	0.58†	1.08±0.51	0.87†
Cirrhosis (N=37)	GG (n=1)	50000000	-*	145	-*	148	-*	1.4	-*
	GT (n=17)	262710466.2±334138521.0	-**	155.3±29.0	-**	127.0±52.1	-**	0.97±0.33	-**
	TT (n=19)	3861538962.0±14182680442.0	0.30#	179.3±99.8	0.34#	175.3±102.9	0.09#	0.84±0.33	0.24#
	GG+GT(n=18)	250893218.1±328016221.8	0.28##	154.7±28.2	0.31##	128.2±50.8	0.08##	0.99±0.33	0.17##
	GT+TT (n=36)	2162092172.0±10335324103.0	0.75†	168.0±75.2	0.21†	152.5±85.4	0.76†	0.90±0.33	0.29†

\* Student's t test (GG vs. GT), \*\* (GG vs. TT), # (GT+TT), ## (GT+GG vs. TT), † one-way ANOVA - (b/w all pairs), p value <0.05 was considered significant, ALT: Alanine aminotransferase; AST: Aspartate aminotransferase.

#### 4.3.4.6 Genotyping SNP rs3923716 (G/T)

Specific primers were designed for the amplification of SNP rs3923716 G/T, further restriction digestion was performed overnight by using *Bse*RI (New England Biolabs). The primer pair was checked for their specificity using the primer-BLAST tool and was further checked for their specificity by IDT OligoAnalyzer tool [325, 326]. The **Table 4.43** shows the primer sequences, amplified product size and expected fragment sizes after RFLP analysis.

**Table 4.43** Depiction of the primer sequences, amplified product size, restriction enzyme and expected fragment sizes of rs3923716 G/T after the RFLP analysis

ULK1 SNP	Primer sequences 5'– 3'	Amplified product size (bp)	Restriction enzyme	Banding pattern (bp)
rs3923716 (G/T)	F:CTGCGAGTGGCTTGTGAGTCG R:TAGGGTGGCCGAGGCAGGAA	525 bp	<i>Bse</i> RI	GG- 355 bp and 170 bp; GT- 525 bp, 355 bp and 170 bp TT- 525 bp

##### 4.3.4.6.1 PCR RFLP

For the amplification of rs3923716 G/T annealing temperature, Taq DNA polymerase concentration, and primer concentration were optimized as mentioned in the **Table 4.44**. Amplified PCR products were analyzed on 1.5% agarose gel stained with ethidium bromide.

**Table 4.44** Optimized condition for genotyping rs3923716 G/T

ULK1 Polymorphism	PCR components	Gradient range	Optimal condition
rs3923716 (G/T)	Annealing temperature	48–65 °C	58 °C
	Taq DNA polymerase	0.5 U–5.0 U	2.5U
	Primers	0.05 - 0.4 μmol	0.2μmol

The optimized PCR conditions were used to amplify DNA segments from 500 HBV infected samples and 200 healthy control samples in order to genotype the SNP rs3923716 G/T as shown in **Table 4.45**. After restriction digestion with *Bse*RI we observed homozygous wild GG (355 and 170 bp), heterozygous GT (525, 355 and 170 bp) and homozygous mutant TT (525bp) genotypes in different HBV infected as well as in healthy control samples. The representative agarose gel picture is shown in **Figure 4.19**.

**Table 4.45** The optimized PCR conditions for genotyping SNP rs3923716 G/T

PCR Step	Temperature	Duration
<b>Initial Denaturation</b>	95°C	2 minutes
<b>Denaturation</b>	95°C	45seconds
<b>Annealing</b>	<b>58°C</b>	1 minute
<b>Extension</b>	72°C	45 seconds
		} 35 cycles
<b>Final extension</b>	72°C	5 minutes

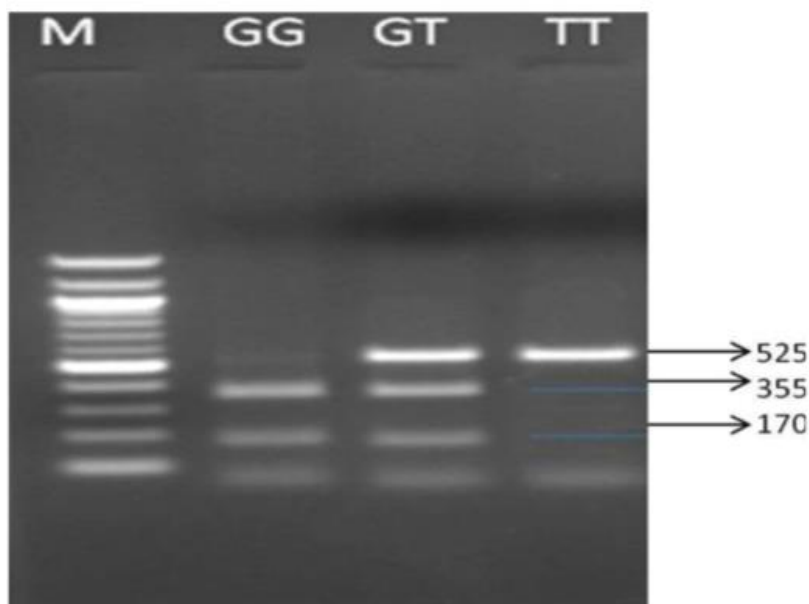


**Figure 4.19** The representative agarose gel picture for genotyping rs3923716 G/T in HBV samples.

#### 4.3.4.6.2 Role of rs3923716 G/T in genetic susceptibility of HBV infection

The genotyping data were compiled and compared for calculating the allelic and genotyping frequencies in 500 HBV infected and 200 healthy control samples. The SNP rs3923716 G/T was found to be associated with HBV infection susceptibility in the allelic model (OR 1.41; 95% CI-1.07 to 1.87; p-0.01) and homozygous model (OR 2.09; 95% CI-1.10 to 3.95; p-0.02) (Table 4.46).

**Table 4.46** Genotypic and allelic frequencies of ULK1 polymorphism rs3923716 G/T in HBV cases and healthy control samples (N = total number of samples)

ULK1 SNP rs3923716 (G/T)	HBV (N=500)	Control (N =200)	Odds ratio [95% CI]	p-value
GG	280 (56%)	127 (63.5%)	Ref.	
GT	160 (32%)	60 (30%)	1.20 (0.84-1.73)	0.30
TT	60 (12%)	13 (6.5%)	<b>2.09 (1.10-3.95)</b>	<b>0.02</b>
GT+TT	220 (44%)	73 (36.5%)	1.36 (0.97-1.91)	0.06
GT+GG	440 (88%)	140 (70%)	0.95 (0.69-1.32)	0.80
G allele	720 (72%)	314 (78.5%)	Ref.	
T allele	280 (28%)	86 (21.5%)	<b>1.41 (1.07–1.87)</b>	<b>0.01</b>

#### 4.3.4.6.3 Genetic correlation of rs3923716 G/T in hepatitis B patients with different clinical groups

When the clinical groups of HBV infected patients were compared to healthy individuals, regression analysis for ULK1 SNP rs3923716 G/T provided a significant outcome (Table 4.46). As shown in Table 4.47, SNP rs3923716 G/T also showed a significant association with two clinical categories, i.e. Asymptomatic patients group (OR 1.48; 95% CI-1.04 to 2.10; p-0.02) and liver cirrhosis group (OR- 1.91; 95% CI-1.08 to 3.37; p-0.02), but no such association was seen with acute hepatitis (OR 1.27; 95% CI-0.87 to 1.86; p-0.21), while protective association was observed in chronic hepatitis (OR 0.20; 95% CI-0.11 to 0.34; p-0.0001) group.

**Table 4.47** Allelic frequencies of ULK1 polymorphism rs3923716 G/T in HBV subgroup and healthy control samples (N = total number of samples)

SNP	Clinical Group	Allele frequency		OR (95% CI)	p-value	
		HBV	Control			
<b>rs3923716</b> <b>(G/T)</b>	Asymptomatic (142)	G	209(74%)	314(78.5%)	<b>1.48 (1.04-2.10)</b>	<b>0.02</b>
		T	75(26%)	86(21.5%)		
	Acute Hepatitis (114)	G	165(72%)	314(78.5%)	1.27 (0.87-1.86)	0.21
		T	63(28%)	86(21.5%)		
	Chronic Hepatitis (207)	G	297(72%)	314(78.5%)	0.20 (0.11-0.34)	0.0001
		T	117(28%)	86(21.5%)		
	Liver cirrhosis (37)	G	49(66%)	314(78.5%)	<b>1.91 (1.08-3.37)</b>	<b>0.02</b>
		T	25(34%)	86(21.5%)		

A 'p-value' <0.05 was considered significant. The significant values are shown in bold.

**Table 4.48** Analysis of the virological and biochemical parameters of HBV infected patients with rs3923716 G/T genotype

HBV infection category (N=no of samples)	Genotypes (n=no of samples)	Viral load (IU/ml) [Mean±SD]	p value	AST (U/L) [Mean±SD]	p value	ALT (U/L) [Mean±SD]	p value	Bilirubin (mg/dL) [Mean±SD]	P value
Asymptomatic (N=142)	GG (n=87)	134.7±113.9	0.88*	56.2±44.8	0.65*	50.6±79.7	0.69*	0.54±0.24	0.21*
	GT(n=35)	131.3±113.1	<b>0.04**</b>	59.9±28.5	0.18**	45.1±37.8	0.76**	0.60±0.25	0.42**
	TT(n=20)	91.4±88.9	0.18#	69.4±58.7	0.42#	55.5±81.7	0.52#	0.50±0.27	0.17#
	GG+GT(n=122)	133.7±113.2	0.11##	57.2±40.9	0.24##	49.0±70.2	0.70##	0.56±0.24	0.31##
	GT+TT (n=55)	116.8±105.8	0.35†	63.4±41.7	0.12†	48.7±57.2	0.42†	0.59±0.25	0.46†
Acute (N=114)	GG (n=65)	1774.4±1532.9	0.71*	70.5±55.4	0.59*	89.2±60.2	0.53*	0.90±0.41	0.81*
	GT (n=35)	1658.0±1529.1	<b>0.05**</b>	64.8±41.7	0.56**	82.1±40.9	0.38**	0.88±0.41	0.40**
	TT (n=14)	937.9±974.9	0.11#	61.5±41.0	0.80#	72.9±75.4	0.58#	0.80±0.38	0.53#
	GG+GT(n=100)	1733.7±1524.8	0.06##	68.5±50.9	0.59##	86.7±54.1	0.39##	0.89±0.41	0.43##
	GT+TT (n=49)	1452.3±1421.8	0.12†	63.9±41.1	0.47†	79.5±52.4	0.48†	0.86±0.40	0.49†
Chronic (N=207)	GG (n=114)	3028665.9±6979398.5	0.43*	106.0±74.8	0.23*	106.4±88.5	0.34*	1.07±0.50	0.61*
	GT (n=69)	2394414.3±5014089.7	0.91**	106.9±108.4	0.27**	111.4±123.6	0.83**	1.07±0.53	0.20**
	TT (n=24)	1919036.3±3911720.7	0.18#	93.0±24.6	0.15#	95.9±28.1	0.21#	1.1±0.37	0.92#
	GG+GT(n=183)	2789521.8±6303384	0.51##	106.4±88.9	0.41##	108.3±102.8	0.76##	1.07±0.51	0.89##
	GT+TT (n=93)	2271736.1±4738320.1	0.95†	103.3±94.2	0.50†	107.4±107.4	0.65†	1.08±0.49	0.97†
Cirrhosis (N=37)	GG (n=14)	346348077.4±359153341.7	0.39*	170.8±69.6	0.90*	142.0±93.5	0.42*	0.78±0.32	<b>0.02*</b>
	GT (n=21)	3472117326.0±13510034516	0.29**	167.7±81.6	0.77**	165.6±78.8	0.41**	1.03±0.31	0.80**
	TT (n=2)	60990640.5±5946566.5	0.71#	139.0±24	0.18#	85.5±55.8	0.43#	0.63±0.32	0.13#
	GG+GT(n=35)	2221809627.0±10479909600	<0.52##	169.0±76.0	0.44##	156.2±84.4	0.08##	0.93±0.33	0.79##
	GT+TT (n=23)	3175497614.0±12918747202	0.85†	165.2±78.4	0.32†	158.6±79.5	0.14†	1.0±0.32	0.93†

\* Student's t test (GG vs. GT), \*\* (GG vs. TT), # (GT+TT), ## (GT+GG vs. TT), † one-way ANOVA - (b/w all pairs), p value <0.05 was considered significant, ALT: Alanine aminotransferase; AST: Aspartate aminotransferase.



#### 4.3.5 Haplotype analysis of nsSNPs of ULK1

Moreover, when haplotype analysis was performed in the context of nsSNPs of ULK1, one high-risk haplotype, i.e, ATCC (OR- 1.74; 95% CI- 1.03 to 2.94; p- 0.039) illustrated the relationship with the susceptibility/clinical presentation of HBV as represented in **Figure 4.19**. Also, for the first time, a correlation of haplotype (ULK1-ATCC) with HBV infection was reported. Importantly, the transition of SNP variation at rs61942435 C→T seems to influence the association of haplotype ATCC with HBV infection susceptibility.

	rs79965940.A.T	rs61942435.C.T	rs55824543.C.T	rs56364352.C.T	Freq	OR (95% CI)	P-value
1	A	C	C	C	0.2629	1.00	---
2	A	C	C	T	0.1593	0.75 (0.48 - 1.16)	0.2
3	C	C	C	C	0.1224	1.16 (0.75 - 1.79)	0.52
4	A	T	C	C	0.0894	<b>1.74 (1.03 - 2.94)</b>	0.039
5	A	C	T	C	0.0686	1.42 (0.83 - 2.43)	0.2
6	C	C	C	T	0.059	0.57 (0.27 - 1.19)	0.14
7	A	T	C	T	0.042	0.70 (0.30 - 1.65)	0.41
8	C	C	T	C	0.0389	0.67 (0.31 - 1.46)	0.31
9	A	C	T	T	0.0352	0.69 (0.31 - 1.57)	0.38
10	C	T	C	T	0.032	0.48 (0.16 - 1.41)	0.18
11	A	T	T	C	0.0237	1.46 (0.60 - 3.55)	0.41
12	C	C	T	T	0.023	0.90 (0.35 - 2.28)	0.82

**Figure 4.20** The haplotype analysis of four nsSNPs of ULK1.

# DISCUSSION

## 5. Discussion

The hepatitis B virus is perhaps a fatal liver infection and can cause both acute and chronic disease; which eventually proceed to liver cirrhosis (LC) and hepatocellular carcinoma (HCC). Nearly 257 million people are alive with hepatitis B virus infection and 8,87,000 people die every year due to acute or chronic consequences of hepatitis B (WHO fact sheet, 2017). Human HBV is a model member which belongs to genus *Orthohepadnavirus* of *Hepadnaviridae* family of viruses. This virus infects hepatocytes. The genome of this virus is the smallest known for mammalian viruses which is about 3020–3320 nucleotides long. Human HBV is also capable of infecting chimpanzees, baboons and other great apes as well as various marsupials [40]. Various viral and environmental factors involved in the progression of the infection have been studied broadly but the host related factors such as age, gender, immune status of the individual and genetic variations are still less studies [142]. The host response to this infection is mainly immune mediated i.e. cytotoxic T-lymphocytes (CTLs) eliminate hepatocytes where viral antigens are processed and displayed in association with MHC class I molecules, which further results into liver injuries [328]. Despite safe vaccine available for HBV, it remains a severe civic health problem, particularly in Asia, Africa, and South America, and may possibly end in death [329]. The development of chronic hepatitis B (CHB) to severe liver disorder, like LC and HCC, is determined by the genetic characteristics of the host, in addition to environmental and viral factors [330].

Although HBV vaccines have reduced the number of new HBV infections, but they do not benefit patients already with chronic HBV infection, who have a high risk of developing liver cirrhosis and hepatocellular carcinoma [331]. The HBx protein is an essential viral protein that is required for successful replication and maintenance of viral infection in mouse models and various cultured cell systems [332]. As stated earlier, HBx can induce autophagy in liver cell lines by up-regulating BECN1 (Beclin 1) expression [68]. HBx can trigger autophagy by directly interacting with the class III phosphatidylinositol 3-kinase (PtdIns3K) to favour virus replication [63]. Similarly, Hepatitis small surface proteins (SHBs) have also been found to induce autophagy by triggering endoplasmic reticulum (ER) stress [162]. Many studies are available that show role of this autophagy in liver pathology [333-336]. Moreover, genetic factors play important role in many diseases and variants in the genes of autophagy pathways have been shown to play role in susceptibility of various

diseases. Till date, no one has targeted autophagy gene ULK1 for its involvement in HBV infection susceptibility.

The human serine/threonine-protein kinase ULK1, a gene involved in the initiation of autophagy pathway was identified as the human homolog of *C. elegans* Unc-51 kinase and of the *S. cerevisiae* autophagy-related protein kinase Apg1p/Atg1 in 1998 [337-339]. Sequence analysis showed that, at the amino acid level, ULK1 is 57%, 20%, and 27% similar to the kinase (located in the N-terminus), the proline/serine-rich, and the C-terminal domains of Atg1, respectively. Compared to the same domains of Unc-51, ULK1 presents 74%, 22%, and 46% similarity, respectively [338]. Although presenting high homology with Unc-51, which is expressed exclusively in neurons, ULK1 was found to be ubiquitously expressed in human adult tissues, suggesting that this evolutionary conserved serine/threonine kinase may have acquired diverse functions during vertebrate evolution [338]. Since, the ULK1 complex is an essential regulator of mammalian autophagy and the fact that its function is largely conserved throughout all eukaryotes underlines its importance. Autophagy has a vital role in health maintenance [340]. In general, autophagy is a cytoprotective mechanism that prevents the accumulation of damaged or impaired cellular components that could be detrimental to the cell if left to persist. Therefore, dysfunctional autophagy has been implicated in numerous diseases [341].

Genetic polymorphisms have been implicated in the culmination of HBV infection especially of those host genes, which are directly or indirectly involved in immune response to this infection [342]. One of the significant host genes is ULK1, involved in autophagy pathway. So far, SNPs in ULK1 gene has been studied in context with various diseases such as Crohn's disease (CD), Behcet syndrome [70], Ulcerative colitis [343], latent tuberculosis [287], lymphatic metastasis [344], pulmonary tuberculosis [287] and uveomeningoencephalitic syndrome [70]. ULK1 has been intensively studied with HBV infection, which further promotes autophagy in hepatocytes via the activation of ULK1. Higher levels of autophagy have been suggested to help the HBV replication. The inhibition of this process decreases HBV replication and might be a new target for anti-HBV therapy [200]. In our study, we have analysed nsSNPs as well as SNPs present in regulatory region of ULK1 for their role in HBV infection susceptibility in North Indian population.

## 5.1 *In silico* analysis

### 5.1.1 Phylogenetic analysis reveals ULK1 as evolutionary conserved gene

By using MEGA5 for phylogenetic analysis of the ULK1, it was found that *Homo sapiens* and *P. troglodytes* have 100% evolutionary relationship depicting that the ULK1 gene present in these species is identical and could have originated from the same ancestors. On the other hand, *R. norvegicus* and *M. musculus* have 93% similarity and could have the same ancestral origin as *C. griseus*. *X. (Silurana) tropicalis*, a species of amphibian family shows a vast difference in its origin and evolution from others, when studied based on protein sequence of ULK1.

### 5.1.2 Imperative regulatory elements and transcription factor binding sites distributed throughout the ULK1 gene

Four potential regulatory elements in ULK1 gene were identified, out of which three are UTRs (corresponding 75% of the total regulatory region in ULK1 gene) and another is a single intron region representing 25% of the total regulatory region. In addition, 23 transcription factors in UTR and intron regions were identified; these transcription factors bind directly or in the form of the complex to the transcriptional regulatory region of ULK1, which could further control its expression. Between these detected, CHOP1 and E2F1 enhance the autophagy process where as NFE2 and STAT suppress the process of autophagy. The interaction of these classes of transcription factors with the ULK1 gene could alter its expression, which can further amend the autophagy pathway.

### 5.1.3 Putative functional sites present in ULK1

Post-translational modification (PTM) of proteins plays crucial role in determining protein structure, activity and function [345]. These modifications include, but are not limited to, phosphorylation to regulate catalytic activity and protein-protein interactions, glycosylation to ensure proper protein folding, ubiquitination to signal degradation, and lipidation to enable insertion into phospholipid membranes [346]. Execution of autophagy requires proper functioning of ULK1 complex, and the activity of this complex and autophagy pathway is highly dependent on the regulatory post-translational modifications specifically phosphorylation [347]. Hence, detection of phosphorylation sites in ULK1 could be beneficial to apprehend its various functional aspects. Therefore, we analyzed PTM sites and

detected 84 vital phosphorylation sites in ULK1 gene. Out of these 84 identified phosphorylation sites, 26 have already been verified experimentally as mentioned in **Table 4.5**. From the rest 58 newly identified phosphorylation sites, 25 were present in kinase domain, 29 were present in Ser/Thr rich domain and 4 were present in CTD domain. We also identified a single phosphorylation site at amino acid position 295 of Y residue in the kinase domain with a significant score (0.809), which has not been verified experimentally and can be studied further to unravel its impact on protein function. Besides the identification of phosphorylation sites among PTMs, we also detected 4 palmitoylation sites at positions 426, 927, 1003 and 1049. Identification of palmitoylation sites was an important component of this study, as it supports detection of added palmitic acid; resulting in increasing the hydrophobicity of proteins and helps in their association to the membranes [304]. The identification of these sites would help understand the complex processes such as sub-cellular trafficking between the membrane compartments [348] and protein–protein interactions that occur due to palmitoylation. Many autophagy related proteins have been studied for the palmitoylation sites [349]. In mammals, ATG101, an important autophagy related protein, interacts with ATG13 (ULK1 interacting protein), which is a component of macroautophagy [349]. ATG101 is localized to the isolation membrane or phagophore, which surrounds the materials to be degraded in the lysosome. The interaction of ATG101 with the phagophore may be due to the palmitoylation site present at the third amino acid, i.e. cysteine [349]. Identification of these palmitoylation sites would help us in exploring diverse interactions with ULK1 and their sub-cellular localizations.

#### **5.1.4 Prediction of nsSNPs destabilize ULK1 protein**

Protein structure and function can be altered by a single base change in the coding region of DNA, which leads to changes in amino acids, present in the protein. These single base changes are known as nsSNPs which have been the subject of many recent studies and a large amount of data now exists in public repositories like SWISSPROT [350], dbSNP [351] and HGVBbase [352]. These polymorphisms could show damaging effect towards the protein structure and function, which can lead to disease development, but not in, all cases. Here we have identified 4 nsSNPs i.e. rs79965940 (N148T), rs61942435 (A991V), rs55824543 (T503M) and rs56364352 (S298L) which could have harmful functional outcomes on the ULK1 protein. The iPTREE-STAB suggest that the three mutations (N148T, T503M and S298L) decrease the protein stability while the mutation A991V increases the protein

stability, whereas i-MUTANT 2.0 suggests that all the four mutations (N148T, A991V, T503M and S298L) decrease the protein stability. Similarly, DUET and ERIS tools were used for prediction of protein stability change at structural level. These online servers also analyze Gibbs free energy change to predict whether the mutation present is stabilizing or destabilizing the protein. DUET indicates that both mutations (N148T and A991V) decrease the protein stability while ERIS suggests that the mutation N148T decreases the protein stability and the mutation A991V increases the protein stability. Also, it was found that rs79965940 nsSNP (N148T) increased the total energy of the protein structure and hence could be regarded as a destabilizing mutation. On the other hand, the nsSNP rs61942435 (A991V), decreased the total energy and hence could be regarded as stabilizing mutation. Overall, the nsSNP rs61942435 was found to increase the protein stability while, the nsSNPs rs79965940, rs55824543, and rs56364352 were found to decrease the protein stability both at sequence and structure level. Therefore, we selected these four nsSNPs along with two other SNPs (rs3923716 and rs12303764) which were found to be associated with Crohn's disease in New Zealand population, for genotyping in the HBV patient samples for determining their role in disease susceptibility or progression.

## **5.2 Genotyping of predicted nsSNPs and non-coding SNPs**

The selected nsSNPs rs79965940, rs55824543, rs56364352, rs61942435 and other two non-coding SNPs rs3923716 and rs12303764 were genotyped in 500 HBV infected patients and 200 healthy control samples to find their role in the susceptibility to HBV infection. The target region of the selected six polymorphisms was amplified through PCR and the genotyping was done by RFLP and T-ARMS PCR (as applicable) followed by agarose gel electrophoresis. The statistical analysis was performed to reveal their association with HBV infection. Viral and biochemical parameters in various genotypes of these polymorphisms were also compared to uncover their role in HBV infection.

### **5.2.1 nsSNPs rs79965940 A/C (N148T), rs56364352 C/T (S298L) and non-coding SNP rs3923716 G/T increase risk of HBV infection, while rs12303764 (G/T) show protective role against HBV infection**

The nsSNP rs79965940 A/C (N148T) was found to destabilize ULK1 protein both in sequence as well as in structural level. Furthermore, this nsSNP was observed to be significantly associated with HBV infection susceptibility and the mutant allele C was found to be significantly linked with HBV risk (OR- 1.4; 95% CI-1.08 to 1.81; p-0.01). The

genotype CC was also significantly associated with HBV infection risk (OR- 1.85; 95% CI- 1.11 to 3.10; p-0.01). The mutant allele C was also found to be associated with two clinical stages of infection, i.e. acute patients group (OR 1.5; 95% CI-1.08 to 2.18; p-0.01) and chronic hepatitis B patients group (OR- 1.4; 95% CI-1.03 to 1.90; p-0.02), but no such association was seen with asymptomatic patients group (OR- 1.3; 95% CI- 0.94 to 1.84; p- 0.01) and liver cirrhosis patients group (OR- 1.2; 95% CI-0.74 to 2.20; p-0.36). Furthermore, viral load in different HBV infection categories was also correlated with the genotypes of HBV infected patients. Also, there was a significant difference (p- 0.004) observed in the mean viral load between the mutant genotype CC in acute infection group. Viral load was also found to be high in all patients with the mutant genotype CC in all the sub-categories of HBV infected patients. No significant variation was observed in biochemical parameters in relation to the genotype of patients.

The nsSNP rs56364352 was found to be significantly associated with HBV infection susceptibility and mutant T allele was found to be significantly linked with the HBV risk (OR- 1.68; 95% CI-1.30 to 2.16; p-< 0.01). The mutant genotype TT was also found to be significantly associated with HBV infection risk (OR- 2.36; 95% CI-1.40 to 3.97; p-< 0.01). Similarly, the heterozygous genotype CT was also found to be associated with HBV risk (OR- 1.72; 95% CI-1.10 to 2.47; p < 0.01). When analyzed with the sub-clinical categories, rs56364352 nsSNP showed a significant association with three clinical categories, i.e. asymptomatic patients group (OR 1.72; 95% CI-1.20 to 2.30; p<0.01), acute patients group (OR 1.97; 95% CI-1.40 to 2.77; p<0.01) and chronic hepatitis B patients group (OR- 1.70; 95% CI-1.27 to 2.28; p<0.01), but no such association was seen with liver cirrhosis patients group. Furthermore, viral load in different HBV infection categories was also correlated with the genotypes of HBV infected patients. Also, there was a significant difference observed in the mean viral load between the mutant genotype TT in acute infection group (p-0.04) and in chronic infection group (p<0.001). The viral load was also found to be high in all patients with the mutant genotype TT in all the sub-categories of HBV infected patients. Significant results were also observed between the mutant genotype TT and bilirubin level in asymptomatic (p-0.03) and chronic infection (p-0.04) group. No such significance was observed in other biochemical parameters in relation to the genotype of patients.

Non-coding SNP, rs3923716 was earlier reported in two studies associated with Crohn's Disease in New Zealand population [73, 75]. In our study, rs3923716 was found to be



significantly associated with HBV infection susceptibility and the mutant T allele also established a significant link with HBV risk (OR- 1.41; 95% CI-1.07 to 1.87; p-0.01). The mutant genotype TT also depicted no association with HBV infection risk (OR- 2.09; 95% CI-1.10 to 3.95; p-0.02). When analyzed with sub-clinical categories, the nsSNP rs3923716 mutant allele T provided a valuable outcome to our above mentioned results, showing a significant association with asymptomatic patients (OR- 1.48; 95% CI-1.04 to 2.10; p-0.02) and with liver cirrhosis patients (OR- 1.91; 95% CI-1.08 to 3.37; p-0.02) group, but no such association was seen with acute hepatitis patients and chronic hepatitis patients group. However, the odds ratio seems to increase with the increase of the severity of HBV infection, indicating a significant role played by this SNP in the progression of the infection. No significant variation was observed in biochemical parameters in relation to the genotype of patients.

There are studies which have shown protective role of mutant allele against the disease progression [353-355]. We have also found that mutant allele of rs12303764 is associated with HBV protection in allelic model (OR 0.64; 95% CI-0.49 to 0.82; p- <0.05), further analysing data of different clinical groups, significant protective association of rs12303764 was observed in acute (OR 0.51; 95% CI- 0.36 to 0.72; p-0.0002) and chronic (OR- 0.59; 95% CI- 0.44 to 0.79; p-0.0006) hepatitis B patient groups suggesting that this SNP might be associated with protection against HBV infection in our population.

### **5.2.2 No significant association was observed for nsSNP rs61942435 C/T (A991V) and rs55824543 (C/T) (T503M)**

In-silico analysis shows that rs61942435 C/T (A991V), rs55824543 (C/T) (T503M) destabilizes ULK1 protein but we could not find any association of these polymorphisms when we compared with total HBV infected patients as well as in different clinical categories of these patients. For these SNPs we have observed that their OR and 95% CI are close to value 1, indicating that increasing the number of samples may show their association with HBV infection in nearby future studies.

The process of HBV infection is a multi-stage process, after HBV infection, the immune response can be induced to eliminate the virus. As a crucial autophagy gene, ULK1, whose expression can be effected by the polymorphisms in the regulatory regions. Studies have also demonstrated that increased/decreased autophagy function may promote/suppress the development of HBV. In this way, variable levels of autophagy can lead to HBV infection/ progression; causing liver damage in susceptible subjects. The foremost findings reported here with respect to nsSNPs of *ULK1* gene was that, rs79965940 and rs56364352 were independently associated with HBV infection which has revealed the importance of these polymorphisms with susceptibility to HBV infection. Results revealed a substantial association of ULK1 rs79965940 with two subclinical HBV groups i.e. acute and CHB risk groups. Similarly, rs56364352 have also shown noteworthy association with three sub-clinical HBV groups i.e. acute, asymptomatic and CHB risk group. Eventually, on analysis of mutant genotypes of rs56364352 and rs79965940, it was clearly observed that there was an increase in hepatitis B viral load as HBV infection progresses from asymptomatic infection to LC. Here, we have also investigated the possible connection of ULK1 SNPs rs3923716 and rs12303764 with HBV infection. The logistic regression analysis illustrated that G allele of rs3923716 is associated with HBV infection. Further, an extensive analysis on different clinical groups of HBV infection depicts interesting results showing that G allele of rs3923716 is associated with asymptomatic infection and liver cirrhosis but not associated with acute hepatitis and chronic hepatitis. These results suggest that TT genotype and T allele of rs3923716 is involved in disease progression as this allele is maximally represented among patients that are either at the first stage of liver disease or at the last stage. Similarly, when mutant TT was compared with hepatitis B viral load among clinical groups, it was observed that the viral load increases when HBV infection progresses from asymptomatic to LC infected patients. In other words, the patients with rs3923716 TT genotype and T allele of ULK1 gene are more likely to have a progressive status in HBV infection. It is projected that nsSNPs and their damaging or deleterious impact could be examined in other populations as well for their possible involvement in various diseases associated with ULK1 and autophagy.

# CONCLUSION

## Conclusion

The major objective in the field of human genomics is to identify mutations that may act as biomarkers for disease susceptibility. GWAS and immunogenetic studies have already provided great insights into the pathogenesis of HBV. Recent studies showed that susceptibility to HBV infection with the potential of destructive liver inflammation is based on host genetic factors that may predispose to or protect from disease [356-358]. Hence, autophagy alone may not necessarily participate in HBV infection, but it may provoke disease in the context of other risk variables, such as host genotype, ageing, and/or behavioural habits such as alcohol intake. Previous studies have also demonstrated that increased/decreased autophagy function may promote/suppress the development of HBV [266]. In this way, variable levels of autophagy can lead to HBV infection/ progression; causing liver damage in susceptible subjects [359]. Since, autophagy has been thoroughly known for its role associated to HBV, still genetic variants such as of ULK1 has not been examined with context to HBV infection. Owing to these facts, the current study investigated whether nsSNPs rs61942435, rs79965940, rs55824543 and rs56364352 and non-coding SNPs rs12303764 and rs3923716 in ULK1 gene might be linked with the susceptibility to HBV infection or its progression to various stages of HBV infection.

This investigation is the first explorative approach focusing on the relation between genetic variants of ULK1 and HBV. We predicted four nsSNPs rs61942435, rs79965940, rs55824543 and rs56364352 [360]. Further analyzed their impact on protein stability and genotyped these polymorphisms for understanding their role in HBV infection. The results from in-silico sequence-based analysis suggest that all the nsSNPs (rs61942435, rs79965940, rs55824543 and rs56364352) decreased the protein stability. Furthermore, these nsSNPs were mapped on the ULK1 protein structures (4WNO [rs79965940] and ULK1A [rs61942435]) to predict the protein stability change at the structural level. On the basis of CHARMM force field, rs79965940 nsSNP (N148T) was found to increase the total energy of the protein structure and hence could be regarded as a destabilizing mutation. On the other hand, the nsSNP rs61942435 (A991V) decreased the total energy and hence could be regarded as stabilizing mutation. Overall, the nsSNP rs61942435 was found to increase the protein stability while, the nsSNPs rs79965940, rs55824543 and rs56364352 were found to decrease the protein stability both at sequence and structure level. Therefore, we selected these four

nsSNPs for genotyping in the HBV infected patient samples in order to determine their role in disease susceptibility or progression.

Using a large, well-characterized north Indian population group, the foremost findings reported here with respect to nsSNPs of *ULK1* gene was that, although all the genotype variants were detected both in the patients and controls but rs79965940 and rs56364352 were independently associated with HBV infection whereas nsSNPs rs61942435 and rs55824543 were not associated with HBV infection respectively. The statistically significant association shown by rs79965940 and rs56364352 has revealed the importance of these polymorphisms with susceptibility to HBV infection. Further, we assessed if these 4 nsSNPs have any association with clinical HBV infected groups. Interestingly our results revealed a substantial association of *ULK1* rs79965940 with two subclinical HBV groups i.e. acute and CHB risk groups. Similarly, rs56364352 have also shown noteworthy association with three sub-clinical HBV groups i.e. acute, asymptomatic and CHB risk group. Eventually, on analysis of mutant genotypes of rs56364352 and rs79965940, it was clearly observed that there was an increase in hepatitis B viral load as HBV infection progresses from asymptomatic infection to LC.

In our work, we have also investigated the possible connection of *ULK1* SNPs rs3923716 and rs12303764 with HBV infection in North Indian population. Where in the frequencies of GG genotype (56%) and G allele (72%) of rs3923716 were different in the HBV patients compared with those in healthy controls. The logistic regression analysis illustrated that G allele of rs3923716 is associated with HBV infection. Further, an extensive analysis on different clinical groups of HBV infection depicts interesting results showing that G allele of rs3923716 is associated with asymptomatic infection and liver cirrhosis but not associated with acute hepatitis and chronic hepatitis. These results suggest that TT genotype and T allele of rs3923716 is involved in disease progression as this allele is maximally represented among patients that are either at the first stage of liver disease or at the last stage. Similarly, when mutant TT was compared with hepatitis B viral load among clinical groups, it was observed that the viral load increases when HBV infection progresses from asymptomatic to LC infected patients. In addition, higher serum ALT, AST levels in HBV patients were associated with rs79965940. In other words, the patients with rs3923716 TT genotype and T allele of *ULK1* gene are more likely to have a progressive status in HBV infection.

This is the first study of its kind, presenting genetic association between polymorphisms of ULK1 gene with HBV infectious patients. The study focuses on the prediction of nsSNPs of ULK1 gene and their susceptibility to HBV infection in north Indian population. The results of this study demonstrate that mutant alleles of rs79965940 and rs56364352 destabilize the ULK1 protein structure. On further comprehensive analysis and assessment (**Figure 5.1**), it is now evident that rs79965940, rs56364352 and rs3923716 are associated with higher risk of HBV infection developing from initial asymptomatic infection to more severe chronic infection. It is proposed that nsSNPs and their damaging or deleterious impact could be examined in other populations as well for their possible involvement in various diseases associated with ULK1 and autophagy. Moreover, the identification of haplotype ATCC in the study is statistically associated HBV infection development. In conclusion, we anticipate that these analyzed SNPs can be used as genetic biomarkers and can act as a bridge between the research gap on autophagy and HBV relation.

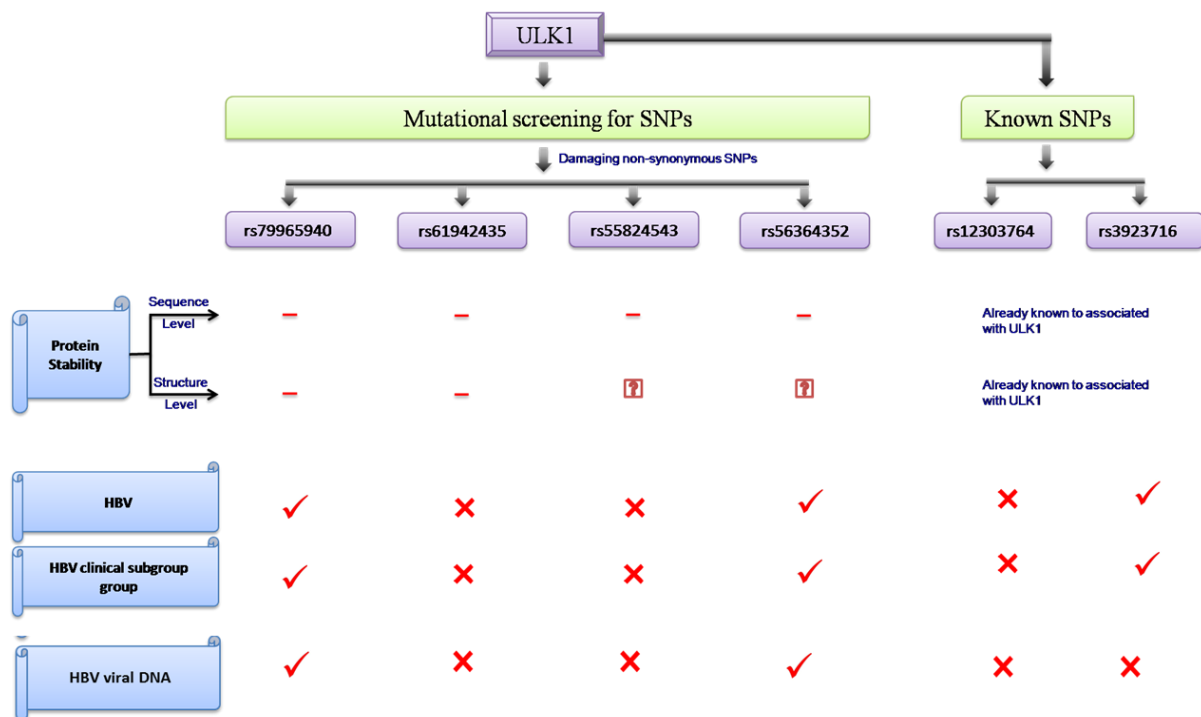


Figure 5.1 Representation of overall conclusion of the study.

# REFERENCES

## 7. References

- [1] F. Becker, C. G. van El, D. Ibarreta, E. Zika, S. Hogarth, P. Borry, *et al* "Genetic testing and common disorders in a public health framework: how to assess relevance and possibilities. Background Document to the ESHG recommendations on genetic testing and common disorders," *Eur J Hum Genet*, vol. 19 Suppl 1, pp. S6-44, Apr 2011.
- [2] W. S. Bush and J. H. Moore, "Chapter 11: Genome-wide association studies," *PLoS Comput Biol*, vol. 8, p. e1002822, 2012.
- [3] B. Rabbani, H. Nakaoka, S. Akhondzadeh, M. Tekin, and N. Mahdieh, "Next generation sequencing: implications in personalized medicine and pharmacogenomics," *Mol Biosyst*, vol. 12, pp. 1818-30, May 24 2016.
- [4] G. G, " Personalized medicine: Promises and pitfalls," *CRC Press*, 2016 Apr 5.
- [5] D. Langlais, N. Fodil, and P. Gros, "Genetics of Infectious and Inflammatory Diseases: Overlapping Discoveries from Association and Exome-Sequencing Studies," *Annu Rev Immunol*, vol. 35, pp. 1-30, Apr 26 2017.
- [6] N. Nishida, K. Tokunaga, and M. Mizokami, "Genome-Wide Association Study Reveals Host Genetic Factors for Liver Diseases," *J Clin Transl Hepatol*, vol. 1, pp. 45-50, Sep 2013.
- [7] W. Xie, D. Agniel, A. Shevchenko, S. V. Malov, A. Svitin, N. Cherkasov, M. K. Baum, A. Campa, S. Gaseitsiwe, H. Bussmann, J. Makhema, R. Marlink, V. Novitsky, T. H. Lee, T. Cai, S. J. O'Brien, and M. Essex, "Genome-Wide Analyses Reveal Gene Influence on HIV Disease Progression and HIV-1C Acquisition in Southern Africa," *AIDS Res Hum Retroviruses*, vol. 33, pp. 597-609, Jun 2017.
- [8] A. L. Harper, L. V. McKinney, L. R. Nielsen, L. Havlickova, Y. Li, M. Trick, *et al.*, "Molecular markers for tolerance of European ash (*Fraxinus excelsior*) to dieback disease identified using Associative Transcriptomics," *Sci Rep*, vol. 6, p. 19335, Jan 13 2016.
- [9] N. Fodil, D. Langlais, and P. Gros, "Primary Immunodeficiencies and Inflammatory Disease: A Growing Genetic Intersection," *Trends Immunol*, vol. 37, pp. 126-40, Feb 2016.
- [10] W. A, "Genome-Wide Association Studies: A Comprehensive Tool to Explore Comparative Genomic Variations and Interactions," *Translational Bioinformatics and Its Application*, pp. 205-222, 2017.
- [11] J. Yang, R. J. Loos, J. E. Powell, S. E. Medland, E. K. Speliotes, D. I. Chasman, *et al.* , "FTO genotype is associated with phenotypic variability of body mass index," *Nature*, vol. 490, pp. 267-72, Oct 11 2012.



- [12] H. Lango Allen, K. Estrada, G. Lettre, S. I. Berndt, M. N. Weedon, F. Rivadeneira, et al. "Hundreds of variants clustered in genomic loci and biological pathways affect human height," *Nature*, vol. 467, pp. 832-8, Oct 14 2010.
- [13] A. Fujimoto, J. Ohashi, N. Nishida, T. Miyagawa, Y. Morishita, T. Tsunoda, R. Kimura, and K. Tokunaga, "A replication study confirmed the EDAR gene to be a major contributor to population differentiation regarding head hair thickness in Asia," *Hum Genet*, vol. 124, pp. 179-85, Sep 2008.
- [14] M. Horikoshi, R. N. Beaumont, F. R. Day, N. M. Warrington, M. N. Kooijman, J. Fernandez-Tajes, et al., "Genome-wide associations for birth weight and correlations with adult disease," *Nature*, vol. 538, pp. 248-252, Oct 13 2016.
- [15] C. S. Tang, H. Zhang, C. Y. Cheung, M. Xu, J. C. Ho, W. Zhou, et al., "Exome-wide association analysis reveals novel coding sequence variants associated with lipid traits in Chinese," *Nat Commun*, vol. 6, p. 10206, Dec 22 2015.
- [16] N. Sikhayeva, A. Iskakova, N. Saigi-Morgui, E. Zholdybaeva, C. B. Eap, and E. Ramanculov, "Association between 28 single nucleotide polymorphisms and type 2 diabetes mellitus in the Kazakh population: a case-control study," *BMC Med Genet*, vol. 18, p. 76, Jul 24 2017.
- [17] H. Zhao, D. R. Nyholt, Y. Yang, and J. Wang, "Improving the detection of pathways in genome-wide association studies by combined effects of SNPs from Linkage Disequilibrium blocks," *Sci Rep*, vol. 7, p. 3512, Jun 14 2017.
- [18] C. C. Chang, C. C. Chow, L. C. Tellier, S. Vattikuti, S. M. Purcell, and J. J. Lee, "Second-generation PLINK: rising to the challenge of larger and richer datasets," *Gigascience*, vol. 4, p. 7, 2015.
- [19] J. Fellay, K. V. Shianna, D. Ge, S. Colombo, B. Ledergerber, M. Weale, K. Zhang, C. Gumbs, A. Castagna, A. Cossarizza, A. Cozzi-Lepri, A. De Luca, P. Easterbrook, P. Francioli, S. Mallal, J. Martinez-Picado, J. M. Miro, N. Obel, J. P. Smith, J. Wyniger, P. Descombes, S. E. Antonarakis, N. L. Letvin, A. J. McMichael, B. F. Haynes, A. Telenti, and D. B. Goldstein, "A whole-genome association study of major determinants for host control of HIV-1," *Science*, vol. 317, pp. 944-7, Aug 17 2007.
- [20] M. Jallow, Y. Y. Teo, K. S. Small, K. A. Rockett, P. Deloukas, T. G. Clark, et al. "Genome-wide and fine-resolution association analysis of malaria in West Africa," *Nat Genet*, vol. 41, pp. 657-65, Jun 2009.
- [21] T. Thye, F. O. Vannberg, S. H. Wong, E. Owusu-Dabo, I. Osei, J. Gyapong, et al., "Genome-wide association analyses identifies a susceptibility locus for tuberculosis on chromosome 18q11.2," *Nat Genet*, vol. 42, pp. 739-741, Sep 2010.

- [22] F. R. Zhang, W. Huang, S. M. Chen, L. D. Sun, H. Liu, Y. Li, *et al.* "Genomewide association study of leprosy," *N Engl J Med*, vol. 361, pp. 2609-18, Dec 31 2009.
- [23] S. Davila, V. J. Wright, C. C. Khor, K. S. Sim, A. Binder, W. B. Breunis, D. Inwald, S. Nadel, H. Betts, E. D. Carrol, R. de Groot, P. W. Hermans, J. Hazelzet, M. Emonts, C. C. Lim, T. W. Kuijpers, F. Martinon-Torres, A. Salas, W. Zenz, M. Levin, and M. L. Hibberd, "Genome-wide association study identifies variants in the CFH region associated with host susceptibility to meningococcal disease," *Nat Genet*, vol. 42, pp. 772-6, Sep 2010.
- [24] D. Burgner, S. Davila, W. B. Breunis, S. B. Ng, Y. Li, C. Bonnard, *et al.*, "A genome-wide association study identifies novel and functionally related susceptibility Loci for Kawasaki disease," *PLoS Genet*, vol. 5, p. e1000319, Jan 2009.
- [25] Y. Kamatani, S. Wattanapokayakit, H. Ochi, T. Kawaguchi, A. Takahashi, N. Hosono, *et al.*, "A genome-wide association study identifies variants in the HLA-DP locus associated with chronic hepatitis B in Asians," *Nat Genet*, vol. 41, pp. 591-5, May 2009.
- [26] H. Zhang, Y. Zhai, Z. Hu, C. Wu, J. Qian, W. Jia, *et al.*, "Genome-wide association study identifies 1p36.22 as a new susceptibility locus for hepatocellular carcinoma in chronic hepatitis B virus carriers," *Nat Genet*, vol. 42, pp. 755-8, Sep 2010.
- [27] A. Rauch, S. Gaudieri, C. Thio, and P. Y. Bochud, "Host genetic determinants of spontaneous hepatitis C clearance," *Pharmacogenomics*, vol. 10, pp. 1819-37, Nov 2009.
- [28] M. P. Martin and M. Carrington, "Immunogenetics of viral infections," *Curr Opin Immunol*, vol. 17, pp. 510-6, Oct 2005.
- [29] M. d. A. MacLennan, Pedro Lara; Vaitsman, Jeni, "Health policy in emerging economies: Innovations and challenges," *Policy in Focus*, vol. 35, 2016.
- [30] P. Desikan and Z. Khan, "Prevalence of hepatitis B and hepatitis C virus co-infection in India: A systematic review and meta-analysis," *Indian J Med Microbiol*, vol. 35, pp. 332-339, Jul-Sep 2017.
- [31] B. Terziroli Beretta-Piccoli, G. Mieli-Vergani, and D. Vergani, "Serology in autoimmune hepatitis: A clinical-practice approach," *Eur J Intern Med*, Oct 19 2017.
- [32] MedlinePlus, "Hepatitis."
- [33] N. Allard, A. Dev, J. Dwyer, G. Srivatsa, A. Thompson, and B. Cowie, "Factors associated with poor adherence to antiviral treatment for hepatitis B," *J Viral Hepat*, vol. 24, pp. 53-58, Jan 2017.
- [34] A. Bertoletti, A. T. Tan, and S. Koh, "T-cell therapy for chronic viral hepatitis," *Cytotherapy*, Aug 25 2017.

- [35] M. E. Guicciardi, H. Malhi, J. L. Mott, and G. J. Gores, "Apoptosis and necrosis in the liver," *Compr Physiol*, vol. 3, pp. 977-1010, Apr 2013.
- [36] WHO, "Hepatitis B Fact sheet," 2017.
- [37] "Global, regional, and national age-sex specific all-cause and cause-specific mortality for 240 causes of death, 1990-2013: a systematic analysis for the Global Burden of Disease Study 2013," *Lancet*, vol. 385, pp. 117-71, Jan 10 2015.
- [38] WHO, 2015.
- [39] P. Puri, "Tackling the Hepatitis B Disease Burden in India," *J Clin Exp Hepatol*, vol. 4, pp. 312-9, Dec 2014.
- [40] C. Seeger and W. S. Mason, "Hepatitis B virus biology," *Microbiol Mol Biol Rev*, vol. 64, pp. 51-68, Mar 2000.
- [41] R. Horvat, "Diagnostic and Clinical Relevance of HBV Mutations," *LABMEDICINE*, vol. 42(8), pp. 488-96, 2011.
- [42] N. Patel, S. J. White, R. F. Thompson, R. Bingham, E. U. Weiss, D. P. Maskell, A. Zlotnick, E. Dykeman, R. Tuma, R. Twarock, N. A. Ranson, and P. G. Stockley, "HBV RNA pre-genome encodes specific motifs that mediate interactions with the viral core protein that promote nucleocapsid assembly," *Nat Microbiol*, vol. 2, p. 17098, Jun 19 2017.
- [43] T. M. Block, H. Guo, and J. T. Guo, "Molecular virology of hepatitis B virus for clinicians," *Clin Liver Dis*, vol. 11, pp. 685-706, vii, Nov 2007.
- [44] M. I. Lusida, Surayah, H. Sakugawa, M. Nagano-Fujii, Soetjipto, Mulyanto, R. Handajani, Boediwarsono, P. B. Setiawan, C. A. Nidom, S. Ohgimoto, and H. Hotta, "Genotype and subtype analyses of hepatitis B virus (HBV) and possible co-infection of HBV and hepatitis C virus (HCV) or hepatitis D virus (HDV) in blood donors, patients with chronic liver disease and patients on hemodialysis in Surabaya, Indonesia," *Microbiol Immunol*, vol. 47, pp. 969-75, 2003.
- [45] H. Norder, A. M. Courouce, and L. O. Magnius, "Molecular basis of hepatitis B virus serotype variations within the four major subtypes," *J Gen Virol*, vol. 73 ( Pt 12), pp. 3141-5, Dec 1992.
- [46] H. Norder, B. Hammas, S. D. Lee, K. Bile, A. M. Courouce, I. K. Mushahwar, and L. O. Magnius, "Genetic relatedness of hepatitis B viral strains of diverse geographical origin and natural variations in the primary structure of the surface antigen," *J Gen Virol*, vol. 74 ( Pt 7), pp. 1341-8, Jul 1993.
- [47] K. Kidd-Ljunggren, E. Myhre, and J. Blackberg, "Clinical and serological variation between patients infected with different Hepatitis B virus genotypes," *J Clin Microbiol*, vol. 42, pp. 5837-41, Dec 2004.

- [48] A. Kramvis, "Genotypes and genetic variability of hepatitis B virus," *Intervirology*, vol. 57, pp. 141-50, 2014.
- [49] L. Stuyver, S. De Gendt, C. Van Geyt, F. Zoulim, M. Fried, R. F. Schinazi, and R. Rossau, "A new genotype of hepatitis B virus: complete genome and phylogenetic relatedness," *J Gen Virol*, vol. 81, pp. 67-74, Jan 2000.
- [50] W. Q. Xiang, W. F. Feng, W. Ke, Z. Sun, Z. Chen, and W. Liu, "Hepatitis B virus X protein stimulates IL-6 expression in hepatocytes via a MyD88-dependent pathway," *J Hepatol*, vol. 54, pp. 26-33, Jan 2011.
- [51] X. Zhang, H. Zhang, and L. Ye, "Effects of hepatitis B virus X protein on the development of liver cancer," *J Lab Clin Med*, vol. 147, pp. 58-66, Feb 2006.
- [52] B. Liu, M. Fang, Y. Hu, B. Huang, N. Li, C. Chang, R. Huang, X. Xu, Z. Yang, Z. Chen, and W. Liu, "Hepatitis B virus X protein inhibits autophagic degradation by impairing lysosomal maturation," *Autophagy*, vol. 10, pp. 416-30, Mar 2014.
- [53] B. Levine, N. Mizushima, and H. W. Virgin, "Autophagy in immunity and inflammation," *Nature*, vol. 469, pp. 323-35, Jan 20 2011.
- [54] V. Deretic and B. Levine, "Autophagy, immunity, and microbial adaptations," *Cell Host Microbe*, vol. 5, pp. 527-49, Jun 18 2009.
- [55] H. Yang, Q. Fu, C. Liu, T. Li, Y. Wang, H. Zhang, X. Lu, X. Sang, S. Zhong, J. Huang, and Y. Mao, "Hepatitis B virus promotes autophagic degradation but not replication in autophagosome," *Biosci Trends*, vol. 9, pp. 111-6, Apr 2015.
- [56] S. Ghavami, R. H. Cunnington, S. Gupta, B. Yeganeh, K. L. Filomeno, D. H. Freed, S. Chen, T. Klonisch, A. J. Halayko, E. Ambrose, R. Singal, and I. M. Dixon, "Autophagy is a regulator of TGF-beta1-induced fibrogenesis in primary human atrial myofibroblasts," *Cell Death Dis*, vol. 6, p. e1696, 2015.
- [57] Y. Feng, D. He, Z. Yao, and D. J. Klionsky, "The machinery of macroautophagy," *Cell Res*, vol. 24, pp. 24-41, Jan 2014.
- [58] C. Mauvezin, P. Nagy, G. Juhasz, and T. P. Neufeld, "Autophagosome-lysosome fusion is independent of V-ATPase-mediated acidification," *Nat Commun*, vol. 6, p. 7007, May 11 2015.
- [59] I. G. Ganley, P. M. Wong, N. Gammoh, and X. Jiang, "Distinct autophagosomal-lysosomal fusion mechanism revealed by thapsigargin-induced autophagy arrest," *Mol Cell*, vol. 42, pp. 731-43, Jun 24 2011.
- [60] B. Levine and G. Kroemer, "Autophagy in the pathogenesis of disease," *Cell*, vol. 132, pp. 27-42, Jan 11 2008.

- [61] N. Mizushima, "Autophagy: process and function," *Genes Dev*, vol. 21, pp. 2861-73, Nov 15 2007.
- [62] G. Kroemer, G. Marino, and B. Levine, "Autophagy and the integrated stress response," *Mol Cell*, vol. 40, pp. 280-93, Oct 22 2010.
- [63] D. Sir, Y. Tian, W. L. Chen, D. K. Ann, T. S. Yen, and J. H. Ou, "The early autophagic pathway is activated by hepatitis B virus and required for viral DNA replication," *Proc Natl Acad Sci U S A*, vol. 107, pp. 4383-8, Mar 2 2010.
- [64] Y. Tian, D. Sir, C. F. Kuo, D. K. Ann, and J. H. Ou, "Autophagy required for hepatitis B virus replication in transgenic mice," *J Virol*, vol. 85, pp. 13453-6, Dec 2011.
- [65] P. M. Wong, C. Puente, I. G. Ganley, and X. Jiang, "The ULK1 complex: sensing nutrient signals for autophagy activation," *Autophagy*, vol. 9, pp. 124-37, Feb 01 2013.
- [66] D. J. Klionsky and Y. Ohsumi, "Vacuolar import of proteins and organelles from the cytoplasm," *Annu Rev Cell Dev Biol*, vol. 15, pp. 1-32, 1999.
- [67] J. Li, Y. Liu, Z. Wang, K. Liu, Y. Wang, J. Liu, H. Ding, and Z. Yuan, "Subversion of cellular autophagy machinery by hepatitis B virus for viral envelopment," *J Virol*, vol. 85, pp. 6319-33, Jul 2011.
- [68] H. Tang, L. Da, Y. Mao, Y. Li, D. Li, Z. Xu, F. Li, Y. Wang, P. Tiollais, T. Li, and M. Zhao, "Hepatitis B virus X protein sensitizes cells to starvation-induced autophagy via up-regulation of beclin 1 expression," *Hepatology*, vol. 49, pp. 60-71, Jan 2009.
- [69] D. J. Horne, A. D. Graustein, J. A. Shah, G. Peterson, M. Savlov, S. Steele, M. Narita, and T. R. Hawn, "Human ULK1 Variation and Susceptibility to Mycobacterium tuberculosis Infection," *J Infect Dis*, Aug 2 2016.
- [70] M. Zheng, H. Yu, L. Zhang, H. Li, Y. Liu, A. Kijlstra, and P. Yang, "Association of ATG5 Gene Polymorphisms With Behcet's Disease and ATG10 Gene Polymorphisms With VKH Syndrome in a Chinese Han Population," *Invest Ophthalmol Vis Sci*, vol. 56, pp. 8280-7, Dec 2015.
- [71] G. Costain, A. C. Lionel, L. Ogura, C. R. Marshall, S. W. Scherer, C. K. Silversides, and A. S. Bassett, "Genome-wide rare copy number variations contribute to genetic risk for transposition of the great arteries," *Int J Cardiol*, vol. 204, pp. 115-21, Feb 1 2016.
- [72] S. Rufini, C. Ciccacci, D. Di Fusco, A. Ruffa, F. Pallone, G. Novelli, L. Biancone, and P. Borgiani, "Autophagy and inflammatory bowel disease: Association between variants of the autophagy-related IRGM gene and susceptibility to Crohn's disease," *Dig Liver Dis*, vol. 47, pp. 744-50, Sep 2015.

- [73] A. R. Morgan, W. J. Lam, D. Y. Han, A. G. Fraser, and L. R. Ferguson, "Association Analysis of ULK1 with Crohn's Disease in a New Zealand Population," *Gastroenterol Res Pract*, vol. 2012, p. 715309, 2012.
- [74] X. Qu, J. Yu, G. Bhagat, N. Furuya, H. Hibshoosh, A. Troxel, J. Rosen, E. L. Eskelinen, N. Mizushima, Y. Ohsumi, G. Cattoretti, and B. Levine, "Promotion of tumorigenesis by heterozygous disruption of the beclin 1 autophagy gene," *J Clin Invest*, vol. 112, pp. 1809-20, Dec 2003.
- [75] L. Henckaerts, I. Cleynen, M. Brinar, J. M. John, K. Van Steen, P. Rutgeerts, and S. Vermeire, "Genetic variation in the autophagy gene ULK1 and risk of Crohn's disease," *Inflamm Bowel Dis*, vol. 17, pp. 1392-7, Jun 2011.
- [76] Z. H. Zhang, C. C. Wu, X. W. Chen, X. Li, J. Li, and M. J. Lu, "Genetic variation of hepatitis B virus and its significance for pathogenesis," *World J Gastroenterol*, vol. 22, pp. 126-44, Jan 07 2016.
- [77] S. Ogholikhan and K. B. Schwarz, "Hepatitis Vaccines," *Vaccines (Basel)*, vol. 4, Mar 11 2016.
- [78] A. Biswas, R. Panigrahi, M. Pal, S. Chakraborty, P. Bhattacharya, S. Chakrabarti, and R. Chakravarty, "Shift in the hepatitis B virus genotype distribution in the last decade among the HBV carriers from eastern India: possible effects on the disease status and HBV epidemiology," *J Med Virol*, vol. 85, pp. 1340-7, Aug 2013.
- [79] J. Hu and K. Liu, "Complete and Incomplete Hepatitis B Virus Particles: Formation, Function, and Application," *Viruses*, vol. 9, Mar 21 2017.
- [80] S. Datta, S. Chatterjee, V. Veer, and R. Chakravarty, "Molecular biology of the hepatitis B virus for clinicians," *J Clin Exp Hepatol*, vol. 2, pp. 353-65, Dec 2012.
- [81] N. Gupta, M. Goyal, C. H. Wu, and G. Y. Wu, "The Molecular and Structural Basis of HBV-resistance to Nucleos(t)ide Analogs," *J Clin Transl Hepatol*, vol. 2, pp. 202-11, Sep 2014.
- [82] F. V. Chisari, M. Isogawa, and S. F. Wieland, "Pathogenesis of hepatitis B virus infection," *Pathol Biol (Paris)*, vol. 58, pp. 258-66, Aug 2010.
- [83] A. Chen, Y. F. Kao, and C. M. Brown, "Translation of the first upstream ORF in the hepatitis B virus pregenomic RNA modulates translation at the core and polymerase initiation codons," *Nucleic Acids Res*, vol. 33, pp. 1169-81, 2005.
- [84] M. J. Feige and L. M. Hendershot, "Disulfide bonds in ER protein folding and homeostasis," *Curr Opin Cell Biol*, vol. 23, pp. 167-75, Apr 2011.
- [85] J. Y. Lee and S. Locarnini, "Hepatitis B virus: pathogenesis, viral intermediates, and viral replication," *Clin Liver Dis*, vol. 8, pp. 301-20, May 2004.

- [86] R. A. Crowther, "The Leeuwenhoek lecture 2006. Microscopy goes cold: frozen viruses reveal their structural secrets," *Philos Trans R Soc Lond B Biol Sci*, vol. 363, pp. 2441-51, Jul 27 2008.
- [87] R. Toita, T. Kawano, J. H. Kang, and M. Murata, "Applications of human hepatitis B virus preS domain in bio- and nanotechnology," *World J Gastroenterol*, vol. 21, pp. 7400-11, Jun 28 2015.
- [88] U. Lauer, L. Weiss, P. H. Hofschneider, and A. S. Kekule, "The hepatitis B virus pre-S/S(t) transactivator is generated by 3' truncations within a defined region of the S gene," *J Virol*, vol. 66, pp. 5284-9, Sep 1992.
- [89] K. Madalinski, B. Burczynska, K. H. Heermann, A. Uy, and W. H. Gerlich, "Analysis of viral proteins in circulating immune complexes from chronic carriers of hepatitis B virus," *Clin Exp Immunol*, vol. 84, pp. 493-500, Jun 1991.
- [90] J. Quarleri, "Core promoter: a critical region where the hepatitis B virus makes decisions," *World J Gastroenterol*, vol. 20, pp. 425-35, Jan 14 2014.
- [91] Y. J. Lin, L. R. Huang, H. C. Yang, H. T. Tzeng, P. N. Hsu, H. L. Wu, P. J. Chen, and D. S. Chen, "Hepatitis B virus core antigen determines viral persistence in a C57BL/6 mouse model," *Proc Natl Acad Sci U S A*, vol. 107, pp. 9340-5, May 18 2010.
- [92] X. Yu, L. Jin, J. Jih, C. Shih, and Z. H. Zhou, "3.5A cryoEM structure of hepatitis B virus core assembled from full-length core protein," *PLoS One*, vol. 8, p. e69729, 2013.
- [93] R. Walsh and S. Locarnini, "Hepatitis B precore protein: pathogenic potential and therapeutic promise," *Yonsei Med J*, vol. 53, pp. 875-85, Sep 2012.
- [94] M. S. R. M. Bruce R. Korf (auth.), PhD, Cam Patterson MD (eds.), "Principles of Molecular Medicine," *Humana Press*, 2006.
- [95] S. A. Jones and J. Hu, "Hepatitis B virus reverse transcriptase: diverse functions as classical and emerging targets for antiviral intervention," *Emerg Microbes Infect*, vol. 2, p. e56, Sep 2013.
- [96] J. E. Tavis, X. Cheng, Y. Hu, M. Totten, F. Cao, E. Michailidis, R. Aurora, M. J. Meyers, E. J. Jacobsen, M. A. Parniak, and S. G. Sarafianos, "The hepatitis B virus ribonuclease H is sensitive to inhibitors of the human immunodeficiency virus ribonuclease H and integrase enzymes," *PLoS Pathog*, vol. 9, p. e1003125, Jan 2013.
- [97] D. N. Clark and J. Hu, "Hepatitis B virus reverse transcriptase - Target of current antiviral therapy and future drug development," *Antiviral Res*, vol. 123, pp. 132-7, Nov 2015.
- [98] G. Y. Hwang, C. Y. Lin, L. M. Huang, Y. H. Wang, J. C. Wang, C. T. Hsu, S. S. Yang, and C. C. Wu, "Detection of the hepatitis B virus X protein (HBx) antigen and anti-HBx antibodies in cases of human hepatocellular carcinoma," *J Clin Microbiol*, vol. 41, pp. 5598-603, Dec 2003.

- [99] D. Y. Gong, E. Q. Chen, F. J. Huang, X. H. Leng, X. Cheng, and H. Tang, "Role and functional domain of hepatitis B virus X protein in regulating HBV transcription and replication in vitro and in vivo," *Viruses*, vol. 5, pp. 1261-71, May 22 2013.
- [100] M. A. Mathew, S. C. Kurian, A. P. Varghese, S. Oommen, and M. G, "HBx Gene Mutations in Hepatitis B Virus and Hepatocellular Carcinoma," *Gastroenterology Res*, vol. 7, pp. 1-4, Feb 2014.
- [101] W. Li, "The hepatitis B virus receptor," *Annu Rev Cell Dev Biol*, vol. 31, pp. 125-47, 2015.
- [102] N. Fay and N. Pante, "Nuclear entry of DNA viruses," *Front Microbiol*, vol. 6, p. 467, 2015.
- [103] NicolettaPrevisaniDaniellLavanchy, "Hepatitis B," *Perspectives in Medical Virology*, vol. 10, pp. 31-97, 26/11/2003 2003.
- [104] C. Seeger and W. S. Mason, "Molecular biology of hepatitis B virus infection," *Virology*, vol. 479-480, pp. 672-86, May 2015.
- [105] C. Shih, S. F. Chou, C. C. Yang, J. Y. Huang, G. Chojijilsuren, and R. S. Zhou, "Control and Eradication Strategies of Hepatitis B Virus," *Trends Microbiol*, vol. 24, pp. 739-49, Sep 2016.
- [106] M. M. Minor and B. L. Slagle, "Hepatitis B virus HBx protein interactions with the ubiquitin proteasome system," *Viruses*, vol. 6, pp. 4683-702, Nov 24 2014.
- [107] C. J. Liu and J. H. Kao, "Global perspective on the natural history of chronic hepatitis B: role of hepatitis B virus genotypes A to J," *Semin Liver Dis*, vol. 33, pp. 97-102, May 2013.
- [108] A. Kramvis, "The clinical implications of hepatitis B virus genotypes and HBeAg in pediatrics," *Rev Med Virol*, vol. 26, pp. 285-303, Jul 2016.
- [109] Y. Suzuki, M. Kobayashi, K. Ikeda, F. Suzuki, Y. Arfase, N. Akuta, T. Hosaka, S. Saitoh, T. Someya, M. Matsuda, J. Sato, S. Watabiki, Y. Miyakawa, and H. Kumada, "Persistence of acute infection with hepatitis B virus genotype A and treatment in Japan," *J Med Virol*, vol. 76, pp. 33-9, May 2005.
- [110] K. Watanabe, T. Takahashi, S. Takahashi, S. Okoshi, T. Ichida, and Y. Aoyagi, "Comparative study of genotype B and C hepatitis B virus-induced chronic hepatitis in relation to the basic core promoter and precore mutations," *J Gastroenterol Hepatol*, vol. 20, pp. 441-9, Mar 2005.
- [111] Y. H. Ni, M. H. Chang, K. J. Wang, H. Y. Hsu, H. L. Chen, J. H. Kao, S. H. Yeh, Y. M. Jeng, K. S. Tsai, and D. S. Chen, "Clinical relevance of hepatitis B virus genotype in children with chronic infection and hepatocellular carcinoma," *Gastroenterology*, vol. 127, pp. 1733-8, Dec 2004.
- [112] M. F. Yuen, D. K. Wong, E. Sablon, E. Tse, I. O. Ng, H. J. Yuan, C. W. Siu, T. J. Sander, E. J. Bourne, J. G. Hall, L. D. Condreay, and C. L. Lai, "HBsAg seroclearance in chronic hepatitis B in



- the Chinese: virological, histological, and clinical aspects," *Hepatology*, vol. 39, pp. 1694-701, Jun 2004.
- [113] B. S. Guirgis, R. O. Abbas, and H. M. Azzazy, "Hepatitis B virus genotyping: current methods and clinical implications," *Int J Infect Dis*, vol. 14, pp. e941-53, Nov 2010.
- [114] E. Orito, T. Ichida, H. Sakugawa, M. Sata, N. Horiike, K. Hino, K. Okita, T. Okanoue, S. Iino, E. Tanaka, K. Suzuki, H. Watanabe, S. Hige, and M. Mizokami, "Geographic distribution of hepatitis B virus (HBV) genotype in patients with chronic HBV infection in Japan," *Hepatology*, vol. 34, pp. 590-4, Sep 2001.
- [115] E. Orito, F. Sugauchi, Y. Tanaka, T. Ichida, M. Sata, E. Tanaka, T. Okanoue, H. Sakugawa, H. Watanabe, H. Miyakawa, S. Nishiguchi, H. Kumada, R. Ueda, and M. Mizokami, "Differences of hepatocellular carcinoma patients with hepatitis B virus genotypes of Ba, Bj or C in Japan," *Intervirology*, vol. 48, pp. 239-45, 2005.
- [116] M. R. Pourkarim, S. Amini-Bavil-Olyaei, F. Kurbanov, M. Van Ranst, and F. Tacke, "Molecular identification of hepatitis B virus genotypes/subgenotypes: revised classification hurdles and updated resolutions," *World J Gastroenterol*, vol. 20, pp. 7152-68, Jun 21 2014.
- [117] C. M. Croagh, P. V. Desmond, and S. J. Bell, "Genotypes and viral variants in chronic hepatitis B: A review of epidemiology and clinical relevance," *World J Hepatol*, vol. 7, pp. 289-303, Mar 27 2015.
- [118] S. Locarnini, A. Hatzakis, D. S. Chen, and A. Lok, "Strategies to control hepatitis B: Public policy, epidemiology, vaccine and drugs," *J Hepatol*, vol. 62, pp. S76-86, Apr 2015.
- [119] C. J. Clements, Y. Baoping, A. Crouch, D. Hipgrave, O. Mansoor, C. B. Nelson, S. Treleaven, R. van Konkelenberg, and S. Wiersma, "Progress in the control of hepatitis B infection in the Western Pacific Region," *Vaccine*, vol. 24, pp. 1975-82, Mar 15 2006.
- [120] H. L. Chan and J. Jia, "Chronic hepatitis B in Asia-new insights from the past decade," *J Gastroenterol Hepatol*, vol. 26 Suppl 1, pp. 131-7, Jan 2011.
- [121] R. Zampino, A. Boemio, C. Sagnelli, L. Alessio, L. E. Adinolfi, E. Sagnelli, and N. Coppola, "Hepatitis B virus burden in developing countries," *World J Gastroenterol*, vol. 21, pp. 11941-53, Nov 14 2015.
- [122] N. C. Nayak, S. K. Panda, A. J. Zuckerman, M. K. Bhan, and D. K. Guha, "Dynamics and impact of perinatal transmission of hepatitis B virus in North India," *J Med Virol*, vol. 21, pp. 137-45, Feb 1987.
- [123] C. Pande, S. K. Sarin, S. Patra, K. Bhutia, S. K. Mishra, S. Pahuja, M. Jain, S. Srivastava, S. B. Dar, S. S. Trivedi, C. K. Mukhopadhyay, and A. Kumar, "Prevalence, risk factors and virological

- profile of chronic hepatitis B virus infection in pregnant women in India," *J Med Virol*, vol. 83, pp. 962-7, Jun 2011.
- [124] R. Behal, R. Jain, K. K. Behal, A. Bhagoliwal, N. Aggarwal, and T. N. Dhole, "Seroprevalence and risk factors for hepatitis B virus infection among general population in Northern India," *Arq Gastroenterol*, vol. 45, pp. 137-40, Apr-Jun 2008.
- [125] T. Kurien, S. P. Thyagarajan, L. Jeyaseelan, A. Peedicayil, P. Rajendran, S. Sivaram, S. G. Hansdak, G. Renu, P. Krishnamurthy, K. Sudhakar, and J. C. Varghese, "Community prevalence of hepatitis B infection and modes of transmission in Tamil Nadu, India," *Indian J Med Res*, vol. 121, pp. 670-5, May 2005.
- [126] T. Kumar, A. Shrivastava, A. Kumar, K. F. Laserson, J. P. Narain, S. Venkatesh, L. S. Chauhan, and F. Averhoff, "Viral Hepatitis Surveillance--India, 2011-2013," *MMWR Morb Mortal Wkly Rep*, vol. 64, pp. 758-62, Jul 24 2015.
- [127] S. A. Meo, A. A. Assad, F. M. Sanie, N. D. Baksh, A. Al-Qahtani, and Z. A. Shaikh, "Transmission of hepatitis-B virus through salivary blood group antigens in saliva," *J Coll Physicians Surg Pak*, vol. 20, pp. 444-8, Jul 2010.
- [128] H. Komatsu, A. Inui, T. Murano, T. Tsunoda, T. Sogo, and T. Fujisawa, "Lack of infectivity of HBV in feces from patients with chronic hepatitis B virus infection, and infection using chimeric mice," *BMC Res Notes*, vol. 8, p. 366, Aug 20 2015.
- [129] E. M. Beltrami, I. T. Williams, C. N. Shapiro, and M. E. Chamberland, "Risk and management of blood-borne infections in health care workers," *Clin Microbiol Rev*, vol. 13, pp. 385-407, Jul 2000.
- [130] Z. Zheng, X. Zhao, Y. Hong, B. Xu, J. Tong, and L. Xia, "The safety of intracytoplasmic sperm injection in men with hepatitis B," *Arch Med Sci*, vol. 12, pp. 587-91, Jun 01 2016.
- [131] W. R. Kim, "Epidemiology of hepatitis B in the United States," *Hepatology*, vol. 49, pp. S28-34, May 2009.
- [132] J. M. Miller, R. Astles, T. Baszler, K. Chapin, R. Carey, L. Garcia, L. Gray, D. Larone, M. Pentella, A. Pollock, D. S. Shapiro, E. Weirich, and D. Wiedbrauk, "Guidelines for safe work practices in human and animal medical diagnostic laboratories. Recommendations of a CDC-convened, Biosafety Blue Ribbon Panel," *MMWR Suppl*, vol. 61, pp. 1-102, Jan 06 2012.
- [133] M. Belopolskaya, V. Avrutin, S. Firsov, and A. Yakovlev, "HBsAg level and hepatitis B viral load correlation with focus on pregnancy," *Ann Gastroenterol*, vol. 28, pp. 379-384, Jul-Sep 2015.
- [134] C. M. Croagh and J. S. Lubel, "Natural history of chronic hepatitis B: phases in a complex relationship," *World J Gastroenterol*, vol. 20, pp. 10395-404, Aug 14 2014.
- [135] T. J. Liang, "Hepatitis B: the virus and disease," *Hepatology*, vol. 49, pp. S13-21, May 2009.

- [136] M. Krajden, G. McNabb, and M. Petric, "The laboratory diagnosis of hepatitis B virus," *Can J Infect Dis Med Microbiol*, vol. 16, pp. 65-72, Mar 2005.
- [137] T. T. Lao, D. S. Sahota, L. W. Law, Y. K. Cheng, and T. Y. Leung, "Age-specific prevalence of hepatitis B virus infection in young pregnant women, Hong Kong Special Administrative Region of China," *Bull World Health Organ*, vol. 92, pp. 782-9, Nov 01 2014.
- [138] A. N. Erena and T. B. Tefera, "Prevalence of hepatitis B surface antigen (HBsAg) and its risk factors among individuals visiting Goba General Hospital, South East Ethiopia, 2012," *BMC Res Notes*, vol. 7, p. 833, Nov 24 2014.
- [139] B. Rauff, M. Idrees, S. A. Shah, S. Butt, A. M. Butt, L. Ali, A. Hussain, R. Irshad Ur, and M. Ali, "Hepatitis associated aplastic anemia: a review," *Virology*, vol. 8, p. 87, Feb 28 2011.
- [140] J. D. Shiela Sherlock, "Diseases of the Liver and Biliary System," 2008.
- [141] T. Inoue and Y. Tanaka, "Hepatitis B virus and its sexually transmitted infection - an update," *Microb Cell*, vol. 3, pp. 420-437, Sep 05 2016.
- [142] H. B. El-Serag, "Epidemiology of viral hepatitis and hepatocellular carcinoma," *Gastroenterology*, vol. 142, pp. 1264-1273 e1, May 2012.
- [143] E. G. Giannini, R. Testa, and V. Savarino, "Liver enzyme alteration: a guide for clinicians," *CMAJ*, vol. 172, pp. 367-79, Feb 01 2005.
- [144] S. Y. Kwon and C. H. Lee, "Epidemiology and prevention of hepatitis B virus infection," *Korean J Hepatol*, vol. 17, pp. 87-95, Jun 2011.
- [145] Z. S. Niu, X. J. Niu, and W. H. Wang, "Genetic alterations in hepatocellular carcinoma: An update," *World J Gastroenterol*, vol. 22, pp. 9069-9095, Nov 07 2016.
- [146] C. Bosetti, F. Turati, and C. La Vecchia, "Hepatocellular carcinoma epidemiology," *Best Pract Res Clin Gastroenterol*, vol. 28, pp. 753-70, Oct 2014.
- [147] N. A. Terrault, N. H. Bzowej, K. M. Chang, J. P. Hwang, M. M. Jonas, and M. H. Murad, "AASLD guidelines for treatment of chronic hepatitis B," *Hepatology*, vol. 63, pp. 261-83, Jan 2016.
- [148] S. Arora, C. L. Martin, and M. Herbert, "Myth: interpretation of a single ammonia level in patients with chronic liver disease can confirm or rule out hepatic encephalopathy," *CJEM*, vol. 8, pp. 433-5, Nov 2006.
- [149] M. D. Zeng, L. G. Lu, Y. M. Mao, D. K. Qiu, J. Q. Li, M. B. Wan, C. W. Chen, J. Y. Wang, X. Cai, C. F. Gao, and X. Q. Zhou, "Prediction of significant fibrosis in HBeAg-positive patients with chronic hepatitis B by a noninvasive model," *Hepatology*, vol. 42, pp. 1437-45, Dec 2005.
- [150] M. Mohamadnejad, G. Montazeri, A. Fazlollahi, F. Zamani, J. Nasiri, H. Nobakht, M. H. Forouzanfar, S. Abedian, S. M. Tavangar, A. Mohamadkhani, F. Ghoujehi, A. Estakhri, N.

- Nouri, Z. Farzadi, A. Najjari, and R. Malekzadeh, "Noninvasive markers of liver fibrosis and inflammation in chronic hepatitis B-virus related liver disease," *Am J Gastroenterol*, vol. 101, pp. 2537-45, Nov 2006.
- [151] A. Kumar, S. Pant, and S. Narang, "Significance of alanine aminotransferase testing in diagnosis of acute and chronic HBV infection," *Asian Pac J Cancer Prev*, vol. 10, pp. 1171-2, 2009.
- [152] C. Mao, A. Liu, and B. Cao, "Virus-based chemical and biological sensing," *Angew Chem Int Ed Engl*, vol. 48, pp. 6790-810, 2009.
- [153] T. C. Zhou, X. Li, L. Li, X. F. Li, L. Zhang, and J. Wei, "Evolution of full-length genomes of HBV quasispecies in sera of patients with a coexistence of HBsAg and anti-HBs antibodies," *Sci Rep*, vol. 7, p. 661, Apr 06 2017.
- [154] N. Yentur Doni, Z. Simsek, Z. Keklik, G. Gurses, and F. Y. Zeyrek, "Epidemiology of hepatitis B in the reproductive-age female farmworkers of southeastern Turkey," *Hepat Mon*, vol. 14, p. e22120, Nov 2014.
- [155] L. Wang, K. Wang, and Z. Q. Zou, "Crosstalk between innate and adaptive immunity in hepatitis B virus infection," *World J Hepatol*, vol. 7, pp. 2980-91, Dec 28 2015.
- [156] M. I. Lusida, Juniastuti, and Y. Yano, "Current hepatitis B virus infection situation in Indonesia and its genetic diversity," *World J Gastroenterol*, vol. 22, pp. 7264-74, Aug 28 2016.
- [157] H. Gregorek, K. Madalinski, M. Woynarowski, J. Mikolajewicz, M. Syczewska, and J. Socha, "IgG subclass distribution of hepatitis B surface antigen antibodies induced in children with chronic hepatitis B infection after interferon-alpha therapy," *J Infect Dis*, vol. 181, pp. 2059-62, Jun 2000.
- [158] N. S. Sheikh, A. S. Sheikh, A. A. Sheikh, S. Yahya, and M. Lateef, "Sero-prevalence of hepatitis B virus infection in Balochistan Province of Pakistan," *Saudi J Gastroenterol*, vol. 17, pp. 180-4, May-Jun 2011.
- [159] C. Bozza, M. Cinausero, D. Iacono, and F. Puglisi, "Hepatitis B and cancer: A practical guide for the oncologist," *Crit Rev Oncol Hematol*, vol. 98, pp. 137-46, Feb 2016.
- [160] Z. N. Said, "An overview of occult hepatitis B virus infection," *World J Gastroenterol*, vol. 17, pp. 1927-38, Apr 21 2011.
- [161] N. Horiike, B. S. Blumberg, and M. A. Feitelson, "Characteristics of hepatitis B X antigen, antibodies to X antigen, and antibodies to the viral polymerase during hepatitis B virus infection," *J Infect Dis*, vol. 164, pp. 1104-12, Dec 1991.
- [162] S. Y. Wu, S. H. Lan, and H. S. Liu, "Autophagy and microRNA in hepatitis B virus-related hepatocellular carcinoma," *World J Gastroenterol*, vol. 22, pp. 176-87, Jan 07 2016.

- [163] L. M. Villar, H. M. Cruz, J. R. Barbosa, C. S. Bezerra, M. M. Portilho, and P. Scalioni Lde, "Update on hepatitis B and C virus diagnosis," *World J Virol*, vol. 4, pp. 323-42, Nov 12 2015.
- [164] B. E. Stranger, E. A. Stahl, and T. Raj, "Progress and promise of genome-wide association studies for human complex trait genetics," *Genetics*, vol. 187, pp. 367-83, Feb 2011.
- [165] K. Yano, E. Yamamoto, K. Aya, H. Takeuchi, P. C. Lo, L. Hu, M. Yamasaki, S. Yoshida, H. Kitano, K. Hirano, and M. Matsuoka, "Genome-wide association study using whole-genome sequencing rapidly identifies new genes influencing agronomic traits in rice," *Nat Genet*, vol. 48, pp. 927-34, Aug 2016.
- [166] Y. R. Li and B. J. Keating, "Trans-ethnic genome-wide association studies: advantages and challenges of mapping in diverse populations," *Genome Med*, vol. 6, p. 91, 2014.
- [167] A. L. Price, C. C. Spencer, and P. Donnelly, "Progress and promise in understanding the genetic basis of common diseases," *Proc Biol Sci*, vol. 282, p. 20151684, Dec 22 2015.
- [168] X. Wang, N. R. Tucker, G. Rizki, R. Mills, P. H. Krijger, E. de Wit, V. Subramanian, E. Bartell, X. X. Nguyen, J. Ye, J. Leyton-Mange, E. V. Dolmatova, P. van der Harst, W. de Laat, P. T. Ellinor, C. Newton-Cheh, D. J. Milan, M. Kellis, and L. A. Boyer, "Discovery and validation of sub-threshold genome-wide association study loci using epigenomic signatures," *Elife*, vol. 5, May 10 2016.
- [169] C. R. Farber, "Systems-level analysis of genome-wide association data," *G3 (Bethesda)*, vol. 3, pp. 119-29, Jan 2013.
- [170] N. A. Rosenberg, L. Huang, E. M. Jewett, Z. A. Szpiech, I. Jankovic, and M. Boehnke, "Genome-wide association studies in diverse populations," *Nat Rev Genet*, vol. 11, pp. 356-66, May 2010.
- [171] A. L. Price, N. A. Zaitlen, D. Reich, and N. Patterson, "New approaches to population stratification in genome-wide association studies," *Nat Rev Genet*, vol. 11, pp. 459-63, Jul 2010.
- [172] A. C. Nica and E. T. Dermitzakis, "Using gene expression to investigate the genetic basis of complex disorders," *Hum Mol Genet*, vol. 17, pp. R129-34, Oct 15 2008.
- [173] J. M. Kwon and A. M. Goate, "The candidate gene approach," *Alcohol Res Health*, vol. 24, pp. 164-8, 2000.
- [174] F. S. Collins, M. S. Guyer, and A. Chakravarti, "Variations on a theme: cataloging human DNA sequence variation," *Science*, vol. 278, pp. 1580-1, Nov 28 1997.
- [175] B. J. Peters, A. S. Rodin, A. de Boer, and A. H. Maitland-van der Zee, "Methodological and statistical issues in pharmacogenomics," *J Pharm Pharmacol*, vol. 62, pp. 161-6, Feb 2010.

- [176] N. J. White, S. Pukrittayakamee, T. T. Hien, M. A. Faiz, O. A. Mokuolu, and A. M. Dondorp, "Malaria," *Lancet*, vol. 383, pp. 723-35, Feb 22 2014.
- [177] G. Band, Q. S. Le, L. Jostins, M. Pirinen, K. Kivinen, M. Jallow, F. Sisay-Joof, K. Bojang, M. Pinder, G. Sirugo, D. J. Conway, V. Nyirongo, D. Kachala, M. Molyneux, T. Taylor, C. Ndila, N. Peshu, K. Marsh, T. N. Williams, D. Alcock, R. Andrews, S. Edkins, E. Gray, C. Hubbart, A. Jeffreys, K. Rowlands, K. Schuldt, T. G. Clark, K. S. Small, Y. Y. Teo, D. P. Kwiatkowski, K. A. Rockett, J. C. Barrett, and C. C. Spencer, "Imputation-based meta-analysis of severe malaria in three African populations," *PLoS Genet*, vol. 9, p. e1003509, May 2013.
- [178] C. Timmann, T. Thye, M. Vens, J. Evans, J. May, C. Ehmen, J. Sievertsen, B. Muntau, G. Ruge, W. Loag, D. Ansong, S. Antwi, E. Asafo-Adjei, S. B. Nguah, K. O. Kwakye, A. O. Akoto, J. Sylverken, M. Brendel, K. Schuldt, C. Loley, A. Franke, C. G. Meyer, T. Agbenyega, A. Ziegler, and R. D. Horstmann, "Genome-wide association study indicates two novel resistance loci for severe malaria," *Nature*, vol. 489, pp. 443-6, Sep 20 2012.
- [179] "Reappraisal of known malaria resistance loci in a large multicenter study," *Nat Genet*, vol. 46, pp. 1197-204, Nov 2014.
- [180] G. Band, K. A. Rockett, C. C. Spencer, and D. P. Kwiatkowski, "A novel locus of resistance to severe malaria in a region of ancient balancing selection," *Nature*, vol. 526, pp. 253-7, Oct 08 2015.
- [181] P. An and C. A. Winkler, "Host genes associated with HIV/AIDS: advances in gene discovery," *Trends Genet*, vol. 26, pp. 119-31, Mar 2010.
- [182] J. Fellay, K. V. Shianna, A. Telenti, and D. B. Goldstein, "Host genetics and HIV-1: the final phase?," *PLoS Pathog*, vol. 6, p. e1001033, Oct 14 2010.
- [183] M. Dean, M. Carrington, C. Winkler, G. A. Huttley, M. W. Smith, R. Allikmets, J. J. Goedert, S. P. Buchbinder, E. Vittinghoff, E. Gomperts, S. Donfield, D. Vlahov, R. Kaslow, A. Saah, C. Rinaldo, R. Detels, and S. J. O'Brien, "Genetic restriction of HIV-1 infection and progression to AIDS by a deletion allele of the *CCR5* structural gene. Hemophilia Growth and Development Study, Multicenter AIDS Cohort Study, Multicenter Hemophilia Cohort Study, San Francisco City Cohort, ALIVE Study," *Science*, vol. 273, pp. 1856-62, Sep 27 1996.
- [184] M. P. Martin, M. Dean, M. W. Smith, C. Winkler, B. Gerrard, N. L. Michael, B. Lee, R. W. Doms, J. Margolick, S. Buchbinder, J. J. Goedert, T. R. O'Brien, M. W. Hilgartner, D. Vlahov, S. J. O'Brien, and M. Carrington, "Genetic acceleration of AIDS progression by a promoter variant of *CCR5*," *Science*, vol. 282, pp. 1907-11, Dec 04 1998.
- [185] H. Hendel, S. Caillat-Zucman, H. Lebuane, M. Carrington, S. O'Brien, J. M. Andrieu, F. Schachter, D. Zagury, J. Rappaport, C. Winkler, G. W. Nelson, and J. F. Zagury, "New class I

- and II HLA alleles strongly associated with opposite patterns of progression to AIDS," *J Immunol*, vol. 162, pp. 6942-6, Jun 01 1999.
- [186] P. O. Flores-Villanueva, H. Hendel, S. Caillat-Zucman, J. Rappaport, A. Burgos-Tiburcio, S. Bertin-Maghit, J. A. Ruiz-Morales, M. E. Teran, J. Rodriguez-Tafur, and J. F. Zagury, "Associations of MHC ancestral haplotypes with resistance/susceptibility to AIDS disease development," *J Immunol*, vol. 170, pp. 1925-9, Feb 15 2003.
- [187] M. Carrington, M. P. Martin, and J. van Bergen, "KIR-HLA intercourse in HIV disease," *Trends Microbiol*, vol. 16, pp. 620-7, Dec 2008.
- [188] T. Hirota, A. Takahashi, M. Kubo, T. Tsunoda, K. Tomita, S. Doi, K. Fujita, A. Miyatake, T. Enomoto, T. Miyagawa, M. Adachi, H. Tanaka, A. Niimi, H. Matsumoto, I. Ito, H. Masuko, T. Sakamoto, N. Hizawa, M. Taniguchi, J. J. Lima, C. G. Irvin, S. P. Peters, B. E. Himes, A. A. Litonjua, K. G. Tantisira, S. T. Weiss, N. Kamatani, Y. Nakamura, and M. Tamari, "Genome-wide association study identifies three new susceptibility loci for adult asthma in the Japanese population," *Nat Genet*, vol. 43, pp. 893-6, Jul 31 2011.
- [189] P. An, C. Winkler, L. Guan, S. J. O'Brien, and Z. Zeng, "A common HLA-DPA1 variant is a major determinant of hepatitis B virus clearance in Han Chinese," *J Infect Dis*, vol. 203, pp. 943-7, Apr 01 2011.
- [190] X. Guo, Y. Zhang, J. Li, J. Ma, Z. Wei, W. Tan, and S. J. O'Brien, "Strong influence of human leukocyte antigen (HLA)-DP gene variants on development of persistent chronic hepatitis B virus carriers in the Han Chinese population," *Hepatology*, vol. 53, pp. 422-8, Feb 2011.
- [191] L. Wang, X. P. Wu, W. Zhang, D. H. Zhu, Y. Wang, Y. P. Li, Y. Tian, R. C. Li, Z. Li, X. Zhu, J. H. Li, J. Cai, L. Liu, X. P. Miao, Y. Liu, and H. Li, "Evaluation of genetic susceptibility loci for chronic hepatitis B in Chinese: two independent case-control studies," *PLoS One*, vol. 6, p. e17608, Mar 08 2011.
- [192] T. R. O'Brien, I. Kohaar, R. M. Pfeiffer, D. Maeder, M. Yeager, E. E. Schadt, and L. Prokunina-Olsson, "Risk alleles for chronic hepatitis B are associated with decreased mRNA expression of HLA-DPA1 and HLA-DPB1 in normal human liver," *Genes Immun*, vol. 12, pp. 428-33, Sep 2011.
- [193] N. Nishida, H. Sawai, K. Matsuura, M. Sugiyama, S. H. Ahn, J. Y. Park, *et al.*, "Genome-wide association study confirming association of HLA-DP with protection against chronic hepatitis B and viral clearance in Japanese and Korean," *PLoS One*, vol. 7, p. e39175, 2012.
- [194] J. Vermehren, J. Lotsch, S. Susser, S. Wicker, A. Berger, S. Zeuzem, C. Sarrazin, and A. Doehring, "A common HLA-DPA1 variant is associated with hepatitis B virus infection but fails to distinguish active from inactive Caucasian carriers," *PLoS One*, vol. 7, p. e32605, 2012.

- [195] R. Thomas, C. L. Thio, R. Apps, Y. Qi, X. Gao, D. Marti, J. L. Stein, K. A. Soderberg, M. A. Moody, J. J. Goedert, G. D. Kirk, W. K. Hoots, S. Wolinsky, and M. Carrington, "A novel variant marking HLA-DP expression levels predicts recovery from hepatitis B virus infection," *J Virol*, vol. 86, pp. 6979-85, Jun 2012.
- [196] A. Al-Qahtani, H. G. Khalak, F. S. Alkuraya, W. Al-hamoudi, K. Alswat, M. A. Al Balwi, I. Al Abdulkareem, F. M. Sanai, and A. A. Abdo, "Genome-wide association study of chronic hepatitis B virus infection reveals a novel candidate risk allele on 11q22.3," *J Med Genet*, vol. 50, pp. 725-32, Nov 2013.
- [197] Y. J. Kim, H. Y. Kim, J. H. Lee, S. J. Yu, J. H. Yoon, H. S. Lee, C. Y. Kim, J. Y. Cheong, S. W. Cho, N. H. Park, B. L. Park, S. Namgoong, L. H. Kim, H. S. Cheong, and H. D. Shin, "A genome-wide association study identified new variants associated with the risk of chronic hepatitis B," *Hum Mol Genet*, vol. 22, pp. 4233-8, Oct 15 2013.
- [198] H. Yan, G. Zhong, G. Xu, W. He, Z. Jing, Z. Gao, Y. Huang, Y. Qi, B. Peng, H. Wang, L. Fu, M. Song, P. Chen, W. Gao, B. Ren, Y. Sun, T. Cai, X. Feng, J. Sui, and W. Li, "Sodium taurocholate cotransporting polypeptide is a functional receptor for human hepatitis B and D virus," *Elife*, vol. 1, p. e00049, Nov 13 2012.
- [199] H. Yan, B. Peng, Y. Liu, G. Xu, W. He, B. Ren, Z. Jing, J. Sui, and W. Li, "Viral entry of hepatitis B and D viruses and bile salts transportation share common molecular determinants on sodium taurocholate cotransporting polypeptide," *J Virol*, vol. 88, pp. 3273-84, Mar 2014.
- [200] T. Yamai, H. Hikita, T. Nakabori, Y. Makino, Y. Nozaki, Y. Saito, T. Kodama, R. Sakamori, T. Tatsumi, and T. Takehara, "HBV infection promotes autophagy by ULK-1 activation leading to increase of HBV replication," in *Hepatology*, 2017, pp. 784A-784A.
- [201] Z. Yang and D. J. Klionsky, "Eaten alive: a history of macroautophagy," *Nat Cell Biol*, vol. 12, pp. 814-22, Sep 2010.
- [202] S. Kaushik and A. M. Cuervo, "Chaperone-mediated autophagy: a unique way to enter the lysosome world," *Trends Cell Biol*, vol. 22, pp. 407-17, Aug 2012.
- [203] E. Arias and A. M. Cuervo, "Chaperone-mediated autophagy in protein quality control," *Curr Opin Cell Biol*, vol. 23, pp. 184-9, Apr 2011.
- [204] I. Tasset and A. M. Cuervo, "Role of chaperone-mediated autophagy in metabolism," *FEBS J*, vol. 283, pp. 2403-13, Jul 2016.
- [205] J. L. Schneider, J. Villarroya, A. Diaz-Carretero, B. Patel, A. M. Urbanska, M. M. Thi, F. Villarroya, L. Santambrogio, and A. M. Cuervo, "Loss of hepatic chaperone-mediated autophagy accelerates proteostasis failure in aging," *Aging Cell*, vol. 14, pp. 249-64, Apr 2015.



- [206] F. Reggiori and D. J. Klionsky, "Autophagic processes in yeast: mechanism, machinery and regulation," *Genetics*, vol. 194, pp. 341-61, Jun 2013.
- [207] T. Saito and J. Sadoshima, "Molecular mechanisms of mitochondrial autophagy/mitophagy in the heart," *Circ Res*, vol. 116, pp. 1477-90, Apr 10 2015.
- [208] Z. Yang and D. J. Klionsky, "An overview of the molecular mechanism of autophagy," *Curr Top Microbiol Immunol*, vol. 335, pp. 1-32, 2009.
- [209] R. Sahu, S. Kaushik, C. C. Clement, E. S. Cannizzo, B. Scharf, A. Follenzi, I. Potolicchio, E. Nieves, A. M. Cuervo, and L. Santambrogio, "Microautophagy of cytosolic proteins by late endosomes," *Dev Cell*, vol. 20, pp. 131-9, Jan 18 2011.
- [210] I. Orhon and F. Reggiori, "Assays to Monitor Autophagy Progression in Cell Cultures," *Cells*, vol. 6, Jul 07 2017.
- [211] D. J. Klionsky, E. L. Eskelinen, and V. Deretic, "Autophagosomes, phagosomes, autolysosomes, phagolysosomes, autophagolysosomes... wait, I'm confused," *Autophagy*, vol. 10, pp. 549-51, Apr 2014.
- [212] Z. Yin, C. Pascual, and D. J. Klionsky, "Autophagy: machinery and regulation," *Microb Cell*, vol. 3, pp. 588-596, Dec 01 2016.
- [213] D. C. Rubinsztein, J. E. Gestwicki, L. O. Murphy, and D. J. Klionsky, "Potential therapeutic applications of autophagy," *Nat Rev Drug Discov*, vol. 6, pp. 304-12, Apr 2007.
- [214] X. Yang, D. D. Yu, F. Yan, Y. Y. Jing, Z. P. Han, K. Sun, L. Liang, J. Hou, and L. X. Wei, "The role of autophagy induced by tumor microenvironment in different cells and stages of cancer," *Cell Biosci*, vol. 5, p. 14, 2015.
- [215] Y. Lee, H. Y. Lee, and A. B. Gustafsson, "Regulation of autophagy by metabolic and stress signaling pathways in the heart," *J Cardiovasc Pharmacol*, vol. 60, pp. 118-24, Aug 2012.
- [216] C. H. Jung, S. H. Ro, J. Cao, N. M. Otto, and D. H. Kim, "mTOR regulation of autophagy," *FEBS Lett*, vol. 584, pp. 1287-95, Apr 02 2010.
- [217] Y. T. Wu, H. L. Tan, G. Shui, C. Bauvy, Q. Huang, M. R. Wenk, C. N. Ong, P. Codogno, and H. M. Shen, "Dual role of 3-methyladenine in modulation of autophagy via different temporal patterns of inhibition on class I and III phosphoinositide 3-kinase," *J Biol Chem*, vol. 285, pp. 10850-61, Apr 02 2010.
- [218] J. D. Rabinowitz and E. White, "Autophagy and metabolism," *Science*, vol. 330, pp. 1344-8, Dec 3 2010.
- [219] S. A. Tooze and T. Yoshimori, "The origin of the autophagosomal membrane," *Nat Cell Biol*, vol. 12, pp. 831-5, Sep 2010.

- [220] K. Abounit, T. M. Scarabelli, and R. B. McCauley, "Autophagy in mammalian cells," *World J Biol Chem*, vol. 3, pp. 1-6, Jan 26 2012.
- [221] A. Longatti and S. A. Tooze, "Vesicular trafficking and autophagosome formation," *Cell Death Differ*, vol. 16, pp. 956-65, Jul 2009.
- [222] M. Mari and F. Reggiori, "Atg9 reservoirs, a new organelle of the yeast endomembrane system?," *Autophagy*, vol. 6, pp. 1221-3, Nov 2010.
- [223] A. Orsi, M. Razi, H. C. Dooley, D. Robinson, A. E. Weston, L. M. Collinson, and S. A. Tooze, "Dynamic and transient interactions of Atg9 with autophagosomes, but not membrane integration, are required for autophagy," *Mol Biol Cell*, vol. 23, pp. 1860-73, May 2012.
- [224] H. Nakatogawa, "Two ubiquitin-like conjugation systems that mediate membrane formation during autophagy," *Essays Biochem*, vol. 55, pp. 39-50, 2013.
- [225] T. Hanada, N. N. Noda, Y. Satomi, Y. Ichimura, Y. Fujioka, T. Takao, F. Inagaki, and Y. Ohsumi, "The Atg12-Atg5 conjugate has a novel E3-like activity for protein lipidation in autophagy," *J Biol Chem*, vol. 282, pp. 37298-302, Dec 28 2007.
- [226] N. Fujita, T. Itoh, H. Omori, M. Fukuda, T. Noda, and T. Yoshimori, "The Atg16L complex specifies the site of LC3 lipidation for membrane biogenesis in autophagy," *Mol Biol Cell*, vol. 19, pp. 2092-100, May 2008.
- [227] J. Geng and D. J. Klionsky, "The Atg8 and Atg12 ubiquitin-like conjugation systems in macroautophagy. 'Protein modifications: beyond the usual suspects' review series," *EMBO Rep*, vol. 9, pp. 859-64, Sep 2008.
- [228] A. Landajuena, J. H. Hervas, Z. Anton, L. R. Montes, D. Gil, M. Valle, J. F. Rodriguez, F. M. Goni, and A. Alonso, "Lipid Geometry and Bilayer Curvature Modulate LC3/GABARAP-Mediated Model Autophagosomal Elongation," *Biophys J*, vol. 110, pp. 411-22, Jan 19 2016.
- [229] J. M. Hyttinen, M. Niittykoski, A. Salminen, and K. Kaarniranta, "Maturation of autophagosomes and endosomes: a key role for Rab7," *Biochim Biophys Acta*, vol. 1833, pp. 503-10, Mar 2013.
- [230] B. Schroeder and M. A. McNiven, "Importance of endocytic pathways in liver function and disease," *Compr Physiol*, vol. 4, pp. 1403-17, Oct 2014.
- [231] C. Burman and N. T. Ktistakis, "Regulation of autophagy by phosphatidylinositol 3-phosphate," *FEBS Lett*, vol. 584, pp. 1302-12, Apr 02 2010.
- [232] I. Monastyrska, E. Rieter, D. J. Klionsky, and F. Reggiori, "Multiple roles of the cytoskeleton in autophagy," *Biol Rev Camb Philos Soc*, vol. 84, pp. 431-48, Aug 2009.
- [233] Z. Sztamari and M. Sass, "The autophagic roles of Rab small GTPases and their upstream regulators: a review," *Autophagy*, vol. 10, pp. 1154-66, Jul 2014.

- [234] B. Levine and D. J. Klionsky, "Autophagy wins the 2016 Nobel Prize in Physiology or Medicine: Breakthroughs in baker's yeast fuel advances in biomedical research," *Proc Natl Acad Sci U S A*, vol. 114, pp. 201-205, Jan 10 2017.
- [235] S. Wesselborg and B. Stork, "Autophagy signal transduction by ATG proteins: from hierarchies to networks," *Cell Mol Life Sci*, vol. 72, pp. 4721-57, Dec 2015.
- [236] L. R. Lapierre, C. Kumsta, M. Sandri, A. Ballabio, and M. Hansen, "Transcriptional and epigenetic regulation of autophagy in aging," *Autophagy*, vol. 11, pp. 867-80, 2015.
- [237] S. Alers, A. S. Loffler, S. Wesselborg, and B. Stork, "The incredible ULKs," *Cell Commun Signal*, vol. 10, p. 7, Mar 13 2012.
- [238] E. Y. Chan, S. Kir, and S. A. Tooze, "siRNA screening of the kinome identifies ULK1 as a multidomain modulator of autophagy," *J Biol Chem*, vol. 282, pp. 25464-74, Aug 31 2007.
- [239] K. Ogura and Y. Goshima, "The autophagy-related kinase UNC-51 and its binding partner UNC-14 regulate the subcellular localization of the Netrin receptor UNC-5 in *Caenorhabditis elegans*," *Development*, vol. 133, pp. 3441-50, Sep 2006.
- [240] A. Melendez, Z. Talloczy, M. Seaman, E. L. Eskelinen, D. H. Hall, and B. Levine, "Autophagy genes are essential for dauer development and life-span extension in *C. elegans*," *Science*, vol. 301, pp. 1387-91, Sep 05 2003.
- [241] F. McAlpine, L. E. Williamson, S. A. Tooze, and E. Y. Chan, "Regulation of nutrient-sensitive autophagy by uncoordinated 51-like kinases 1 and 2," *Autophagy*, vol. 9, pp. 361-73, Mar 2013.
- [242] X. Zhou, J. R. Babu, S. da Silva, Q. Shu, I. A. Graef, T. Oliver, T. Tomoda, T. Tani, M. W. Wooten, and F. Wang, "Unc-51-like kinase 1/2-mediated endocytic processes regulate filopodia extension and branching of sensory axons," *Proc Natl Acad Sci U S A*, vol. 104, pp. 5842-7, Apr 03 2007.
- [243] D. Papinski and C. Kraft, "Regulation of Autophagy By Signaling Through the Atg1/ULK1 Complex," *J Mol Biol*, vol. 428, pp. 1725-41, May 08 2016.
- [244] M. Kundu, "ULK1, mammalian target of rapamycin, and mitochondria: linking nutrient availability and autophagy," *Antioxid Redox Signal*, vol. 14, pp. 1953-8, May 15 2011.
- [245] S. Di Bartolomeo, M. Corazzari, F. Nazio, S. Oliverio, G. Lisi, M. Antonioli, V. Pagliarini, S. Matteoni, C. Fuoco, L. Giunta, M. D'Amelio, R. Nardacci, A. Romagnoli, M. Piacentini, F. Cecconi, and G. M. Fimia, "The dynamic interaction of AMBRA1 with the dynein motor complex regulates mammalian autophagy," *J Cell Biol*, vol. 191, pp. 155-68, Oct 04 2010.
- [246] H. I. Mack, B. Zheng, J. M. Asara, and S. M. Thomas, "AMPK-dependent phosphorylation of ULK1 regulates ATG9 localization," *Autophagy*, vol. 8, pp. 1197-214, Aug 2012.

- [247] I. G. Ganley, H. Lam du, J. Wang, X. Ding, S. Chen, and X. Jiang, "ULK1.ATG13.FIP200 complex mediates mTOR signaling and is essential for autophagy," *J Biol Chem*, vol. 284, pp. 12297-305, May 01 2009.
- [248] Y. Kamada, K. Yoshino, C. Kondo, T. Kawamata, N. Oshiro, K. Yonezawa, and Y. Ohsumi, "Tor directly controls the Atg1 kinase complex to regulate autophagy," *Mol Cell Biol*, vol. 30, pp. 1049-58, Feb 2010.
- [249] J. W. Lee, S. Park, Y. Takahashi, and H. G. Wang, "The association of AMPK with ULK1 regulates autophagy," *PLoS One*, vol. 5, p. e15394, Nov 03 2010.
- [250] N. Hosokawa, T. Hara, T. Kaizuka, C. Kishi, A. Takamura, Y. Miura, S. Iemura, T. Natsume, K. Takehana, N. Yamada, J. L. Guan, N. Oshiro, and N. Mizushima, "Nutrient-dependent mTORC1 association with the ULK1-Atg13-FIP200 complex required for autophagy," *Mol Biol Cell*, vol. 20, pp. 1981-91, Apr 2009.
- [251] H. Cheong, U. Nair, J. Geng, and D. J. Klionsky, "The Atg1 kinase complex is involved in the regulation of protein recruitment to initiate sequestering vesicle formation for nonspecific autophagy in *Saccharomyces cerevisiae*," *Mol Biol Cell*, vol. 19, pp. 668-81, Feb 2008.
- [252] D. Papinski, M. Schuschnig, W. Reiter, L. Wilhelm, C. A. Barnes, A. Maiolica, I. Hansmann, T. Pfaffenwimmer, M. Kijanska, I. Stoffel, S. S. Lee, A. Brezovich, J. H. Lou, B. E. Turk, R. Aebersold, G. Ammerer, M. Peter, and C. Kraft, "Early steps in autophagy depend on direct phosphorylation of Atg9 by the Atg1 kinase," *Mol Cell*, vol. 53, pp. 471-83, Feb 06 2014.
- [253] C. Kraft, M. Kijanska, E. Kalie, E. Siergiejuk, S. S. Lee, G. Semplicio, I. Stoffel, A. Brezovich, M. Verma, I. Hansmann, G. Ammerer, K. Hofmann, S. Tooze, and M. Peter, "Binding of the Atg1/ULK1 kinase to the ubiquitin-like protein Atg8 regulates autophagy," *EMBO J*, vol. 31, pp. 3691-703, Sep 12 2012.
- [254] S. Alers, A. S. Loffler, F. Paasch, A. M. Dieterle, H. Keppeler, K. Lauber, D. G. Campbell, B. Fehrenbacher, M. Schaller, S. Wesselborg, and B. Stork, "Atg13 and FIP200 act independently of Ulk1 and Ulk2 in autophagy induction," *Autophagy*, vol. 7, pp. 1423-33, Dec 2011.
- [255] J. S. Stephan, Y. Y. Yeh, V. Ramachandran, S. J. Deminoff, and P. K. Herman, "The Tor and PKA signaling pathways independently target the Atg1/Atg13 protein kinase complex to control autophagy," *Proc Natl Acad Sci U S A*, vol. 106, pp. 17049-54, Oct 06 2009.
- [256] Y. Y. Yeh, K. Wrasman, and P. K. Herman, "Autophosphorylation within the Atg1 activation loop is required for both kinase activity and the induction of autophagy in *Saccharomyces cerevisiae*," *Genetics*, vol. 185, pp. 871-82, Jul 2010.

- [257] M. Tarocchi, S. Polvani, G. Marroncini, and A. Galli, "Molecular mechanism of hepatitis B virus-induced hepatocarcinogenesis," *World J Gastroenterol*, vol. 20, pp. 11630-40, Sep 07 2014.
- [258] C. A. Lamb, T. Yoshimori, and S. A. Tooze, "The autophagosome: origins unknown, biogenesis complex," *Nat Rev Mol Cell Biol*, vol. 14, pp. 759-74, Dec 2013.
- [259] S. W. Tang, A. Ducroux, K. T. Jeang, and C. Neuveut, "Impact of cellular autophagy on viruses: Insights from hepatitis B virus and human retroviruses," *J Biomed Sci*, vol. 19, p. 92, Oct 30 2012.
- [260] K. Reifenberg, H. Wilts, J. Lohler, P. Nusser, R. Hanano, L. G. Guidotti, F. V. Chisari, and H. J. Schlicht, "The hepatitis B virus X protein transactivates viral core gene expression in vivo," *J Virol*, vol. 73, pp. 10399-405, Dec 1999.
- [261] P. Arbuthnot and M. Kew, "Hepatitis B virus and hepatocellular carcinoma," *Int J Exp Pathol*, vol. 82, pp. 77-100, Apr 2001.
- [262] C. M. Osowski and F. Urano, "Measuring ER stress and the unfolded protein response using mammalian tissue culture system," *Methods Enzymol*, vol. 490, pp. 71-92, 2011.
- [263] G. S. Hotamisligil, "Endoplasmic reticulum stress and the inflammatory basis of metabolic disease," *Cell*, vol. 140, pp. 900-17, Mar 19 2010.
- [264] L. Wang and J. H. Ou, "Hepatitis C virus and autophagy," *Biol Chem*, vol. 396, pp. 1215-22, Nov 2015.
- [265] I. J. Su, L. H. Wang, W. C. Hsieh, H. C. Wu, C. F. Teng, H. W. Tsai, and W. Huang, "The emerging role of hepatitis B virus pre-S2 deletion mutant proteins in HBV tumorigenesis," *J Biomed Sci*, vol. 21, p. 98, Oct 15 2014.
- [266] J. Wang, Y. Shi, and H. Yang, "[Infection with hepatitis B virus enhances basal autophagy]," *Wei Sheng Wu Xue Bao*, vol. 50, pp. 1651-6, Dec 2010.
- [267] A. M. Zhang, H. F. Wang, H. B. Wang, J. H. Hu, W. P. He, H. B. Su, J. Chen, N. Du, and X. Z. Duan, "[Association between HBV genotype and chronic/severe liver disease with HBV infection in Chinese patients]," *Zhonghua Shi Yan He Lin Chuang Bing Du Xue Za Zhi*, vol. 24, pp. 178-80, Jun 2010.
- [268] D. Sir, D. K. Ann, and J. H. Ou, "Autophagy by hepatitis B virus and for hepatitis B virus," *Autophagy*, vol. 6, pp. 548-9, May 2010.
- [269] Z. Xu, T. S. Yen, L. Wu, C. R. Madden, W. Tan, B. L. Slagle, and J. H. Ou, "Enhancement of hepatitis B virus replication by its X protein in transgenic mice," *J Virol*, vol. 76, pp. 2579-84, Mar 2002.

- [270] D. Sir and J. H. Ou, "Autophagy in viral replication and pathogenesis," *Mol Cells*, vol. 29, pp. 1-7, Jan 2010.
- [271] M. Sunbul, "Hepatitis B virus genotypes: global distribution and clinical importance," *World J Gastroenterol*, vol. 20, pp. 5427-34, May 14 2014.
- [272] Y. Deng, Y. Du, Q. Zhang, X. Han, and G. Cao, "Human cytidine deaminases facilitate hepatitis B virus evolution and link inflammation and hepatocellular carcinoma," *Cancer Lett*, vol. 343, pp. 161-71, Feb 28 2014.
- [273] C. L. Thio, D. L. Thomas, P. Karacki, X. Gao, D. Marti, R. A. Kaslow, J. J. Goedert, M. Hilgartner, S. A. Strathdee, P. Duggal, S. J. O'Brien, J. Astemborski, and M. Carrington, "Comprehensive analysis of class I and class II HLA antigens and chronic hepatitis B virus infection," *J Virol*, vol. 77, pp. 12083-7, Nov 2003.
- [274] Y. G. Jiang, Y. M. Wang, T. H. Liu, and J. Liu, "Association between HLA class II gene and susceptibility or resistance to chronic hepatitis B," *World J Gastroenterol*, vol. 9, pp. 2221-5, Oct 2003.
- [275] S. H. Ahn, K. H. Han, J. Y. Park, C. K. Lee, S. W. Kang, C. Y. Chon, Y. S. Kim, K. Park, D. K. Kim, and Y. M. Moon, "Association between hepatitis B virus infection and HLA-DR type in Korea," *Hepatology*, vol. 31, pp. 1371-3, Jun 2000.
- [276] C. L. Thio, M. Carrington, D. Marti, S. J. O'Brien, D. Vlahov, K. E. Nelson, J. Astemborski, and D. L. Thomas, "Class II HLA alleles and hepatitis B virus persistence in African Americans," *J Infect Dis*, vol. 179, pp. 1004-6, Apr 1999.
- [277] Y. J. Kim, H. S. Lee, J. H. Yoon, C. Y. Kim, M. H. Park, L. H. Kim, B. L. Park, and H. D. Shin, "Association of TNF-alpha promoter polymorphisms with the clearance of hepatitis B virus infection," *Hum Mol Genet*, vol. 12, pp. 2541-6, Oct 01 2003.
- [278] Y. Liu, X. H. Guo, T. Du, J. H. Li, X. L. Zhu, J. R. Gao, L. P. Lu, C. Y. Gou, Z. Li, and H. Li, "[Association of TNFA polymorphisms with the outcomes of HBV infection]," *Zhonghua Yi Xue Yi Chuan Xue Za Zhi*, vol. 22, pp. 406-10, Aug 2005.
- [279] L. P. Lu, X. W. Li, Y. Liu, G. C. Sun, X. P. Wang, X. L. Zhu, Q. Y. Hu, and H. Li, "Association of -238G/A polymorphism of tumor necrosis factor-alpha gene promoter region with outcomes of hepatitis B virus infection in Chinese Han population," *World J Gastroenterol*, vol. 10, pp. 1810-4, Jun 15 2004.
- [280] J. Ma, X. Guo, X. Wu, J. Li, X. Zhu, Z. Li, L. Pan, T. Li, H. Li, and Y. Liu, "Association of NKG2D genetic polymorphism with susceptibility to chronic hepatitis B in a Han Chinese population," *J Med Virol*, vol. 82, pp. 1501-7, Sep 2010.

- [281] S. Romani, S. M. Hosseini, S. R. Mohebbi, S. Kazemian, S. Derakhshani, M. Khanyaghma, P. Azimzadeh, A. Sharifian, and M. R. Zali, "Interleukin-16 gene polymorphisms are considerable host genetic factors for patients' susceptibility to chronic hepatitis B infection," *Hepat Res Treat*, vol. 2014, p. 790753, 2014.
- [282] J. Yuan, Y. Zhang, F. T. Yan, and X. Zheng, "Association of PRKAA1 gene polymorphisms with chronic hepatitis B virus infection in Chinese Han population," *Braz J Infect Dis*, vol. 20, pp. 564-568, Nov - Dec 2016.
- [283] Z. Heidari, B. Moudi, H. Mahmoudzadeh Sagheb, and M. Moudi, "Association of TNF-alpha Gene Polymorphisms with Production of Protein and Susceptibility to Chronic Hepatitis B Infection in the South East Iranian Population," *Hepat Mon*, vol. 16, p. e41984, Nov 2016.
- [284] P. C. Robinson and M. A. Brown, "Genetics of ankylosing spondylitis," *Mol Immunol*, vol. 57, pp. 2-11, Jan 2014.
- [285] X. Zhang, R. Han, M. Wang, X. Li, X. Yang, Q. Xia, R. Liu, Y. Yuan, X. Hu, M. Chen, G. Jiang, Y. Ma, J. Yang, S. Xu, J. Xu, Z. Shuai, and F. Pan, "Association between the autophagy-related gene ULK1 and ankylosing spondylitis susceptibility in the Chinese Han population: a case-control study," *Postgrad Med J*, vol. 93, pp. 752-757, Dec 2017.
- [286] A. Kaser, S. Zeissig, and R. S. Blumberg, "Inflammatory bowel disease," *Annu Rev Immunol*, vol. 28, pp. 573-621, 2010.
- [287] D. J. Horne, A. D. Graustein, J. A. Shah, G. Peterson, M. Savlov, S. Steele, M. Narita, and T. R. Hawn, "Human ULK1 Variation and Susceptibility to Mycobacterium tuberculosis Infection," *J Infect Dis*, vol. 214, pp. 1260-7, Oct 15 2016.
- [288] R. C. Edgar, "MUSCLE: multiple sequence alignment with high accuracy and high throughput," *Nucleic Acids Res*, vol. 32, pp. 1792-7, 2004.
- [289] K. Katoh, K. Misawa, K. Kuma, and T. Miyata, "MAFFT: a novel method for rapid multiple sequence alignment based on fast Fourier transform," *Nucleic Acids Res*, vol. 30, pp. 3059-66, Jul 15 2002.
- [290] K. Tamura, D. Peterson, N. Peterson, G. Stecher, M. Nei, and S. Kumar, "MEGA5: molecular evolutionary genetics analysis using maximum likelihood, evolutionary distance, and maximum parsimony methods," *Mol Biol Evol*, vol. 28, pp. 2731-9, Oct 2011.
- [291] V. Gotea and I. Ovcharenko, "DiRE: identifying distant regulatory elements of co-expressed genes," *Nucleic Acids Res*, vol. 36, pp. W133-9, Jul 01 2008.
- [292] A. T. Kwon, D. J. Arenillas, R. Worsley Hunt, and W. W. Wasserman, "oPOSSUM-3: advanced analysis of regulatory motif over-representation across genes or CHIP-Seq datasets," *G3 (Bethesda)*, vol. 2, pp. 987-1002, Sep 2012.

- [293] A. Sandelin, W. Alkema, P. Engstrom, W. W. Wasserman, and B. Lenhard, "JASPAR: an open-access database for eukaryotic transcription factor binding profiles," *Nucleic Acids Res*, vol. 32, pp. D91-4, Jan 01 2004.
- [294] P. C. Ng and S. Henikoff, "SIFT: Predicting amino acid changes that affect protein function," *Nucleic Acids Res*, vol. 31, pp. 3812-4, Jul 01 2003.
- [295] V. Ramensky, P. Bork, and S. Sunyaev, "Human non-synonymous SNPs: server and survey," *Nucleic Acids Res*, vol. 30, pp. 3894-900, Sep 01 2002.
- [296] G. A. Thorisson, A. V. Smith, L. Krishnan, and L. D. Stein, "The International HapMap Project Web site," *Genome Res*, vol. 15, pp. 1592-3, Nov 2005.
- [297] J. C. Barrett, B. Fry, J. Maller, and M. J. Daly, "Haploview: analysis and visualization of LD and haplotype maps," *Bioinformatics*, vol. 21, pp. 263-5, Jan 15 2005.
- [298] L. T. Huang, M. M. Gromiha, and S. Y. Ho, "iPTREE-STAB: interpretable decision tree based method for predicting protein stability changes upon mutations," *Bioinformatics*, vol. 23, pp. 1292-3, May 15 2007.
- [299] E. Capriotti, P. Fariselli, and R. Casadio, "I-Mutant2.0: predicting stability changes upon mutation from the protein sequence or structure," *Nucleic Acids Res*, vol. 33, pp. W306-10, Jul 01 2005.
- [300] D. E. Kim, D. Chivian, and D. Baker, "Protein structure prediction and analysis using the Robetta server," *Nucleic Acids Res*, vol. 32, pp. W526-31, Jul 01 2004.
- [301] D. E. Pires, D. B. Ascher, and T. L. Blundell, "DUET: a server for predicting effects of mutations on protein stability using an integrated computational approach," *Nucleic Acids Res*, vol. 42, pp. W314-9, Jul 2014.
- [302] S. Yin, F. Ding, and N. V. Dokholyan, "Eris: an automated estimator of protein stability," *Nat Methods*, vol. 4, pp. 466-7, Jun 2007.
- [303] A. Bononi, C. Agnoletto, E. De Marchi, S. Marchi, S. Patergnani, M. Bonora, C. Giorgi, S. Missiroli, F. Poletti, A. Rimessi, and P. Pinton, "Protein kinases and phosphatases in the control of cell fate," *Enzyme Res*, vol. 2011, p. 329098, 2011.
- [304] W. Wu, W. Tian, Z. Hu, G. Chen, L. Huang, W. Li, X. Zhang, P. Xue, C. Zhou, L. Liu, Y. Zhu, L. Li, L. Zhang, S. Sui, B. Zhao, and D. Feng, "ULK1 translocates to mitochondria and phosphorylates FUNDC1 to regulate mitophagy," *EMBO Rep*, vol. 15, pp. 566-75, May 2014.
- [305] J. V. Olsen, M. Vermeulen, A. Santamaria, C. Kumar, M. L. Miller, L. J. Jensen, F. Gnad, J. Cox, T. S. Jensen, E. A. Nigg, S. Brunak, and M. Mann, "Quantitative phosphoproteomics reveals widespread full phosphorylation site occupancy during mitosis," *Sci Signal*, vol. 3, p. ra3, Jan 12 2010.



- [306] Y. T. Wang, C. F. Tsai, T. C. Hong, C. C. Tsou, P. Y. Lin, S. H. Pan, T. M. Hong, P. C. Yang, T. Y. Sung, W. L. Hsu, and Y. J. Chen, "An informatics-assisted label-free quantitation strategy that depicts phosphoproteomic profiles in lung cancer cell invasion," *J Proteome Res*, vol. 9, pp. 5582-97, Nov 05 2010.
- [307] L. Shang, S. Chen, F. Du, S. Li, L. Zhao, and X. Wang, "Nutrient starvation elicits an acute autophagic response mediated by Ulk1 dephosphorylation and its subsequent dissociation from AMPK," *Proc Natl Acad Sci U S A*, vol. 108, pp. 4788-93, Mar 22 2011.
- [308] N. Blom, S. Gammeltoft, and S. Brunak, "Sequence and structure-based prediction of eukaryotic protein phosphorylation sites," *J Mol Biol*, vol. 294, pp. 1351-62, Dec 17 1999.
- [309] A. Kreegipuu, N. Blom, and S. Brunak, "PhosphoBase, a database of phosphorylation sites: release 2.0," *Nucleic Acids Res*, vol. 27, pp. 237-9, Jan 01 1999.
- [310] F. Zhou, Y. Xue, X. Yao, and Y. Xu, "CSS-Palm: palmitoylation site prediction with a clustering and scoring strategy (CSS)," *Bioinformatics*, vol. 22, pp. 894-6, Apr 01 2006.
- [311] D. Szklarczyk, A. Franceschini, M. Kuhn, M. Simonovic, A. Roth, P. Minguez, T. Doerks, M. Stark, J. Muller, P. Bork, L. J. Jensen, and C. von Mering, "The STRING database in 2011: functional interaction networks of proteins, globally integrated and scored," *Nucleic Acids Res*, vol. 39, pp. D561-8, Jan 2011.
- [312] X. Sole, E. Guino, J. Valls, R. Iriarte, and V. Moreno, "SNPStats: a web tool for the analysis of association studies," *Bioinformatics*, vol. 22, pp. 1928-9, Aug 01 2006.
- [313] S. Gumeni, Z. Evangelakou, V. G. Gorgoulis, and I. P. Trougakos, "Proteome Stability as a Key Factor of Genome Integrity," *Int J Mol Sci*, vol. 18, Sep 22 2017.
- [314] A. del Sol, H. Fujihashi, D. Amoros, and R. Nussinov, "Residue centrality, functionally important residues, and active site shape: analysis of enzyme and non-enzyme families," *Protein Sci*, vol. 15, pp. 2120-8, Sep 2006.
- [315] G. Heinrich and C. J. Pagtakhan, "Both 5' and 3' flanks regulate Zebrafish brain-derived neurotrophic factor gene expression," *BMC Neurosci*, vol. 5, p. 19, May 21 2004.
- [316] V. Deretic, T. Saitoh, and S. Akira, "Autophagy in infection, inflammation and immunity," *Nat Rev Immunol*, vol. 13, pp. 722-37, Oct 2013.
- [317] J. Fullgrabe, D. J. Klionsky, and B. Joseph, "The return of the nucleus: transcriptional and epigenetic control of autophagy," *Nat Rev Mol Cell Biol*, vol. 15, pp. 65-74, Jan 2014.
- [318] T. W. Whitfield, J. Wang, P. J. Collins, E. C. Partridge, S. F. Aldred, N. D. Trinklein, R. M. Myers, and Z. Weng, "Functional analysis of transcription factor binding sites in human promoters," *Genome Biol*, vol. 13, p. R50, Sep 26 2012.

- [319] R. R. Beerli, B. Dreier, and C. F. Barbas, 3rd, "Positive and negative regulation of endogenous genes by designed transcription factors," *Proc Natl Acad Sci U S A*, vol. 97, pp. 1495-500, Feb 15 2000.
- [320] J. G. Mandell and C. F. Barbas, 3rd, "Zinc Finger Tools: custom DNA-binding domains for transcription factors and nucleases," *Nucleic Acids Res*, vol. 34, pp. W516-23, Jul 01 2006.
- [321] C. O. Pabo, E. Peisach, and R. A. Grant, "Design and selection of novel Cys2His2 zinc finger proteins," *Annu Rev Biochem*, vol. 70, pp. 313-40, 2001.
- [322] J. E. Smotryś and M. E. Linder, "Palmitoylation of intracellular signaling proteins: regulation and function," *Annu Rev Biochem*, vol. 73, pp. 559-87, 2004.
- [323] N. Watanabe and H. Osada, "Phosphorylation-dependent protein-protein interaction modules as potential molecular targets for cancer therapy," *Curr Drug Targets*, vol. 13, pp. 1654-8, Dec 2012.
- [324] F. R. Marin-Martin, C. Soler-Rivas, R. Martin-Hernandez, and A. Rodriguez-Casado, "A Comprehensive In Silico Analysis of the Functional and Structural Impact of Nonsynonymous SNPs in the ABCA1 Transporter Gene," *Cholesterol*, vol. 2014, p. 639751, 2014.
- [325] J. Ye, G. Coulouris, I. Zaretskaya, I. Cutcutache, S. Rozen, and T. L. Madden, "Primer-BLAST: a tool to design target-specific primers for polymerase chain reaction," *BMC Bioinformatics*, vol. 13, p. 134, Jun 18 2012.
- [326] S. F. Altschul, W. Gish, W. Miller, E. W. Myers, and D. J. Lipman, "Basic local alignment search tool," *J Mol Biol*, vol. 215, pp. 403-10, Oct 05 1990.
- [327] S. K. Sarin, M. Kumar, G. K. Lau, Z. Abbas, H. L. Chan, C. J. Chen, *et al.*, "Asian-Pacific clinical practice guidelines on the management of hepatitis B: a 2015 update," *Hepatol Int*, vol. 10, pp. 1-98, Jan 2016.
- [328] K. Jooss, H. C. Ertl, and J. M. Wilson, "Cytotoxic T-lymphocyte target proteins and their major histocompatibility complex class I restriction in response to adenovirus vectors delivered to mouse liver," *J Virol*, vol. 72, pp. 2945-54, Apr 1998.
- [329] L. C. Meireles, R. T. Marinho, and P. Van Damme, "Three decades of hepatitis B control with vaccination," *World J Hepatol*, vol. 7, pp. 2127-32, Aug 28 2015.
- [330] T. Chitapanarux and K. Phornphutkul, "Risk Factors for the Development of Hepatocellular Carcinoma in Thailand," *J Clin Transl Hepatol*, vol. 3, pp. 182-8, Sep 28 2015.
- [331] H. A. Torres and M. Davila, "Reactivation of hepatitis B virus and hepatitis C virus in patients with cancer," *Nat Rev Clin Oncol*, vol. 9, pp. 156-66, Jan 24 2012.

- [332] M. A. Feitelson, B. Bonamassa, and A. Arzumanyan, "The roles of hepatitis B virus-encoded X protein in virus replication and the pathogenesis of chronic liver disease," *Expert Opin Ther Targets*, vol. 18, pp. 293-306, Mar 2014.
- [333] S. Y. Wu, S. H. Lan, S. R. Wu, Y. C. Chiu, X. Z. Lin, I. J. Su, T. F. Tsai, C. J. Yen, T. H. Lu, F. W. Liang, C. Y. Li, H. J. Su, C. L. Su, and H. S. Liu, "Hepatocellular carcinoma-related cyclin D1 is selectively regulated by autophagy degradation system," *Hepatology*, Jan 12 2018.
- [334] Y. Fukuo, S. Yamashina, H. Sonoue, A. Arakawa, E. Nakadera, T. Aoyama, A. Uchiyama, K. Kon, K. Ikejima, and S. Watanabe, "Abnormality of autophagic function and cathepsin expression in the liver from patients with non-alcoholic fatty liver disease," *Hepatol Res*, vol. 44, pp. 1026-36, Sep 2014.
- [335] S. Fu, J. Wang, X. Hu, R. R. Zhou, Y. Fu, D. Tang, R. Kang, Y. Huang, L. Sun, N. Li, and X. G. Fan, "Crosstalk between hepatitis B virus x and high-mobility group box 1 facilitates autophagy in hepatocytes," *Mol Oncol*, Jan 5 2018.
- [336] S. Yu, Y. Wang, L. Jing, F. X. Claret, Q. Li, T. Tian, X. Liang, Z. Ruan, L. Jiang, Y. Yao, K. Nan, Y. Lv, and H. Guo, "Autophagy in the "inflammation-carcinogenesis" pathway of liver and HCC immunotherapy," *Cancer Lett*, vol. 411, pp. 82-89, Dec 28 2017.
- [337] A. Matsuura, M. Tsukada, Y. Wada, and Y. Ohsumi, "Apg1p, a novel protein kinase required for the autophagic process in *Saccharomyces cerevisiae*," *Gene*, vol. 192, pp. 245-50, Jun 19 1997.
- [338] H. Kuroyanagi, J. Yan, N. Seki, Y. Yamanouchi, Y. Suzuki, T. Takano, M. Muramatsu, and T. Shirasawa, "Human ULK1, a novel serine/threonine kinase related to UNC-51 kinase of *Caenorhabditis elegans*: cDNA cloning, expression, and chromosomal assignment," *Genomics*, vol. 51, pp. 76-85, Jul 1 1998.
- [339] K. Ogura, C. Wicky, L. Magnenat, H. Tobler, I. Mori, F. Muller, and Y. Ohshima, "Caenorhabditis elegans unc-51 gene required for axonal elongation encodes a novel serine/threonine kinase," *Genes Dev*, vol. 8, pp. 2389-400, Oct 15 1994.
- [340] V. Todde, M. Veenhuis, and I. J. van der Klei, "Autophagy: principles and significance in health and disease," *Biochim Biophys Acta*, vol. 1792, pp. 3-13, Jan 2009.
- [341] J. L. Schneider and A. M. Cuervo, "Autophagy and human disease: emerging themes," *Curr Opin Genet Dev*, vol. 26, pp. 16-23, Jun 2014.
- [342] B. Moudi, Z. Heidari, and H. Mahmoudzadeh-Sagheb, "Impact of host gene polymorphisms on susceptibility to chronic hepatitis B virus infection," *Infect Genet Evol*, vol. 44, pp. 94-105, Oct 2016.

- [343] E. Hoefkens, K. Nys, J. M. John, K. Van Steen, I. Arijs, J. Van der Goten, G. Van Assche, P. Agostinis, P. Rutgeerts, S. Vermeire, and I. Cleynen, "Genetic association and functional role of Crohn disease risk alleles involved in microbial sensing, autophagy, and endoplasmic reticulum (ER) stress," *Autophagy*, vol. 9, pp. 2046-55, Dec 2013.
- [344] K. J. Schmitz, C. Ademi, S. Bertram, K. W. Schmid, and H. A. Baba, "Prognostic relevance of autophagy-related markers LC3, p62/sequestosome 1, Beclin-1 and ULK1 in colorectal cancer patients with respect to KRAS mutational status," *World J Surg Oncol*, vol. 14, p. 189, Jul 22 2016.
- [345] M. Audagnotto and M. Dal Peraro, "Protein post-translational modifications: In silico prediction tools and molecular modeling," *Comput Struct Biotechnol J*, vol. 15, pp. 307-319, 2017.
- [346] G. Duan and D. Walther, "The roles of post-translational modifications in the context of protein interaction networks," *PLoS Comput Biol*, vol. 11, p. e1004049, Feb 2015.
- [347] Y. Xie, R. Kang, X. Sun, M. Zhong, J. Huang, D. J. Klionsky, and D. Tang, "Posttranslational modification of autophagy-related proteins in macroautophagy," *Autophagy*, vol. 11, pp. 28-45, 2015.
- [348] O. Rocks, A. Peyker, M. Kahms, P. J. Verveer, C. Koerner, M. Lumbierres, J. Kuhlmann, H. Waldmann, A. Wittinghofer, and P. I. Bastiaens, "An acylation cycle regulates localization and activity of palmitoylated Ras isoforms," *Science*, vol. 307, pp. 1746-52, Mar 18 2005.
- [349] C. A. Mercer, A. Kaliappan, and P. B. Dennis, "A novel, human Atg13 binding protein, Atg101, interacts with ULK1 and is essential for macroautophagy," *Autophagy*, vol. 5, pp. 649-62, Jul 2009.
- [350] B. Boeckmann, A. Bairoch, R. Apweiler, M. C. Blatter, A. Estreicher, E. Gasteiger, M. J. Martin, K. Michoud, C. O'Donovan, I. Phan, S. Pilbout, and M. Schneider, "The SWISS-PROT protein knowledgebase and its supplement TrEMBL in 2003," *Nucleic Acids Res*, vol. 31, pp. 365-70, Jan 1 2003.
- [351] S. T. Sherry, M. H. Ward, M. Kholodov, J. Baker, L. Phan, E. M. Smigielski, and K. Sirotkin, "dbSNP: the NCBI database of genetic variation," *Nucleic Acids Res*, vol. 29, pp. 308-11, Jan 1 2001.
- [352] D. Fredman, G. Munns, D. Rios, F. Sjolholm, M. Siegfried, B. Lenhard, H. Lehvaslaiho, and A. J. Brookes, "HGvbase: a curated resource describing human DNA variation and phenotype relationships," *Nucleic Acids Res*, vol. 32, pp. D516-9, Jan 1 2004.

- [353] H. Price, P. Lacap, J. Tuff, C. Wachihi, J. Kimani, T. B. Ball, M. Luo, and F. A. Plummer, "A TRIM5alpha exon 2 polymorphism is associated with protection from HIV-1 infection in the Pumwani sex worker cohort," *AIDS*, vol. 24, pp. 1813-21, Jul 31 2010.
- [354] A. V. Grant, M. I. Araujo, E. V. Ponte, R. R. Oliveira, P. Gao, A. A. Cruz, K. C. Barnes, and T. H. Beaty, "Functional polymorphisms in IL13 are protective against high *Schistosoma mansoni* infection intensity in a Brazilian population," *PLoS One*, vol. 7, p. e35863, 2012.
- [355] J. Castiblanco, D. C. Varela, N. Castano-Rodriguez, A. Rojas-Villarraga, M. E. Hincapie, and J. M. Anaya, "TIRAP (MAL) S180L polymorphism is a common protective factor against developing tuberculosis and systemic lupus erythematosus," *Infect Genet Evol*, vol. 8, pp. 541-4, Sep 2008.
- [356] A. Kunanopparat, I. Kimkong, T. Palaga, P. Tangkijvanich, B. Sirichindakul, and N. Hirankarn, "Increased ATG5-ATG12 in hepatitis B virus-associated hepatocellular carcinoma and their role in apoptosis," *World J Gastroenterol*, vol. 22, pp. 8361-8374, Oct 7 2016.
- [357] A. Kotsafti, F. Farinati, R. Cardin, U. Cillo, D. Nitti, and M. Bortolami, "Autophagy and apoptosis-related genes in chronic liver disease and hepatocellular carcinoma," *BMC Gastroenterol*, vol. 12, p. 118, Aug 28 2012.
- [358] T. Doring and R. Prange, "Rab33B and its autophagic Atg5/12/16L1 effector assist in hepatitis B virus naked capsid formation and release," *Cell Microbiol*, vol. 17, pp. 747-64, May 2015.
- [359] K. Wang, "Autophagy and apoptosis in liver injury," *Cell Cycle*, vol. 14, pp. 1631-42, 2015.
- [360] R. Randhawa, M. Sehgal, T. R. Singh, A. Duseja, and H. Changotra, "Unc-51 like kinase 1 (ULK1) in silico analysis for biomarker identification: a vital component of autophagy," *Gene*, vol. 562, pp. 40-9, May 10 2015.

# APPENDIX

## Appendix

**Institutional Ethics Committee (IEC)****Chairman**

Professor TC Bhalla  
 Professor and Head, Department of Biotechnology  
 HPU, Shimla, bhallatc@rediffmail.com  
 +919418439910

**Member Secretary**

Professor RS Chauhan  
 Head, Department of BT & BI  
 JUIT, Wagnaghat, Solan  
 rajinder.chuhan@juit.ac.in +919418405536

No. IEC/project no-6-2014

Dated: 23.05.2014

**Approval of Institutional Ethics Committee**

To

Dr. Harish Changotra, Ph.D.  
 Department of Biotechnology and Bioinformatics  
 Jaypee University of Information Technology,  
 Solan, Himachal Pradesh – 173 234

The Institutional Ethics Committee of Jaypee University of Information Technology, Wagnaghat reviewed and discussed your application to conduct the research work titled "*Identification of Single Nucleotide Polymorphisms in the transcriptional regulatory region of autophagy gene, ULK1 and their role in susceptibility to chronic hepatitis B virus infection*", hereby assigned IEC/project no-6-2014" in the meeting of the committee held on 23.05.2014 at 11:00 AM in the in the board room at JUIT Wakanaghat Solan. The following Members of the Ethics Committee were present in the meeting.

Professor TC Bhalla; Chairman  
 Ms. Ambika Sharma, Media Correspondent  
 Dr. SS Kanwar, Department of Biotechnology, HPU, Shimla; Member  
 Dr. Omesh Bharti, Epidemiologist (M.A.E), Directorate of Health, Kasumpti, Shimla; Member  
 Dr. Meenakshi F Paul, Center of Evening Studies, HPU, Shimla; Member  
 Dr. RS Chauhan Head, Professor & Head, Department of BT & BI JUIT, Wagnaghat; Member Secretary

**Decision:** The committee members after due consideration and discussion approved the project.

The institutional Ethics Committee needs to be informed at regular intervals about:

- Copy of all consent forms, filled and signed
- Any serious adverse event occurring during the study
- A copy of the final report of the study
- The Institutional Ethics Committee has to be informed and permission taken before any changes in the protocol
- Please note that members of IEC have the right to monitor the trial with prior information.



Member Secretary

**A. Buffers and reagents used in DNA isolation****1. Tris (hydroxymethyl) aminomethane-chloride (Tris-Cl)**

<b>Ingredients</b>	<b>Amount (g)</b>	<b>Final Concentration</b>
Tris base	<b>12.11</b>	<b>1 M</b>
pH was set to 8.0 by using 1n HCL. Added autoclaved distilled water to amke up the final volume to 100ml		

**2. Ammonium Chloride (NH<sub>4</sub>Cl)**

<b>Ingredients</b>	<b>Amount (g)</b>	<b>Final Concentration</b>
Ammonium Chloride (NH <sub>4</sub> Cl)	<b>5.35</b>	<b>1 M</b>
5.35 grams of NH <sub>4</sub> Cl dissolved in 80ml of distilled water and final volume was made up to 100ml		

**3. Di-sodium ethylene diamine tetra acetate (Na<sub>2</sub>EDTA)**

<b>Ingredients</b>	<b>Amount (g)</b>	<b>Final Concentration</b>
EDTA	<b>18.61</b>	<b>0.5 M</b>
18.61 grams of EDTA was dissolved in 50ml of distilled water and placed over magnetic stirrer. 10M NaOH was added to teh above mixture. Allowed the salt to dissolve completely. Final volume was made up to 100 ml and pH was set at 8.0.		



**4. Red Blood cell (RBC) lysis buffer**

<b>Ingredients</b>	<b>Volume (ml)</b>	<b>Final Concentration</b>
Tris (8.0)	10	1M
EDTA	2	0.5M
NH <sub>4</sub> Cl (pH-8.0)	125	1M
Final volume was made 1000ml with distilled water		

**5. Tris EDTA (TE) buffer (pH-8.0)**

<b>Ingredients</b>	<b>Volume (ml)</b>	<b>Final Concentration</b>
Tris Cl	10	1M
EDTA	2	0.5M
Final volume was made 1000ml with distilled water		

**6. Tris EDTA (TE) buffer (pH-7.0)**

<b>Ingredients</b>	<b>Volume (ml)</b>	<b>Final Concentration</b>
Tris Cl (pH-7.3)	10	1M
EDTA	2	0.5M
Final volume was made 1000ml with distilled water		

**7. Sodium dodecyl sulphate (SDS) (10%)**

<b>Ingredients</b>	<b>Amount (g)</b>	<b>Final Concentration</b>
SDS	10	10%
Final volume was made 100ml with distilled water		

**8. Ammonium acetate (7.5M)**

<b>Ingredients</b>	<b>Amount (g)</b>	<b>Final Concentration</b>
Ammonium acetate	28.9	7.5M
28.9 grams of the salt was dissolved in 20 ml of distilled water and final volume was made 50ml with distilled water		

**9. Ethyl alcohol (70%)**

<b>Ingredients</b>	<b>Volume (ml)</b>	<b>Final Concentration</b>
Dehydrated ethyl alcohol	70	70%
70 ml of Dehydrated ethyl alcohol was mixed in 30ml of autoclaved distilled water to obtain final volume of 100ml		

**10. Tris-acetic acid-EDTA (TAE) buffer (50X)**

<b>Ingredients</b>	<b>Amount (g)</b>	<b>Final Concentration</b>
Tris base	242	50X
Dissolved in 500ml of distilled autoclaved water and 57.1 ml of glacial acetic acid and 100ml of 0.5M EDTA (pH-8.0) was added. Final volume was made 1000ml.		

**11. Agarose gel**

<b>Ingredients</b>	<b>Amount (g)</b>	<b>Final Concentration</b>
Agarose	1.5 gm	3%
Dissolve in 1X TAE buffer, dissolved completely by heating in microwave oven		

**12. Ethidium Bromide (EtBr) (10mg/ml)**

<b>Ingredients</b>	<b>Amount (mg)</b>	<b>Final Concentration</b>
Ethidium Bromide	50	10mg/ml
Added 5ml of distilled autoclaved water and completely dissolved by heating in microwave oven		

**B. Table 1.** Complete list of phosphorylation sites in ULK1 gene

NAME	POSITION	CONTEXT SEQUENCE	SCORE	PREDICTION	PREDICTED KINASE	PUBMED IDS
ULK1_HUMAN	17	KFEFSRKDL	0.997	*S*	-	-
ULK1_HUMAN	56	NLAQSQTLL	0.648	*S*	-	-
ULK1_HUMAN	111	MRTLSEDTI	0.896	*S*	-	-
ULK1_HUMAN	225	FQASSPQDL	0.993	*S*	-	19807128
ULK1_HUMAN	283	DASPSVRKS	0.939	*S*	-	-
ULK1_HUMAN	287	SVRKSPVP	0.996	*S*	-	-
ULK1_HUMAN	298	SYPSSGSGS	0.717	*S*	-	-
ULK1_HUMAN	300	PSSGSGSSS	0.819	*S*	-	-
ULK1_HUMAN	302	SGSGSSSSS	0.951	*S*	-	-
ULK1_HUMAN	303	GSGSSSSSS	0.92	*S*	-	-
ULK1_HUMAN	304	SGSSSSSSS	0.967	*S*	-	-
ULK1_HUMAN	305	GSSSSSSST	0.977	*S*	-	-
ULK1_HUMAN	306	SSSSSSSTS	0.953	*S*	-	-
ULK1_HUMAN	307	SSSSSTSH	0.984	*S*	-	-
ULK1_HUMAN	308	SSSSSTSHL	0.977	*S*	-	-
ULK1_HUMAN	310	SSSTSHLAS	0.979	*S*	-	-
ULK1_HUMAN	314	SHLASPPSL	0.915	*S*	-	-
ULK1_HUMAN	317	ASPPSLGEM	0.732	*S*	PKC $\alpha$	22932492
ULK1_HUMAN	330	KTLASPADT	0.992	*S*	-	-
ULK1_HUMAN	340	GFLHSSRDS	0.991	*S*	-	-
ULK1_HUMAN	344	SSRDSGGSK	0.994	*S*	-	-
ULK1_HUMAN	347	DSGGSKDSS	0.967	*S*	-	-
ULK1_HUMAN	350	GSKDSSCDT	0.997	*S*	-	-
ULK1_HUMAN	351	SKDSSCDTD	0.921	*S*	-	-
ULK1_HUMAN	374	AEAPSAKPP	0.941	*S*	-	-
ULK1_HUMAN	381	PPDSL MCS	0.686	*S*	-	-
ULK1_HUMAN	397	AGLESHGRT	0.975	*S*	-	-
ULK1_HUMAN	403	GRTSPSPSP	0.924	*S*	GSK3 $\beta$	22932492
ULK1_HUMAN	405	TPSPSPPCS	0.987	*S*	GSK3 $\beta$	21383122
ULK1_HUMAN	409	SPPCSSSPS	0.678	*S*	-	-
ULK1_HUMAN	411	PCSSSPSPS	0.895	*S*	GSK3 $\beta$ , ERK1	22932492
ULK1_HUMAN	413	SSSPSPSGR	0.947	*S*	-	-
ULK1_HUMAN	415	SPSPSGRAG	0.993	*S*	-	-
ULK1_HUMAN	422	AGPFSSSRC	0.756	*S*	-	-
ULK1_HUMAN	424	PFSSSRCGA	0.53	*S*	-	-

ULK1_HUMAN	460	TPRSSAIRR	0.962	*S*	-	-
ULK1_HUMAN	465	AIRRSGSTS	0.984	*S*	-	16964243
ULK1_HUMAN	467	RRSGSTSPL	0.986	*S*	AMPK, PKC $\delta$ , 14-3-3	19807128
ULK1_HUMAN	469	SGSTSPLGF	0.975	*S*	ERK1	21383122
ULK1_HUMAN	477	FARASPSPP	0.989	*S*	ERK1	18691976
ULK1_HUMAN	479	RASPSPPAH	0.891	*S*	CDC2, CDK5	21383122, 18691976, 19807128
ULK1_HUMAN	495	ARKMSLGGG	0.969	*S*	AMPK AKT PKA PKC $\delta$ PKC $\mu$ 14-3-3	22932492
ULK1_HUMAN	533	RGGRSPRPG	0.994	*S*	CDK5	21383122
ULK1_HUMAN	538	PRPGSSAPE	0.787	*S*	-	-
ULK1_HUMAN	539	RPGSSAPEH	0.943	*S*	-	-
ULK1_HUMAN	544	APEHSPRTS	0.986	*S*	CDC2 CDK5	22932492
ULK1_HUMAN	548	SPRTSGLGC	0.713	*S*	-	-
ULK1_HUMAN	556	CRLHSAPNL	0.807	*S*	AMPK 14-3-3	21383122, 21205641, 18669648, 18846507.
ULK1_HUMAN	588	PPQASPPQP	0.782	*S*	-	-
ULK1_HUMAN	598	HGLQSCRNL	0.773	*S*	-	-
ULK1_HUMAN	605	NLRGSPKLP	0.998	*S*	-	-
ULK1_HUMAN	630	KAVPSFDFP	0.786	*S*	-	-
ULK1_HUMAN	665	LPDLSEVGP	0.899	*S*	-	-
ULK1_HUMAN	694	GRSFSTSRL	0.987	*S*	AKT 14-3-3	22932492
ULK1_HUMAN	716	PDPGSTESL	0.894	*S*	CK1	22932492
ULK1_HUMAN	719	GSTESLQEK	0.574	*S*	CK1	22932492
ULK1_HUMAN	747	AGGTSSPSP	0.551	*S*	-	16964243
ULK1_HUMAN	750	TSSPSPVVF	0.913	*S*	-	-
ULK1_HUMAN	761	GSPPSGSTP	0.575	*S*	-	16964243
ULK1_HUMAN	775	TRMFSAGPT	0.983	*S*	-	21383122
ULK1_HUMAN	784	GSASSSARH	0.955	*S*	-	-

ULK1_HUMAN	785	SASSSARHL	0.926	*S*	-	-
ULK1_HUMAN	866	ALKGSASEA	0.886	*S*	-	19807128
ULK1_HUMAN	891	ISLLSREWG	0.951	*S*	-	-
ULK1_HUMAN	916	SGLQSAIDQ	0.985	*S*	-	-
ULK1_HUMAN	973	DRIHSITAE	0.949	*S*	-	-
ULK1_HUMAN	1042	ERRLSALLT	0.99	*S*	AMPK	19807128
					PKA	
ULK1_HUMAN	8	GRGGTETVG	0.633	*T*	-	-
ULK1_HUMAN	10	GGTETVGKF	0.595	*T*	-	-
ULK1_HUMAN	109	HAMRTLSED	0.791	*T*	-	-
ULK1_HUMAN	114	LSEDTIRLF	0.966	*T*	-	-
ULK1_HUMAN	180	MMAATLCGS	0.563	*T*	-	-
ULK1_HUMAN	247	IPRETSAPL	0.942	*T*	-	-
ULK1_HUMAN	401	SHGRTPSPS	0.582	*T*	-	-
ULK1_HUMAN	456	TQFQTPRSS	0.971	*T*	-	18669648
ULK1_HUMAN	503	GRPYTPSPQ	0.877	*T*	-	-
ULK1_HUMAN	510	PQVGTIPER	0.584	*T*	-	-
ULK1_HUMAN	520	GWSGTPSPQ	0.571	*T*	-	-
ULK1_HUMAN	636	DFPKTPSSQ	0.671	*T*	CDK5	22932492
ULK1_HUMAN	695	RSFSTSRLT	0.975	*T*	-	-
ULK1_HUMAN	746	RAGGTSSPS	0.783	*T*	-	-
ULK1_HUMAN	834	LPEETLMEQ	0.721	*T*	-	-
ULK1_HUMAN	295	PVPSYPSSG	0.809	*Y*	-	-

## Consent Form

**Project Title:** *Identification of Single Nucleotide Polymorphisms in the transcriptional Regulatory region of autophagy gene, ULK1 and their role in susceptibility to chronic hepatitis B virus infection*

**Name and Complete Address of the Project Implementing Agency.**

*Department of Biotechnology,*

*Govt. of India, New Delhi.*

**Name, Address and Telephone Number of the Principal Investigator**

*Dr. Harish Changotra,*

*Assistant Professor, Dept. Of Biotechnology & Bioinformatics*

*Jaypee University of Information Technology, Waknaghat, Solan*

I have been explained the purposes of the research being undertaken, and I have understood them. Yes/ No

I have had the opportunity to ask questions and I am satisfied with the answers provided to me. Yes/ No

I have been informed of the risks of participation and donation. Yes/ No

I have been informed of the steps to be implemented for protecting my privacy and confidentiality and I am satisfied with them. Yes/ No

I have been informed that certain screening tests may be performed on the blood/tissue samples donated by me and that I will not be provided with the results of these tests. Yes/ No

I have been informed that no private results pertaining to me that are generated during the course of this research will be provided to me. Yes/ No

I have been informed that I will not derive any direct benefits resulting from this research. Yes/ No

I am freely donating my sample for the purpose of this research study and I confirm that I have not been pressurized, directly or indirectly, to donate my sample.

**Donor's Name:**

**Date**

<b>Patient Information:</b>
-----------------------------

Name:			
Mobile:			
Address:			
State:			
Occupation:			
Email:			
Age:			
Sex:			
Blood Type:			
Current Symptoms:			
Family History:			
Alcohol:			
Infection Type:			
Anti HBe			
HBsAg			
HBeAg			
anti-HCV			
Total Bilirubin			
HBV DNA level (viral load)			
AST (SGOT) test			
ALT (SGPT) test			
Medication Prescribed			



# PUBLICATIONS

## LIST OF PUBLICATIONS

### Journal Publications

- **Randhawa R**, Duseja A, Changotra H. (2017) A novel Tetra-primer ARMS-PCR based assay for genotyping SNP rs12303764 (G/T) of human Unc-51 like kinase 1 gene. *Molecular biology reports*. 44(1): 1-4.
- Vij A, **Randhawa R**, Prakash J and Changotra H (2016) Investigating regulatory signatures of human autophagy related gene 5 (ATG5) through functional In Silico analysis. *Meta Gene*. 9: 237-248.
- Agarwal S, Kaur G, **Randhawa R**, Mahajan V, Bansal R, Changotra H (2016) Liver X receptor- $\alpha$  polymorphisms (rs11039155 and rs2279238) are associated with susceptibility to vitiligo. *Meta Gene*. 8: 33-36.
- **Randhawa R**, Sehgal M, Singh TR, Duseja A, Changotra H (2015) Unc-51 like kinase 1 (ULK1) *in silico* analysis for biomarkers identification: A vital component of autophagy. *Gene*. 562: 40–49.

### Paper/Poster Presentations

- Dogra T, Mukharjee S, Joshi V, **Randhawa R**, Khosla R and Changotra H. Role of Genetic Variants in Autophagy Related Gene 7 (ATG7) (rs35807939) in Asthma in North Indian Population. National Conference on Recent Trends in Biomedical Engineering, Cancer Biology, Bioinformatics and Applied Biotechnology (BECBAB-2015). *Jawaharlal Nehru University*, New Delhi, India. 28 November 2015.
- **Randhawa R**, Sehgal M, Singh TR, Duseja A and Changotra H. Computational analysis of unc-51 like kinase 1 (ULK1) gene and its association with autophagy. International Conference on “Stem Cell Research, Cancer Biology, Biomedical Sciences, Bioinformatics and Applied Biotechnology, *Jawaharlal Nehru University*, New Delhi, India, 1st -2nd November, 2014.

- **Randhawa R** and Changotra H. Interleukin-28B SNPs rs12979860 and rs8099917 allele frequencies from North India using a novel in-house multiplex T-ARMS-PCR. International Conference on “Stem Cell Research, Cancer Biology, Biomedical Sciences, Bioinformatics and Applied Biotechnology, *Jawaharlal Nehru University*, New Delhi, India, 1st -2nd November, 2014.
- **Randhawa R** and Changotra H. A Novel Multiplex T-ARMS-PCR Assay to Genotype IL28B Single Nucleotide Polymorphisms rs12979860 and rs8099917, simultaneously. National Conference on New insights into Pharmacogenomics, Drug Development and Personalized Medicine, *Bhagwan Mahavir Medical Research Institute*, Hyderabad, India, July 18 – 19, 2014.